

Microwave Electronics

**DESIGN AND DEVELOPMENT OF COMPACT
PRINTED ULTRA WIDE BAND ANTENNAS**

A thesis submitted by

SHAMEENA V.A

in partial fulfillment of the requirements for the degree of

DOCTOR OF PHILOSOPHY

Under the guidance of

Prof. P. MOHANAN



**DEPARTMENT OF ELECTRONICS
FACULTY OF TECHNOLOGY
COCHIN UNIVERSITY OF SCIENCE AND TECHNOLOGY
KOCHI-22, INDIA**

January 2012

“Design and Development of Compact Printed Ultra Wide Band Antennas”

Ph.D. Thesis under the Faculty of Technology

Author

Shameena V.A

Research Scholar

Department of Electronics

Cochin University of Science and Technology

Kochi - 682022

Email: shameenava@gmail.com

Supervising Guide

Dr. P. Mohanan

Professor

Department of Electronics

Cochin University of Science and Technology

Kochi - 682022

Email: drmohan@gmail.com

January 2012

Dedicated to my daughter Abida...





**DEPARTMENT OF ELECTRONICS
COCHIN UNIVERSITY OF SCIENCE AND TECHNOLOGY,
KOCHI – 682 022**

Dr. P. Mohanan
Professor

Ph: 0484 2576418
E-mail: drmohan@cusat.ac.in

Certificate

This is to certify that this thesis entitled “**Design and Development of Compact Printed Ultra Wide Band Antennas**” is a bonafide record of the research work carried out by Ms. SHAMEENA V.A under my supervision in the Department of Electronics, Cochin University of Science and Technology. The results embodied in this thesis or parts of it have not been presented for any other degree.

Cochin-22
25th January 2012

Dr. P. Mohanan
(Supervising Teacher)

Declaration

I hereby declare that the work presented in this thesis entitled “**Design and Development of Compact Printed Ultra Wide Band Antennas**” is a bonafide record of the research work done by me under the supervision of Dr. P. Mohanan, Professor, Department of Electronics, Cochin University of Science and Technology, India and that no part thereof has been presented for the award of any other degree.

Cochin-22
25th January 2012

Shameena V.A
Research Scholar
Department of Electronics
Cochin University of Science
and Technology

Words of Gratitude...

The work presented in this thesis would not have been possible without the support of a number of individuals and organizations and I gratefully acknowledge all of them. First of all, I would like to thank my supervisor Prof.P.Mohanan for guiding me throughout this work with his patience. He has been a constant source of encouragement and I am impressed by his notable academic background and profound understanding of the subjects, which have proved to be immense benefits to me. It has been my great pleasure and honour to be under his supervision and work with him.

I take this opportunity to thank Prof.K.G.Nair for his vision in setting up Center for Research in Electromagnetics and Antennas (CREMA) at CUSAT. I also wish to thank him for his valuable personnel and professional suggestions throughout my research period.

I am grateful to Prof. K. Vasudevan, Dean Faculty of Technology and former Head, Department of Electronics for his well-timed care in my research, valuable suggestions and constant encouragements to improve my work.

In this context let me also thank Prof. P.R.S. Pillai, Head of the Department of Electronics for his whole hearted support, constant encouragement, and for extending the facilities of Department of Electronics for my research.

A special and sincere acknowledgement goes to Dr. C. K. Aanandan, Professor, Department of Electronics, Cochin University of Science and Technology for his valuable suggestions and constant encouragement, which helped me very much to improve my research work.

My sincere thanks to Dr. Tessamma Thomas, Dr. James Kurien, Dr. M.H. Supriya, and all other faculty members of Department of Electronics for the help and assistance

extended to me. My sincere thanks to all non teaching staff of Department of Electronics for their amicable relation, sincere cooperation and valuable helps.

I wish to thank UGC, Govt. of India for financial assistance in the form of Research fellowship for meritorious students (RFSMS).

Speaking of people I am indebted to at the center, I am especially grateful to have known and interacted with such a high caliber of cohort. In particular I would like to thank Dr. Suma M.N and Dr Rohith. K, Raj for guiding me properly during the initial stage of my research. I also wish to acknowledge Dr.Manoj Joseph ,Dr.Deepu V, Dr. Gijo Augustine, Dr. Jitha B, Dr. Bybi , Dr.Gopikrishna and Dr.Deepti Das Krishna for their support.

Very special thanks to Mr.Sujith,Mr. Sarin, Mrs.Nishamol.M.S and Mrs.Laila.D, for offering their immense care, technical and scientific talks shared together during my research period . May the road rise up to meet you .These friends will be in my heart forever.

Words will not be enough to thank Mr. Nijas.C.M for his extreme care, helps and support. I will also miss the company of Mr.Deepak,Mr. Dinesh, , Mr.Tony.D , Mr.Abdul Rasheed, Mr .Vinesh P V, Mr. Sreejith .M.Nair,Mr. Lindo.A.O, Ms.Anju.P.Mathews, and Mrs.Sarah Jacob Mr. Ullas.G.Kalappura, Mr.Paulbert Thomas, Mr.Sreenath.S, Mr.Ashkarali.P, Ms. Sreekala, Mr. Sumesh, Mr. Cyriac M O: discussing research,coffee breaks and because of the incredible amount of unforgettable moments that we have shared. I also want to acknowledge Mrs. Sreekala Thomas and Ms. Indhu K,K for their whole hearted support and prayers.

I remember with gratitude, Dr.Mridula, faculty, School of Engineering, CUSAT for her guidance and encouragement towards my research. Special thanks to Dr. Binu Paul and Mrs. Anju Pradeep for their whole hearted support, helps and above all the association with me.

I would also like to thank the colleagues at Centre for Ocean Electronics (CUCENTOL), Microwave Tomography and Material Research Laboratory (MTMR) and

Audio and Image Research Lab (AIRL), Department of Electronics, Cochin University of Science and Technology.

One cannot attribute success only to work related people. My Family, consisting of Father, Mother, Brother and sister being there always an incredible pillar of support. My parents each of them had their own special way to make my life great. They are my source of courage to face even the hardest situation. Special thanks to my brother whose words inspired me very much for coming in to the research field.

Mere words will not be enough to thank my daughter Abida for her sacrifice and adjustment during the period of my research.

Above all there is that supreme power whose blessings and kindness helped me a lot to tide over.

Shameena V.A.

Abstract

In recent years, there is a visible trend for products/services which demand seamless integration of cellular networks, WLANs and WPANs. This is a strong indication for the inclusion of high speed short range wireless technology in future applications. In this context UWB radio has a significant role to play as an extension/complement to existing cellular/access technology.

In the present work, three major types of ultra wide band planar antennas are investigated: Monopole and Slot. Three novel compact UWB antennas, suitable for portable applications, are designed and characterized, namely

- 1) Ground modified monopole
- 2) Serrated monopole
- 3) Triangular slot

The performance of these designs have been studied using standard simulation tools used in industry/academia and they have been experimentally verified. Antenna design guidelines are also deduced by accounting the resonances in each structure.

In addition to having compact sized, high efficiency and broad bandwidth antennas, one of the major criterion in the design of impulse-UWB systems have been the transmission of narrow band pulses with minimum distortion. The key challenge is not only to design a broad band antenna with constant and stable gain but to maintain a flat group delay or linear phase response in the frequency domain or excellent transient response in time domain. One of the major contributions of the thesis lies in the analysis of the frequency and time-domain response of the designed UWB antennas to confirm their suitability for portable pulsed-UWB systems. Techniques to avoid narrowband interference by engraving narrow slot resonators on the antenna is also proposed and their effect on a nano-second pulse have been investigated.

CONTENTS

Chapter -1

INTRODUCTION	01- 37
1.1 Introduction-----	2
1.2 Over view of Antenna Research-----	3
1.3 Short-Range Wireless Communications-----	5
1.3.1 Bluetooth-----	7
1.4 Ultra-Wideband (UWB) Technology-----	9
1.4.1 Overview of Ultra-Wideband Communications-----	12
1.4.2 UWB antenna characteristics-----	15
1.4.2.1 Frequency independent antennas-----	17
1.4.2.2 Multi-resonant antennas-----	19
1.4.2.3 Travelling wave antennas-----	19
1.4.2.4 Small element antennas-----	20
1.4.3 UWB Transmission Schemes-----	21
1.4.4 UWB regulation and standards-----	24
1.4.5 Advantages and Limitations of UWB-----	26
1.4.6 UWB Applications-----	28
1.5 Motivation for the work-----	29
1.6 Thesis Organization-----	31
References-----	34

Chapter -2

METHODOLOGY AND LITERATURE REVIEW.....	39 - 78
2.1 Antenna Fabrication-----	40
2.2 Antenna measurement facilities-----	40
2.2.1 HP 8510C Vector Network Analyzer-----	40
2.2.2 Anechoic Chamber-----	42
2.2.3 Turn table assembly for far field radiation pattern measurement --	42
2.3 Antenna Characterization-----	43
2.3.1 Return loss Measurement-----	43
2.3.2 Efficiency Measurement:-----	43
2.3.3 Radiation Pattern Measurement.-----	45
2.3.4 Antenna Gain Measurement-----	45
2.4 Ansoft HFSS- The CAD tool-----	46
2.5 Time domain antenna analysis-----	46
2.5.1 Behavior of UWB Antenna System-----	47

2.5.1.1	Description of UWB Antenna System	47
2.5.2	Group Delay	49
2.5.3	Choice of Source Pulse	51
2.5.4	Transfer function determination	54
2.5.5	Implementation in MATLAB R ^o	54
2.5.6	Received Signal Waveforms	54
2.6	Pulse Distortion Analysis: Fidelity Factor	55
2.7	Effective Isotropically Radiated Power (EIRP)	56
2.8	Monopole UWB Antennas-Review	59
2.8.1	UWB Planar monopole antennas	61
2.9	Chapter Conclusion	70
	References	70

Chapter -3

TOP LOADED MONOPOLE ULTRA WIDE BAND ANTENNAS.....79 - 156

3.1	Ground Modified Monopole Antenna	81
3.1.1	Finite Ground Coplanar Waveguide (FGCPW) fed Strip Monopole Antenna	83
3.1.1.1	Resonance mechanism	84
3.1.1.2	Effect of ground plane length L_g	86
3.1.1.3	Effect of ground plane width W_g	87
3.1.1.4	Effect of Monopole length S	88
3.1.2	Top Loaded Strip Monopole Antenna	90
3.1.2.1	Simulated current distribution and radiation pattern of the top loaded strip monopole antenna	91
3.1.3	Compact Ground Modified Monopole Antenna	93
3.1.3.1	Geometry of Ground Modified Monopole Antenna	93
3.1.3.2	Reflection characteristics of Ground Modified Monopole Antenna	94
3.1.3.3	Parametric Analysis of Ground Modified Monopole Antenna	95
3.1.3.3.1	Effect of radius of quarter circle (R)	95
3.1.3.3.2	Effect of top loaded rectangle L_1	96
3.1.3.3.3	Effect of gap distance S	97
3.1.3.4	Simulated Current distribution and radiation pattern of the ground modified monopole antenna	98
3.1.3.5	Measured Radiation Pattern of the ground modified monopole antenna	99
3.1.3.6	Gain and Efficiency of the ground modified monopole antenna	101
3.1.3.7	Design of the ground modified monopole antenna	101
3.2	Planar Serrated Microstrip Fed Monopole UWB Antenna	104
3.2.1	Evolution of the Antenna	104

3.2.1.1	A simple microstrip fed monopole Antenna (Antenna I) ----	105
3.2.1.2	Top loaded strip monopole antenna (Antenna II) -----	108
3.2.1.3	Microstrip fed serrated monopole Antenna (Antenna III) ---	112
3.2.1.3.1	Reflection Characteristics of Micro strip fed serrated monopole Antenna-----	113
3.2.1.3.2	Current distribution and radiation pattern of the serrated monopole antenna-----	114
3.2.1.3.3	Measured radiation pattern of the serrated monopole antenna -----	115
3.2.1.3.4	Parametric Analysis of Serrated Monopole Antenna-117	
3.2.1.3.4.1	Effect of width W_1 of patch-----	117
3.2.1.3.4.2	Effect of gap d -----	117
3.2.1.3.5	Design of serrated monopole antenna -----	118
3.2.1.3.6	Gain and Efficiency of Serrated Monopole Antenna ----	120
3.3	Band notch Design -----	121
3.3.1	5.8 GHz Band notched UWB serrated monopole antenna -----	123
3.3.2	Reconfigurable Antennas-----	129
3.3.2.1	Implementation of the switch by means of a PIN diode ----	130
3.4	A Compact CPW fed serrated UWB antenna -----	132
3.4.1	Geometry of CPW fed serrated antenna -----	132
3.4.2	Reflection Characteristics of CPW fed Serrated Monopole Antenna -----	133
3.4.3	Design of CPW fed Serrated Monopole Antenna -----	134
3.5	Time Domain Analysis of UWB Monopole Antennas -----	139
3.5.1	Group Delay of UWB Monopole Antennas-----	140
3.5.2	Transfer functions of UWB Monopole Antennas -----	141
3.5.3	Impulse Responses of UWB Monopole Antennas -----	144
3.5.4	Received Signal Waveforms of UWB Monopole Antennas -----	147
3.5.5	Fidelity Factor of UWB Monopole Antennas -----	148
3.5.6	EIRP of UWB Monopole Antennas-----	149
3.5.7	Chapter Summary -----	152
References	-----	153

Chapter -4

PLANAR TRIANGULAR SLOT ULTRA WIDEBAND ANTENNA.....157 - 202

4.1	Review on UWB planar Slot Antennas-----	158
4.2	Triangular slot UWB antenna -----	165
4.2.1	Triangular slot Antenna (Antenna 1) -----	166
4.2.2	Signal strip extended Triangular slot Antenna (Antenna 2) -----	167
4.2.3	Triangular Slot UWB Antenna (Antenna 3) -----	169
4.2.3.1	Geometry of the Triangular slot UWB Antenna-----	169
4.2.3.2	Reflection Characteristics of the Triangular slot UWB Antenna-----	170
4.2.3.3	Parametric Analysis of the Triangular slot UWB Antenna --	171
4.2.3.3.1	Effect of rectangle length L -----	171

4.2.3.3.2	Effect of gap distance S. -----	173
4.2.3.3.3	Effect of triangular side L_2 -----	175
4.2.3.3.4	Effect of L_3 -----	175
4.2.3.5	Field distributions and Radiation patterns of the Triangular slot UWB Antenna -----	176
4.2.3.6	Design of the Triangular slot UWB Antenna -----	180
4.2.3.7	Current distribution and radiation pattern of the triangular slot UWB antenna -----	182
4.2.3.8	Gain and Efficiency of the triangular slot UWB antenna. ---	184
4.3	5.8GHz Band Notched Triangular Slot Antenna -----	184
4.3.1	Reflection characteristics of Band Notched Triangular Slot Antenna 185	
4.4	Time Domain Analysis of Triangular Slot UWB Antennas -----	189
4.4.1	Group delay of Triangular Slot UWB Antennas -----	189
4.4.2	Transfer functions of Triangular Slot UWB Antennas -----	190
4.4.3	Impulse Responses of Triangular Slot UWB Antennas -----	192
4.4.4	Received signal waveforms of Triangular Slot UWB Antennas ---	193
4.4.5	Fidelity of Triangular Slot UWB Antennas -----	194
4.4.6	EIRP of Triangular Slot UWB Antennas -----	195
4.5	Chapter Summary -----	197
	References -----	197

Chapter -5

CONCLUSIONS AND FUTURE PERSPECTIVE203 - 208

5.1	Thesis Summary and Conclusions-----	204
5.2	Suggestions for Future Work-----	207

PUBLICATIONS209 - 211

CITATIONS213

CURRICULUM VITAE215 - 217

INDEX219 - 220

Contents	1.1	<i>Introduction</i>
	1.2	<i>Over view of Antenna Research</i>
	1.3	<i>Short-Range Wireless Communications</i>
	1.4	<i>Ultra-Wideband (UWB) Technology</i>
	1.5	<i>Motivation for the work</i>
	1.6	<i>Thesis Organization</i>

This chapter surveys the current and emerging wireless communication standards and highlights the significance of Ultra Wide-Band (UWB) communications. A history of research in the field of UWB antennas are narrated followed by a description about advantages and applications of UWB communication. A description of the stimulus behind the present investigations is presented and the chapter is concluded with the organization of the present thesis.

1.1 Introduction

The antenna is an essential part of any wireless system as it is the component providing transition between a guided wave and a free-space wave. According to IEEE standard definitions for antennas [1], an antenna is defined as a means for radiating or receiving radio waves. During the period 1885-1900, some pioneers invented the antennas and the wireless systems.

The foundations for wireless communication research and industry were established in 1864, when James Clerk Maxwell predicted that the electric and magnetic fields will allow energy to be transported through materials and space at a finite velocity [2]. Heinrich Rudolf Hertz demonstrated Maxwell's theory of electromagnetic radiation in 1888 by his classical spark transmitter. Hertz's apparatus demonstrated the first transmission of regulated radio waves, the 'new form of energy' [3].

The great Indian scientist Jagadish Chandra Bose made a revolutionary attempt to demonstrate radio communication. In 1895, Bose gave his first public demonstration of electromagnetic waves. The wavelengths he used ranged from 2.5 cm to 5 mm. He was playing at 60 GHz over one hundred years ago!. Bose's investigations included measurement of refractive index of a variety of substances. He also made dielectric lenses, oscillators, receivers, and his own polarization device.

Guglielmo Marconi, dubbed the father of the wireless communications, took the discoveries of Maxwell and Hertz to the outside world. It was in 1897 that Marconi demonstrated the practical applications of wireless communication, when he established continuous radio contact between the shore and ships traveling in the English Channel [4]. By mid December in 1901, Marconi took a much greater step by performing the first transcontinental

wireless communication, between England and Canada. This achievement triggered the scientists and engineers all over the world towards wireless communication.

1.2 Over view of Antenna Research

Prior to World War II, most antenna elements were of wire types such as long wires, dipoles, helices, rhombuses etc., and were used either as single element or as arrays. In the year 1926 Yagi-Uda antenna was introduced [5], which received wide popularity due to the simple array structure and excellent radiation performance. It is still being used as home TV antenna.

World War II was the most flourishing period in antenna research. During and after World War II, many other radiators were introduced. Many of these were aperture type such as open ended waveguides, slots, horns, reflectors and lenses. They were employed for radar, remote sensing and deep space applications [6]. In 1950s a breakthrough in antenna evolution was created by V.H Ramsey [7] which extended the bandwidth as great as 40:1 or more. The structure is specified entirely by angles, instead of linear dimensions, they offered an infinite bandwidth and were popularly referred to as frequency independent antennas.

It was not until almost 20 years later that a fundamental new radiating element, which has received a lot of attention and many applications since its inception, was introduced. Microstrip antennas received considerable attention starting in the 1970s, although the idea of a microstrip antenna can be traced to 1953 [8]. Microstrip antenna is simple, lightweight, inexpensive, low profile and conformal to Aircraft, Missile etc. Major advances in millimeter wave antennas have been made in recent years, including integrated antennas where

active and passive circuits are combined with the radiating elements into one compact unit to form monolithic circuits [9].

There has been much interest in electrically small antennas. Antennas that are electrically small, efficient, and have significant bandwidth would fill many needs if antenna engineers could reconcile these usually contradictory requirements. This is especially true recently with increased uses of wireless technologies for communications and sensor networks. It is well known that small electric dipole antenna is an inefficient radiator, i.e., because it has a very small radiation resistance with very large capacitive reactance. Consequently, to obtain a high overall efficiency, considerable effort must be expended on a matching network that produces an impedance that is conjugately matched to the dipole's impedance; i.e., it forces the total reactance to zero by introducing a very large inductive reactance which cancels the very large capacitive reactance of a small electric dipole, and that then matches this resonant system to a feed network. Recently, this problem has been overcome by introducing metamaterials in antennas. A metamaterial medium is introduced in antennas to obtain electrically small antenna element with good efficiency [10].

Research conducted on antennas is driven by several factors. The first factor deals with the increase of the bandwidth and shift of operational frequency to the higher bands. With the ever-increasing need for mobile communication and the emergence of many systems, it has become important to design broadband antennas to cover a wide frequency range. Modern wireless applications require the processing of more and more data in different forms, higher data rates, higher capacity and multi-standard abilities. There are numerous well-known methods to increase the bandwidth of antennas including designs with log-periodic profile, travelling-wave topologies, increase of the

substrate thickness and the use of a low dielectric substrate, various impedance matching and feeding techniques, multiple resonators and slot antenna geometry [11-14].

According to wireless applications and the associated devices, the type of antennas can be very different. For example, the main requirements for an antenna of a cellular mobile radio phone will be small type, low profile and broad/multi bandwidth. Last but not least, in modern wireless communication systems, complex signal processing techniques and digital routines are considered in order to build a device which is flexible enough to run every possible waveform without any restrictions on carrier frequency, bandwidth, modulation format, data rate, etc. This is the philosophy of future radio systems such as Software Defined Radio (SDR) and cognitive radio firstly introduced by Mitola [15,16]. In this context, the antenna becomes not only one of the most important parts in a wireless system but it is also flexible and “intelligent” enough to perform processing function that can be realized by any other device. The antennas are becoming increasingly linked to other components (e.g., system-on-chip) and to other subject areas (such as digital signal processing or propagation channels). To accurately integrate the antenna performance into the design of the overall wireless system, specific models compatible with standard languages are highly desired. Such modeling allows the right design and optimization of wireless RF front-ends including antennas.

1.3 Short-Range Wireless Communications

Radio-based Short-Range Wireless (SRW) communication is an alternative class of emerging technologies designed primarily for indoor use over very short distances. It is intended to provide fast (tens or hundreds of megabits per second) and low cost, cable free connections to the internet and

between portable devices. SRW features transmission powers of several microwatts up to milliwatts, yielding a communication range between 10 and 100 meters. SRW provides connectivity to portable devices such as laptops, PDAs, cell phones and others.

Short-range communications standards fall into two broad but overlapping categories: Personal Area Networks (PAN) and Local Area Networks (LAN). Wireless PAN technologies emphasize low cost and low power consumption, usually at the expense of range and peak speed. In a typical wireless PAN application, a short wireless link, typically under 10 meters, replaces a computer serial cable or USB cable. Standards, such as Bluetooth and Home RF, have been created to regulate short-range wireless communications. Bluetooth has appeared recently in many mobile devices. Bluetooth can transmit data through solid nonmetal objects and supports a nominal link range of 10cm-10m at a moderate baud rate up to 720kb/s (raw data rate is 1Mb/s) [17]. An optional high power mode in the current specifications allows for ranges up to 100m. Because of the nature of radio, Bluetooth is a point to multipoint communication system, which supports connections of two devices as well as ad hoc networking between several devices. In order to prevent unauthorized access, Bluetooth requires sophisticated authentication and encryption mechanisms, which hamper fast connection establishment.

Therefore, Bluetooth is best for applications that require stable point-to-point or point-to multipoint connections for data exchange at moderate speeds, where mobility is a key requirement. Ultra-WideBand (UWB) is an emerging new technology that shows great potential for SRW applications. Unlike conventional wireless communications systems that are carrier-based, UWB-

based communication is baseband. It uses a series of short pulses that spread the energy of the signal from near DC to a few GHz.

Wireless LAN technologies, on the other hand, emphasize a higher peak speed and longer range at the expense of cost and power consumption. Typically, wireless LANs provide wireless links from portable laptops to a wired LAN access point. To date, 802.11b has gained acceptance rapidly as a wireless LAN standard. It has a nominal open-space range of 100m and a peak over-the-air speed of 11Mb/s. Users can expect maximum available speeds of about 5.5Mb/s. Other communication standards offer even higher data rates, like 802.11a and 802.11g.

1.3.1 Bluetooth

In 1994, Ericsson Mobile Communications, the global telecommunications company based in Sweden, initiated a study to investigate the feasibility of a low-power, low-cost radio interface between mobile phones and their accessories. The aim of the study was to find a way to eliminate cables between mobile phones and PC cards, headsets, desktops, and other devices. The study was part of a larger project investigating how different communications devices could be connected to the cellular network via mobile phones. The company determined that the last link in such a connection should be a short-range radio link. As the project progressed, it became clear that the applications for a short-range radio link were virtually unlimited [18]. The Bluetooth specification comprises a system solution consisting of hardware, software and interoperability requirements. The set of Bluetooth specifications developed by Ericsson and other companies answers the need for short-range wireless connectivity for ad hoc networking. The Bluetooth baseband protocol is a combination of circuit and packet switching, making it suitable for both voice and data.

Bluetooth wireless technology is implemented in tiny, inexpensive, short-range transceivers in the mobile devices that are available today, either embedded directly into existing component boards or added into an adapter device such as a PC card inserted into a notebook computer. Potentially, this will make devices using the Bluetooth specification the least expensive wireless technology to implement.

Bluetooth wireless technology uses the globally available unlicensed ISM (Industrial, Scientific, and Medical) radio band of 2.4 GHz. The ISM bands include then frequency ranges at 902—928 MHz and 2.4—2.484 GHz, which do not require an operator's license from the Federal Communications Commission (FCC) or any international regulatory authority. The use of a common frequency band means that devices using the Bluetooth specification can be used virtually anywhere in the world and they will be able to link up with other such devices, regardless of what country they are being operated in.

When it comes to ad hoc networking for data, a device equipped with a radio using the Bluetooth specification establishes instant connectivity with one or more other similarly equipped radios as soon they come into range. Each device has a unique 48-bit Medium Access Control (MAC) address, as specified in the IEEE 802 standards for LANs. For voice, when a mobile phone using Bluetooth wireless technology comes within range of another mobile phone with built-in Bluetooth wireless technology conversations occur over a localized point-to-point radio link. Since the connection does not involve a telecommunications service provider, there is no per-minute usage charge.

The radio link itself is very robust, using frequency-hopping spread-spectrum technology to mitigate the effects of interference and fading. As noted, spread spectrum is a digital coding technique in which the signal is taken

apart or "spread" so that it sounds more like noise to the casual listener. The coding operation increases the number of bits transmitted and expands the bandwidth used.

Using the same spreading code as the transmitter, the receiver correlates and collapses the spread signal back down to its original form. With the signal power spread over a larger band of frequencies, the result is a robust signal that is less susceptible to impairment from electromechanical noise and other sources of interference. It also makes voice and data communications more secure. With the addition of frequency hopping—having the signals hop from one frequency to another—wireless transmissions are made even more secure against eavesdropping.

The objective of the Bluetooth standard is to enable seamless communications of data and voice over short-range wireless links between both mobile and stationary devices. The standard specifies how mobile phones, Wireless Information Devices (WIDs), handheld computers, and Personal Digital Assistants (PDAs) using Bluetooth wireless components can interconnect with each other, with desktop computers, and with office or home phones. With its use of spread-spectrum technology, the first generation of the Bluetooth specification permits the secure exchange of data up to a rate of about 1 Mbps—even in areas with significant electromagnetic activity. With its use of Continuously Variable Slope Delta modulation (CVSD) for voice encoding, the Bluetooth specification allows speech to be carried over short distances with minimal disruption.

1.4 Ultra-Wideband (UWB) Technology

In the short-range application space, ultra-wideband radio technology (UWB-RT) can drive the potential solutions for many of today's problems

identified in the areas of spectrum management and radio systems engineering. The novel and unconventional approach underlying the use of UWB-RT is based on optimally sharing the existing radio spectrum resources rather than looking for still available but possibly unsuitable new bands. This disruptive idea has recently received legal adoption by the regulatory authorities in the United States [19], and efforts to achieve this status have started in both Europe [20] and Asia, particularly Japan and Singapore. It is widely anticipated that UWB-RT will have a sizable impact on the multimedia-driven home networking and entertainment market, and will allow implementation of intelligent networks and devices enabling a truly pervasive and user-centric wireless world.

The bandwidth of UWB systems, as defined by FCC in [21], is more than 20% of a center frequency or more than 0.5 GHz. Clearly, this bandwidth is much greater than the bandwidth used by any current communication technology. UWB implementations can directly modulate an impulse that has a very sharp rise and fall time, thus resulting in a waveform that occupies several GHz of bandwidth. Fractional bandwidth is defined as

$$B_f = 2 \frac{f_h - f_l}{f_h + f_l} \text{-----(1.1)}$$

where, f_h and f_l are the highest and lowest cut-off frequencies (-10 dB point) of a UWB pulse spectrum respectively. The large bandwidth of UWB signals provide robustness to jamming and have low probability of detection properties. UWB devices usually require low transmit power, due to the control over duty cycle, thus supporting a longer battery life for hand-held devices.

This led to the emergence of UWB technology based applications for commercial high-data-rate, short-range communications, radar systems and measurement. They include high-speed file transfers and printing, high-definition

audio/video streaming and a myriad of other applications in the consumer electronics, personal computing and mobile communication arenas. The UWB systems should provide ≈ 50 Mbps through buildings within a range of at least 20m, as well as higher rates (up to 1 Gbps) at shorter distances. UWB circuits need very little power to achieve these data rates (around tens of mW), which is between one tenth and one hundredth of the power required by devices such as mobile telephones and existing WLANs for the equivalent data rates, respectively, and are thus ideal for battery-powered devices [22].

If we have a fixed amount of energy, we can either transmit a great deal of energy density over a small bandwidth or a very small amount of energy density over a large bandwidth. This is measured in terms of the Power Spectral Density (PSD) which is defined as

$$\text{PSD} = P/B \text{ ----- (1.2)}$$

where P is the power transmitted in watts (W), B is the bandwidth of the signal in hertz (Hz), and the unit of PSD is watts/hertz (W/Hz) or dBm/Hz on a logarithmic scale. For UWB systems, the energy is spread out over a very large bandwidth (hence the name ultra wide band) and in general, is of a very low power spectral density. The maximum permitted power levels of the FCC approved UWB technology is low enough at 0.5mW over the entire 7.5GHz bandwidth (i.e. PSD = -41.3dBm/MHz, the same level as unintentional radiation from common electronics devices such as laptop computers). For wireless communications in particular, this allows UWB technology to overlay already available services such as the WiMAX and the IEEE 802.11 WLANs that coexist in the 3.1 to 10.6GHz.

The proponents of the ultra wideband technology have claimed that the system has the ability to utilize the frequency spectrum without causing any interference problem to other conventional communication systems, because it has a low power spectral density. Fig. 1.1 shows spectrum utilization of UWB system and conventional narrowband system.

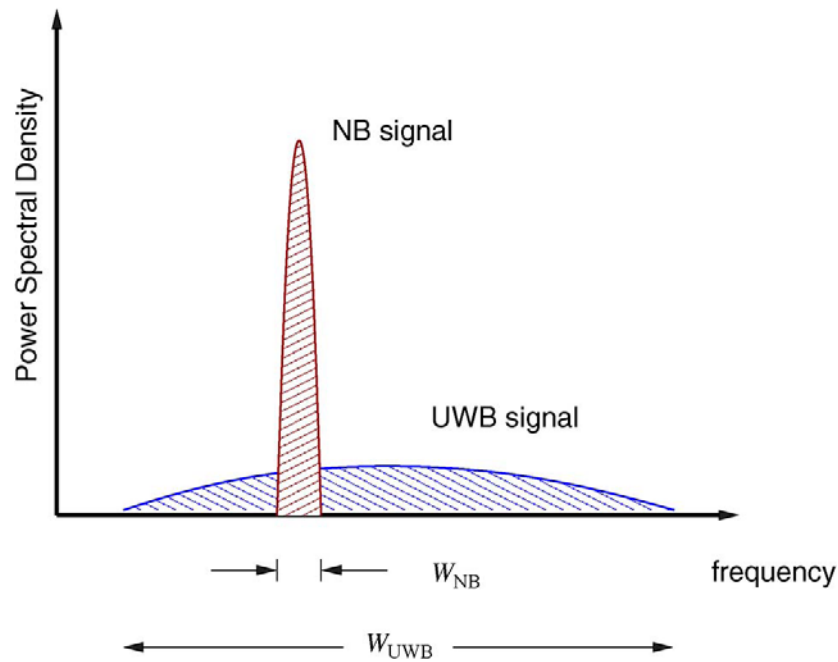


Fig.1.1. Illustration of spectrum utilization by UWB systems

1.4.1 Overview of Ultra-Wideband Communications

In today's world, although it is most common to use sinusoidal signals in wireless communication systems, the earliest electromagnetic communication systems were actually based on pulses [23].

The spark gap generator is known to be the first UWB radio that was used by Hertz and Marconi in the late 1800's [24]. Heinrich Hertz used the spark gap to produce electromagnetic waves for his experiments in 1893. Similarly, Marconi used spark gap generator for electromagnetic data communications [25].

Marconi's spark-gap transmission experiments in 1901 were one of the first experiments about impulse radio. Additionally, Sommerfeld first analyzed the diffraction of a short pulse by a half-plane which is known to be one of the fundamental problems in UWB wave propagation [26]. Therefore, it can be assumed that the first practical UWB systems and theoretical research on UWB radiation goes back to more than a century ago. Nevertheless, the signals generated by the spark-gap transmitters had low spectral efficiency and low bit rate but large bandwidth [27]. During that period, researchers could not utilize this issue and it was perceived as a failure. Therefore, the communications became mainly narrowband after 1910, and ultra wideband research did not get any more interest until the 1960s when the studies began again for time domain electromagnetics with the innovative work of Gerald F. Ross.

In his studies, Ross described the transient behavior of microwave networks through their characteristic impulse responses. Also around this time, the sampling oscilloscope was developed by Hewlett Packard and some techniques were built up for subnano second (baseband) pulse generation. This allowed the analysis of short duration signals in the time domain experimentally and provided the direct observation and measurement of the impulse response for microwave networks.

When the techniques for impulse measurement were developed also for designing wideband antenna structures, researchers recognized that short pulse radar and communication systems could be built up utilizing the same equipments.

Afterwards, the main interest moved towards the techniques for the development of radar and communication devices. Designing high power, short pulse generators for UWB radar systems was investigated by the military. In particular, radar got a lot of interest because it was possible to obtain results

with good accuracy. The low-frequency components were useful in penetrating objects, and ground penetrating radar was developed.

In the 1970s, ultra wideband communications started to get more attention [28]. Ross developed various applications for radar and communications at the Sperry Research Center. In April 1973, he was awarded the first UWB communications patent. Therefore, in the 1970s and 1980s, most of the research and development were in the military or in the works funded by the US Government.

One of the earliest applications of UWB technology was high power military radar. Also, low probability of intercept capability of UWB signals is utilized for covert communications and use of a very wide band of frequencies allowed detection of buried mines in ground penetrating radar applications. The term ultra-wideband was first applied around 1989 by the U.S. Department of Defense and this technology was earlier referred to as baseband carrier-free or impulse radar.

Small companies such as Multispectral Solutions, Inc., Aether Wire and Location, and Pulson Communications (Time Domain Corporation) also started basic research and development on communications and positioning systems, specializing in UWB technology, beginning in the late 1980s [29]. By the mid-1990's, University of Southern California's Ultra Lab was established. Ultra Lab lobbied FCC to allow commercializing the UWB technology.

In May 1998, a workshop sponsored by US Army Research Office and USC Ultra Lab was organized and soon after this conference, the companies working on UWB technology decided to band together and formed an informal industry association, Ultra-Wideband Working Group (<http://www.uwb.org>).

In the late 1990s, there has been a lot of interest regarding the application of UWB technology for wireless communications. Companies such as Time

Domain Corporation, US Radar, Zircon Corporation had requested for permission from FCC to develop a small number of commercialized UWB devices. At the same time, USC's Ultra Lab acquired a license from FCC for experimental studies on UWB radio transmissions.

Since UWB signals occupy a large frequency range, they violate the frequency regulations assigned to other conventional narrowband systems all over the world. However, proponents of the technology in both industry and academia insisted that UWB emissions would not interfere with those other narrowband services. Then, after lengthy deliberations, the FCC issued its first report and order on UWB technology in April 2002[30]. In this ruling, it is specified that the UWB emission is allowed between the frequency ranges of 3.1 GHz and 10.6 GHz. Since the late 1990s, the research and development of ultra wideband technology have widely emerged and become a promising technology which came to be known as impulse radio.

1.4.2 UWB antenna characteristics

In 2003, a history of UWB antennas is presented by H.G. Schantz who emphasizes the relevant past works on UWB antennas and their important wide variety [31]: *“Ultra-Wideband has its roots in the original spark-gap transmitters that pioneered radio technology. This history is well known and has been well documented in both professional histories and in popular treatments. The development of UWB antennas has not been subjected to similar scrutiny. As a consequence, designs have been forgotten and then re-discovered by later investigators”*. Thus, in the recent years, a lot of UWB antenna designs have been reported and presented in the academic literature (32; 33; 34) and in some patents (35).

An antenna is a device that converts a signal transmitted from a source to a transmission line into electromagnetic waves to be broadcasted into free space and vice versa. An antenna is usually required to optimize or concentrate the radiation energy in some directions and to suppress it in the others at certain frequencies. A good design of the antenna can relax system requirements and improve overall system performance. In practice, to describe the performance of an antenna, there are several commonly used antenna parameters, such as impedance bandwidth, radiation pattern, directivity, gain, input impedance, and so on.

However, UWB antennas are firstly antennas! As a consequence, UWB antennas try to achieve the same goals, and are subjected to the same physical constraints (e.g., low cost, small size, integration capability, etc.) and the same electrical constraints (e.g., impedance matching, radiation pattern, directivity, efficiency, polarization, etc.) as in the case of narrowband antennas. Further, due to the large bandwidth, the electrical parameters become frequency dependent complicating the design and analysis. In addition to the conventional characterization parameters, some specific parameters must be examined in order to take into account the distortion effects, notably, critical for IR applications. These specific parameters include group delay, phase response and impulse response. The radiation pattern is desired to be constant within the overall operating frequency in order to guarantee the pulse properties to be same in any direction. The group delay is given by the derivative of the unwrapped phase of an antenna. If the phase is linear throughout the frequency range, the group delay will be constant for the frequency range. This is an important characteristic because it helps to indicate how well a UWB pulse will be transmitted and to what degree it may be distorted or dispersed.

The specifications of the antenna design will be a trade-off of these parameters taking into account not only the expected application but also the technique of transmission (multiple narrow bands or pulsed operation) to be used. Some parameters have to be declared more important than others. Two types of requirements can be distinguished. The physical constraints arise when one strives to develop antennas of small size, low profile and low cost (materials, maintenance and fabrication), and with embeddable capability. The electrical constraints arise while designing antennas with wideband impedance bandwidth covering all sub-bands (for MB-OFDM) or the bandwidth where most of the energy of the source pulse is concentrated (for IR), steady directional or omni-directional radiation patterns, constant gain at directions of interest, constant desired polarization.

UWB antennas may be categorized into different types according to their radiating characteristics: frequency independent antennas, multi-resonant antennas, travelling wave antennas and small element antennas.

1.4.2.1 Frequency independent antennas

Frequency independent antennas, such as biconical, spiral, conical spiral and log periodic antennas are classic broadband and UWB antennas. They can offer real constant impedances and consistent pattern properties over a frequency bandwidth greater than 10:1. There are two principles for achieving frequency independent characteristics.

The first one was introduced by V.H Rumsey in the 1950s. Rumsey's principle suggests that the pattern properties of an antenna will be frequency independent if the antenna shape is specified only in terms of angles. Infinite biconical and spiral antennas are good examples whose shapes are completely described by angles. For the log periodic antennas, the entire shape is not solely specified by angles rather it is also dependent on the length from the origin to

any point on the structure. However, the log periodic antennas can still exhibit frequency independent characteristics. Fig. 1.2 illustrates the geometry of spiral, log periodic and conical spiral antennas.

The second principle accounting for frequency independent characteristics is self complementarities, which was introduced by Mushiake in the 1940s derived from the Babinet's principle in optics. Mushiake discovered that the product of input impedances of a planar electric current antenna (plate) and its corresponding "magnetic current" antenna was the real constant $\frac{\eta^2}{4}$, where η is the intrinsic impedance of free space. Hence, if an antenna is its own complement, the frequency independent impedance behavior is obtained. In Fig. 1.2 (a), if the lengths W and S are the same, i.e., the metal and the air regions of the antenna are equal; the spiral antenna is self-complementary. Fig. 1.2 (d) shows the geometry of a logarithmic spiral antenna.

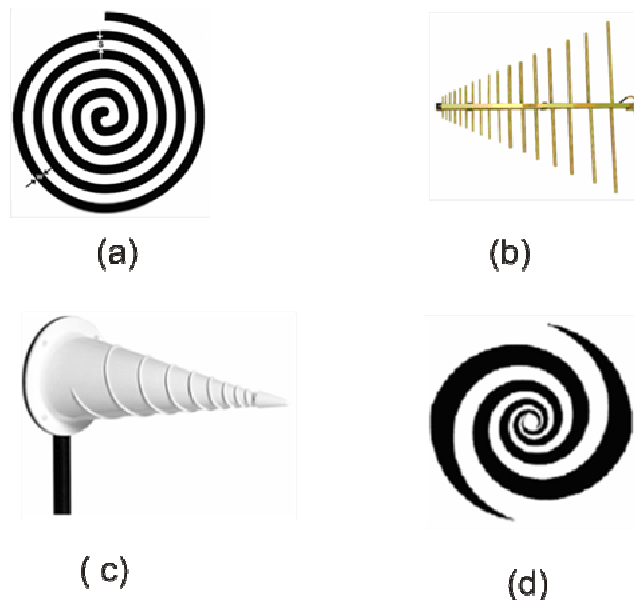


Fig. 1.2(a) Spiral antenna; (b) Log periodic antenna (SAS 510-7 from A.H. Systems Inc); (c) Conical spiral antenna; (d) Logarithmic spiral antenna.

Although the frequency independent antennas can operate over an extremely wide frequency range, they still have some limitations. Firstly, to satisfy Rumsey's requirement, the antenna configuration needs to be infinite in principle but, in practice, it is usually truncated in size. This requirement makes the frequency independent antennas quite large in terms of wavelength. Secondly, the frequency independent antennas tend to be dispersive because they radiate different frequency components from different parts of the antenna, i.e., the smaller-scale part contributes higher frequencies while the large-scale part accounts for lower frequencies. Consequently, the received signal suffers from severe ringing effects and distortions. Due to this drawback, the frequency independent antennas can be used only when the waveform dispersion may be tolerated.

1.4.2.2 Multi-resonant antennas

Multi-resonant antennas are composed of an arrangement of multiple narrowband radiating elements. This type of antenna includes log periodic antennas, Yagi antennas (Fig. 1.2(b)). Planar versions of these antennas also exist. Although these antennas are UWB, yet they are not convenient for IR-UWB systems because their phase centers are not fixed in frequency and therefore exhibit dispersion.

1.4.2.3 Travelling wave antennas

Travelling wave antennas include horn antennas, tapered slot antennas and dielectric rod antennas. These antennas feature a smooth and gradual transition between a guided wave and a radiated wave, and have good properties for UWB. Horn antennas constitute a major class of UWB directional antennas and these are commonly used for measuring radiation patterns or for ground penetrating radar applications. They consist of rectangular or circular waveguides which are inherently broadband. Their bandwidth is relatively large, i.e., 50% - 180%. These antennas present very good polarization, very low dispersion and

very low variation in phase center versus frequency. Fig. 1.3 (a) shows a double ridge horn antenna as an example.

The Tapered Slot Antenna (TSA) is another important class of UWB directional antennas. A typical TSA consists of a tapered slot that has been etched in the metallization on a dielectric substrate. The profile of tapering may take different forms: linear tapered slot antenna (LTSA), constant width slot antenna (CWSA), broken linearly tapered slot antenna (BLTSA) or exponentially tapered slot antenna (Vivaldi) as shown in Fig. 1.3 (b). The TSAs are adapted to a wide bandwidth of 125% - 170%. Their radiation pattern is unidirectional in the plane of the substrate and has a low level of cross-polarization. The directivity increases with frequency and the gains achieved by these antennas can go up to 10 dBi depending on the type of profile.

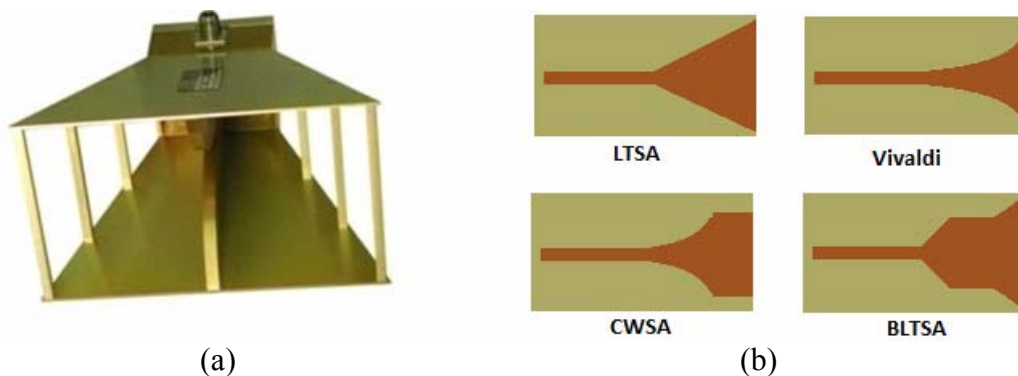


Fig. 1.3 (a) Horn Antenna – SA S571 A.H. Sys. Inc; (b) Tapered slot antennas.

1.4.2.4 Small element antennas

Small-element antennas include Lodge’s biconical and bow-tie antennas, Mater’s diamond dipole, Stohr’s spherical and ellipsoidal antennas, and Thomas’s circular dipole. These antennas are direct evolution of monopole and the basic dipole (doublet of Hertz). Antenna engineers discovered that, starting from a dipole or monopole antenna, thickening the arms results in an increased

bandwidth. Thus, for a thick dipole or monopole antenna, the current distribution is no longer sinusoidal and where this phenomenon hardly affects the radiation pattern of the antenna, there this strongly influences the input impedance too. This band widening effect is even more severe if the thick dipole takes the shape of a biconical antenna.

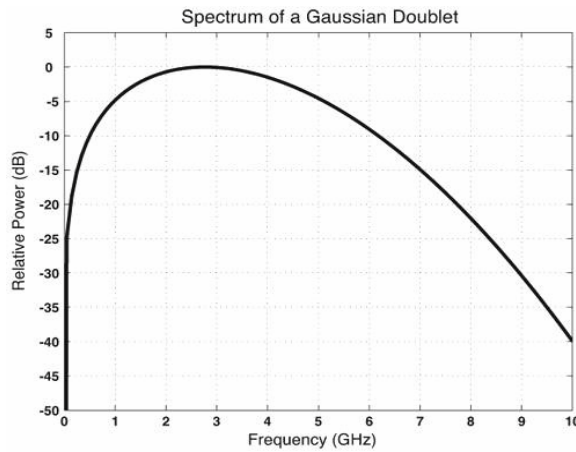
1.4.3 UWB Transmission Schemes

Although the FCC has regulated the spectrum and transmitter power levels for a UWB, there is currently no standard for a UWB transmission scheme. Various pulse generation techniques have been proposed to use the 7.5-GHz license-free UWB spectrum. Generally, UWB transmission approaches can be categorized into two main approaches: single-band and multiband. Figure 1.4 illustrates UWB signals in the time and frequency domains when single and multiband approaches are employed.

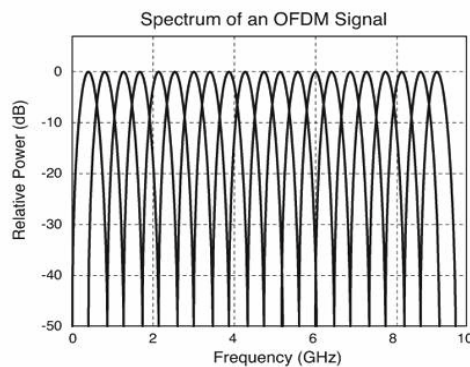
Essentially, UWB communications comes in one of two types,

Single Band: Impulse radio falls in the category of single band UWB system and is based on sending very short duration pulses to convey information. In impulse radio, the signal that represents a symbol consists of serial pulses with a very low duty cycle. The pulse width is very narrow, typically in nanoseconds. As a result it has a better resolution of multi path in UWB channels. The small pulse width gives rise to a large bandwidth as shown in Fig.1.4(a). The high instantaneous power during the brief interval of the pulse helps to overcome interference to UWB systems, but increases the possibility of interference from UWB to narrow band systems. Simple I-UWB systems can be very inexpensive to construct as it eliminates the need for up and down conversion and allows low-complexity transceivers.

Multi Band: Since UWB can be any technique that generates signals occupying at least 500MHz of bandwidth within the spectrum mask placed by FCC, the UWB systems can also be classified as multiband based. Here, the 7500MHz of unlicensed spectrum can be considered to provide a number of UWB “bands” as shown in Fig.1.4(b) and can be exploited in many ways like by using multi-carrier (MC) or OFDM modulation with Hadamard or other spreading codes. MC-UWB is particularly well-suited for avoiding interference because its carrier frequencies can be precisely chosen to avoid narrow band interference to or from narrow band systems.



(a) Spectrum of a Gaussian Monocycle-Based Impulse UWB Signal



(b) Spectrum of an OFDM-based MC-UWB Signal

Fig. 1.4: Comparison of (a) Impulse and (b) Multi carrier UWB spectrums.

Impulse radio faces the very important challenge of coexisting with existing narrowband systems. To mitigate the effects of narrow band interferers, notch filters are required in impulse radios. However, use of such filters may distort a received signal. Multi banded UWB on the other hand, can avoid transmitting on the frequency bands where other wireless systems like 802.11a are present by not using those frequency bands. This approach has the additional benefit of being able to adapt to the different regulatory requirements of various countries due to the flexibility of multi band allocation.

Short duration of the pulses in impulse radio presents several technical challenges as well. The generation of pulses that fit into the spectral mask imposed by regulatory bodies is difficult and their short duration makes them more susceptible to timing jitter. Supporting higher data rates will involve increasing the pulse PRF either by using higher-order modulation or by using spread spectrum technology. The first option makes the system more vulnerable to ISI. The second would increase the peak-to-average power ratio and impose greater linearity requirements on the circuits. The last option requires careful selection of the properties of the codes.

In multi banded UWB, the pulses are not as short. So, the PRF can be lower than that of impulse radio at the same peak power, diminishing the effects of ISI and timing jitter. This approach also eases the requirements of pulse shaping filters and avoids the use of notch filters. Scaling can be achieved by simply adding more bands. Furthermore, more multiple access schemes like FDMA and CDMA are available.

The longer duration of the pulses in a multi banded system lead to milder ISI and equalization requirements, but may also require the suppression of adjacent channel interference. In addition, the number of resolved multipath

components increases as the bandwidth increases. Thus, the number of rake fingers needed for the impulse-based approach is around ten times more than the multi banded approach for a given Signal to Interference Ratio (SIR), leading to a more complex receiver.

These challenges faced by impulse radios have made UWB solution providers and developers to look toward to a multiband approach for their systems. This approach has much greater flexibility in coexisting with other wireless systems and is based on more conventional technology.

1.4.4 UWB regulation and standards

In USA, the FCC approved a UWB spectral mask specified 7.5 GHz of usable spectrum bandwidth between 3.1 GHz and 10.6 GHz for communication devices and protected existing users operating within this spectrum by limiting the UWB signal's EIRP level of -41.3 dBm/MHz (known as Part 15 Limit). In this restriction, the limitation of the power spectral density (PSD) measured in a 1 MHz bandwidth at the output of an isotropic transmit antenna to a spectrum mask is shown in Figure 1.5 for indoor and outdoor environments, respectively.

The FCC issued in April 2002 UWB Regulations, under Part 15 of the Commission's rules, permitting ultra-wideband intentional emissions subject to certain frequencies and power limitations that will mitigate interference risk to those sharing the same spectrum. UWB signals may be transmitted between 3.1 GHz and 10.6 GHz at power levels up to -41 dBm/MHz, with higher degree of attenuation required for the out of band region for outdoor communication.

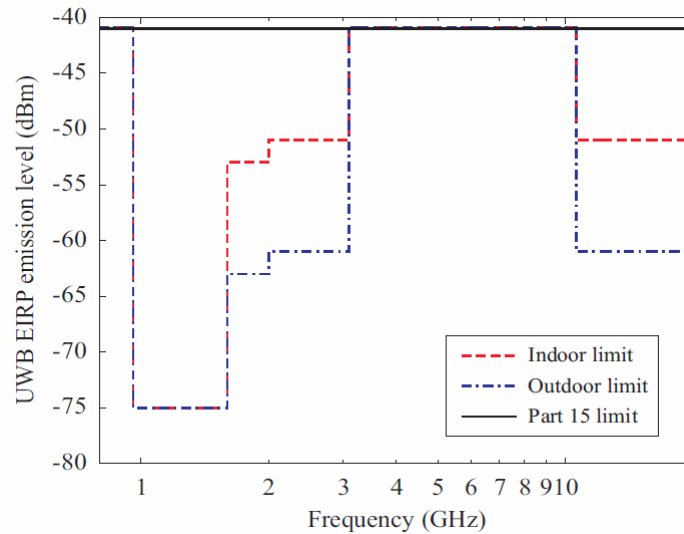


Fig.1.5 FCC Spectrum Mask for Transmissions by UWB Communication Devices

Although UWB currently is legal only in the United States, international regulatory bodies are considering possible rules and emission limits that would help it enable worldwide operation of UWB devices. Fig.1.6 shows the graph of the worldwide spectrum mask that is defined now for UWB communication devices. There is difference in EIRP levels among USA, Europe, Japan and Singapore. In some countries, there is an exclusive obligation to protect the existing communication systems. Countries that have a sole obligation to protect existing users tend to be much more conservative in international for a that are designed to achieve spectrum harmonization, such as the international Telecommunication Union (ITU). Therefore, it is extremely necessary to gain compromises and agreement among all of them for making the international UWB policy because UWB is not only a new technology but also a new regulatory paradigm. In the processes of the compromise for UWB policy, there are two useful technologies to prevent the interference with other signal. One is Detect and Avoid (DAA) and the other is Low Duty Cycle (LDC). The former

is a technology to mitigate interference potential by searching for broadband wireless signals and then automatically switching the UWB devices to another frequency to prevent any conflict. The latter reduces interference with other signal by using the UWB signal with very low duty cycle.

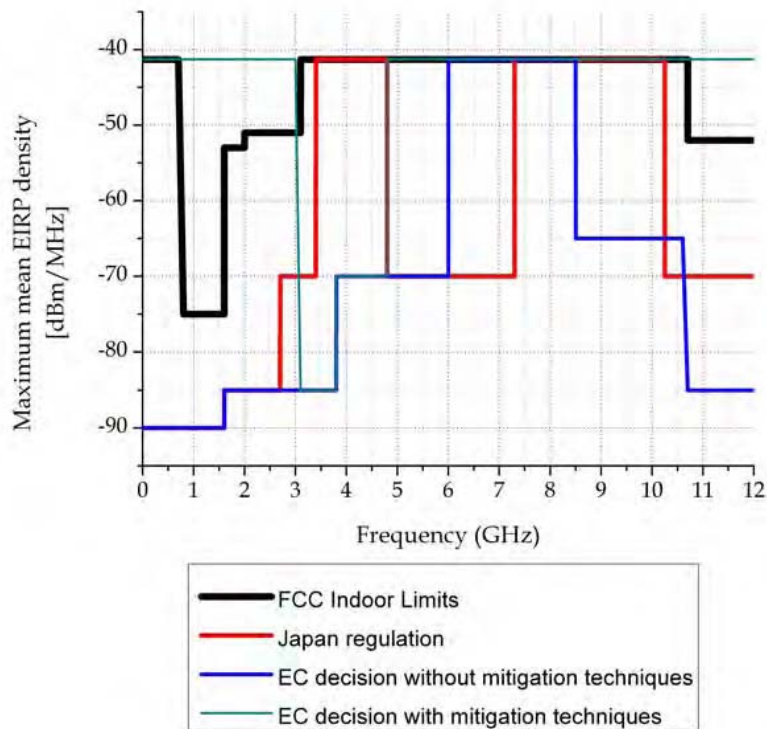


Fig. 1.6 The worldwide spectrum masks for UWB communication devices

1.4.5 Advantages and Limitations of UWB

The main advantages and benefits of UWB systems can be summarized as follows:

In military communications, there are many potential threats about the security of the signal. Ultra wideband signals are usually at noise floor level due to the very large spreading factor. Therefore they provide low probability of detection for military communication and cannot be detected using conventional receivers.

Also, UWB signals immune to jamming and interference from other radio systems because of the large spreading factor.

In UWB communication system, the pulses can easily penetrate walls, doors, and other objects. Since UWB signals contain significant low frequency components, it has the ability to penetrate materials that are normally more resistive to higher frequencies.

The extremely high transmission bandwidth of an UWB signal provides very accurate timing information to be resolved. Accurate range measurements and positioning can be achieved due to the resolving capability of multipath. This ability combined with the penetration through materials makes UWB suitable for accurate positioning applications.

Multiple users can transmit simultaneously on the same frequency range as long as they use different spreading codes. Due to the very large spreading gain of UWB systems, it can enable multiple access capability and a large number of users can be fitted in a UWB system.

Since the UWB technology is the transmission and reception of baseband signals, its complexity is relatively low and it provides inexpensive implementation compared to conventional narrowband systems. UWB systems do not require RF modulators and demodulators in the transmitter and receiver design. The absence of RF & IF stages, linear amplifiers, and the required filters reduces the complexity and the cost of the system.

Another advantage of UWB transmission for communications is its high data rate. Higher data rates can enable new applications and devices. The extremely large bandwidth occupied by UWB gives this potential.

The main disadvantages and limitations of UWB systems can be summarized as follows:

UWB antennas need to be optimized over a wide range of frequencies such that the antennas employed in UWB systems are required to efficiently radiate electromagnetic signals over several gigahertz bandwidth. This makes the design procedure more complicated than for other conventional narrowband antennas. The transmission range of an UWB radio is very limited without use of a power amplifier. Designing small-size, efficient wideband power amplifiers and directional antennas is still a challenge even though medium-range communications using low-power UWB signals is claimed to be possible.

Since UWB extends over an extremely wide bandwidth, many other wireless systems would be affected and need to be convinced that UWB will not cause too much interference to their existing services. Although it has been claimed that the interference between UWB and other systems is minimal, a large amount of UWB transmissions could still cause a problem for systems such as GPS. Moreover, if higher power UWB signals are used for longer range transmissions, the interference problem may arise.

1.4.6 UWB Applications

FCC's First Report and Order permits the marketing and operation of certain type of new products incorporating ultra-wideband technology. Depending on the operational characteristics and the potential for causing interference to other services, each system is allowed to operate in their allocated frequency bands. According to these restrictions, the FCC report categorizes UWB devices into following categories: imaging systems, communications and measurement systems, and vehicular radar systems.

Ground penetrating radar systems (GPRs), wall imaging systems, through wall imaging systems, and medical systems can be included in the imaging systems.

GPRs are used for detecting the buried objects. The operational frequencies are required to be below 960 MHz or in between 3.1-10.6 GHz. Law enforcement, fire and rescue, scientific research institutions, mining companies, and construction companies are placed in this category.

Medical systems are used for health care applications to observe the location or movement of objects inside the body of a human or animal. These systems must operate in the frequency band 3.1-10.6 GHz. Operation must be carried out under the guidance of licensed health care practitioners.

Communication and measurement systems include devices that are subject to certain frequency and power limitations under the Part 15 of the FCC's rules. UWB high-speed home and business networking devices, storage tank measurement can be included in this group. The operational frequency band is 3.1-10.6 GHz.

Vehicular radar system devices are used to detect the location and movement of objects near a vehicle. They operate in 24 GHz band using directional antennas on terrestrial transportation vehicles. The center frequency of the emission and the frequency at which the highest radiated emission occurs are greater than 24.075 GHz.

1.5 Motivation for the work

The UWB technology has undergone remarkable achievements during the past few years. In spite of all the promising prospects featured by UWB, there

are still challenges in making this technology fulfill its full potential. One particular challenge is the UWB antenna.

In recent years, many varieties of UWB antennas have been proposed and investigated. They present a simple structure and UWB characteristics with nearly omni-directional radiation patterns. However, for some space-limited applications, UWB antennas need to feature a compact size while maintaining UWB characteristics. Therefore, miniaturization of UWB antennas becomes an interesting research topic and deserves a comprehensive investigation and analysis.

The issues concerning interference between wide band devices with other existing narrow band communication networks can be sorted by implementing filters to notch out the required frequency bands. However, since additional filters would increase the size of the devices, embedded filters on the antenna is preferred.

Consumer electronics like wireless USB & next G bluetooth applications requires narrow planar antennas with a width of ≈ 11 to 24mm. However, with the reduction of antenna size, impedance bandwidth degrades. Since compact antennas show significant ground plane length/shape effects on its performance, it is important to design antennas resistant to it. The conflicting requirements of good performance and compact size make the design of such antennas challenging.

The aim of the thesis is to investigate the requirements for a wide band behavior of compact planar antenna designs. This work looks in detail the wide band performance of the monopole and slot antennas and identifies the design parameters of the same. Several novel designs on commercially available

microwave substrates are proposed that could be successfully implemented in consumer electronics applications. It is important to characterize the designed UWB antennas in terms of their transient performance. To throw light on their suitability for pulse communications, their time-domain behavior is studied in the final part of the thesis.

The shortcoming of the planar antenna designs, usually reported, is that they are based on the lengthy trial and error method that involves computationally intensive full wave electromagnetic simulations. When one decides to design an antenna using a different dielectric substrate, the time consuming design process has to be fully repeated. In such circumstances, the designers are interested in having simple design formulas that provide a very good approximation to the final design when sophisticated EM analysis and design software packages are applied. This thesis addresses this issue and provides simple design formulas, which are suitable for the antennas designed. It is shown that the antenna design parameters obtained using the equations developed in this thesis do not differ much from the optimized values obtained using the commercial software.

1.6 Thesis Organization

Chapter 1 gives the introduction of the thesis. This chapter gives basic information about UWB technology and also the history of research in the field of UWB antennas. The motivation of the work and thesis organization is also included in this chapter.

Chapter 2 starts with the methodology used for developing the antennas reported in this thesis. Measurements in the frequency domain such as return loss, radiation pattern, gain are explained. The relevant theory behind the time domain characterization of the antenna, are deduced from the measurements,

are explained. Then a detailed literature review about monopole UWB antennas is conducted.

Chapters 3 & 4 concentrate on UWB Monopole and Slot antennas respectively. In this section, a common approach is followed for the antenna development. The chapters begin with a detailed literature review of the available designs belonging to this broad category, followed by a description on the evolution of the antennas. The proposed antenna designs are simulated and their resonant modes are identified. The antennas are CPW-fed for easy fabrication and better integration with monolithic microwave circuits except in some cases where it is microstrip-feed. The surface current and field distributions on the antenna at the resonant modes and their corresponding radiation patterns are analyzed in detail.

The results of the analysis along with the parametric studies have enabled to deduce their design equations and design methodologies on any substrate for the desired operating frequencies. The measured results of the fabricated antennas are then plotted with their corresponding simulated results which are found to conform well in all cases. Further, to notch out selected narrow band frequencies in the wide operating band, thin slot resonator is embedded in the serrated monopole antenna.

There are two novel compact designs of planar monopole antennas presented in chapter 4: a ground modified antenna and a serrated antenna. These antennas perform well in terms of its impedance match and gain, over a wide band and easily comply with the FCC UWB frequency band of 3.1 to 10.6GHz. The radiation patterns are omni-directional but in case of ground modified antenna they are distorted at the higher end of the spectrum. This is overcome a little bit by the serrated antenna which has the advantage of a compact size as

well. A band notched serrated antenna to notch out the 5.8GHz WLAN band by etching a inverted U slot from the patch is also presented. Electronic reconfiguration of the notch band by integrating a PIN diode across $\lambda/2$ inverted 'U' slot is also demonstrated. A CPW fed serrated monopole antenna is also developed and presented.

The triangular slot antenna developed in chapter 4 overcomes the problem of pattern deterioration at higher frequencies observed in the case of monopole antennas. Antenna structure is compact and covers the FCC specified UWB band. To reduce the interference with the conventional WLAN, a notch band is also introduced.

In the final sections of chapters 3&4, the influence of the antenna on radiation of a UWB pulse to confirm their suitability for I-UWB applications is investigated. The transfer function measurements are performed in the azimuthal plane and their impulse responses are deduced. The influence of the antenna on pulse transmissions is evaluated by convoluting the impulse response with a UWB pulse. The time domain distortions for the different designs are then characterized in terms of mathematically tractable parameter Fidelity.

Finally the thesis is concluded in Chapter 5, by compiling the overall work and their results along with a brief description on the scope for future study.

References

- [1] “IEEE Standard Definitions of Terms for Antennas”, IEEE Std 145-1993, ISBN: 1-55937-317-2, USA.
- [2] K.Fujimoto and J.R.James, ”Mobile Antenna Systems Handbook”, Artech House, 1994.
- [3] M.E Bialkowski, “Wireless: From Marconi – The Way Ahead”, IWTS 1997, Shah Alum, Malaysia,1997.
- [4] T.S. Rappaport, “Wireless Communications, Principles and Practice”, Prentice Hall, 1996.
- [5] S. Uda, “Wireless Beam of short electric waves”, J. IEE (Japan), pp. 273-282, March 1926 and pp. 1209-1219, Nov. 1927.
- [6] W.V. T. Rusch, “The current State of the Reflector Antenna Art-Entering the 1990’s”, Proc. IEEE, vol. 80, No.1, pp. 113-126, Jan. 1992.
- [7] V. H. Rumsey, “Frequency Independent Antennas”, 1957 IRE National Convention Record, Part 1, pp. 114-118.
- [8] G.A. Deschamps, “Microstrip Microwave Antennas”, presented at the Third USAF symposium on Antennas, 1953
- [9] F.K. Schwering, “Millimeter wave antennas”, Proc. IEEE, vol. 80, No.1, pp. 92-102.
- [10] Richard W. Ziolkowski and Aycan Erentok, “Metamaterial-Based Efficient Electrically Small Antennas”, IEEE Transactions on Antennas and Propagation, Vol. 54, No. 7, July 2006.

-
- [11] Walter, C.H. (1990), "Traveling Wave Antennas", Peninsula Pub, ISBN: 0-9321-4651-1.
- [12] Agrawal, P. Kumar, G Ray & K.P, "New Wide-Band Monopole Antennas, Proceedings of IEEE International Symposium on Antennas and Propagation", pp. 248-251, ISBN: 0-7803-4178-3, Montréal, Québec, July 1997.
- [13] Ammann, M.J. & Chen, Z.J,"Wideband monopole antennas for multiband wireless systems", IEEE Antennas and Propagation Magazine, Vol. 45, () 5 , ISSN: 1045-9243, April 2003.
- [14] Islam, M.T.; Shakib, M.N.; Misran, N. & Sun, T.S "Broadband Microstrip Patch Antenna", European Journal of Scientific Research, Vol. 27, No. 2, ISSN: 1450-216X,2009.
- [15] Mitola,J,"The Software Radio Architecture", IEEE Communications Magazine, Vol. 33, No. 5, ISSN: 0163-6804, May 1995.
- [16] Mitola, J. & Maguire, G.Q, "Cognitive Radio: Making Software radios More Personal", IEEE Personal Communications, Vol. 6, No. 4, ISSN: 1070-9916, August 1999.
- [17] "Specifications of the Bluetooth System", Version 1.0B, 1999. <http://www.bluetooth.com> (Accessed on March 4th 2004).
- [18] N.J. Muller, "Bluetooth Demystified", New York, Mc Graw Hill, 2001.
- [19] FCC, "Revision of Part 15 of the Commission's Rules Regarding Ultra-Wideband Transmission Systems", ET-Docket 98-153, <http://www.fcc.gov/oet/dockets/et98-153>,2004.
- [20] CEPT Euro," Radio communication Committee Workshop On Introduction of UWB Services in Europe", RegTP, Mainz, Mar. 20, 2001; [http://www.ero.dk/ERCWGActivities/ Short-Range Devices](http://www.ero.dk/ERCWGActivities/Short-Range%20Devices), 2004.

- [21] “FCC First Report and Order, Revision of the Part 15 Commission’s Rules Regarding Ultra-Wideband Transmission Systems”, pp. 98–153, April 22, 2003.
- [22] P.Smyth, “Ultra-wideband and its capabilities. In Mobile and Wireles Communications, Key Technologies and Future Applications, BT Communication Technology Series 9”,pp.81–100. The Institution of Engineering and Technology, London, UK, 2004.
- [23] Ghavami, M., Michael, L.B., and Kohno, R,” Ultra Wideband Signals and Systems in Communication Engineering”, John Wiley & Sons, England, 2004.
- [24] Weightman, G,”Signor Marconi’s Magic Box: The Most Remarkable Invention of the 19th Century and the Amateur Inventor Whose Genius Sparked a Revolution”, da Capo Press, 2003.
- [25] Molisch, A.F “Introduction to UWB Signals and Systems”, B. Allen, M. Dohler, E. Okon, W. Malik, A.Brown, D. Edwards, Ultra Wideband Antennas and Propagation for Communications, Radar and Imaging, John Wiley & Sons, 1-17, 2006.
- [26] QUI, R. “Propagation Effects”, M.G.Di Benedetto et al., (ed.), “UWB Communications Systems”: A Comprehensive Overview, EURASIP publishing, 2005.
- [27] MOLISCH, A.F, Introduction to UWB Signals and Systems, B. Allen, M. Dohler, E. Okon, W. Malik, A.Brown, D. Edwards, “Ultra Wideband Antennas and Propagation for Communications”, Radar and Imaging, John Wiley & Sons, 1-17, 2006.

- [28] HARMUTH H.F, “Nonsinusoidal Waves for Radar and Radio Communication”, Academic Press, New York,1981.
- [29] Scholtz, R.A., Pozar, D.M., Namgoong.W,”Ultra-Wideband Radio, EURASIP Journal on Applied Signal Processing”, vol. 3: 252-2722005.
- [30] “Federal Communications Commission. First report and order, revision of Part 15 of commission’s rule regarding ultra-wide band transmission systems”, FCC 02-48, 2002.
- [31] Schantz, H.G “A Brief History of UWB antennas, Proceedings of IEEE Ultra Wideband Systems and Technologies Conference”, pp. 209-213, ISBN: 0-7803-8187-4, Virginia, USA, November 2003.
- [32] Schantz, H.G., The Art and Science of Ultra-Wideband Antennas, Artech House Publisher, ISBN: 1-5805-3888-6, England,2005.
- [33] Wiesbeck, W. & Adamiuk, G. “Antennas for UWB Systems, Proceedings of International ITG Conference on Antennas, pp. 66-71, ISBN: 978-3-00-021643-5, Munich, Germany, March 2007.
- [34] Chang, D.C, “UWB Antennas and Their Applications, Proceedings of International Workshop on Antenna Technology: Small Antennas and Novel Metamaterials, pp. 14-19, ISBN: 978-1-4244-1522-9, Chiba, Japan, May 2008.
- [35] Akdagli, A.; Ozdemir, C.; Yamacli, S,” A Review of Recent Patents on Ultra Wide Band (UWB) Antennas”, Recent Patents on Electrical Engineering, Vol. 1, No. 1, 8 (68-75), ISSN: 1874-4761, January 2008.



METHODOLOGY AND LITERATURE REVIEW

<i>Contents</i>	<i>2.1 Antenna Fabrication</i>
	<i>2.2 Antenna measurement facilities</i>
	<i>2.3 Antenna Characterization</i>
	<i>2.4 Ansoft HFSS- The CAD tool</i>
	<i>2.5 Time domain antenna analysis</i>
	<i>2.6 Pulse Distortion Analysis: Fidelity Factor</i>
	<i>2.7 Effective Isotropically Radiated Power (EIRP)</i>
	<i>2.8 Monopole Uwb Antennas-Review</i>
	<i>2.9 Chapter Conclusion</i>

This chapter provides the experimental and simulation methodology utilized for the analysis of antennas described in this thesis. The prototypes of different antenna were fabricated using photolithographic process and the antenna characterization was done using Vector Network Analyzer in the anechoic chamber. Parametric analysis of different antenna parameters was carried out using Ansoft HFSS. A detailed account of the measurement techniques, for frequency and time domain studies, are presented in this chapter. A review of literature about monopole antennas is also conducted.

2.1 Antenna Fabrication

The accuracy of the antenna dimension is very critical at microwave frequencies. Therefore photolithographic technique is used to fabricate the antenna. Photolithography is the process of transferring geometrical shapes from a photo-mask to a surface.

The CAD drawing of the antenna is printed on a high quality butter paper with a high resolution laser printer. The copper clad of suitable dimension is cleaned with a suitable chemical like acetone to remove any impurities. A thin layer of photo resist material is then applied over the copper clad using a high speed spinner. The antenna mask is carefully aligned over the photo resist coated clad and exposed to UV. Extreme care must be taken to ensure that no dust or impurities are present in between the mask and copper clad. The layer of photo resist material in the exposed portions hardens, while the unexposed region remains unaffected and it can be removed by carefully rinsing with a suitable developer solution. The unwanted copper over the copper clad can be removed by processing the copper clad in a ferric chloride (FeCl_3) solution. The laminate is then cleaned to remove the hardened photo resist using acetone solution.

2.2 Antenna measurement facilities

A brief description of equipments and facilities used for the measurements of antenna characteristics is presented in this section.

2.2.1 HP 8510C Vector Network Analyzer

The HP 8510C series microwave vector network analyzers provide a complete solution for characterizing the linear behavior of either active or passive networks over the 45 MHz to 50 GHz frequency range [1]. The network analyzer measures the magnitude, phase, and group delay of two-port networks

to characterize their linear behavior. The analyzer is also capable of displaying a network's time domain response to an impulse or a step waveform by computing the inverse Fourier transform of the frequency domain response.

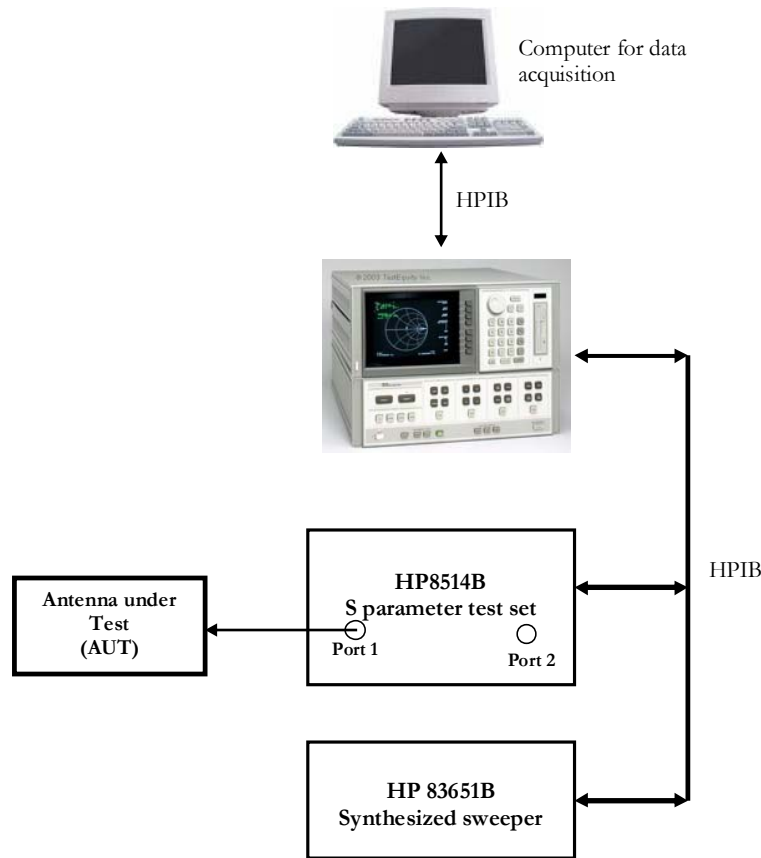


Fig.2.1. Block diagram of HP8510C Vector Network Analyzer

The HP 8510C network analyzer comprises of a microwave generator, S-parameter test set, signal processor and the display unit as depicted in fig. 2.1. The synthesized sweeper generator, HP 83651B, uses an open loop YIG tuned element to generate the RF stimulus. The frequencies can be synthesized in step mode or ramp mode, depending upon the desired measurement accuracy. The antenna under test is connected to the two-port s-parameter Test unit, HP8514B. This module

isolates the incident, reflected and transmitted signals at the two ports. The signals are then down converted to an intermediate frequency and fed to the IF detector. These signals are suitably processed to display the magnitude and phase information of S-parameters in log-magnitude, linear-magnitude, or Smith chart formats. All these constituent modules of the network analyzer are connected using the HP1B system bus. A completely automated data acquisition is made possible using the HP-BASIC based MERLSOFT, developed indigenously at the Center for Research in Electromagnetics and Antennas (CREMA), Department of Electronics, Cochin University of Science and Technology.

2.2.2 Anechoic Chamber

The Anechoic chamber is a room used to measure the antenna characteristics accurately [2]. The room consists of microwave absorbers fixed on the walls, roof and floor to avoid EM reflections. High quality low foam impregnated with dielectrically magnetically lossy medium is used to make the microwave absorber. The tapered shapes of the absorber provide good impedance match for the microwave power impinging upon it. Aluminium sheets are used to shield the chamber from electromagnetic interference from surroundings.

2.2.3 Turn table assembly for far field radiation pattern measurement

A turntable assembly consists of a microcontroller based antenna positioner, interfaced with the PC for the radiation pattern measurement. The antenna under test (AUT) is mounted over the turntable assembly and a linearly polarized; wideband standard horn antenna is used as the transmitter for the radiation pattern measurement. The main lobe tracking for gain measurement as well as the polarization pattern measurement are carried out through this setup. The matlab based graphical user interface (GUI) manages the antenna characterization by synchronizing each component in the system.

2.3 Antenna Characterization

The major antenna characterization procedures are depicted in the following sessions.

2.3.1 Return loss Measurement

In order to measure the return loss characteristics of the antenna under test, the test antenna is connected to any one of the network analyzer ports and operating the VNA in S_{11} or S_{22} mode. The specific port of the analyzer should be calibrated for the frequency range of interest using the standard open, short and matched load, prior to the measurement. The S_{11} values of the antenna in the entire frequency band are then stored in a computer in Comma Separated Variable, “CSV”, format with the help of “CREMA SOFT”-the indigenously developed measurement automation software. The frequency at which the return loss value minimum is taken as the resonant frequency of the antenna. The range of frequencies for which the return loss value is within the -10dB points is usually treated as the band width of the antenna.

2.3.2 Efficiency Measurement:

The IEEE definition of the antenna efficiency is the ratio of total radiated power to the net accepted power by the antenna at its terminals during the radiation process [3]. A more reasonable definition would include the reflected power due to mismatch as an explicit loss and radiation efficiency is defined as the ratio of the total power radiated by the antenna to the net power applied at its terminals.

A method for assessing the efficiency over the UWB, that explicitly include mismatch reflected power as a loss term, is presented in [4]. This method is a modification of the Wheeler Cap method conventionally used to

measure radiation efficiency of narrow band antennas. Rather than inhibiting radiation efficiency from the antenna to a radiation sphere with radius $r = \lambda/2\pi$ as in the narrow band approach, UWB Wheeler Cap method allows the antenna to radiate freely and then receive its own transmitted-reflected signal.

The power budget for a transmit antenna may be expressed in terms of power fractions. A fraction of the incident energy is dissipated in losses ($l = P_{\text{loss}}/P_{\text{in}}$), a fraction is reflected away due to mismatch ($m = P_{\text{refl}}/P_{\text{in}}$), and a fraction is radiated ($\eta = P_{\text{rad}}/P_{\text{in}}$). Averaging over a suitable time interval and applying conservation of energy yields:

$$l + m + \eta = 1 \text{ ----- (2.1)}$$

The spherical shell surrounding the AUT enforces a near ideal time reversal of the transmitted signal. Thus the antenna receives the reflected signal with negligible structural scattering, and the antenna mode scattering term is simply the mismatch fraction ($m = |S_{11} - F_s|^2$). The receive and transmit efficiencies (η) are identical by reciprocity. The scattering coefficient inside the UWB Wheeler Cap becomes:

$$\begin{aligned} |S_{11} - F_s|^2 &= m + \eta^2 + \eta^2 m^2 + \eta^2 m^2 + \eta^2 m^2 \dots\dots\dots \\ &= |S_{11} - F_s|^2 + \eta^2 \sum_{n=0} |S_{11} - F_s|^{2n} \text{ ----- (2.2)} \\ &= |S_{11} - F_s|^2 + \eta^2 \frac{1}{1 - |S_{11} - F_s|^2} \end{aligned}$$

$$\eta = \sqrt{(1 - |S_{11} - F_s|^2) \left((|S_{11} - W_c|^2) - |S_{11} - F_s|^2 \right)} \text{ ----- (2.3)}$$

For measurements, an oblate metallic chamber with diameter 70cm is used. First, the AUT is placed in free space and the return loss $S_{11}-F_s$ is measured. It is then placed at the center of the closed metallic chamber and the $S_{11}-W_c$ is measured. Finally, eqn.(2.3) is employed to calculate the radiation efficiency. The measurement is repeated several times and the average value at discrete frequency intervals is computed.

2.3.3 Radiation Pattern Measurement.

The radiation pattern measurement is carried out in the anechoic chamber with the help of HP 8510C VNA. The antenna under test is mounted on a turntable assembly in the anechoic chamber and connected to one port of the network analyzer configured in the receiver mode. The other port of the network analyzer is connected to a wideband horn which act as the transmitter. The network analyzer and the turntable controller are interfaced to a computer which runs the measurement automation software “CREMA SOFT”. The measurement automation software requires *the measurement band, start angle, stop angle angular step size and file name* as input. The system automatically undergoes THRU calibration prior to the measurement and performs the transmission measurement for each step angle and records the angular transmission characteristics in a data file.

2.3.4 Antenna Gain Measurement

Gain transfer method is employed to measure the gain of the antenna [5]. The experimental setup for determining the gain is similar to the radiation pattern measurement setup. The gain of the AUT is measured relative to the power levels detected by a standard gain antenna. In order to measure the gain of AUT, the standard gain antenna is mounted on the turntable and a THRU

calibration is performed at boresight direction. The AUT is again boresighted. The relative power level is obtained from the analyzer and this provides the gain with respect to the standard antenna. The gain of the standard antenna is added to the relative gain to obtain the gain of the AUT.

2.4 Ansoft HFSS- The CAD tool

Ansoft HFSS is one of the globally accepted commercial Finite Element Method(FEM) solver for electromagnetic structures [6]. The optimization tool available with HFSS is very useful for antenna engineers to optimize the antenna parameters very accurately. There are many kinds of boundary schemes available in HFSS. Radiation and PEC boundaries are widely used in this work. The vector as well as scalar representation of E, H and J values of the device under simulation gives a good insight in to the problem under simulation.

2.5 Time domain antenna analysis

UWB systems often employ short pulses to deliver information, in other words, enormous bandwidth is occupied. Therefore the influence of the antenna on the transmitted signal emerges as a vital issue. The antenna cannot be treated as a “spot filter” any more but a “band-pass filter”. In this regard, antenna parameters will have to be evaluated as functions of frequency and some elemental antenna parameters need to be re-addressed or re-assessed within the UWB definition scope and due to UWB’s unique features, it is essential to study UWB antennas from a time domain perspective. Ideally, the received UWB signal should maintain exactly the same shape as the source pulse. Practically, the signal waveforms reaching the receiver usually do not resemble the input pulse at the transmitter. The received signals normally are distorted in shape and sometimes present a long tail termed the “ringing effect”. The

antenna, therefore, should be carefully designed to avoid unwanted distortions and a time domain study of UW antennas is indispensable.

2.5.1 Behavior of UWB Antenna System

2.5.1.1 Description of UWB Antenna System

Consider a typical transmitting / receiving antenna system in UWB radio systems [7], as shown in figure 2.2.

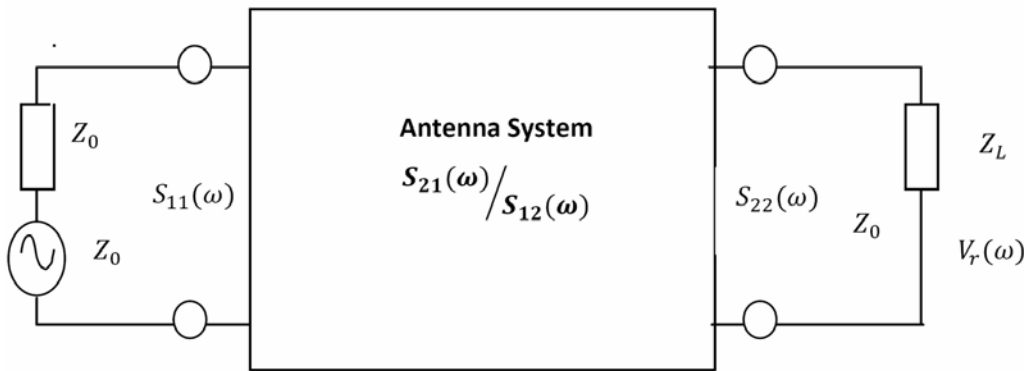


Fig. 2.2. Schematic diagram of UWB antenna system.

The Friis Transmission Equation relates the received power to the transmitted power between two antennas [8], as given in equation 2.4.

$$\frac{P_r}{P_t} = (1 - |\tau_t|^2)(1 - |\tau_r|^2) G_t G_r |P_t^{\wedge} P_r^{\wedge}|^2 \left(\frac{\lambda}{4\pi d} \right)^2 |P_t^{\wedge} P_r^{\wedge}|^2 \text{-----} (2.4)$$

where P_t , P_r : time average input power of the transmitting antenna and time average output power of the receiving antenna; Γ_t , Γ_r : reflection coefficient at the input of the transmitting antenna and the output of the receiving antenna; G_t , G_r : gain of the transmitting antenna and the receiving antenna polarisation match factor between the transmitting and receiving antenna; λ : operating wavelength; and d : distance between the two antennas.

As UWB systems operate over a huge frequency range, all of the parameters in equation 2.4 are frequency-dependent. The formula can be rewritten as follows

$$\frac{P_r(\omega)}{P_t(\omega)} = (1 - |\tau_t(\omega)|^2)(1 - |\tau_r(\omega)|^2) G_t(\omega) G_r(\omega) |P_t(\omega) P_r(\omega)|^2 \left(\frac{\lambda}{4\pi d}\right)^2 \quad \text{---(2.5)}$$

For reflection and polarisation matched antennas aligned for maximum directional radiation and reception, equation 2.5 reduces to:

$$\frac{P_r(\omega)}{P_t(\omega)} = \left(\frac{\lambda}{4\pi d}\right)^2 G_r(\omega) G_t(\omega) \quad \text{-----(2.6)}$$

The system transfer function, i.e. S_{21} , is defined to describe the relation between the source and the output signal. According to Fig. 2.2

$$\frac{V_t^2(\omega)}{2} = P_t(\omega) Z_0$$

$$\frac{V_r^2(\omega)}{2} = P_r(\omega) Z_0$$

So S_{21} is given by

$$S_{21}(\omega) = \frac{V_r(\omega)}{V_t(\omega)} = \sqrt{\frac{P_r(\omega) Z_L}{P_t(\omega) 4Z_L}} e^{-j\varphi(\omega)}$$

$$= |S_{21}(\omega)| e^{-j\varphi(\omega)}$$

$$\varphi(\omega) = \varphi_t(\omega) + \varphi_r(\omega) + \frac{\omega d}{c} \quad \text{-----(2.7)}$$

In equation 2.7, c denotes velocity of light $\varphi_t(\omega)$ and $\varphi_r(\omega)$ are the phase variation related to the transmitting and receiving antennas, respectively.

It is evident in equation 2.5 and equation 2.7 that the transfer function is determined by the characteristics of both transmitting and receiving antennas, such as impedance match, gain, polarisation match and the spacing between the two antennas. S_{21} also integrates all of the important system performance, such as path loss and phase delay. Thus, it can be used to assess the behaviour of antenna systems.

In addition, the system response can be fully determined when the transfer function is known. To reduce distortions in the received waveform, the transfer function should feature a flat magnitude and linear phase response across the operating band.

2.5.2 Group Delay

A good measure of the performance of a filter is its group delay, defined as the negative derivative of the filter phase with respect to frequency. When a signal passes through a device or medium, it experiences both amplitude and phase distortion. The amount of distortion depends on the characteristics of the device/medium. A waveform incident at the input of a filter may have several frequency components. The group delay gives an indication of the average time delay the input signal suffers at each frequency. Stated differently, this parameter gives an indication of the dispersive nature of the device.

Mathematically, the device response and group delay are given by:

$$H(f) = A(\omega) e^{j\theta(\omega)} \text{-----} (2.8)$$

$$\tau_g = \frac{-d\theta(\omega)}{d(\omega)}$$

If the device has a non-linear phase response, the group delay will vary with frequency causing the input signal to experience different delays at different frequencies. As a result, the output waveform is likely to be distorted. For a filter to be linear phase (have constant group delay), its phase response must satisfy one of the following relationships:

$$\theta(\omega) = -\alpha\omega; \theta(\omega) = \beta - \alpha\omega. \text{-----}(2.9)$$

It can be shown that in order to satisfy either one of the above conditions of linear phase, the impulse response of an FIR filter must have positive or negative symmetry [9]. The UWB antenna can be viewed as a filter with some magnitude and phase response. By representing the Rx/Tx antenna system as a filter, we can determine its phase linearity within the frequency band of interest by looking at its group delay. The phase response and group delay are related to the antenna magnitude (gain) response. For example, if there is a null in the magnitude, it implies a nonlinear phase, and therefore, a non-constant group delay. Unless there are large variations in the magnitude, it is difficult to determine the phase linearity by simply looking at the phase plots.

The group delay plot is able to clearly show any nonlinearity that may be present in the phase. The pulse input to the antenna system has an extremely large bandwidth and hence, any variation in group delay across the pass band of the transmitted pulse is likely to distort the pulse. To characterize the antenna, the peak to- peak variations of the gain and group delay within the 10dB bandwidth of the input pulse is determined.

Antennas are oriented in two extreme cases: face to face and side by side as in Fig.2.3 and their corresponding group delays are determined.

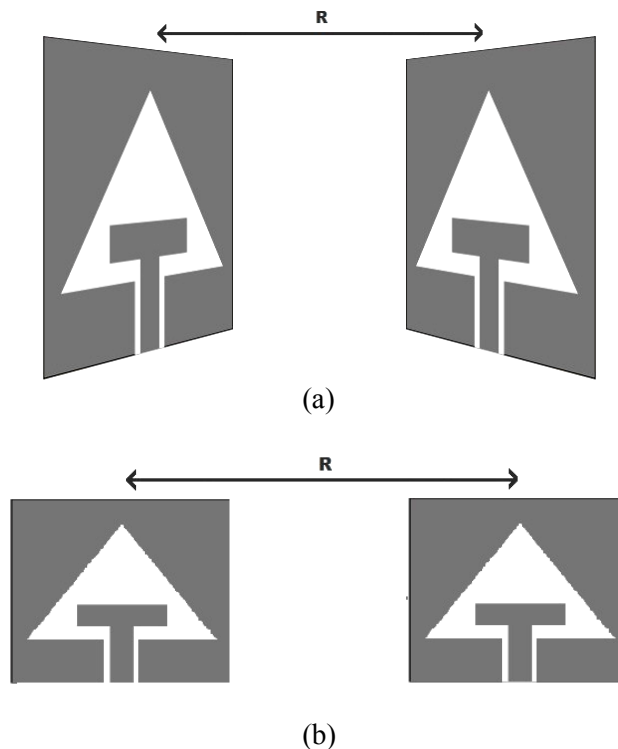


Fig.2.3. (a)Face to face and (b) side by side orientations of antennas

2.5.3 Choice of Source Pulse

In impulse radio, the signal that represents a symbol consists of serial pulses with a very low duty cycle. The pulse width is very narrow, typically in nanoseconds, and it can be any function which satisfies the spectral mask regulatory requirements. Several non-damped waveforms have been proposed in the literature for UWB systems, such as Gaussian, Rayleigh, Laplacian, cubic and modified Hermitian monocycles.

In all these waveforms, the goal is a nearly flat frequency domain spectrum over the bandwidth of the pulse with no DC component [10]. In principle, all the impulses with the spectra wider than 500MHz, stipulated by the FCC, can be used as signals. However, the choice of the pulse shape is a

key design decision in UWB systems. Given the stringent transmission power limitations, maximizing the received SNR requires efficient utilization of the bandwidth and power allowed by the FCC masks [11].

A Gaussian pulse has been the original proposal for UWB radar and communication systems [12]. However, its PSD has a direct current offset and hence will not radiate effectively. In addition, it does not fit in to the emission mask for any value of the pulse width.

One approach to the design of digital pulse shapers that comply with the FCC spectral masks is to employ prolate spheroidal wave functions to generate pulses from the dominant eigen vectors of a channel matrix that is constructed by sampling the spectral mask [13], [14], [15]. The pulses generated from different eigenvectors are mutually orthogonal, but require a high sampling rate that could lead to implementation difficulties.

Another possible solution for this is to shift the center frequency and adjust the bandwidth so as to satisfy the requirements. This could be done by modulating the monocycle with a sinusoid to shift the center frequency and by varying the pulse width. Impulse radio being a carrier less system, modulation will increase the cost and complexity.

Other pulse shaping methods include exploiting the properties of Hermite orthogonal polynomials [16], and fine-tuning higher-order derivatives of the Gaussian pulse [17].

Owing to unique temporal and spectral properties, a family of differentiated Gaussian pulses which resemble sinusoids modulated by a Gaussian envelope, $v_n(t)$, is widely used as the source pulses in the UWB systems.

$$V_n(t) = \frac{d^n}{d^n t} \left[e^{-2\pi \left(\frac{t}{\tau}\right)^2} \right] \quad (2.10)$$

where the pulse parameter σ stands for the time in radians when $v_0(\sigma) = e^{-1}$ as shown in Fig.2.4(a) and n is the order of differentiation. Some of the higher order derivative of gaussian pulses can match the UWB band directly, such as the fourth-order Rayleigh pulses as shown in Fig.2.4(b), with the σ chosen such that the pulse spectrum peaks at 5.5GHz. This is the waveform template chosen for pulse distortion analysis in this thesis. Note that the waveforms are shifted in X-axis for clearer distinction in Fig.2.4(a).

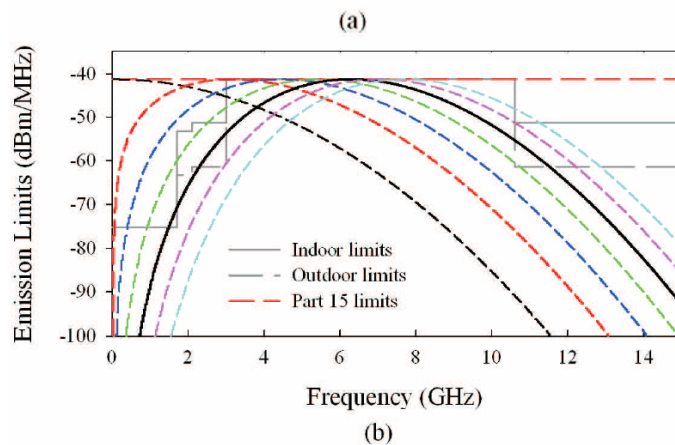
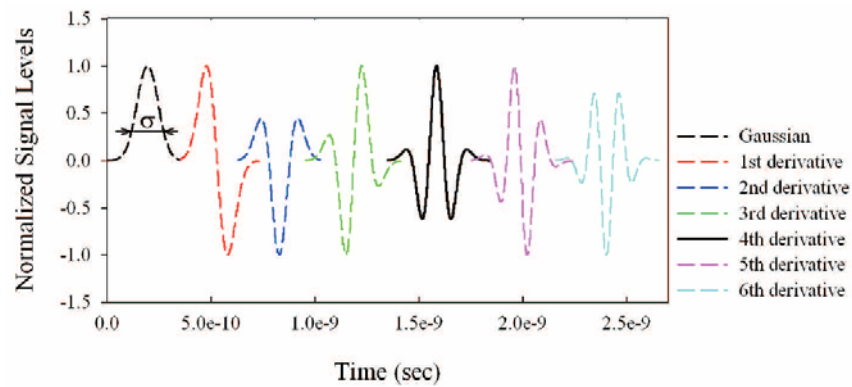


Fig.2.4 Gaussian pulse and its derivatives (a) waveforms in the time domain and (b) their power spectral densities.

2.5.4 Transfer function determination

The transfer function of the antennas are determined from the measured values of S_{21} in the frequency domain. Using two identical antennas oriented along various angles, the following relation is used to find the transfer function

$$H(\omega) = \sqrt{(2\pi R c S_{21}(\omega) e^{j\omega R/c}) / j\omega} \text{ ----- (2.11)}$$

Where $H(\omega)$ is the transfer function, c is the free space velocity and R is the distance between the two antennas. The measured transfer function is first transformed to time domain [$H(t)$] by performing the inverse fourier transform.

2.5.5 Implementation in MATLAB R•

The impulse responses are deduced from the measured transfer functions by taking their inverse fast fourier transforms (IFFT) but with certain precautions. The measured data used in this thesis is over a frequency range 2 to 12GHz. The data is complemented by zero padding for 0 to 2GHz and 12GHz to f_{max} . It is assumed that the antenna's response is so poor out of band that the data obtained is clearly dominated by noise and it might be advantageous to blank or zero data in those frequency ranges [18]. To correspond to the spectrum of a real signal, the conjugate of the zero-padded data is taken and reflected to the negative frequencies resulting in a spectrum which is symmetric around DC. The IFFT of the resulting measured data in frequency domain gives a real impulse waveform.

2.5.6 Received Signal Waveforms

For a UWB system, the received signal is desired to resemble the source pulse with minimum distortions. The received waveform is determined by both the source pulse and the system transfer function which has already considered

the effects from the entire system including the transmitting and receiving antennas.

The transfer function measured by the vector network analyser is a frequency response of the system. However, the frequency domain information can be transformed to the time domain. Here, Hermitian processing is used for the data conversion [19]. Firstly, the pass-band signal is obtained with zero padding from the lowest frequency down to DC (Direct Current). Secondly, the conjugate of the signal is taken and reflected to the negative frequencies. The resulting double-sided spectrum corresponds to a real signal, i.e. the system impulse response. It is then transformed to the time domain using Inverse Fast Fourier Transform (IFFT). Finally, the system impulse response is convolved with the input signal to obtain the received pulse.

2.6 Pulse Distortion Analysis: Fidelity Factor

Ideally, an impulse antenna should faithfully replicate the transmitted pulse on reception. But the changes in the phase center position and radiation characteristics alter the integrity of the transmitted pulses. The non-linearity in the antenna phase response leads to pulse dispersion. In addition, its radiation characteristics also have a significant impact on its performance. Any distortion of the signal in the frequency domain causes distortion of the transmitted pulse shape, therefore increases the complexity of the detection mechanism at the receiver.

The antenna gain should be smooth across the frequency band in order to avoid frequency selective distortion of the transmitted pulse. Since the antenna gain typically appears different from different angles, the shape of received pulse show spatial dependence [20].

From the spatio-temporal antenna impulse responses, we are able to calculate the pulse distortions introduced by the antenna along different orientations. These distortions are often quantized as the fidelity factor which is a measure of the faithfulness with which a device reproduces the time shape of the input signal. For UWB systems, the commonly used receivers are based on the pulse energy detection or correlation with the template waveform. Therefore we need to examine the pulse distortions by calculating the fidelity factor [21].

Fidelity factor F is defined by

$$F = \max_{\tau} \frac{\int x(t) \cdot \int y(t - \tau) dt}{\sqrt{\int |x(t)|^2 dt \int |y(t)|^2 dt}} \quad (2.12)$$

where τ is the delay which is varied to maximize the numerator. The fidelity parameter F , is the maximum of the cross-correlation function and compares only shape of the waveforms not the amplitudes. It is deduced from the measured and simulated data for different RX antenna orientations, with $y(t)$ as the incident and $x(t)$ as the received waveform [22].

To assess antenna performance as a system, we have considered a pair of the designed planar antennas. One antenna is assumed to be transmitting and the other receiving. The distance between the transmitting and the receiving antennas is 120cms of free space, which is more than 12 wavelengths at the lowest frequency of the considered band of operation i.e. the antennas are in the far field of each other.

2.7 Effective Isotropically Radiated Power (EIRP)

The ultimate goal of an indoor UWB communication system is to transmit and receive high speed data via a wireless link. This makes the study of

antennas an inevitable part of the system design. FCC spectral mask constrains the effective isotropically radiated power (EIRP) of the antenna rather than PSD of pulses before transmission. This requires some further study of the antenna effects on UWB pulses.

For an isotropic antenna the gain is identical in all directions, so that

$$G_T(f, \theta, \phi) = G_T(f)$$

where G_T is the transmit antenna gain, where Φ is the elevation angle and θ is the azimuth angle in the spherical coordinate system. The radiation power density is

$$\rho(f) = \frac{P_T(f)G_T(f)}{4\pi d^2}$$

over a sphere of radius d . $IRP(f)$ is the transmitted power density.

The radiated power of an isotropic antenna at a reference distance d_{ref} is

$$IRP(f) = d_{ref}^2 \int_0^{2\pi} \int_0^\pi \frac{P_T(f)G_T(f) \sin \theta d\theta d\phi}{4\pi d_{ref}^2}$$

For an arbitrary antenna, not necessarily isotropic, the FCC requires that on any point of the sphere at d_{ref} the radiated power should not exceed that of an isotropic antenna, hence the term EIRP.

$$\begin{aligned} IRP(f) &= \max_{\phi, \theta} P_T(f)G_T(f, \phi, \theta) \text{ ----- (2.13)} \\ &= P_T(f)G_T(f, \phi_0, \theta_0) \end{aligned}$$

where (Φ_0, θ_0) represents the direction of maximal gain.

For simplicity we will write $G_T(f)$ for the maximal gain of frequency f for any direction,

hence

$$EIRP(f) = P_T(f)G_T(f)$$

A general procedure for determining the EIRP per unit bandwidth is the use of the Friis power transmission formula in its simple form where antennas are assumed to be both impedance and polarization matched [23]

$$EIRP(f) = P_T(f)G_R(f) \left(\frac{c}{4\pi df} \right)^2 \text{-----} (2.14)$$

where $P_R(f)$ is the received power density, $G_R(f)$ is the receive antenna gain, c is the speed of light, d is the far field radial distance between the transmitter and the receiver and f is the frequency of operation. Equation (2.14) is valid for r larger than $2D_{\max}^2/\lambda$, where D_{\max} is the maximum dimension of the transmit antenna and λ is the free space wavelength. When D_{\max} is much greater than the wavelength, the far field criterion becomes very large and the field strength that must be measured at the far field location is less than the receiver noise floor. In such cases, the near field measurement techniques should be used for EIRP determination [24]. The dimensions of antenna and the maximum frequency of interest (10 GHz) in our case result in a reasonable far field distance where (2.14) is still valid. To obtain the EIRP, we use similar transmit (Tx) and receive (Rx) antennas and measure, using a network analyzer, the total frequency response of system,

$$H_{CH}(f) = \frac{P_R(f)}{P_T(f)}$$

This channel response, H_{CH} , includes free space propagation and transmit and receive antennas responses. The orientations of antennas are carefully adjusted so that they see each other with the same angle. Thus, for similar transmit and receive antennas (identical models), $G(f) = G_T(f) = G_R(f)$ and from (2.13) and (2.14) we have

$$H_{CH}(f) = \frac{P_R(f)}{P_T(f)}$$

$$EIRP(f) = \sqrt{H_{CH}(f)} \left(\frac{4\pi df}{c} \right) \text{-----} \quad (2.15)$$

Under the assumption no multipath reflections in the Friis formula. This condition can be created experimentally by attenuating the major reflections by placing RF absorbers around the antennas during H_{CH} measurement; all remaining multipath reflections are easily removed by truncating the channel impulse response. The truncated impulse response is then Fourier transformed and used in (2.15) for the EIRP calculation.

2.8 Monopole UWB Antennas-Review

The wire monopole is one of the most widely used antenna for wireless communication systems due to simple structure, low cost and omnidirectional radiation pattern. The bandwidth of a straight wire monopole is typically around 10% - 20%, depending on the radius-to-length ratio of the monopole. When the monopole radius is too large relatively to the feeding line, the impedance mismatch between them becomes significant and the bandwidth is limited. Finally, a method to obtain enhanced bandwidth is to replace the wire element with a plate which is obviously much "fatter". This plate can take various

configurations, such as triangle, circle, square, trapezoid, pentagon, hexagon, ellipse and so on (Fig.2.5).

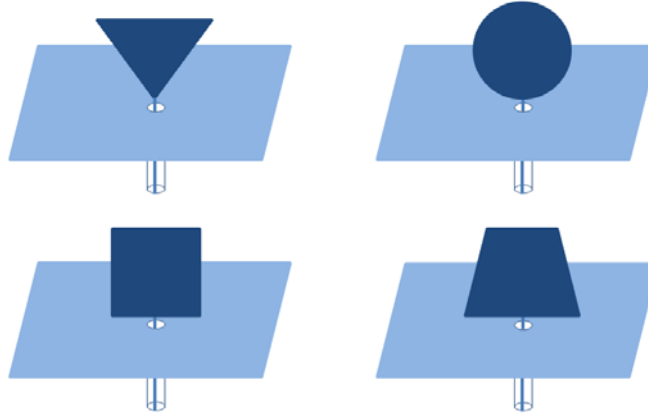


Fig. 2.5. Examples of triangle, circle, square and trapezoid monopoles.

Recent research focuses on antennas that can be easily integrated into other RF circuits or UWB devices. This triggered the scientists all over the world to intensify research on planar and printed UWB antennas. The printed monopole antennas offered wideband matching characteristic, omni directional radiation pattern and high radiation efficiency. Moreover, they are compact in size also. Many microstrip UWB antenna designs were proposed during the last decade. The planar radiators are etched onto the dielectric substrate. The ground plane may be either coplanar with the radiators or under the radiating element. The radiators can be fed by a microstrip line or coaxial probe.

The UWB printed monopole antenna consists of a monopole patch and a ground plane, both printed on the same or opposite side of the substrate. Compared with the ultra-wideband metal-plate monopole antenna, the UWB printed monopole antenna does not need a perpendicular ground plane. Therefore, the antenna consumes less volume and is suitable for integrating with monolithic microwave integrated circuits (MMIC). To broaden the

bandwidth of this kind of antennas, different monopole shapes have been developed. The UWB printed monopoles are more suitable for compact portable devices where volume is a significant factor. In such devices the main requirement for antennas is the capability to transmit a pulse with minimum distortion to preserve the shape of the pulse.

2.8.1 UWB Planar monopole antennas

The development of the planar antenna resulted in compact communication gadgets. The planar antennas are easy to integrate with the handheld communication devices while maintaining the radiation characteristics. Recent works in planar antenna are described below.

S. Honda et al. [25] presented a circular disk monopole antenna with 1:8 impedance band width and omni-directional radiation characteristics. M.Hammoud et al. [26] proposed a circular disc monopole antenna having a large band width. The antenna provides a broad band width of 2.25-17.25 GHz for VSWR<2.

Z. N. Chen presented [27] a new planar monopole antenna for broad band application. The antenna consists of a square parasitic planar radiator and a probe fed strip, which are separated by a thin dielectric slab. The electromagnetic coupling of the planar radiator improves the impedance characteristics of a conventional monopole antenna.

As mentioned above, broadband antennas have been used for many decades. In the past, traditional broadband antennas satisfied the requirements for commercial UWB systems. However, the UWB technology has gained more and more popularity and has become a good candidate for short-distance high-speed wireless communication since the approval of UWB by the FCC in 2002.

The proposed commercial UWB radio concept with its frequency 3.1 GHz to 10.6 GHz differs significantly from traditional wideband, short-pulse applications, such as radar. Furthermore, UWB antennas need different requirements due to its applications such as portable electronics and mobile communications. These requirements are not satisfied with the conventional UWB antennas. To satisfy different requirements like size, gain and radiation patterns, many novel antennas are proposed.

Although biconical antennas are attractive due to its broadband characteristics, they are so massive and impractical to use for compact electronic gadgets. Therefore, the modified planar structures of the biconical antennas are required. Most of monopole type UWB antenna requires a horizontal ground plane. UWB planar antennas can be fed using microstrip or coplanar waveguide (CPW). M. J. Ammann introduced the pentagonal planar monopole antenna having 6.6:1 impedance bandwidth (2.1~12.5 GHz) [28].

Qit Jinghui et al. presented a circular monopole antenna for UWB systems[29]. It consists of a $9 \times 9 \text{ cm}^2$ ground plane and a metal plate of radius of 2.5 cm. It is fed by a single coaxial cable that passed through the ground plane and connects to the bottom metal plate. The proposed antenna's return loss is better than 10 dB from 1.25 GHz to more than 30 GHz.

Daniel Valderas et al. introduced UWB folded plate monopole antenna which is based on a rectangular plate monopole antenna. Folded configurations are also presented to reduce antenna size and improve radiation pattern maintaining the planar monopole radiation characteristics[30]. They have received great attention due to ease of fabrication, small size and low cost. Furthermore, Shiwei et al. and Tu Zhen et al. respectively introduced quadrate bowtie antenna with round corners and ultra wideband dipole antenna[31,32].

The former antenna offered better return loss in high frequency with small size and high gain, by rounding the corners on the rectangular bowtie antenna. The Tu Zhen et.al developed the UWB dipole antenna from the cone antenna. The folded bowtie antenna also called as sectorial loop antennas (SLA) is suitable for UWB operation [33]. Its performance is improved by adding a shorting loop to the outside of a bowtie antenna. The optimized antenna has a 8.5:1 impedance bandwidth and consistent radiation properties over 4.5:1 frequency range with excellent polarization purity over the entire 8.5:1 frequency range.

The planar monopole antenna for UWB systems can be classified according to feeding methods like microstrip feeding and coplanar waveguide feeding. Commonly employed radiating patch shapes in the microstrip fed UWB antennas are rectangular, triangular, circular and elliptical. Seok H. Choi et al. proposed a new ultra-wideband antenna[34]. Three techniques to achieve wide bandwidth are (i) two steps(ii) a partial ground plane and (iii) a single slot on the patch, which can lead to a good impedance match. Jinhak Jun[35] et al. introduced a small wideband microstrip monopole antenna which consists of a rectangular patch with two notches at the two lower corners of the patch and a truncated notched ground plane. Triangular patch and its modified structures of microstrip fed UWB antenna are introduced by Lin et al.,[35]. The structure is based on the triangular monopole antenna. It consists of a tapered radiating element fed by a microstrip line. The 3:1 VSWR bandwidth of the antenna is from 4 to 10 GHz.

A new antenna, the planar inverted cone antenna (PICA) proposed by Seong-Youp Suh[36] provides ultra wide band performance with a radiation pattern similar to monopole disk antenna with reduced size. Extensive simulations and experiments were presented to demonstrate that the PICA

antenna provides more than 10:1 impedance bandwidth (for VSWR 2) and supports a monopole type omni directional pattern over 4:1 bandwidth.

Z.N.Chen[37] presented a bi-arm rolled monopole for ultrawide-band applications. The roll monopole is constructed by wrapping a planar monopole. The impedance and radiation characteristics of the proposed roll monopole are experimentally compared with a rectangular planar monopole and strip monopole. Furthermore, the transfer responses of transmit–receive antenna systems comprising two identical monopoles are examined across the UWB band.

Maciej Klemm[38] presented a paper on a novel small-size directional antenna for ultrawide-band wireless body area networks/wireless personal area networks applications. The design is based on a typical slot antenna structure with an added reflector in order to achieve directionality. The effects of different antenna parameters and human body proximity on the radiation characteristics are analyzed. Antenna measurements with an optic RF setup were performed in order to characterize the small-size antenna far field radiation pattern.

Jeongpyo Kim[39], presented an ultra wide-band (UWB) antenna with a printed monopole structure fed by a coplanar waveguide (CPW) line. The antenna is analyzed using the Finite-Difference Time-Domain (FDTD) method and Genetic Algorithm (GA). The measured frequency response shows a 2:1 VSWR impedance bandwidth of 7.25 GHz from 3.3 to 10.55 GHz.

In 2005, J. Liang presented a paper on coplanar waveguide (CPW) fed circular disc monopole antenna for ultra-wideband (UWB) applications[40]. A circular disc monopole printed on a dielectric substrate and fed by a 50Ω CPW on the same layer can yield an ultra-wide band with satisfactory radiation patterns.

C.-C. Lin presented a paper on a printed PTMA by using the FR-4 printed circuit board substrate. The measured voltage standing wave ratio is less than 3 from 4 to 10 GHz[41]. In the UWB communication frequency range, the measured phase distribution of the input impedance is quite linear and the H-plane patterns are almost omni-directional.

Joeri R. Verbiest[42] presented a novel antenna topology based on the printed tapered monopole antenna (PTMA) in view of ultra-wideband (UWB) wireless body area network (WBAN) applications. First, the bandwidth in the presence of a human arm is studied. Second, the pulse distortion of a modulated Gaussian pulse is investigated, based on measured S_{21} -parameters.

Y.-J. Ren [43]proposed an elliptical ring antenna fed by a coplanar waveguide line for ultra-wideband applications. The wideband performance is achieved by extending the length of the elliptical ring's major axis. The elliptical ring antenna has a 2:1 VSWR from 4.6 to 10.3 GHz and has an average gain of 4.48 dBi. The antenna radiation patterns show stable characteristics within its operation band. The parameters determining the antenna wideband characteristic are discussed and the measured performance is presented.

Maciej Klemm presented a new ultra wideband (UWB) textile antenna designed for UWB wireless body area network (WBAN) applications[44]. Unlike previous textile antennas, these antennas offer a direct integration into clothing. They realized two different designs of textile antennas: coplanar waveguide fed printed UWB disc monopole and UWB annular slot antenna. Moreover, measured transfer functions show that these textile antennas possess excellent transient characteristics, when operating in free space as well as on the human body.

A novel, ultrawideband (UWB) monopole antenna suitable to be mounted on the printed circuit board (PCB) of a Wireless, Universal, Serial-bus (USB) dongle as is presented[45]. The proposed antenna is a U-shaped, metal-plate monopole antenna, easily fabricated from bending a simple metal plate onto a foam base of size $6 \times 11 \times 20 \text{ mm}^3$.

A variation of the novel technique called defected microstrip structure (DMS) is employed to enlarge the bandwidth of a planar ultrawideband monopole. It is demonstrated that introducing a defect in the feeding microstrip line, the lower bandwidth limit is lowered without affecting the antenna gain and radiation pattern. The bevel technique in the ground plane near to the feeding point is used to increase the highest bandwidth limit. By using these techniques, a 50 mm x50-mm planarized omnidirectional antenna was developed, achieving a voltage standing wave ratio (VSWR) ≤ 2 from 2.1 to 12.3 GHz[46].

In the study proposed by Ching-Wei Ling[47] ,a new edge curve, characterized by the binomial function was proposed for designing ultra wideband antenna. The effect on the impedance bandwidth through the change with the different order of the binomial function and the gap width between the antenna and ground plane has been investigated and analyzed.

A compact rectangular monopole with an equal-width ground plane was presented[48]. This novel structural configuration could significantly improve its radiation performance with decreased size. The feeding structure composed of a trident-shaped strip and a tapered impedance transformer is presented and discussed. Its impedance bandwidth is from 2.75 to 16.2 GHz. Both numerical and experimental results show that the proposed monopole antenna has stable omni-directional H-plane radiation patterns with low cross-polarization level

within its impedance bandwidth. This novel monopole antenna has ultrawide impedance bandwidth, very compact size (30 mm*8 mm), low fabrication cost, and omni-directional H-plane radiation patterns, which are suitable for various broadband applications.

A planar ultrawideband (UWB) monopole antenna was proposed by Xue-Song Yang[49]. The proposed antenna is incorporated with the rectangular/rounded-corner ground plane to further improve the monopole performances such as impedance bandwidth. In this paper, all of the requirements can be easily accomplished by making use of the recently developed Jumping Genes (JGs) multiobjective optimization scheme.

An ultrawideband (UWB) omnidirectional monopole antenna was presented by Xuan Hui Wu[50]. It is shaped by symmetrically wrapping a PEC sheet that has two trapezoidal cuts at the bottom corners. The antenna features about 132% impedance bandwidth over the UWB band. The monopole antenna is investigated both experimentally and numerically using FDTD method.

A balloon-shaped ultrawideband (UWB) antenna was developed, and its scattering characteristics are theoretically and experimentally studied in both the frequency and time domain[51]. The radar cross-section (RCS) and scattering waveforms of the UWB antenna terminated with three different loads are simulated and measured. The results are in good agreement with the numerical results. The balloon-shaped antenna offers almost omnidirectional scattering pattern, and its scattering mode and structural mode are obviously separated in the time domain. Therefore, this antenna is a suitable candidate for the passive ultrawideband-enabled radio-frequency identification (UWB-RFID) tag applications.

A novel omni-directional ultrawideband (UWB) monopole antenna was described by Alipour [52]. In the first part, the monopole antenna which is in the shape of an eye placed above a flat ground plane is designed and fabricated. This antenna operates from 3–20 GHz with low voltage standing wave ratio (VSWR) (1.5). To keep the main radiating beam fixed over the frequency range of interest without degrading the VSWR, shaped ground plane is introduced leading the antenna to the operate from 3–20 GHz with low VSWR (< 1.8). This eye antenna is fed by a coaxial probe through a SMA connector.

An internal ultra wideband monopole antenna for portable wireless communication applications was presented by Jaewon Lee[53]. The proposed antenna is compact and its dimension is $12 \times 16 \times 4.5 \text{ mm}^3$. It consists of a radiating patch, a matching stub, and a ground plane. The antenna was fabricated with a case and had a wide bandwidth of more than 8.7 GHz (2.3–11 GHz) for a return loss less than 10 dB. With this ultra wideband capability, the antenna could cover the wireless-broadband (2.3–2.39 GHz), Bluetooth (2.4–2.4835GHz), S-DMB (2.605–2.655GHz), and UWB (3.1–10.6 GHz) bands. The performances of the proposed antenna on a laptop computer was investigated and discussed.

M. Ojaroudi presented a novel modified printed monopole antenna (PMA) for ultra-wideband (UWB) applications[54]. It consists of a truncated ground plane and radiating patch with two tapered steps, which provides wideband behaviour and relatively good matching. Moreover, the effects of a modified trapezoid-shaped slot inserted in the radiating patch, on the impedance match and radiation behaviour is investigated. The antenna has a small area of $14 \times 20 \text{ mm}^2$ and offers an impedance bandwidth as high as 100%. It offered a frequency bandwidth increase of 18% with respect to the previous similar

antenna. Simulated and experimental results obtained for this antenna show that it exhibits good radiation behaviour within the UWB frequency range.

Ching-Wei Ling proposed a simple and compact printed ultrawideband (UWB) antenna[55]. The antenna is mainly composed of a monopole section and a quasi-transmission line section. The input signal from the feed line first passes through the line section then enters the monopole. The quasi-transmission line section provides different functions as the operating frequency changes. It serves not only as an impedance matching circuit but also a main radiator, which leads to the UWB performance of the antenna. The resonance mechanisms across the full band are described, followed by a thorough study of the antenna's geometrical parameters.

Mohammad Ojaroudi presented a printed monopole antenna for ultrawideband (UWB) applications[56]. The proposed antenna consists of a square radiating patch with two rectangular slots and a ground plane with inverted T-shaped notch to provide a wide usable fractional bandwidth of more than 120%(3.12–12.73 GHz). The proposed antenna is simple and small in size. Simulated and experimental results obtained for this antenna show that it exhibits good radiation behavior within the UWB frequency range

R.A. Sadeghzadeh-Sheikhan [57] proposed a planar monopole antenna incorporating a resonant structure in the form of a ladder-shape, which is etched on its back-plane. The radiation element of the antenna comprises a simple rectangular-shaped patch. The feature that makes the antenna different from a traditional monopole antenna is the resonant structure's configuration. The resonant structure has an effect of transforming the monopole antenna into an ultra-wideband (UWB) antenna. The prototype antenna's performance was verified through simulations and measurements. This antenna with dimension

of 22 x 22 mm² offered an impedance bandwidth of more than 17 GHz, between 2.7 to 20 GHz.

2.9 Chapter Conclusion

This chapter has discussed the methodology to simulate, optimize and fabricate the various planar antennas mentioned in the following chapters of the thesis. It has deduced the complete theory behind the transfer function characterization and the transient analysis of the antennas, along with their measurement techniques. The performance of the UWB antennas are assessed not only in terms of the conventional antenna parameters like VSWR, return loss, gain and radiation pattern but also in terms of the UWB quality measures like group delay. The antenna's ability to effectively transmit-receive a UWB pulse waveform are also discussed and estimated in terms of the Fidelity factor. Finally a detailed literature review of monopole antennas are also conducted at the end of the chapter.

References

- [1] "HP 8510 C Network Analyzer operating and programming manual", Hewlett Packard, 1988.
- [2] Chung, B.K and Chuah, H.T, "Design and construction of a multipurpose wideband anechoic chamber", IEEE Antennas and Propagation Magazine, Vol.45, No.6,2003.
- [3] IEEE standard test procedures for antennas (IEEE Std 149-1979), 1979.
- [4] H. G. Schantz. Radiation Efficiency of UWB Antennas. Proceedings of the 2002 IEEE UWBST Conference, 2002.

- [5] Constantine A Balanis, *Antenna Theory analysis and design*, John Wiley & Sons, 2005.
- [6] HFSS users manual, version 10, Ansoft Corporation, July 2005.
- [7] L. Guo, J. Liang, C.C. Parini and X. Chen, “A time domain study of CPW-Fed disk monopole for UWB applications”, *Asia-Pacific Microwave Conference 2005*, 4-7 December 2005, Suzhou, China.
- [8] Y. Cho, K. Kim, D. Choi, S. Lee and S. Park, “A Miniature UWB Planar Monopole Antenna With 5-GHz Band-Rejection Filter and the Time-Domain Characteristics”, *IEEE Transactions on Antennas and Propagation*, vol. 54, no. 5, May 2006, pp. 1453-1460.
- [9] E. C Ifeachor, B.W Jervis, *Digital Signal Processing, A practical Approach*, Addison-Wesley, 1993.
- [10] M. Ghavami, L. B. Michael and R. Kohno. Generation of ultra wideband waveforms. In *Ultra Wideband Signals and Systems in Communication Engineering*. John Wiley and Sons, Inc., 2004.
- [11] Z. N. Chen, X. H. Wu, H. F. Li, N. Yang and M. Y. W. Chia. Considerations for source pulses and antennas in UWB radio systems. *IEEE Trans. Antennas Propag.*, vol. 52, no. 7, pages 1739–1748, 2004.
- [12] J. D. Taylor. *Introduction to ultrawideband radar systems*. CRC Press, 1995.
- [13] R. S. Dilmaghani, M. Ghavami, B. Allen and H. Aghvami. Novel UWB pulse shaping using prolate spheroidal wave functions. *Proc. IEEE Int. Symp. on Personal, Indoor and Mobile Radio Communications*, Beijing, vol. 1, pages 602–606, 2003.

- [14] B. Parr, B. Cho, K. Wallace and Z. Ding. *A novel ultra-wideband pulse design algorithm*. IEEE Communications Letters, vol. 7, no. 5, pages 219–221, 2003.
- [15] H. Zhang and R.Kohno. *SSA realization in UWB multiple access systems based on prolate spheroidal wave functions*. Proc. IEEE Wireless Communications and Networking Conf., pages 1794–1799, 2004.
- [16] M. Ghavami, L. B. Michael and R. Kohno. *Hermite function based orthogonal pulses for UWB communication*. Proc. Int. Symp. on Wireless Personal Multimedia Communications, pages 437–440, 2001.
- [17] H. Sheng, P. Orlik, A. M. Haimovich, L. J. Cimini and J. Zhang. *On the spectral and power requirements for ultra-wideband transmission*. Proc. IEEE Int. Conf. on Communications, pages 738–742, 2003.
- [18] J. S. McLean and R. Sutton. *Considerations for source pulses and antennas in UWB radio systems*. Proc. IEEE Int. Conf. on Ultrawideband, vol. 2, pages 113–116, 2008.
- [19] J. Liang, L. Guo, C.C.Chiau and X. Chen, “*Time domain characteristics of UWB disc monopole antennas*”, 35th European Microwave Conference, 3-7 October, 2005, Paris, France.
- [20] N. Fortino, J.-Y. Dauvignac, G. Kossiavas and R. Staraj. *Design optimization of UWB printed antennas for omnidirectional pulse radiation*. IEEE Trans. on Antennas and Propagat., vol. 56, no. 7, pages 1875–1881, 2008.
- [21] D. Lamensdorf and L. Susman. *Baseband-pulse-antenna techniques*. IEEE Antennas and Propagation Magazine, vol. 36, no. 1, pages 20–30, 1994.

- [22] M. Klemm, I. Z. Koves, G. F. Pederson and G. Troster. Novel small-size directional antenna for UWB WBAN/WPAN applications. *IEEE Trans. on Antennas and Propagat.*, vol. 53, no. 12, pages 3884– 3896, 2005.
- [23] D. Pozar, "Microwave engineering," John Wiley & Sons, 3rd Ed, 2005.
- [24] J. D. Brunett, R. M. Ringler, V. V. Liepa, "On measurements for EIRP compliance of UWB devices," *IEEE Electromagnetic Compatibility*, vol. 2, pp. 473- 476, Aug. 2005.
- [25] S. Honda, M. Ito, H. Seki, and Y. Jingo, "A disc monopole antenna with 1:8 impedance bandwidth and omnidirectional radiation pattern", *Proc. Int. Sym. Antennas Propagat.*, Sapporo, Japan, September 1992, pp 1145-1148.
- [26] M. Hammoud, P. Poey and F. Colombel, "Matching the Input Impedance of a Broadband Disc Monopole", *Electronics Letters*, vol. 29, no. 4, 18th February 1993, pp. 406-407.
- [27] Z.N. Chen and M.Y.W. Chia, *Broadband Planar Antennas: Design and Applications*. Chichester: John Wiley & Sons, Ltd, 2006.
- [28] Ammann F. R. (2001), "The Pentagonal Planar Monopole for Digital Mobile Terminals; Bandwidth Considerations and Modelling", *Proceedings of 11th International Conference on Antennas and Propagation*, pp. 82-85, ISBN: 0-85296-733-0, Manchester, UK, 17-20 April 2001, Institution of Electrical Engineers, London.
- [29] Jinghui Q, Jiaran Q. & Wei L, "A Circular Monopole Ultra-Wideband Antenna", *Proceedings of 5th International Conference on Microwave Electronics: Measurement, Identification, Applications*, pp. 45-47 ISBN: 5-7782-0554-6, Novosibirsk, Russia, 13-15 December 2005.

- [30] Valderas D, Legarda J, Gutierrez I. & Sancho J. I,” Design of UWB Folded-Plate Monopole Antennas Based on TLM”, IEEE Transactions on Antennas and Propagation, Vol. 54, No. 6, pp. 1676-1687, ISSN: 0018-926X,2006.
- [31] Qu S. & Ruan C, “Quadrature bowtie antenna with round corners, Proceedings of IEEE International Conference on Ultra-Wideband 2005”, ISBN: 078039397X, Zurich, Switzerland, September 5 - 8, Piscataway, N.J 2005.
- [32] Tu Z.; Chen G. & Zhang G.” The FDTD Analysis of two Ultra Wideband Dipole Antennas, Proceedings of 4th International Conference on Microwave and Millimeter Wave Technology”, pp. 46-49, ISBN: 0-7803-8401-6, Beijing, China, 18-24 August 2004, Institute Of Electrical & Electronics Engineer, NY 2004.
- [33] Behdad N. & Sarabandi K, “A Compact Antenna for Ultrawide-Band Applications”, IEEE Transactions on Antennas and Propagation, Vol. 53, No. 7, pp. 2185-2192, ISSN: 0018-926X,2005.
- [34] Seok H. Choi, Jong K. Park, Sun K. Kim and Jae Y. Park “A new Ultra wide band antenna for UWB applications”, Microwave and Optical Technology Letters, Volume: 40, Issue: 5, pp. 399-401, 2004.
- [35] Jung J.; Choi W. & Choi J,”A Small Wideband Microstrip-fed monopole antenna, IEEE Microwave and Wireless Components Letters”, Vol. 15, No. 19, pp. 703-705, ISSN: 1531-1309, 2005.
- [36] Lin C. C.; Kan Y. C.; Kuo L. C. & Chuang H. R,” A planar triangular monopole antenna for UWB Communication”, IEEE Microwave and Wireless Components Letters, Vol. 15, No. 10, pp. 624-626, ISSN: 1531-1309(2005).

- [37] Seong-Youp Suh, Warren L. Stutzman, and William A. Davis, “A New Ultra wideband Printed Monopole Antenna, The Planar Inverted Cone Antenna (PICA)”, *IEEE Transactions on Antennas and Propagation*, Vol. 52, No. 5, May 2004.
- [38] Zhi Ning Chen, “Novel Bi-Arm Rolled Monopole for UWB Applications”, *IEEE Transactions on Antennas and Propagation*, Vol. 53, No. 2, February 2005.
- [39] Maciej Klemm, István Z. Kovács, Gert F. Pedersen and Gerhard Tröster, IEEE, ” Novel Small-Size Directional Antenna for UWB WBAN/WPAN Applications”, *IEEE Transactions on Antennas and Propagation*, Vol. 53, No. 12, December 2005.
- [40] Jeongpyo Kim, Taeyeoul Yoon, Jaemoung Kim, and Jaehoon Choi, “Design of an Ultra Wide-band Printed Monopole Antenna Using FDTD and Genetic Algorithm”, *IEEE Microwave And Wireless Component Letters*, Vol. 15, No. 6, June 2005.
- [41] J. Liang, L. Guo, C.C. Chiau, X. Chen and C.G. Parini, ”Study of CPW-fed circular disc monopole antenna for ultra wideband applications”, *IEE Proc.-Microw. Antennas Propag.*, Vol. 152, No. 6, December 2005.
- [42] C.-C. Lin, Y.-C. Kan, L.-C. Kuo, and H.-R. Chuang ”A Planar Triangular Monopole Antenna for UWB Communication”, *IEEE Microwave And Wireless Component Letters*, Vol. 15, No. 10, October 2005
- [43] Joeri R. Verbiest, and Guy A. E. Vandenbosch, “A Novel Small-Size Printed Tapered Monopole Antenna for UWB WBAN”, *IEEE Antennas And Wireless Propagation Letters*, Vol. 5, 2006.

- [44] Y.-J. Ren and K. Chang, "Ultra-wideband planar elliptical ring antenna", *Electronic Letters*, 13th April 2006, Vol. 42, No. 8.
- [45] Maciej Klemm and Gerhard Troester, "Textile UWB Antennas for Wireless Body Area Networks", *IEEE Transactions on Antennas and Propagation*, Vol. 54, No. 11, November, 2006.
- [46] Saou-Wen (Stephen) Su, Jui-Hung Chou, and Kin-Lu Wong, "Internal Ultrawideband Monopole Antenna for Wireless USB Dongle Applications", *IEEE Antennas And Wireless Propagation Letters*, Vol. 6, 2007.
- [47] M. A. Peyrot-Solis, J. A. Tirado-Mendez, and H. Jardon-Aguilar, "Design of Multiband UWB Planarized Monopole Using DMS Technique", *IEEE Antennas And Wireless Propagation Letters*, Vol. 6, 2007.
- [48] Ching-Wei Ling, Wen-Hsin Lo, Ran-Hong Yan, and Shyh-Jong Chung, "Planar Binomial Curved Monopole Antennas for Ultrawideband Communication applications", *IEEE Transactions on Antennas and Propagation*, Vol. 55, No. 9, September 2007.
- [49] Qi Wu, Ronghong Jin, Junping Geng, and Min Ding, "Printed Omnidirectional UWB Monopole Antenna with Very Compact Size", *IEEE Transactions on Antennas and Propagation*, vol. 56, issue 3, pp. 896-899.
- [50] Xue-Song Yang, Kai Tat Ng, Sai Ho Yeung, and Kim Fung Man, "Jumping Genes Multiobjective Optimization Scheme for Planar Monopole Ultrawideband Antenna", *IEEE Transactions on Antennas and Propagation*, Vol. 56, No. 12, December 2008.

- [51] Xuan Hui Wu and Ahmed A. Kishk, “Study of an Ultrawideband Omnidirectional Rolled Monopole Antenna With Trapezoidal Cuts”, IEEE Transactions on Antennas and Propagation, Vol. 56, No. 1, January 2008.
- [52] Hu, Choi Look Law, and Wenbin Dou,” A Balloon-Shaped Monopole Antenna for Passive UWB-RFID Tag Applications”, IEEE Antennas And Wireless Propagation Letters, Vol. 7, 2008.
- [53] Alipour and H. R. Hassani,”A Novel Omni-Directional UWB Monopole Antenna”, IEEE Transactions on Antennas and Propagation, Vol. 56, No. 12, December 2008.
- [54] Jaewon Lee, Seokjin Hong, Jaewoong Shin, and Jaehoon Choi,” A Compact Ultrawideband Monopole Antenna for Wireless Communication Application”, IEEE Transactions on Antennas and Propagation, Vol. 57, No. 9, September 2009.
- [55] M. Ojaroudi G. Kohneshahri Ja. Noory “Small modified monopole antenna for UWB application”, IET Microw. Antennas Propag., 2009.
- [56] Ching-Wei Ling and Shyh-Jong Chung, “A Simple Printed Ultrawideband Antenna With a Quasi-Transmission Line Section”, IEEE Transactions on Antennas and Propagation, Vol. 57, No. 10, October 2009.
- [57] Mohammad Ojaroudi, Changiz Ghobadi, and Javad Nourinia, “Small Square Monopole Antenna With Inverted T-Shaped Notch in the Ground Plane for UWB Application” , IEEE Antennas And Wireless Propagation Letters, Vol. 8, 2009.

- [58] R.A. Sadeghzadeh-Sheikhan M. Naser-Moghadasi E. Ebadifallah H. Rosta,M. Katouli,B.S. Virdee ,”Planar monopole antenna employing back-plane ladder-shaped resonant structure for ultra-wideband performance”, IET Microw. Antennas Propag., Vol. 4, Iss. 9, pp. 1327–1335, 2010.

.....✂.....

TOP LOADED MONOPOLE ULTRA WIDE BAND ANTENNAS

Contents	3.1	<i>Ground Modified Monopole Antenna</i>
	3.2	<i>Planar Serrated Microstrip Fed Monopole UWB Antenna</i>
	3.3	<i>Band notch Design</i>
	3.4	<i>A Compact CPW fed serrated UWB antenna</i>
	3.5	<i>Time Domain Antenna Analysis</i>

This chapter concentrates on the development of top loaded planar monopole UWB antennas. The evolution of the antenna designs are presented first. The designs are then simulated and their resonant modes are identified. The surface current & field distributions on the antenna and their radiation patterns at the resonant modes are analyzed in detail. The results of the analysis along with the parametric studies have enabled to deduce their design equations and design methodologies on any substrate for the desired operating frequencies. The performance of the fabricated antennas are then experimentally verified and are found to conform reasonably well with the simulated responses in all cases.

Two novel designs of compact planar monopole antennas are presented in this chapter: a ground modified monopole and a serrated monopole antenna. These antennas perform well in terms of impedance match and gain, over the FCC approved UWB frequencies of 3.1 to 10.6 GHz. However, in the case of ground modified antenna, radiation patterns at the higher end of the band do not exhibit omni-directional characteristics. This defect is mitigated by the serrated monopole antennas with added advantage of compactness. A band notched serrated antenna to notch out the 5.8GHz WLAN band by etching an inverted U slot from the patch is also presented. Electronic reconfiguration of the notch band by integrating a PIN diode across $\lambda/2$ inverted 'U' slot is also demonstrated. A CPW fed serrated monopole antenna is also developed and presented.

The antennas are well suitable for broadband mobile applications in terms of their physical and electrical characteristics. Their suitability for pulsed UWB applications are confirmed by investigating their effects on large fractional bandwidth pulses and this is carried out at the end of the chapter.

Introduction

The monopole antenna is attractive for modern communication systems due to its simple structure, broad bandwidth and nearly omnidirectional radiation characteristics. The monopoles are usually placed vertical to the ground plane which increases the system complexity, size and volume. These types of antennas may create constraints to the performance of the system and uneasiness to the user. Printed monopoles on the other hand, are conformal for modular design and can be fabricated along with the printed circuit board of the system, which make the design simpler and fabrication easier. Usually in the printed monopole designs ground plane is printed on the same substrate parallel to the radiator either on the same side of radiator or on the opposite side. This results in low in profile and low in volume along with added advantage of easy fabrication and integration in the system circuit board of the communication device. The limited space of circuit board will impose another constraint on the size of the ground plane. It is found that the size of the ground plane, adversely affects the antenna performance considerably. Thus the ground plane, an inevitable part of the mobile gadget and its effect on antenna performance are the important issues that have to be addressed in the present scenario. The exhaustive investigations of the ground plane effects have resulted in an interesting inference that the bandwidth of a conventional printed strip quarter wave monopole can be broadened by properly modifying the ground plane.

Thus compact monopole antennas can be designed on truncated ground planes with the additional advantage of broad band behaviour. This intervening property is elaborately discussed in this chapter. Exhaustive parametric analyses were carried out to optimize the ground plane size. From the parametric studies an optimum ground plane dimension to fix the resonance at desired frequency is

derived. Using the optimum ground plane a compact ground modified monopole antenna is designed and experimentally characterized.

3.1 Ground Modified Monopole Antenna

This section deals with the experimental and simulation analysis of a compact ground modified monopole antenna. Design and evolution of this antenna from a finite ground strip monopole antenna is analyzed.

Fig.3.1(a) shows a Finite Ground Coplanar Waveguide (FGCPW) fed strip monopole antenna. The antenna is fabricated on a substrate of $\epsilon_r=4.4$ and $h=1.6\text{mm}$. A truncated ground plane of length 17mm and width 13mm is used. A strip monopole of length 5mm and width 3mm acts as the radiating element. The CPW are designed for 50Ω characteristic impedance[1]. Strip monopole antenna (Fig.3.1 (a)) produces two resonances at 7.7GHz and 11.1GHz respectively with bandwidth ranging from 6.8GHz to 9.5GHz and 10.35GHz to 11.89GHz. This is shown as blue line in Fig.3.2.

The above strip monopole is top loaded with a rectangle of length L_1 and width W_1 as shown in (Fig.3.1(b)). The top loading decreases the resonant frequency from 7.71GHz to 4.55GHz due to the increased length of the monopole. But the resonance at 11.1 GHz is not much affected. Reflection coefficient of top loaded monopole is shown as black line in Fig.3.2. Finally UWB antenna is obtained by removing two quarter circles from the rectangular ground as given in Fig.3.1(c). This produces an additional resonance at 7.5GHz and merging of these three resonances results in the required UWB operation. Reflection coefficient of the ground modified antenna is shown as red line in Fig.3.2(c). From the return loss studies it is found that this UWB antenna is

resonating at three frequencies at 3.6, 7.5 and 10.7GHz. Each antenna is analysed in detail in the remaining sessions.

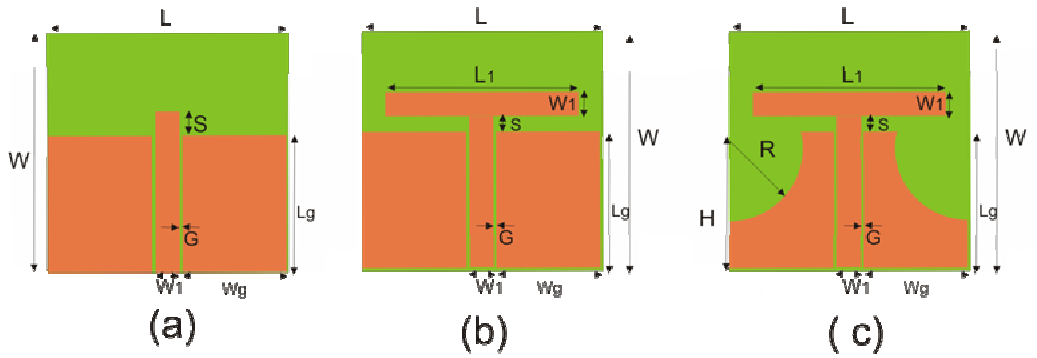


Fig.3.1. Evolution of the ground modified monopole antenna(a) Finite Ground Coplanar Waveguide(FGCPW) fed Strip Monopole Antenna (b)Top loaded monopole antenna(c)Ground modified monopole antenna (L=30mm, W=25mm, L₁=24mm, W₁=3mm, H=15mm, R=9mm, L_r=17mm, W_g=13mm, S=2mm, h=1.6mm, ε_r=4.4, G=0.35mm.)

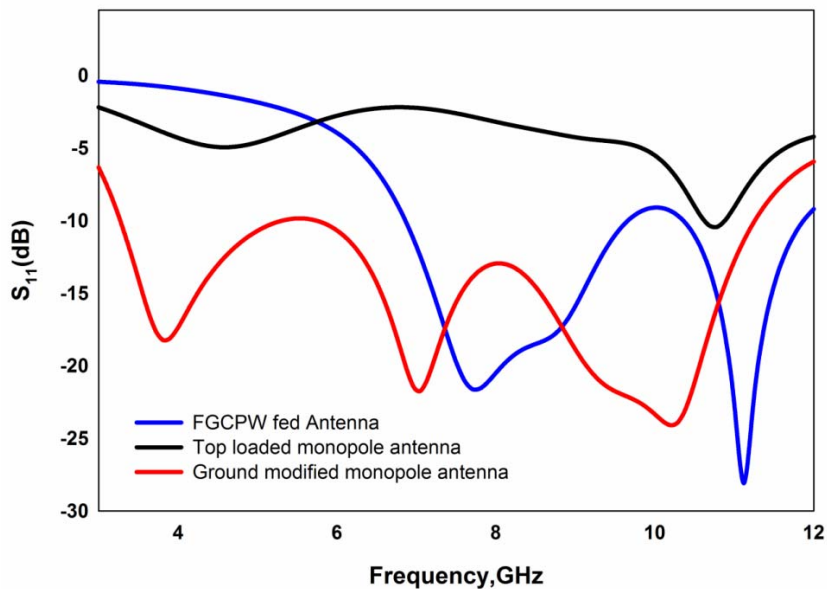


Fig.3.2. Reflection coefficients of FGCPW, top loaded and ground modified monopole antennas (L=30mm, W=25mm, L₁=24mm, W₁=3mm, H=15mm, R=9mm, L_r=17mm, W_g=13mm, S=2mm, h=1.6mm, ε_r=4.4, G=0.35mm.)

3.1.1 Finite Ground Coplanar Waveguide (FGCPW) fed Strip Monopole Antenna

The analysis of a Finite Ground Coplanar Waveguide (FGCPW) fed monopole antenna is carried out in this session. The antenna is fed using a 50Ω CPW fabricated on a substrate of $\epsilon_r=4.4$ and loss tangent $\tan \delta=0.02$. The ground plane dimensions $L_g \times W_g$ are $17\text{mm} \times 13\text{mm}$. The center conductor of the FGCPW is extended to form a strip monopole of length 'S'.

The geometry of the strip monopole antenna is depicted in Fig 3.3.

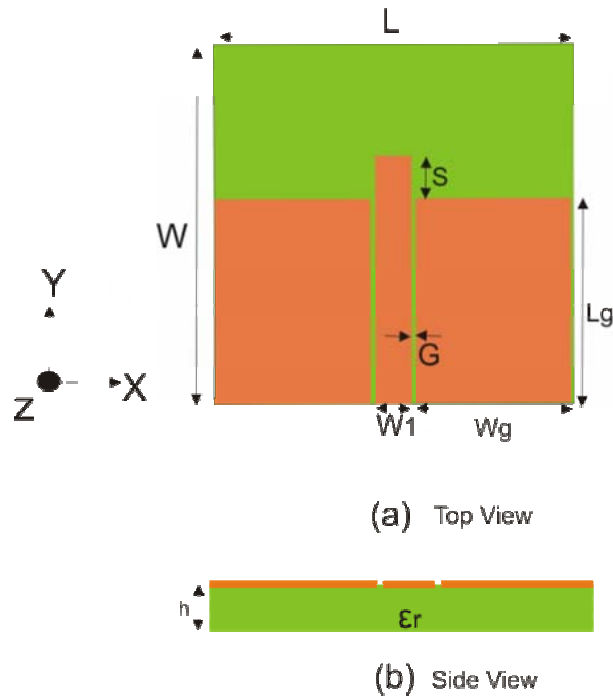


Fig.3.3. Geometry of FGCPW fed Monopole Antenna
 ($L = 30\text{mm}$, $W = 25\text{mm}$, $G = 0.35\text{mm}$, $W_g = 13\text{mm}$ and $L_g = 17\text{mm}$,
 $W_1 = 3\text{mm}$, $S = 5\text{mm}$, $h = 1.6\text{mm}$ and $\epsilon_r = 4.4$).

Reflection coefficient of the antenna is plotted in Fig.3.4 and a 2:1 VSWR bandwidth from 6.8 GHz to 9.5 GHz and 10.3 GHz to 11.8GHz with resonances centered at 7.7 GHz and 11.1 GHz respectively is observed.

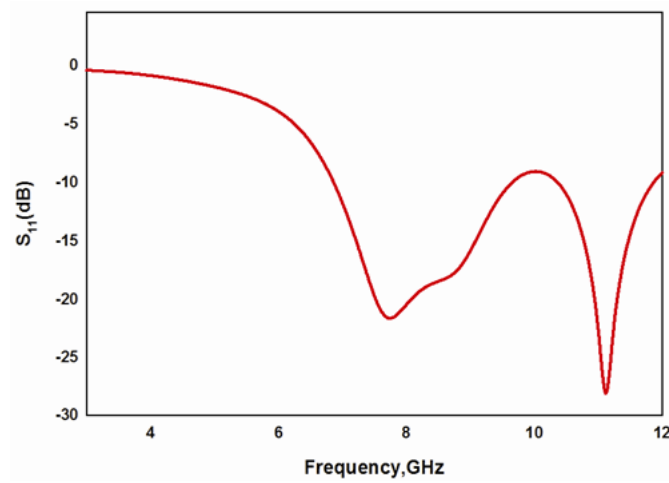


Fig.3.4. Reflection coefficient of FGCPW fed antenna
 ($L = 30\text{mm}$, $W = 25\text{mm}$, $G = 0.35\text{mm}$, $W_g = 13\text{mm}$ and
 $L_g = 17\text{mm}$, $W_1 = 3\text{mm}$, $S = 5\text{mm}$, $h = 1.6\text{mm}$ and $\epsilon_r = 4.4$).

3.1.1.1 Resonance mechanism

The surface current distribution of the antenna is a good tool for finding the resonant mechanism, polarization and hence the radiation characteristics. Surface current distribution of the antenna at 7.71GHz and 11.1GHz are shown in Figs.3.5 and 3.6 respectively. It is clearly evident from Fig.3.5 that there is a quarter wave current variation along the length of monopole strip corresponding to the first resonance. At the fundamental resonance the electric field is polarized along Y direction. From the surface current distribution, it can be observed that a feeble current exists on either sides of the feed and are equal in magnitude but out of phase. This strongly indicates that there is negligible radiation from the ground plane and monopole alone is radiating at this frequency. Since the contribution from the ground plane is virtually small, the electric field is lying along the y direction along the length of the monopole. Thus it can be concluded that first resonance is produced solely due to the strip monopole. This is confirmed from the simulated radiation pattern of the antenna at first resonance shown in Fig.3.7(a).

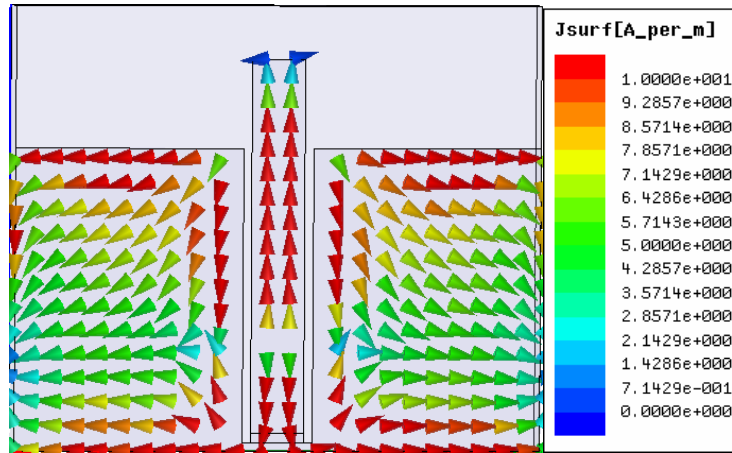


Fig.3.5. Current distribution of the antenna at 7.7GHz
 (L = 30mm, W= 25mm, G = 0.35mm, Wg = 13mm and
 Lg = 17mm, W₁= 3mm, S=5mm, h=1.6mm and $\epsilon_r=4.4$).

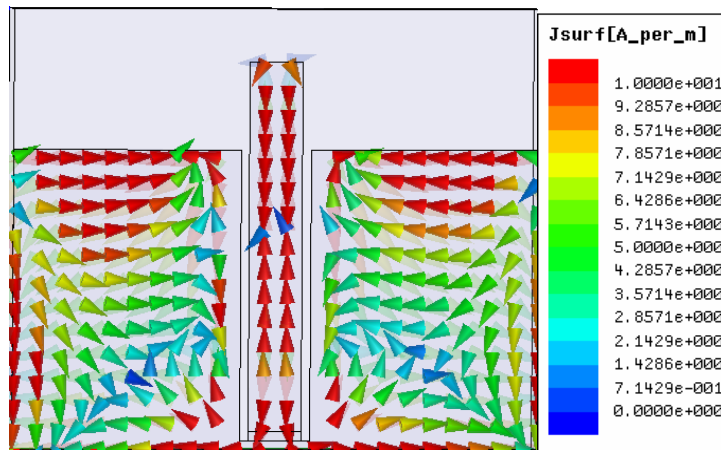


Fig.3.6. Current distribution of the antenna at 11.1GHz
 (L = 30mm, W= 25mm, G = 0.35mm, Wg = 13mm and
 Lg = 17mm, W₁= 3mm, S=5mm, h=1.6mm and $\epsilon_r=4.4$).

But contrary to current distribution at first resonance, there is an the effect of ground plane on the resonance at second resonance as shown in Fig.3.6. But the interesting point to be noted is that ground strip current variation shown in Fig.3.6 is larger in magnitude compared to the earlier case but out of phase. Hence the effect of these currents contributing towards radiation is again

negligible. So in this frequency also the top strip monopole acts as main radiator, yielding vertical polarization same as in the first case. Hence it can be concluded that throughout the resonant band the antenna is vertically polarized along Y direction with similar radiation characteristics. Thus it can be concluded that second resonance is produced due to the combined effect of strip monopole and the ground and this produces degradation in its radiation pattern. Simulated radiation pattern shown in Fig.3.7(b) also reveal that the pattern is distorted at higher frequency due to the combined effect of monopole and ground plane.

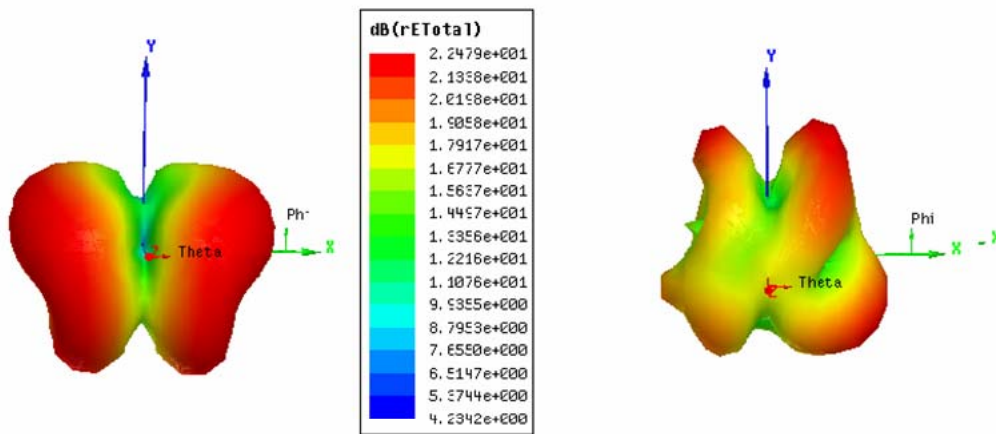


Fig.3.7. Simulated radiation patterns of the antenna at (a) 7.71GHz and (b)11.1GHz
(L = 30mm, W= 25mm, G = 0.35mm, Wg = 13mm and Lg = 17mm, W₁= 3mm, S=5mm, h=1.6mm and $\epsilon_r=4.4$).

3.1.1.2 Effect of ground plane length Lg

Fig 3.8 shows the return loss characteristics with different ground plane lengths of a typical antenna. It is found that for Lg=11mm and 13mm, there are single resonances centered at 4.8GHz and 5.4GHz respectively. But increasing Lg to 15mm results in the production of an additional resonance at 8.5GHz

besides the fundamental resonance at 6.5GHz. At the optimum ground plane length of $L_g=17\text{mm}$, two resonant modes merge together and wide bandwidth is obtained. Further increase in L_g decreases the matching and bandwidth as shown in Fig. So optimum value of $L_g=17\text{mm}$ is chosen. After exhaustive experimental and simulation studies it is found that optimum L_g to obtain UWB operation is found to be $0.674 \lambda_m$ where λ_m is the wavelength corresponding to centre frequency of operating band.

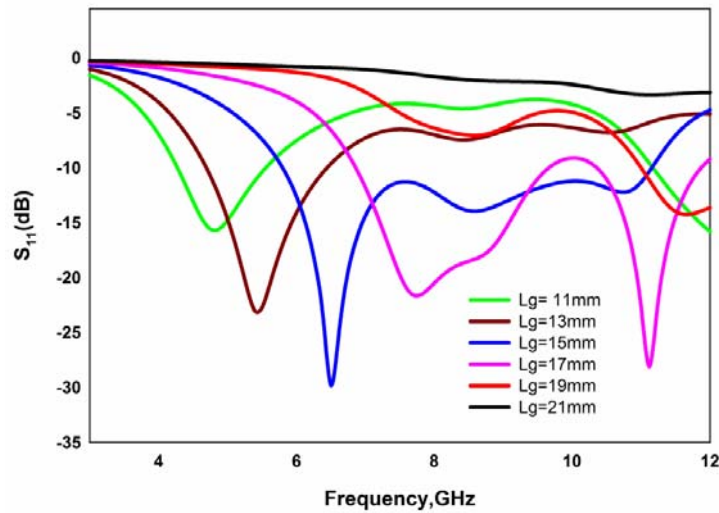


Fig.3.8. Effect of ground length L_g
 ($L = 30\text{mm}$, $W = 25\text{mm}$, $G = 0.35\text{mm}$, $W_g = 13\text{mm}$ and,
 $W_1 = 3\text{mm}$, $S = 5\text{mm}$, $h = 1.6\text{mm}$ and $\epsilon_r = 4.4$).

3.1.1.3 Effect of ground plane width W_g

A thorough parametric analysis is carried out to find the effect of W_g on reflection characteristics and is plotted in Fig.3.9. It is found that increasing W_g decreases both the resonant frequencies. Since bandwidth is maximum for $W_g=13\text{mm}$, it is selected as optimum value. Here also it is found that at optimum $W_g=0.515 \lambda_m$ where λ_m is the wavelength corresponding to centre frequency of operating band.

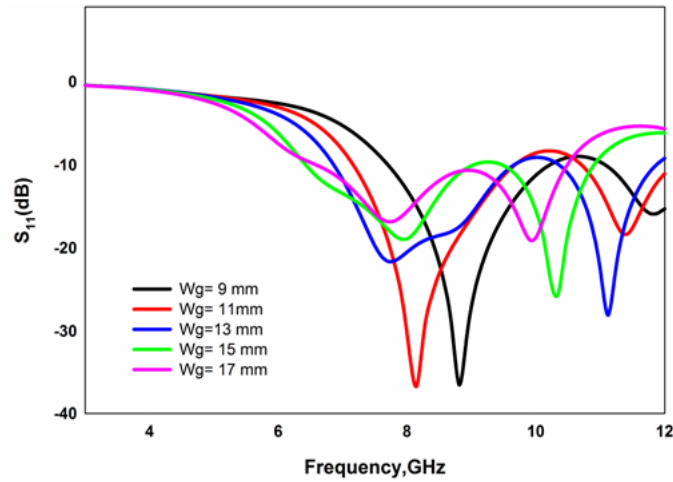


Fig.3.9. Effect of ground width W_g
 ($L = 30\text{mm}$, $W = 25\text{mm}$, $G = 0.35\text{mm}$, $L_g = 17\text{mm}$, $W_1 = 3\text{mm}$,
 $S = 5\text{mm}$, $h = 1.6\text{mm}$ and $\epsilon_r = 4.4$).

3.1.1.4 Effect of Monopole length S

In order to find the effect of monopole length on input reflection coefficient of the antenna, a rigorous parametric analysis has been performed. The variation of resonant frequency with monopole length (S) is shown in Fig.3.10. Monopole length is varied from 0mm to 7mm. When the monopole length is varied, the first resonance corresponding to the monopole mode is significantly affected. For the second resonance, variation in length of the monopole slightly affects the resonance. It is clear from the results that the length of the strip monopole is inversely proportional to the resonant frequency. It is found that maximum bandwidth is obtained for $S = 5\text{mm}$. But when the monopole length is increased the two modes separates and is not able to merge them. This observation again confirms our earlier argument that the first resonance is solely due to the strip monopole and the second mode is the combined effect of strip monopole and the ground plane. It is found that when the length is large the first resonance occurs at lower frequency as expected.

This resonance frequency can be increased by decreasing the length of the radiating strip. Almost similar behavior is observed for second resonant mode also. As stated earlier this variation is rather small compared to the first resonance. Hence by proper selection of the length of the radiating strip and ground plane the two resonant modes can be merged together to obtain large bandwidth. It is found from the experimental studies that optimum length required for the present UWB antenna is $0.079 \lambda_m$ where λ_m is the wavelength corresponding to centre frequency of operating band.

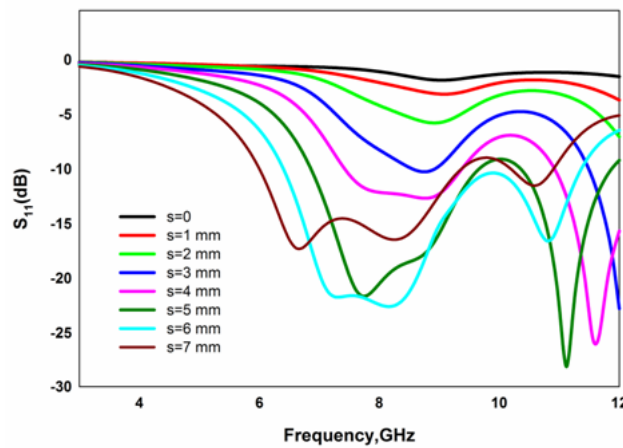


Fig.3.10. Variation of reflection coefficient with signal strip length S
(L = 30mm, W= 25mm, G = 0.35mm, Wg = 13mm,
Lg = 17mm, W₁= 3mm, h=1.6mm and $\epsilon_r=4.4$)

Thus from the above studies we reached in a conclusion that a FGCPW strip monopole produces two resonances at 7.71GHz and 11.1GHz. The first resonance is purely due to the strip monopole and second resonance is due to the combined effect of monopole and ground. Increasing the monopole length decreases the resonant frequency. With an aim to produce resonance in the lower frequency region, a rectangle is top loaded on the monopole. In this case total resonant path increases resulting in a decrease in first resonance. These aspects are elaborately explained in the next section.

3.1.2 Top Loaded Strip Monopole Antenna

Technique of top loading can be effectively applied to the strip monopole for achieving compact mode of operation. In this case resonant frequency is lowered without much affecting the compactness of the antenna. Resulting antenna geometry is shown in Fig.3.11.

The antenna is fed using a 50Ω CPW fabricated on a substrate of $\epsilon_r=4.4$ and loss tangent $\tan \delta=0.02$. The ground plane dimensions $L_g \times W_g$ are selected to be $17\text{mm} \times 13\text{mm}$. The center conductor of the FGCPW is extended to form a strip monopole of length 'S'. A rectangle of length L_1 and width W_1 is top loaded on the monopole.

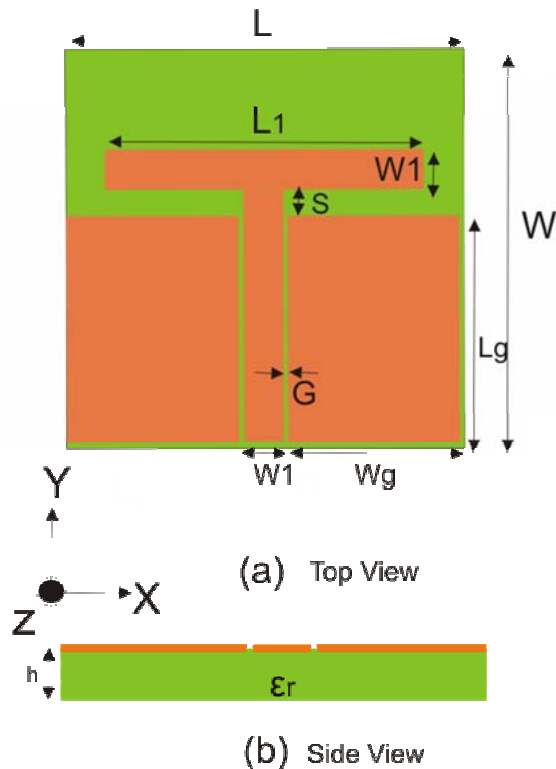


Fig.3.11. Geometry of the Top loaded Strip Monopole Antenna
 ($L = 30\text{mm}$, $W = 25\text{mm}$, $G = 0.35\text{mm}$, $W_g = 13\text{mm}$ and $L_g = 17\text{mm}$, $L_1 = 24\text{mm}$, $W_1 = 3\text{mm}$, $h = 1.6\text{mm}$ and $\epsilon_r = 4.4$).

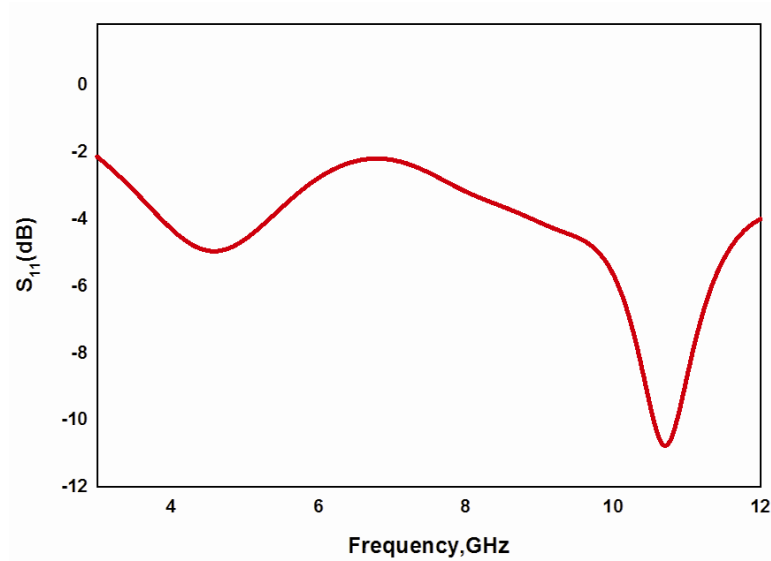


Fig.3.12. Reflection coefficient of Top loaded CPW fed antenna ($L = 30\text{mm}$, $W = 25\text{mm}$, $G = 0.35\text{mm}$, $W_g = 13\text{mm}$ and $L_g = 17\text{mm}$, $L_1 = 24\text{mm}$, $W_1 = 3\text{mm}$, $h = 1.6\text{mm}$ and $\epsilon_r = 4.4$).

From the reflection characteristics shown in Fig.3.13, it is clear that the resonance at 7.7 GHz due to strip monopole is lowered to 4.55GHz due to the top loaded rectangle. After top loading, the total effective length of the monopole increases resulting in a decrease in the first resonance frequency. And second resonance is not much affected.

3.1.2.1 Simulated current distribution and radiation pattern of the top loaded strip monopole antenna

Resonance mechanism of the top loaded antenna can be explained further by examining the current distribution and radiation pattern of the antenna at resonant frequencies and is shown in Fig.3.13 and 3.14. It is found that in the case of first resonance there is a quarter wavelength variation along the length of the monopole. And radiation pattern at this frequency is almost omni directional. But at the second resonance ground plane is also found to contribute to the resonance and hence the pattern is found to be distorted.

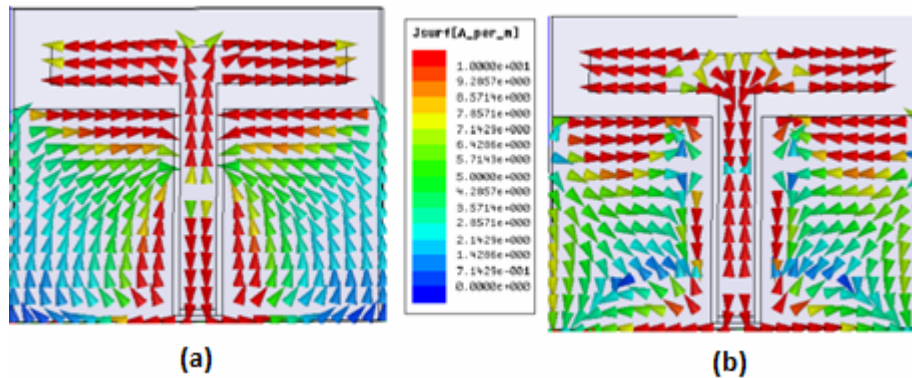


Fig.3.13. Simulated surface current distribution of the top loaded antenna at (a)4.55GHz and (b)10.68GHz
 ($L = 30\text{mm}$, $W = 25\text{mm}$, $G = 0.35\text{mm}$, $W_g = 13\text{mm}$ and $L_g = 17\text{mm}$,
 $L_1=24\text{mm}$, $W_1= 3\text{mm}$, $h=1.6\text{mm}$ and $\epsilon_r=4.4$).

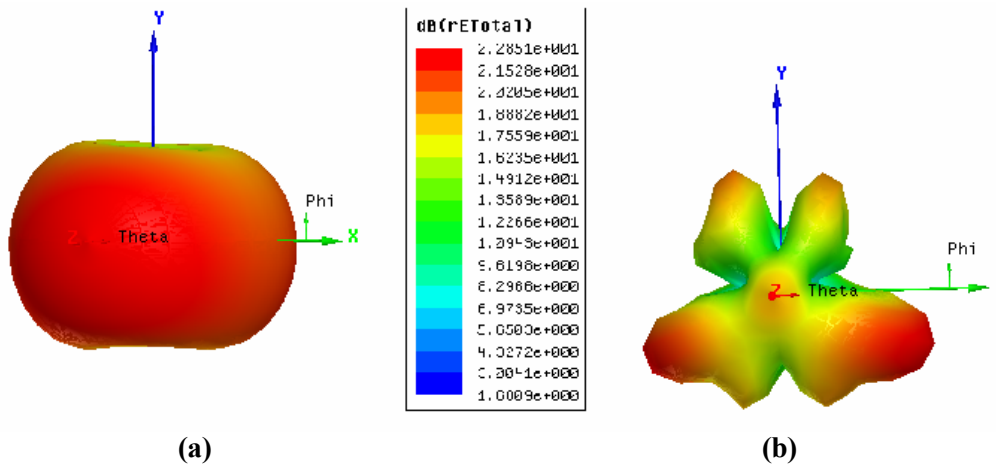


Fig.3.14. Simulated radiation patterns of the top loaded antenna (a)4.55GHz and (b)10.68GHz
 ($L = 30\text{mm}$, $W = 25\text{mm}$, $G = 0.35\text{mm}$, $W_g = 13\text{mm}$ and $L_g = 17\text{mm}$,
 $L_1=24\text{mm}$, $W_1= 3\text{mm}$, $h=1.6\text{mm}$ and $\epsilon_r=4.4$).

It is found that embedding an appropriate notch in the ground plane near the radiating element can increase the impedance bandwidth of antenna. In fact, this modified ground plane structure acts as a matching circuit and controls the bandwidth of antenna [2 –5]. Modifying the ground plane shape also can improve the capability of antenna in preserving the waveform of source signal [6].

3.1.3 Compact Ground Modified Monopole Antenna

3.1.3.1 Geometry of Ground Modified Monopole Antenna

The geometry of the proposed ground modified monopole antenna is shown in Fig.3.15. The T shaped monopole antenna is fed by a coplanar waveguide (CPW) with a partially curved ground plane. Ground is formed by etching two circles of radius R centered at $(0,H,h)$ and (L,H,h) from a normal rectangular ground, as shown in the figure. Antenna is printed on a substrate with dielectric constant $\epsilon_r = 4.4$, loss tangent $\tan\delta = 0.02$ and thickness $h = 1.6$ mm. The strip width (W) and gap (G) of the Coplanar Waveguide (CPW) feed are derived using standard design equations for 50Ω impedance.

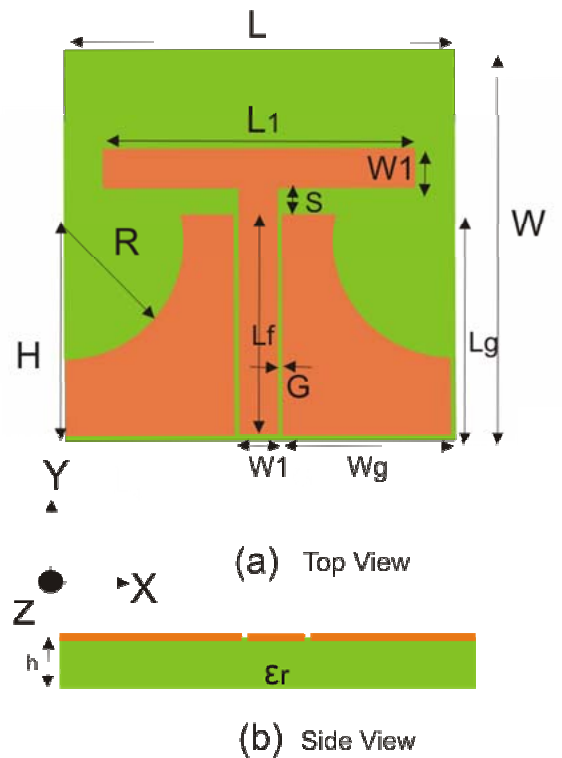


Fig.3.15. Geometry of the ground modified monopole UWB antenna
 ($L=30\text{mm}$, $W=25\text{mm}$, $L_1=24\text{mm}$, $W_1=3\text{mm}$, $H=15\text{mm}$,
 $R=9\text{mm}$, $L_f=17\text{mm}$, $W_g=13\text{mm}$, $S=2\text{mm}$, $h=1.6\text{mm}$, $\epsilon_r=4.4$,
 $G=0.35\text{mm}$.)

The antenna has simple structure with a few geometric parameters and large bandwidth. Due to its excellent characteristics like single layer, small size and large bandwidth, CPW fed antenna is a good candidate for UWB systems. The simulated and experimental results show that the antenna has a 2:1 VSWR band width from 3.1-12GHz with all desired UWB radiation characteristics.

Geometries like rectangle and triangle can be also removed from the ground plane in order to produce UWB operation. But the required UWB performance is obtained only when two quarter circles are removed from the ground plane as described in the next session.

3.1.3.2 Reflection characteristics of Ground Modified Monopole Antenna

Fig.3.16 shows the measured and simulated reflection coefficient of the antenna. The antenna exhibits a 2:1 VSWR bandwidth from 3.1 to 12 GHz with three resonances centered at 4GHz, 7.5GHz and 10.5GHz respectively. It is clear from the figure that both experiment and simulation agree very well.

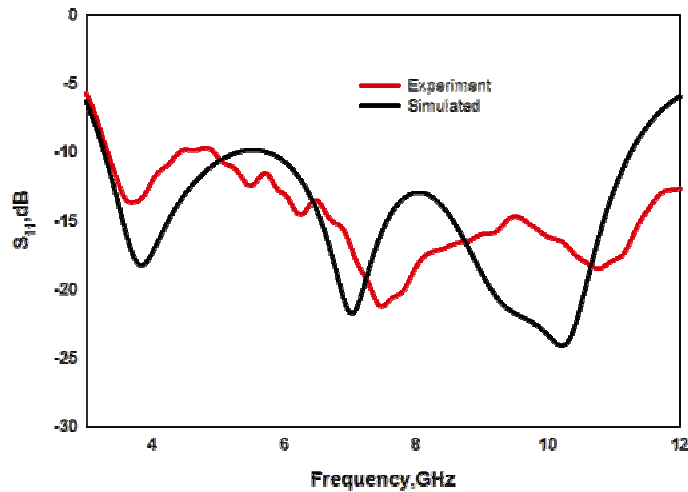


Fig.3.16. Measured and simulated reflection coefficients of the ground modified monopole antenna
($L=30\text{mm}$, $W=25\text{mm}$, $L_1=24\text{mm}$, $W_1=3\text{mm}$, $H=15\text{mm}$, $R=9\text{mm}$, $L_f=17\text{mm}$, $W_g=13\text{mm}$, $S=2\text{mm}$, $h=1.6\text{mm}$, $\epsilon_r=4.4$, $G=0.35\text{mm}$)

Ultra wide band width is produced by merging of the resonances produced due to the combined effect of top loaded rectangle and the modified ground plane. Due to simple strip monopole, two resonances are produced at 7.71GHz and 11.1GHz. By top loading, first and second resonances are shifted to 4.55GHz and 10.6GHz respectively. Removing two quarter circles from the ground results in the creation of a new resonance at 7GHz and merging of these resonances results in UWB operation.

3.1.3.3 Parametric Analysis of Ground Modified Monopole Antenna

In order to investigate the effect of various structural and substrate parameters on the antenna characteristics, a parametric analysis is performed with the help of the simulation software. Results of the parametric analysis along with concluding remarks for each study are narrated in the following sections.

3.1.3.3.1 Effect of radius of quarter circle (R)

The important parameter affecting the performance of ground modified antenna is the radius of the circle R etched from the ground plane. Fig.3.17 shows the variations in reflection coefficients of the antenna with different values of R. When R=0, ie, for normal rectangular ground, the antenna has two resonances at 4.55GHz and 10.6GHz. Increasing R to 7mm improves the matching and a new resonance is created at 6.16GHz. Increasing R shifts the second and third resonances to higher frequencies with the decrease of the first resonance. Maximum matching and bandwidth is obtained for R=9mm. Further increase in R deteriorates the matching and bandwidth. So optimum value of 9 mm is chosen. From the impedance plots also it is clear that impedance matching is obtained for the optimum design compared to rectangular ground. It is found that for better impedance characteristics the optimum radius $R=0.357\lambda_m$ where λ_m is the wavelength corresponding to centre frequency of operating band.

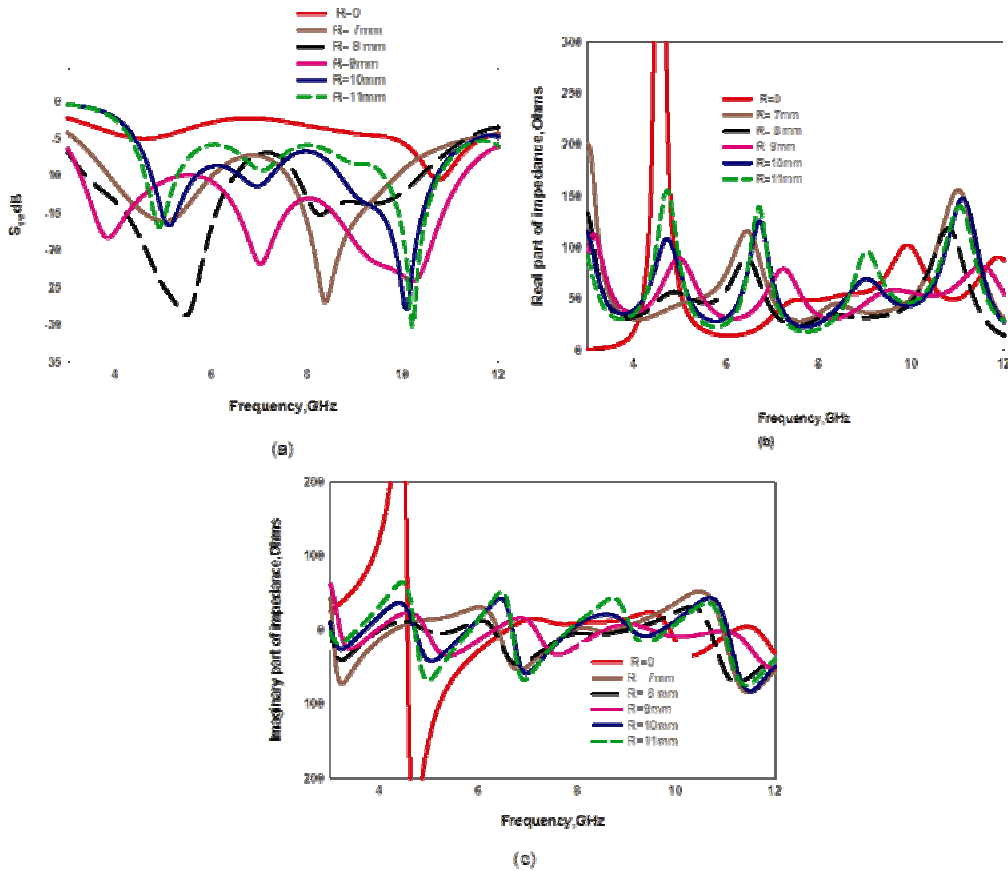


Fig.3.17. Reflection coefficient and input impedances of ground modified monopole antenna for different R
 $(L=30\text{mm}, W=25\text{mm}, L_1=24\text{mm}, W_1=3\text{mm}, H=15\text{mm}, L_f=17\text{mm}, W_g=13\text{mm}, S=2\text{mm}, h=1.6\text{mm}, \epsilon_r=4.4, G=0.35\text{mm})$ (a)Reflection coefficient(b)Real part of impedance(c)Imaginary part of impedance.

3.1.3.3.2 Effect of top loaded rectangle L_1

Figure 3.18 shows the variation of reflection coefficients and impedances of the antenna for different lengths of top loaded rectangle L_1 . It is clear from the figure that optimum performance is obtained for $L_1=24\text{mm}$. For $L_1=20\text{mm}$, impedance matching is poor. Increasing L_1 to 22mm, increases the impedance match and for optimum L_1 of 24mm, required UWB performance is obtained. Further increase in L_1 deteriorates impedance matching. Thus the length of the top loaded rectangle mainly influences the matching of the antenna and

resonances are lightly affected. The optimum L_1 is found to be $0.952\lambda_m$ where λ_m is the wavelength corresponding to centre frequency of operating band.

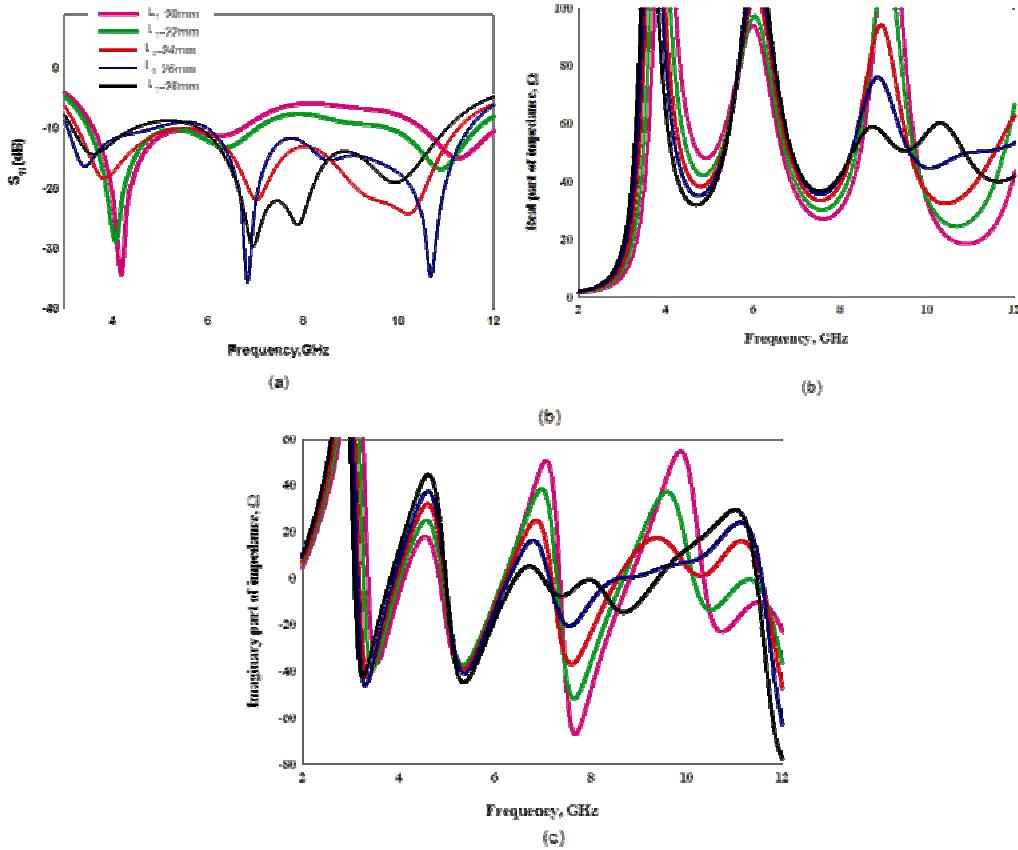


Fig.3.18. Reflection coefficients and input impedances of the ground modified monopole antenna for different L_1 ($L=30\text{mm}$, $W=25\text{mm}$, $W_1=3\text{mm}$, $H=15\text{mm}$, $R=9\text{mm}$, $L_f=17\text{mm}$, $W_g=13\text{mm}$, $S=2\text{mm}$, $h=1.6\text{mm}$, $\epsilon_r= 4.4$, $G=0.35\text{mm}$.)(a)Reflection coefficient (b) Real part (c) Imaginary part.

3.1.3.3.3 Effect of gap distance S

The effect of gap S between the monopole and the ground is also studied. Figure 3.19 shows the variation of reflection coefficients for different values of S . For $S=1\text{mm}$, -10dB band starts from 4GHz with poor matching at the mid frequencies. And for $S=3\text{mm}$, impedance matching is poor. Optimum performance

is obtained for $S=2\text{mm}$. From the impedance plot also it is clear that only for $S=2\text{mm}$, real part of impedance oscillates around 50Ω and imaginary part oscillate around 0Ω . Thus the optimum gap distance S is selected to be $0.079\lambda_m$ where λ_m is the wavelength corresponding to centre frequency of operating band.

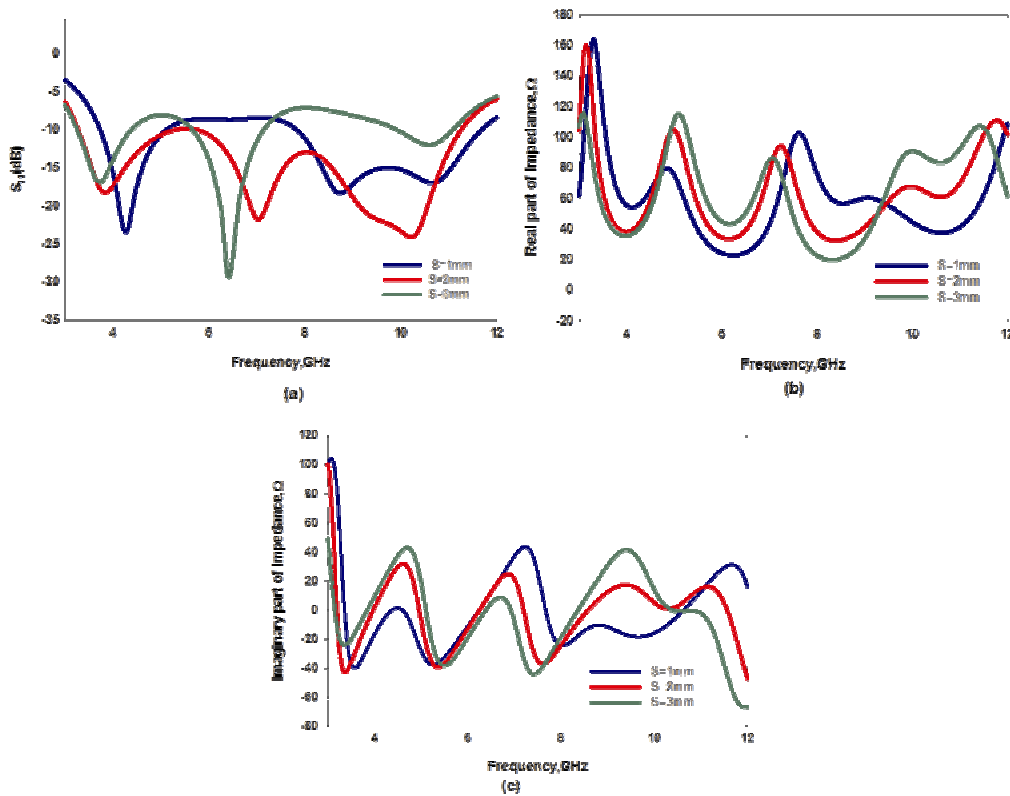


Fig.3.19. Reflection coefficient of ground modified monopole antenna for different S
 $(L=30\text{mm}, W=25\text{mm}, L_1=24\text{mm}, W_1=3\text{mm}, H=15\text{mm}, R=9\text{mm}, L_f=17\text{mm}, W_g=13\text{mm}, h=1.6\text{mm}, \epsilon_r=4.4, G=0.35\text{mm}).$ (a)Reflection coefficient(b)Real part of impedance(c)Imaginary part of Impedance.

3.1.3.4 Simulated Current distribution and radiation pattern of the ground modified monopole antenna

Fig.3.20 shows the surface currents & field distributions on the antenna along with their corresponding 3D radiation patterns at 3.6GHz, 7.5GHz and 10.7GHz. At first resonance, almost omni directional pattern is obtained since

top loaded rectangle is mainly contributing for the resonance. But at second and third resonances, patterns are losing their omnidirectional behavior since ground plane also contributing to these resonances.

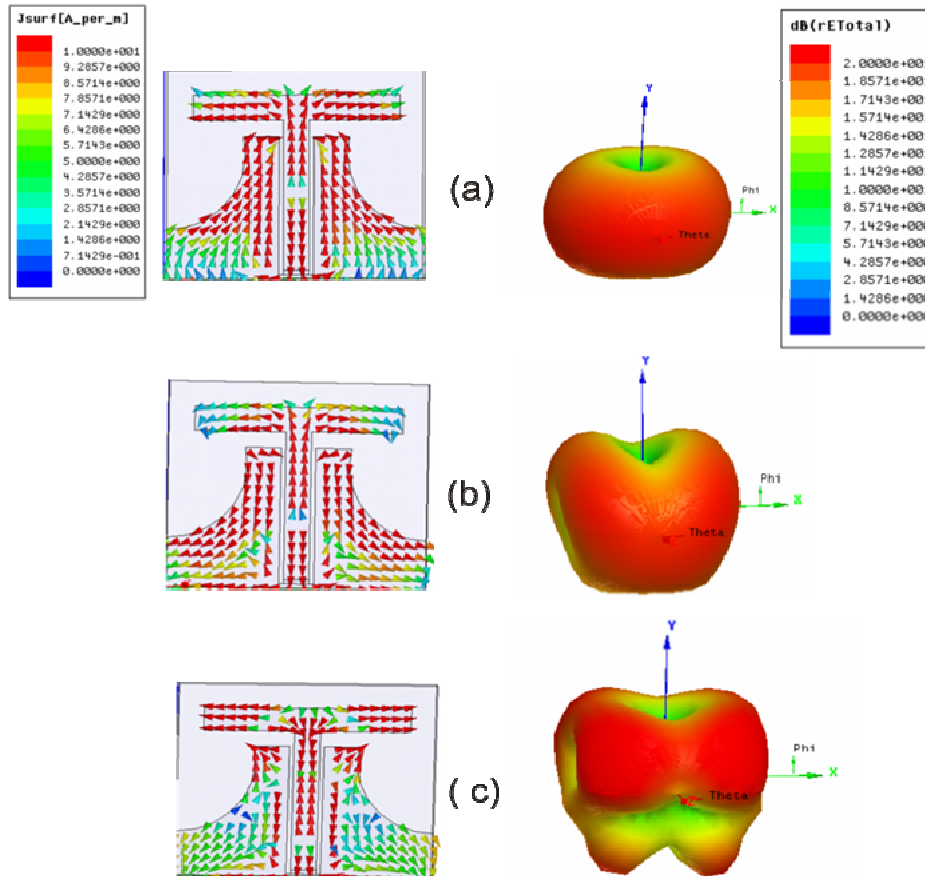


Fig.3.20. Simulated current distribution and radiation pattern of the ground modified monopole antenna at (a)3.6GHz(b) 7.5GHz and (c) 10.7GHz ($L=30\text{mm}$, $W=25\text{mm}$, $L_1=24\text{mm}$, $W_1=3\text{mm}$, $H=15\text{mm}$, $R=9\text{mm}$, $L_f=17\text{mm}$, $W_g=13\text{mm}$, $h=1.6\text{mm}$, $\epsilon_r=4.4$, $G=0.35\text{mm}$).

3.1.3.5 Measured Radiation Pattern of the ground modified monopole antenna

The measured radiation patterns of the antenna in two principle planes at frequencies 3.1GHz, 3.7GHz, 7.4GHz, 10.7GHz and 12GHz are plotted in Fig.3.21(a)-(e).

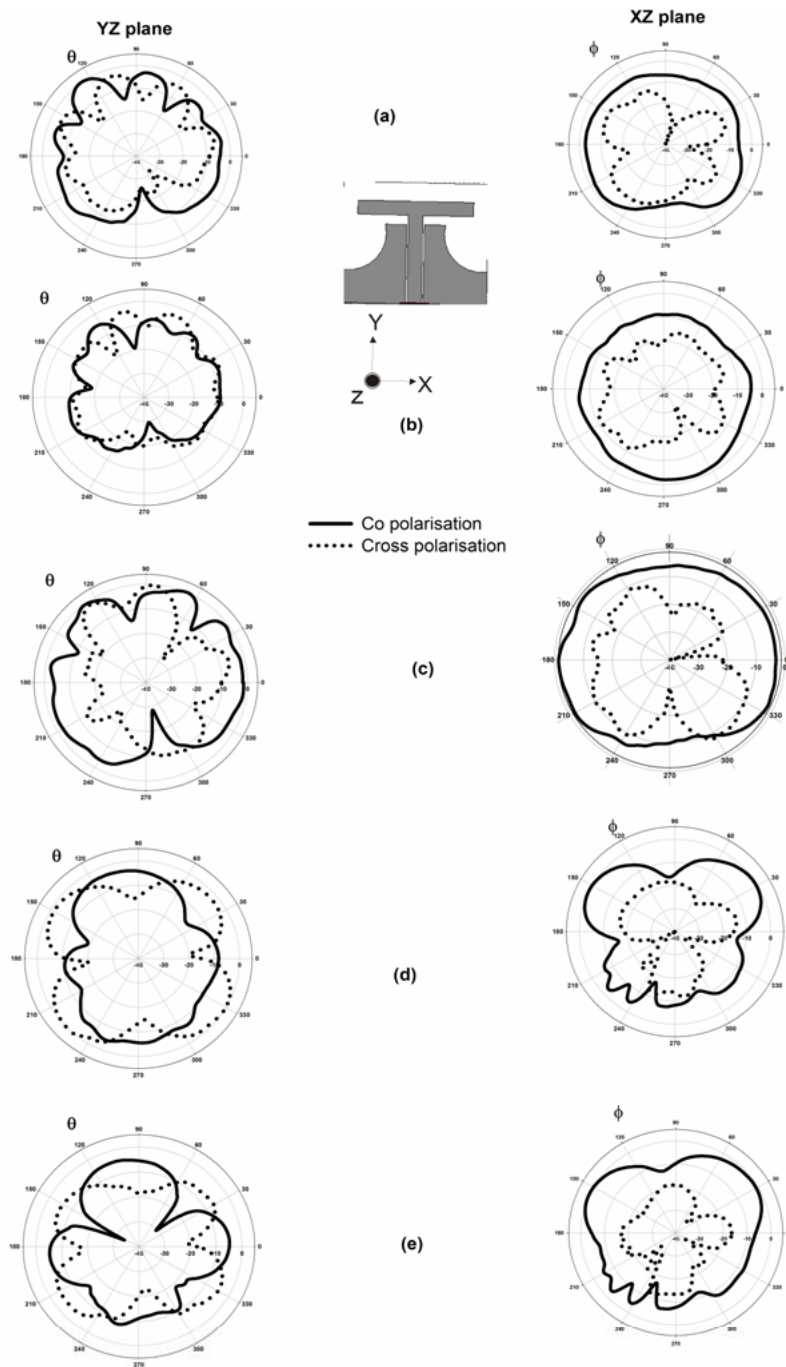


Fig.3.21. Radiation pattern of the ground modified monopole antenna at (a)3.1GHz(b)3.6GHz(c)7.5GHz (d)10.7GHz and (e)12GHz ($L=30\text{mm}$, $W=25\text{mm}$, $L_1=24\text{mm}$, $W_1=3\text{mm}$, $H=15\text{mm}$, $R=9\text{mm}$, $L_f=17\text{mm}$, $W_g=13\text{mm}$, $h=1.6\text{mm}$, $\epsilon_r=4.4$, $G=0.35\text{mm}$).

The antenna shows almost omnidirectional pattern for most of the frequency bands from 3.1 to 7.4GHz. However at higher frequencies patterns are slightly distorted.

3.1.3.6 Gain and Efficiency of the ground modified monopole antenna

The boresight gain is measured using gain comparison method and is shown in Fig.3.22. In the entire band the antenna shows reasonable gain with a peak gain of 5dBi at 9 GHz. The efficiency of the antenna is also measured using Wheeler cap method. An average efficiency of 70% is obtained.

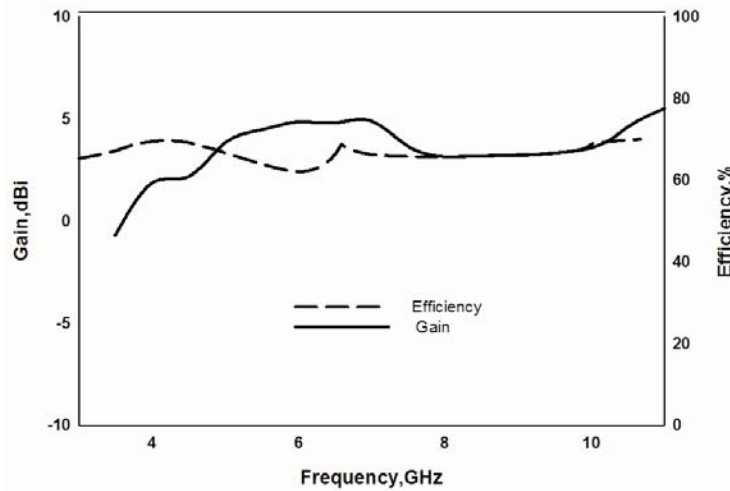


Fig.3.22 Gain and efficiency of the ground modified monopole antenna
 ($L=30\text{mm}$, $W=25\text{mm}$, $L_1=24\text{mm}$, $W_1=3\text{mm}$, $H=15\text{mm}$, $R=9\text{mm}$,
 $L_f=17\text{mm}$, $W_g=13\text{mm}$, $h=1.6\text{mm}$, $\epsilon_r=4.4$, $G=0.35\text{mm}$).

3.1.3.7 Design of the ground modified monopole antenna

Based on the parametric studies aforementioned, a design procedure for the antenna is developed. Since we are interested in the ultra wide band width, mean frequency of operating band is taken into account while deriving the design equations. The step by step procedure for designing the antenna is as follows.

1) Design a 50 Ω CPW line on a substrate with permittivity ϵ_r . Calculate ϵ_{reff} using $\epsilon_{\text{reff}} = (\epsilon_r + 1)/2$ where ϵ_{reff} is the effective permittivity of the substrate.

2) Design the T monopole using the dimensions

$$L_1 = 0.952 \lambda_m \text{(3.1)}$$

$$W_1 = 0.119 \lambda_m \text{(3.2)}$$

where λ_m is the wavelength corresponding to centre frequency of the operating band.

3) Design the ground on both sides of the feed line using

$$L_g = 0.674 \lambda_m \text{(3.3)}$$

$$W_g = 0.515 \lambda_m \text{(3.4)}$$

4) Remove two quarter circles of radius $R = 0.367 \lambda_m$ centered at $(0, H, h)$ and (L, H, h) from the ground where

$$R = 0.357 \lambda_m \text{(3.5)}$$

$$H = 0.59 \lambda_m \text{(3.6)}$$

5) Length of the feedline L_f and the gap S are calculated using

$$L_f = 0.674 \lambda_m \text{(3.7)}$$

$$S = 0.079 \lambda_m \text{(3.8)}$$

In order to justify the design equations, the antenna parameters are computed for different substrates (Table 3.1) and are tabulated in Table 3.2.

Table 3.1. Antenna Description

Laminate	Antenna 1 Rogers 5880	Antenna 2 FR4 Epoxy	Antenna 3 Rogers RO3006	Antenna 4 Rogers6010LM
h(mm)	1.57	1.6	1.28	0.635
ϵ_r	2.2	4.4	6.15	10.2
ϵ_{re}	1.6	2.7	3.575	5.6
W(mm)	4	3	2.58	2.05
G(mm)	0.17	0.35	0.45	0.5

Table 3.2 Computed Geometric Parameters of the Antenna

Parameter (mm)	Antenna 1	Antenna 2	Antenna 3	Antenna 4
L_1	31	24	20.71	16.29
W_1	3.89	3	2.59	2.04
H	19.29	15	12.8	10.11
R	12	9.25	8	6.29
L_f	22	17	14.69	11.55
L_g	22	17	14.69	11.55
W_g	16.8405	13	11.227	8.83
S	2.59	2	1.722	1.354

Fig 3.23 shows the simulated reflection coefficients of different antennas as given in Table 3.2. In all the cases antenna is operating in the UWB region.

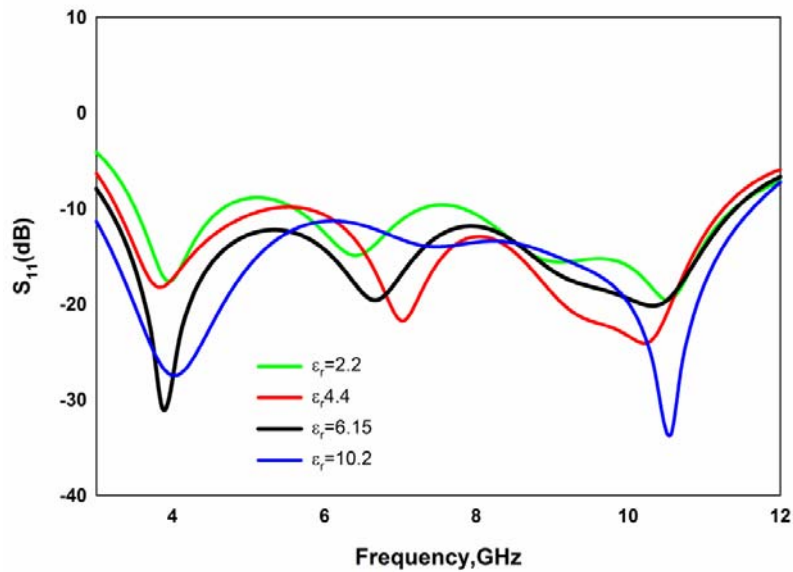


Fig. 3.23. Reflection coefficient of the antenna with computed geometric parameter for different substrates.

3.2 Planar Serrated Microstrip Fed Monopole UWB Antenna

In the previous session, we have analyzed a ground modified monopole antenna. The antenna has a dimension of $30 \times 22 \text{mm}^2$. It is observed that the antenna exhibits poor YZ plane radiation characteristics for the entire band of operation especially at higher frequencies. The above ground modified antenna can be modified to achieve compactness and good radiation characteristics by modifying the patch by increasing the top loaded strip width.

3.2.1 Evolution of the Antenna

Fig.3.24 shows the evolution of the serrated UWB antenna. The design starts with a conventional microstrip fed monopole antenna (Antenna 1). Strip monopole antenna is fabricated on a substrate with relative permittivity $\epsilon_r = 4.4$ and thickness $h = 1.6 \text{mm}$. A strip of length L_m and width W is used. A rectangular ground plane of dimensions $W_g \times L$ is printed on the other side of the substrate parallel and symmetric to the strip.

Top loading this with a rectangle of same length and width results in Antenna 2. Top loading increases the bandwidth of the antenna. Finally UWB antenna is obtained by making serrations both on the ground plane and the patch resulting in antenna 3.

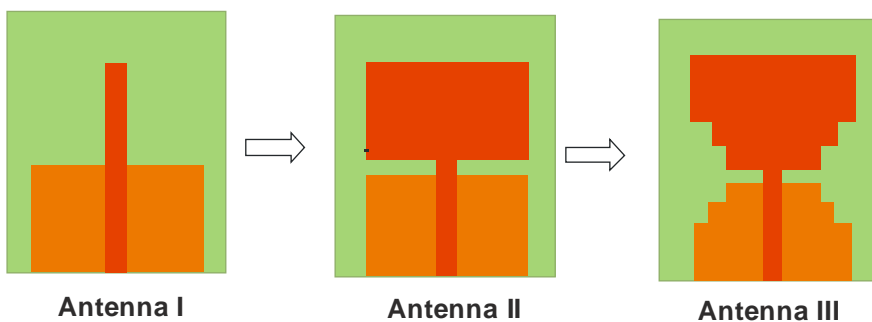


Fig.3.24. Evolution of the serrated monopole antenna(a)Microstrip fed strip monopole antenna(b)Top loaded monopole antenna and(c)Serrated UWB monopole antenna.

3.2.1.1 A simple microstrip fed monopole Antenna (Antenna I)

The conventional monopole antenna mainly consists of a radiating element vertically above the large ground plane. For better radiation performance, the radiating element of quarter wavelength is placed perpendicular to a large ground plane. This classical antenna provides nearly omni-directional radiation pattern with moderate gain and efficiency. The major drawback of this antenna is the large ground plane and not suited for modern communication systems.

The planar version of the conventional monopole antenna is very attractive because, it maintains almost similar radiation performance as that of the conventional monopole along with compactness. These conformal antennas can be fabricated with ground plane on the printed circuit board parallel to the radiator either on the same side or at the opposite side and can be easily integrated to the system circuit board.

A strip monopole antenna, fabricated on a substrate with relative permittivity $\epsilon_r = 4.4$ and thickness $h=1.6\text{mm}$ is depicted in Fig.3.25. A strip of length L_m and width W is used. For the present analysis the width of the radiating monopole is selected as the width of 50Ω microstrip line. A rectangular ground plane of dimensions $W_g \times L$ is printed on the other side of the substrate parallel and symmetric to the strip as shown in Fig.3.25.

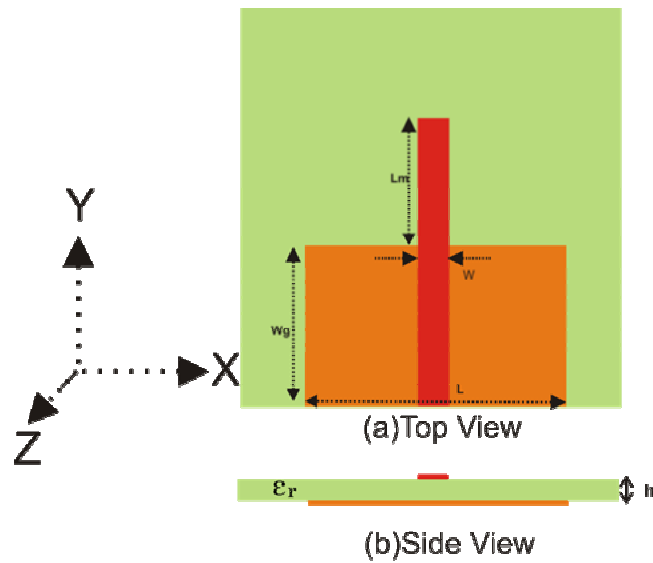


Fig.3.25. Geometry of a strip monopole antenna (Antenna I)
 ($L_m=14\text{mm}$, $W=3\text{mm}$, $W_g=12\text{mm}$, $L=20\text{mm}$, $L_m=14\text{mm}$, $\epsilon_r=4.4$,
 $h=1.6\text{mm}$)

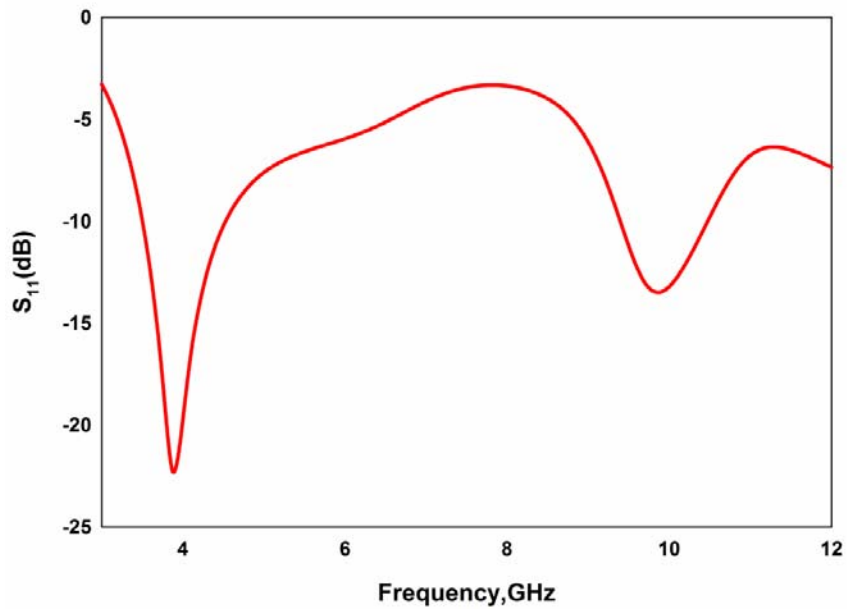


Fig.3.26. Reflection coefficient of strip monopole antenna (Antenna I)
 ($L_m=14\text{mm}$, $W=3\text{mm}$, $W_g=12\text{mm}$, $L=20\text{mm}$, $L_m=14\text{mm}$,
 $\epsilon_r=4.4$, $h=1.6\text{mm}$)

Simulated reflection coefficient curve shown in Fig.3.26 indicates that the antenna has two resonances at 3.87GHz and 9.88GHz respectively. The -10dB bandwidth extends from 3.48 GHz to 4.48 GHz for the first band. Second resonance is at 9.88GHz with bandwidth ranging from 9.36GHz to 10.52GHz.

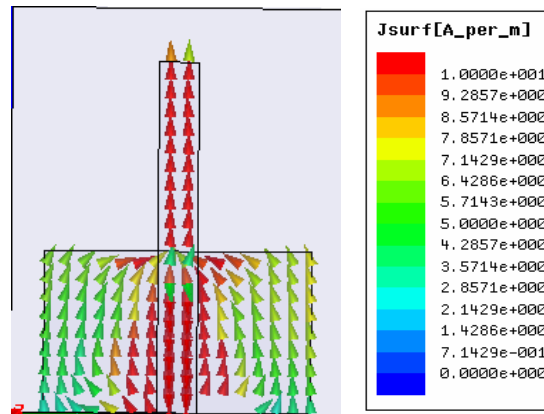


Fig.3.27 Current distribution of Antenna 1 at 3.87GHz
**($L_m=14\text{mm}$, $W=3\text{mm}$, $W_g=12\text{mm}$, $L=20\text{mm}$, $L_m=14\text{mm}$, $\epsilon_r=4.4$,
 $h=1.6\text{mm}$)**

A better understanding about the resonance behavior of the strip monopole is obtained from the current density plot shown in Fig. 3.27. A quarter wave current density variation is found along the strip above the ground plane at first resonant frequency. The current is maximum at the feed point and zero at the open end. The polarization of the antenna can be observed from the current density plot. By analyzing the plot, it is found that, the direction of the current throughout the strip is along the Y-axis and hence it is Y polarized.

A close look at the current distribution at the second resonance in the return loss response is shown in Fig.3.28. According to the current distribution even though the monopole and ground plane are separate entities, they excite a common mode by utilizing the current paths as shown in Figure. In this case an L shaped and reflected L (\perp) shaped current paths are formed by utilizing the top strip monopole and either

side of the ground plane width. But the interesting point to be noted is that ground strip current variation for the second resonance is larger in magnitude compared to the first resonance but out of phase. Hence the effect of these currents contributing towards radiation is again negligible. So in this frequency also the top strip monopole acts as main radiator, yielding Y polarization same as in the first case. Hence it can be concluded that throughout the resonant band the antenna is polarized along Y direction with similar radiation characteristics.

However, the bandwidth of the strip monopole is narrow and not suitable for the present day communication requirements. An attempt is made to increase the bandwidth of the antenna by top loading with a rectangular patch. This aspect is elaborately described in the next section.

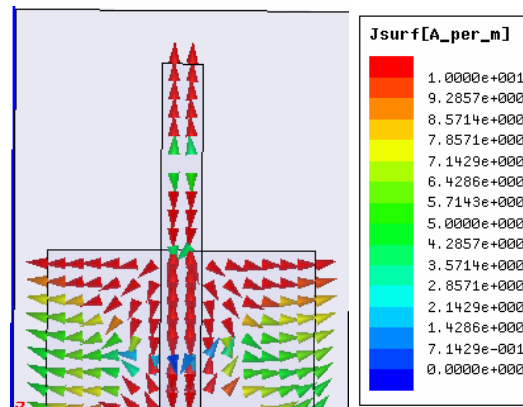


Fig.3.28 Current distribution of Antenna 1 at 9.88GHz
($L_m=14\text{mm}$, $W=3\text{mm}$, $W_g=12\text{mm}$, $L=20\text{mm}$, $L_m=14\text{mm}$, $\epsilon_r=4.4$,
 $h=1.6\text{mm}$)

3.2.1.2 Top loaded strip monopole antenna (Antenna II)

The geometry of the top loaded monopole antenna is shown in Fig.3.29. The strip monopole is loaded with a rectangle of length 20mm and width 12mm. Here the dimension of the ground plane is also same as that of the top loaded patch. Both the strip monopole and the patch are fabricated on

a substrate with relative permittivity, $\epsilon_r = 4.4$ and thickness, $h = 1.6\text{mm}$. Reflection coefficient of the antenna shown in Fig. 3.29 indicates that the resonant frequency of the antenna is shifted to 4.5GHz with a bandwidth 2.28GHz.

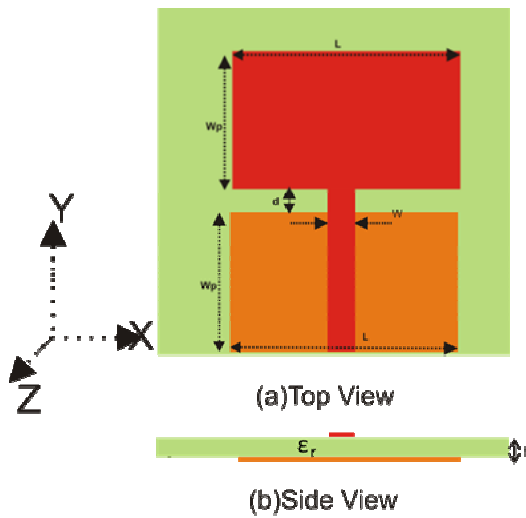


Fig.3.29. Geometry of the top loaded monopole antenna (AntennaII)
 ($L=20\text{mm}, W=3\text{mm}, Wp=12\text{mm}, d=2\text{mm}, \epsilon_r=4.4, h=1.6\text{mm}$)

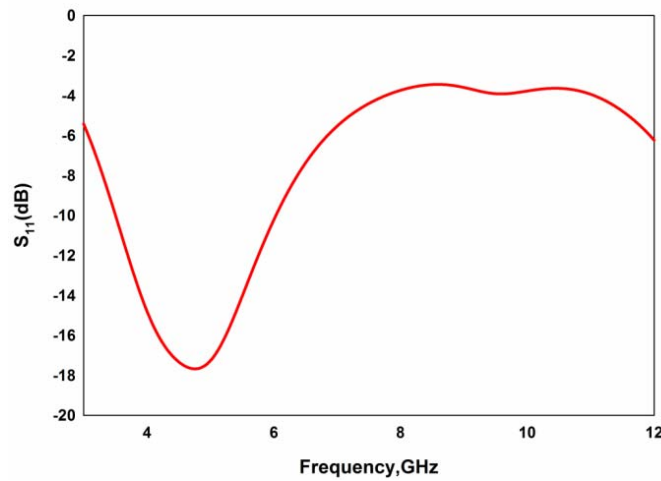


Fig.3.30. Reflection coefficient of strip monopole antenna (AntennaII)
 ($L=20\text{mm}, W=3\text{mm}, Wp=12\text{mm}, d=2\text{mm}, \epsilon_r=4.4, h=1.6\text{mm}$)

Variations of reflection coefficient with width of the top loaded rectangles are done and are shown in Fig.3.31. It is found that increasing W_p decreases the resonant frequency but increases the bandwidth. $W_p=12\text{mm}$ is chosen as optimum considering maximum compactness and bandwidth. After exhaustive experimental studies W_p is optimised to be $0.321 \lambda_c$ where λ_c is the wavelength corresponding to centre frequency of operating band.

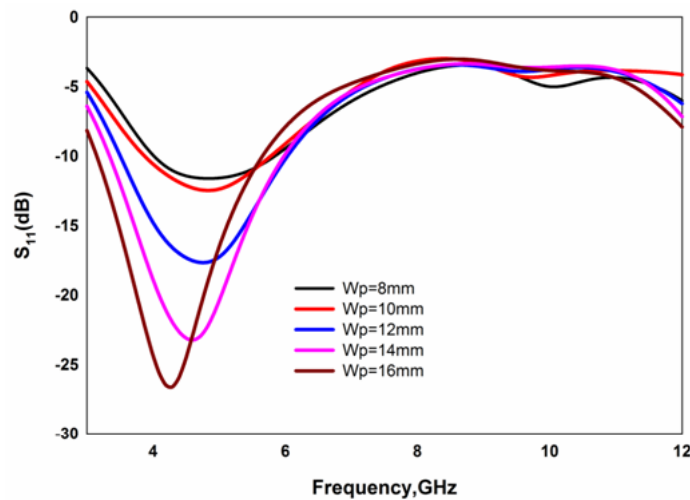


Fig.3.31. Variation of reflection coefficients for different W_p values of top loaded rectangle of Antenna 2 ($L=20\text{mm}$, $W=3\text{mm}$, $d=2\text{mm}$, $\epsilon_r=4.4$, $h=1.6\text{mm}$)

Resonance mechanism of the top loaded monopole can be better understood by examining the surface current distribution. On examining the current distribution at 4.5GHz, as shown in Fig.3.32, we can see that there is a quarter wave variation along the edge of the rectangular patch. Also it is found that surface current at the tip of the patch is minimum. In the ground plane current is maximum at the top. So it is inferred that any variation in these positions may alter the current path and this principle is used in upcoming design procedures.

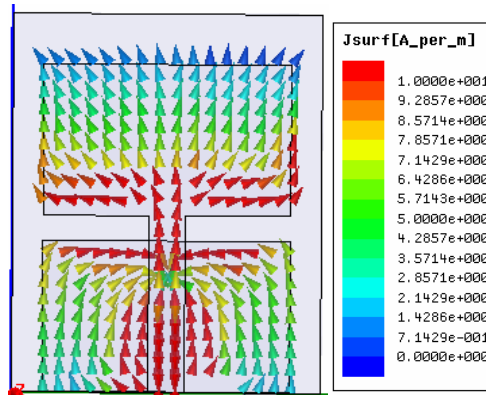


Fig.3.32. Surface current distribution of the antenna II at 4.5GHz
 ($L=20\text{mm}, W=3\text{mm}, W_p=12\text{mm}, d=2\text{mm}, \epsilon_r=4.4, h=1.6\text{mm}$)

With an aim of increasing the bandwidth, serrations are made on the patch and on the ground plane as shown in Fig.3.33 and corresponding reflection coefficients are shown in Fig.3.33. It is found that for a single pair of serrations (Fig.3.33(a)), -10dB bandwidth extends from 3.1GHz to 6.8GHz and is shown as black line on Fig.3.32. But in the case of antenna with two pairs of serrations on the patch (Fig.3.33(b)), -10dB bandwidth is from 3GHz to 7.5GHz (Blue line in Fig.3.34). Finally in addition two pairs of serrations on the radiating patch, a pair of serrations is inserted on the ground plane also (Fig.3.33(c)). In that case -10dB bandwidth extends from 3GHz to 7.8GHz and is shown as red line in Fig.3.34.

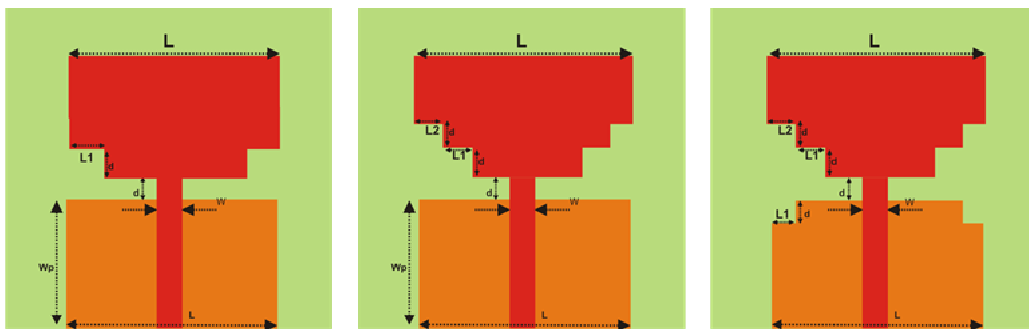


Fig.3.33. Top loaded antenna with (a)A pair of serrations on the patch(b)Two pairs of serrations on the patch(c)Two pair of serrations on the patch and one pair on ground
 ($L=20\text{mm}, W=3\text{mm}, W_p=12\text{mm}, d=2\text{mm}, L_1=4\text{mm}, L_2=2.5\text{mm}$)

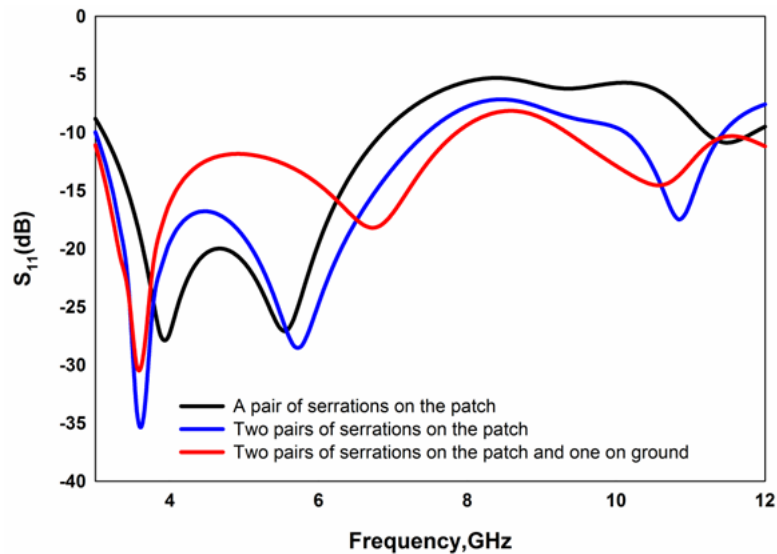


Fig.3.34. Reflection coefficients of antennas shown in Fig.3.33
($L=20\text{mm}$, $W=3\text{mm}$, $W_p=12\text{mm}$, $d=2\text{mm}$, $L_1=4\text{mm}$, $L_2=2.5\text{mm}$)

3.2.1.3 Micro strip fed serrated monopole Antenna (Antenna III)

In the previous sessions, we have analyzed a simple strip monopole antenna and a top loaded strip monopole antenna. It is found that making serrations on the top loaded monopoles increases the bandwidths. With an aim of producing a UWB antenna with this compact dimension, one more pair of serrations are made on the ground plane forming a stair case structure as shown in Fig.3.35.

Making serrations are aimed to change the distance between the lower part of the planar monopole antenna and the ground plane in order to tune the capacitive coupling between the antenna and the ground plane, thereby to widen the impedance bandwidth. For the two steps, the return loss curve is the best, covering 3.17 GHz to 11.5 GHz of frequency ranges. If we increase the number of serrations further, bandwidth degrades.

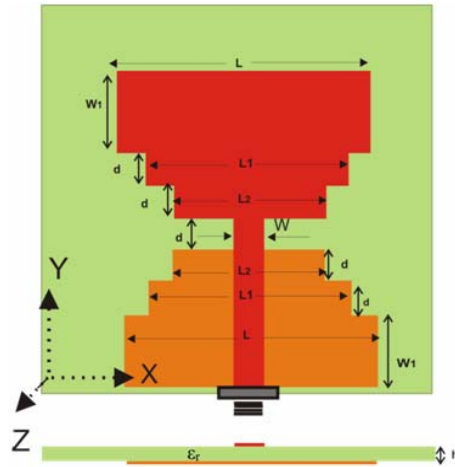


Fig.3.35. Geometry of the serrated monopole antenna(Antenna III)
 ($L=20\text{mm}, L_1=15\text{mm}, L_2=12\text{mm}, d=2\text{mm}, W_1=8\text{mm}, W=3\text{mm},$
 $\epsilon_r= 4.4, h=1.6\text{mm}$)

The ground plane acts as an impedance matching element of the antenna. Modifying the partial ground plane to staircase ground plane has improved the reflection coefficient of antenna, especially at higher frequencies.

3.2.1.3.1 Reflection Characteristics of Micro strip fed serrated monopole Antenna

Fig.3.36 shows measured and simulated reflection coefficients of the antenna III. Antenna shows a 2:1 VSWR bandwidth from 3.09 to 11.6GHz with three resonances centered at 3.6GHz, 6.7GHz and 9.8GHz respectively.

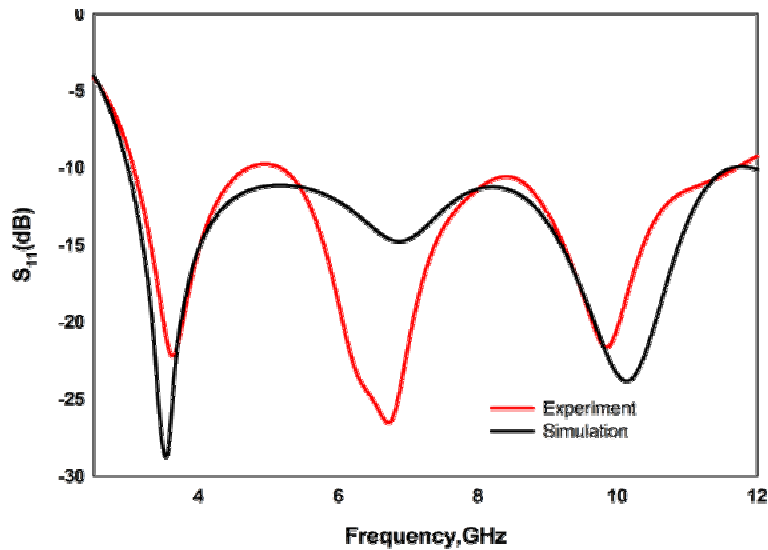


Fig.3.36. Measured and simulated Reflection coefficients of the serrated monopole antenna
**($L=20\text{mm}$, $L_1=15\text{mm}$, $L_2=12\text{mm}$, $d=2\text{mm}$, $W_1=8\text{mm}$, $W=3\text{mm}$,
 $\epsilon_r=4.4$, $h=1.6\text{mm}$)**

3.2.1.3.2 Current distribution and radiation pattern of the serrated monopole antenna

The reflection coefficient can only describe the behavior of an antenna as a lumped load at the end of feeding line. The detailed EM behavior of the antenna can only be revealed by examining the field/current distributions or radiation patterns. The typical current distributions on the antenna at three resonance frequencies are plotted in Fig. 3.37.

These current distributions reveal that the antenna gives almost omnidirectional pattern for the first two resonances. But at the third resonance pattern is slightly distorted. First resonance is found due to a $\lambda/4$ variation along the edge of the steps. It is also found that in all cases current is flowing mainly through step edges.

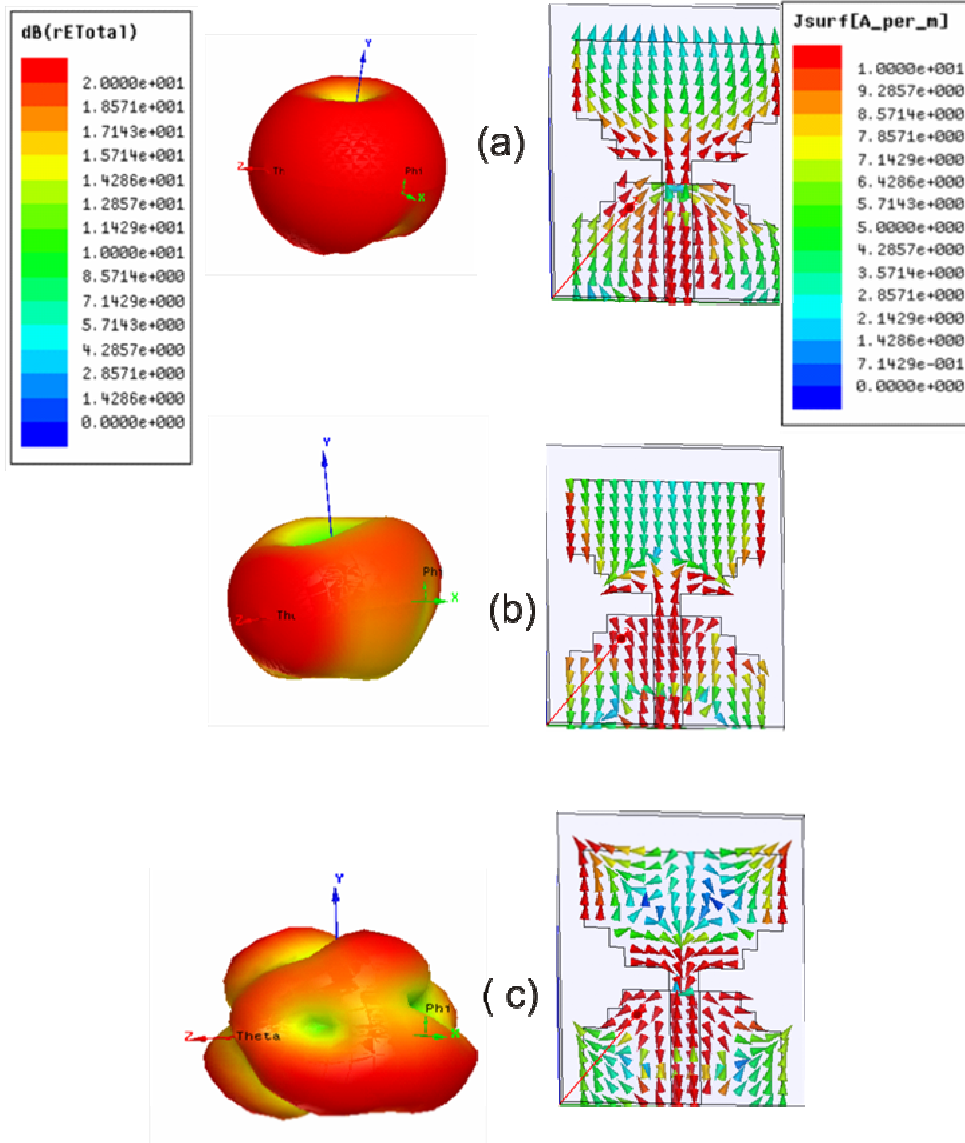


Fig.3.37. Current distribution and radiation pattern of the serrated monopole antenna at (a)3.6 GHz (b)6.7 GHz and (c)9.8GHz ($L=20\text{mm}$, $L_1=15\text{mm}$, $L_2=12\text{mm}$, $d=2\text{mm}$, $W_1=8\text{mm}$, $W=3\text{mm}$, $\epsilon_r=4.4$, $h=1.6\text{mm}$)

3.2.1.3.3 Measured radiation pattern of the serrated monopole antenna

The measured E and H plane radiation patterns of the antenna for three different frequencies are shown in Fig.3.38. Monopole like radiation patterns

are obtained in the YZ plane and nearly omni directional radiation pattern is observed in XZ plane. In addition the antenna is linearly polarized along Y direction in the entire operating band. It is also found that radiation pattern is not much distorted at higher frequencies as in the case of ground modified antenna.

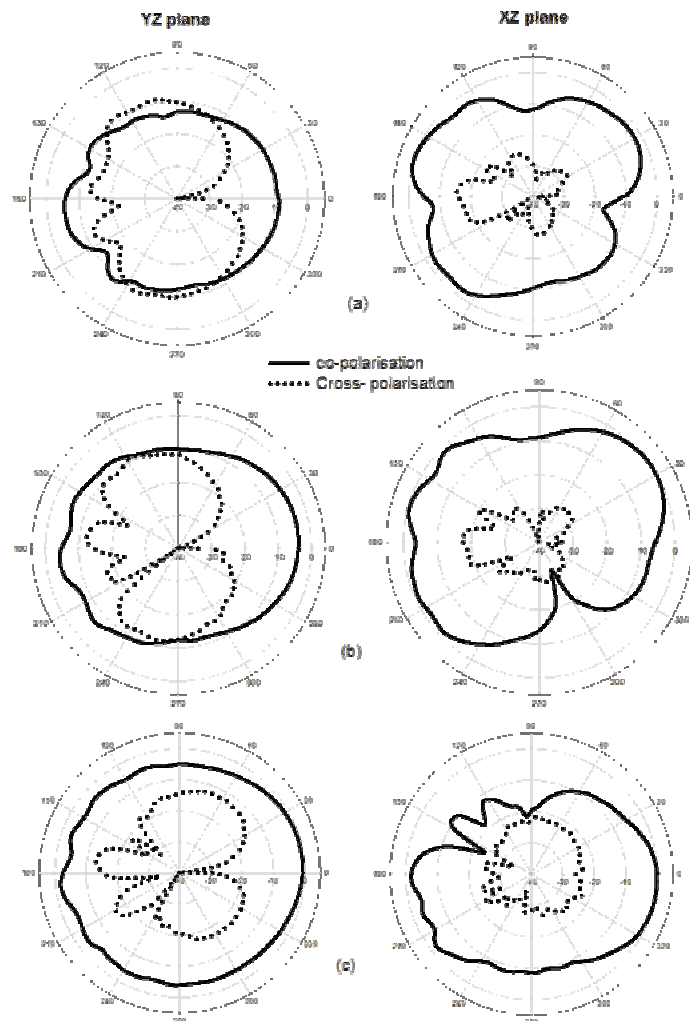


Fig.3.38. Measured radiation patterns of the serrated monopole antenna at (a)3.6 GHz(b)6.7GHz and (c)9.8GHz ($L=20\text{mm}$, $L_1=15\text{mm}$, $L_2=12\text{mm}$, $d=2\text{mm}$, $W_1=8\text{mm}$, $W=3\text{mm}$, $\epsilon_r=4.4$, $h=1.6\text{mm}$)

3.2.1.3.4 Parametric Analysis of Serrated Monopole Antenna

The parametric study is carried out to optimize the antenna and provide more information about the effects of essential design parameters.

3.2.1.3.4.1 Effect of width W_1 of patch

Fig.3.39 shows the reflection coefficient for different values of W_1 . It is observed that start frequency decreases from 3.6GHz to 3GHz when W_1 is varied from 2mm to 8mm. Thus for UWB operation, W_1 is fixed at 8mm. Further increasing W_1 increases the compactness of the antenna.

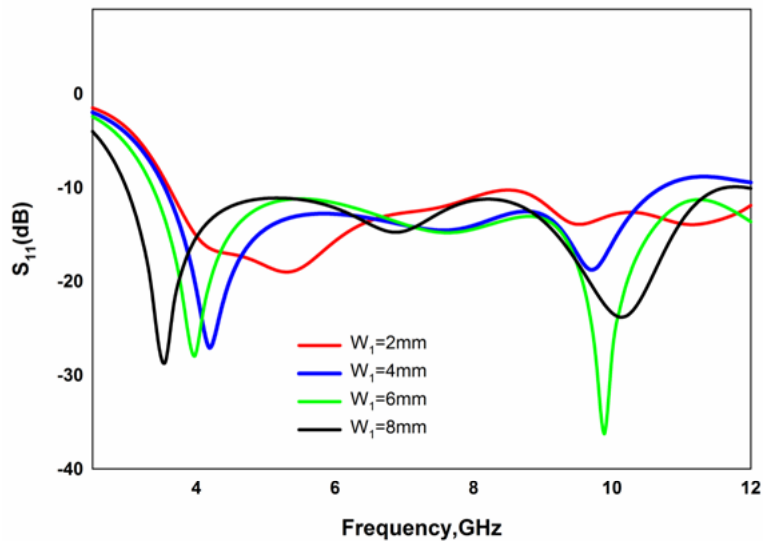


Fig.3.39. Reflection coefficient of serrated monopole antenna for different values of W_1
($L=20$ mm, $L_1=15$ mm, $L_2=12$ mm, $d=2$ mm, $W=3$ mm, $\epsilon_r=4.4$, $h=1.6$ mm)

3.2.1.3.4.2 Effect of gap d

The effect the feed gap distance (d) on the impedance bandwidth is studied. From the simulation results in Figure 3.40, it is found that the impedance bandwidth is effectively improved when separation ' d ' is changed. It is seen that the lower edge frequency of the impedance bandwidth is reduced

with increasing gap but the matching becomes poor for larger values. By varying d , the electromagnetic coupling between the lower edge of the rectangular patch and the ground plane can be properly adjusted. For optimum match ' d ' is fixed at 2mm. It is observed from the figure that variation all the resonances are affected by the gap ' d '. This is because varying d varies the resonant lengths for all the resonances. Thus it is clear that ' d ' is an important parameter affecting both the resonant frequencies as well as the bandwidths of the antenna.

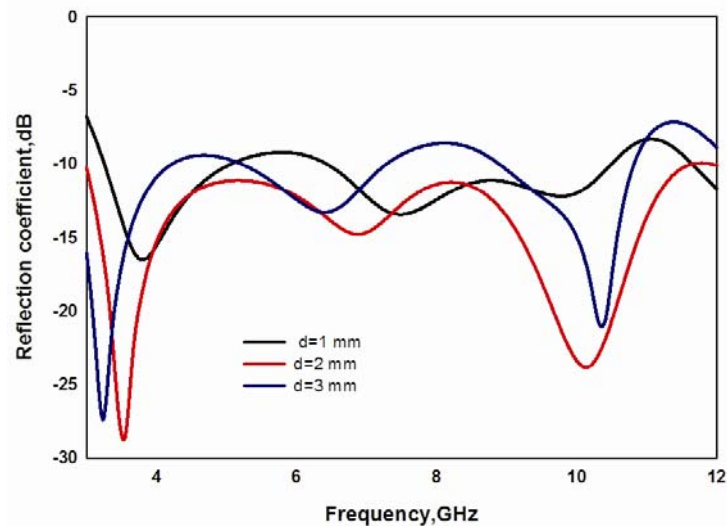


Fig.3.40. Reflection coefficient for different values of d
($L=20\text{mm}$, $L_1=15\text{mm}$, $L_2=12\text{mm}$, $W_1=8\text{mm}$, $W=3\text{mm}$,
 $\epsilon_r = 4.4\text{mm}$, $h=1.6\text{mm}$)

3.2.1.3.5 Design of serrated monopole antenna

Based on the observations aforementioned, the design procedure for the planar serrated antenna is given below.

- a) Feed line: Choose the width of the micro strip feed line W for 50Ω impedance on a substrate with permittivity ϵ_r and thickness h .

- b) Draw ground and patch of length $0.803 \lambda_c$ and width $0.321 \lambda_c$, where λ_c is the wavelength corresponding to the centre frequency of the operating band.
- c) Remove a pair of rectangles of length $0.1 \lambda_c$ and width $0.08\lambda_c$ from the bottom edges of patch.
- d) Remove one more pair of rectangles of length $0.06 \lambda_c$ and width $0.08 \lambda_c$ from the patch.
- e) Remove similar rectangles from the top of the ground also.

In order to justify the design equations, the antenna parameters are computed for different substrates (Table 3.3) and are tabulated in Table 3.4.

Table 3.3 Antenna Description

	Ant. 1	Ant. 2	Ant. 3	Ant. 4
Laminate	Rogers 5880	FR4 Epoxy	Rogers RO3006	Rogers 6010LM
h(mm)	1.57	1.6	1.28	0.635
ϵ_r	2.2	4.4	6.15	10.2
ϵ_{re}	1.6	2.7	3.575	5.6
W(mm)	3	3	3	3

Table 3.4 Computed Geometric Parameters of the Antenna

Parameter (mm)	Ant. 1	Ant.2	Ant. 3	Ant. 4
L₁	25.92	20	17.26	13.85
L₂	10.365	8	6.901	5.53
L₃	3.229	2.5	2.15	1.725
L₄	2.5832	2	1.72	1.38
L₅	1.9374	1.5	1.29	1.035
S	2.5832	2	1.72	1.38
L_f	18.14	14	12.08	9.69

Fig 3.41 shows the reflection coefficients of different antennas as given in Table 3.4. In all the cases antenna is operating in the UWB region.

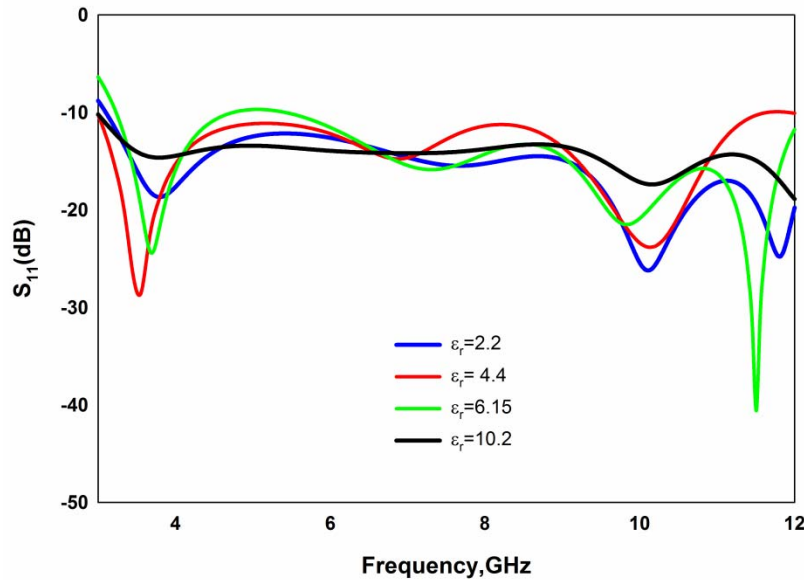


Fig.3.41. Reflection coefficient of the antenna with computed geometric parameter for different substrates.

3.2.1.3.6 Gain and Efficiency of Serrated Monopole Antenna

Measured antenna gain and efficiency of the antenna is plotted in Fig.3.42. It is found that the gain remains constant in the entire operating band with an average value of 2.5. Efficiency of the antenna in the entire band is also calculated using the Wheeler cap method. Average efficiency of the antenna is found to be 85%.

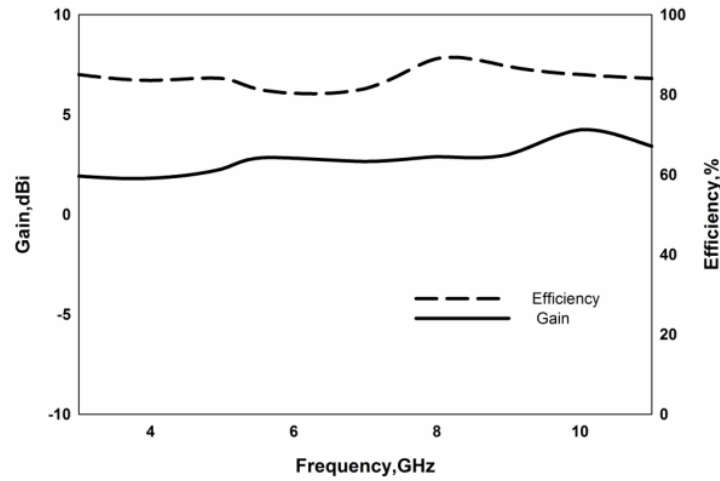


Fig.3.42. Gain and efficiency of the serrated monopole antenna ($L=20\text{mm}$, $L_1=15\text{mm}$, $L_2=12\text{mm}$, $d=2\text{mm}$, $W_1=8\text{mm}$, $W=3\text{mm}$, $\epsilon_r=4.4$, $h=1.6\text{mm}$).

3.3 Band notch Design

Fascinating growth of Ultra Wide Band (UWB) Technology for future short range high speed communication has given a boom in designing wideband antennas. Due to the attractive features like wide bandwidth, simple structure and omni-directional radiation pattern, planar monopole antennas have been studied for UWB communication systems. But, UWB transmitters should not cause any electromagnetic interference (EMI) on nearby communication systems such as wireless LAN (5725–5875 MHz). To avoid the interference between the UWB and WLAN systems, a band-notch filter in UWB systems is necessary. However, the use of a filter will increase the complexity of the UWB system. Therefore, a UWB antenna having frequency band-notch characteristic can be an ideal choice to overcome this handicap. It was shown that by etching a particular geometry in the interior of the radiating element, a planar antenna can exhibit a single narrow frequency notch band while maintaining wideband performance.

The literature review shows a number of methods that are used to achieve the band-notch function. They can be basically categorized in two groups; the first group include the technique of adding a perturbation in the antenna's radiating element. Such a perturbation usually consists of a slot carved in the antenna's radiating element like cutting away a rectangular portion from the upper elliptical patch [7], inverted U-shaped slot in the radiator patch [8], two T-shaped stubs inside an ellipse slot cut in the radiation patch [9].

In the second group, a perturbation on the antenna feeding line and ground plane, rather than on the antenna's radiating element itself, is added. They include U-slot, defected ground structure (DGS) in the ground of the feed line [10], compact coplanar waveguide (CPW) resonant cell [11], L-shaped slots in the ground plane [12]. The perturbation would act as a band stop filter whose stop band is exactly the unwanted 5 to 6 GHz frequency interval.

There are other band-notch techniques like introducing split ring resonators [13], employing a Koch-curve-shaped slot [14], attaching parasitic elements near the radiating patch [15].

A planar monopole antenna with a staircase shape and small volume (25x 26x 1 mm³) is proposed by Young Jun Cho. With the use of a half-bowtie radiating element, the staircase- shape, and a modified ground plane structure, the proposed antenna has a very wide impedance bandwidth of about 11.6 GHz (2.9–14.5 GHz, bandwidth ratio about 1:5) with a notched WLAN band in the vicinity of 5 GHz[16].

T.G.Ma[17] proposed a new band-notched folded strip monopole antenna for ultrawideband applications. This antenna is composed of a fork-shape

radiator and a 50Ω microstrip line. To achieve band-reject property at the WLAN bands, the fork shaped strips are folded back resulting in a pair of coupled lines on the radiator. The length and gap width of the coupled lines primarily determine the notched frequency of the antenna.

In [18], a novel modified microstrip-fed ultra wide-band planar monopole antenna with variable frequency band-notch characteristic is presented. By inserting two slots in the ground plane on both sides of the microstrip feed line, wide impedance bandwidth is produced. A modified H-shaped conductor-backed plane with variable dimensions is used in order to generate the frequency band-stop performance and control band-notch frequency and bandwidth. The designed antenna has a small size of $22 \times 22 \text{ mm}^2$ and operates over the frequency band between 3.1 and 14 GHz for $\text{VSWR} < 2$ while showing the band rejection performance in the 5.1 to 5.9 GHz frequency band.

In [19], an elliptic-card ultra wide band planar antenna is proposed. The design consists of an elliptic radiating element and a rectangular ground plane. The feeding mechanism comprises of a microstrip line on the other side of the substrate and connecting the line to the elliptic element by a via. The structure of the antenna is miniaturized by optimizing the elliptic profile. The ground plane size is only $22 \times 40 \text{ mm}^2$. Housing effects on the antenna performance are also studied in this paper.

3.3.1 5.8 GHz Band notched UWB serrated monopole antenna

Fig.3.43 shows the geometry and dimension of the UWB antenna with band-notch characteristic from 5.04-5.81 GHz band. By removing a U-shaped slot from the stair cased rectangular-radiating patch of antenna III, a band notch performance is created. It is noteworthy that when the band-notched structure is applied to the antenna III, there is no redesigning work needed for the

previously obtained dimensions. In general, the main aim behind the design methodology of the notch behaviour is to tune the total length of the U-shaped slot approximately equal to the half guided wavelength (λ_g) of the desired notch frequency. At the desired notch frequency, the current distribution is around the U-shaped slot. Hence, a destructive interference for the excited surface current will occur, which causes the antenna to be non-responsive at that frequency. The input impedance closer to the feed point, changes abruptly making large reflections at the required notch frequency.

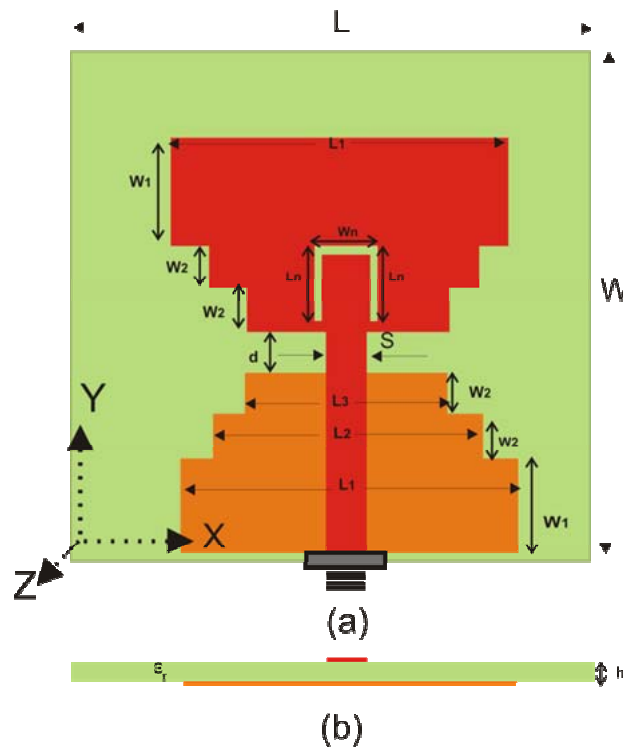
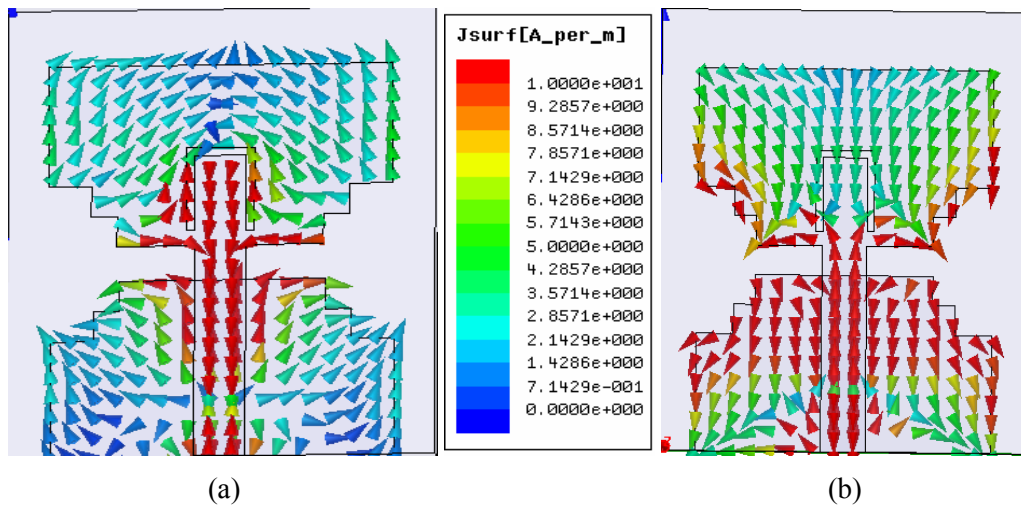


Fig.3.43. Geometry of the band notch design (a)Top View(b)Side view
($L=20\text{mm}, L_1=15\text{mm}, L_2=12\text{mm}, d=2\text{mm}, W_1=8\text{mm}, W=3\text{mm},$
 $h=1.6\text{mm}, L_n=5.5\text{mm}, W_n=4\text{mm}$)

An analysis of the current distribution at the notch frequency, which is shown in Fig. 3.44(a) reveals that the antenna operates as an open circuit at the

notch frequency band. $\lambda/2$ ‘U’ slot can be considered to be parallel combination of two $\lambda/4$ shorted lines. So the net impedance at the centre of ‘U’ slot is high and acts as an open circuit. This may lead to high impedance at the input and most of the energy is reflected back. Hence the current distribution on the surface of the patch is virtually null at this band. Away from this band (Fig.3.44(b), there is no effect of the slot and hence there may be a current distribution on the patch and this may lead to the radiation from the system.



**Fig.3.44. Current distribution of the band notched serrated monopole antenna at (a)5.8GHz(b)7.68GHz
($L=20\text{mm}$, $L_1=15\text{mm}$, $L_2=12\text{mm}$, $d=2\text{mm}$, $W_1=8\text{mm}$, $W=3\text{mm}$, $h=1.6\text{mm}$, $L_n=5.5\text{mm}$, $W_n=4\text{mm}$)**

Measured and simulated reflection coefficients of the antenna are shown in Fig.3.45. Measured and simulated results agree very well. A notched band from 5.04-5.81GHz is obtained.

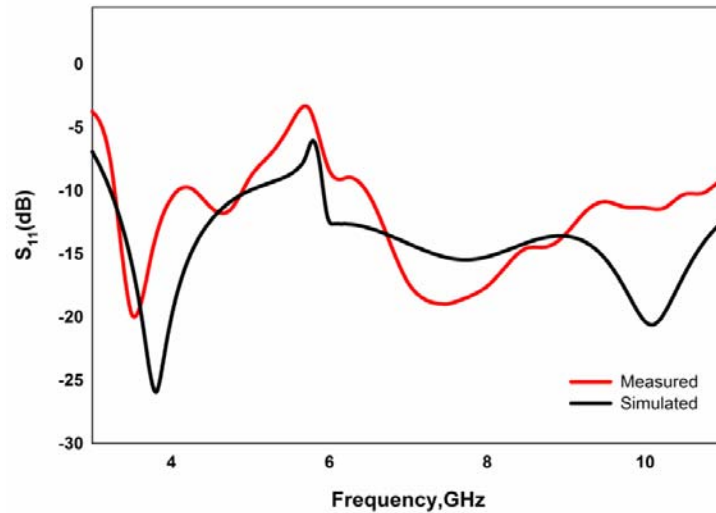


Fig.3.45. Measured and simulated reflection coefficient of the band notched serrated monopole antenna ($L=20\text{mm}$, $L_1=15\text{mm}$, $L_2=12\text{mm}$, $d=2\text{mm}$, $W_1=8\text{mm}$, $W=3\text{mm}$, $h=1.6\text{mm}$, $L_n=5.5\text{mm}$, $W_n=4\text{mm}$)

The 3D radiation patterns at 3.6, 6.7 and 9.8GHz shown in Fig.3.46 are similar to the 3D patterns shown in Fig.3.37. This confirms that radiation patterns at other frequencies are not altered by the notch. At notch frequency (5.8GHz) the radiation pattern of the antenna is very much reduced. This shows that at this frequency the antenna is not radiating or receiving electromagnetic energy.

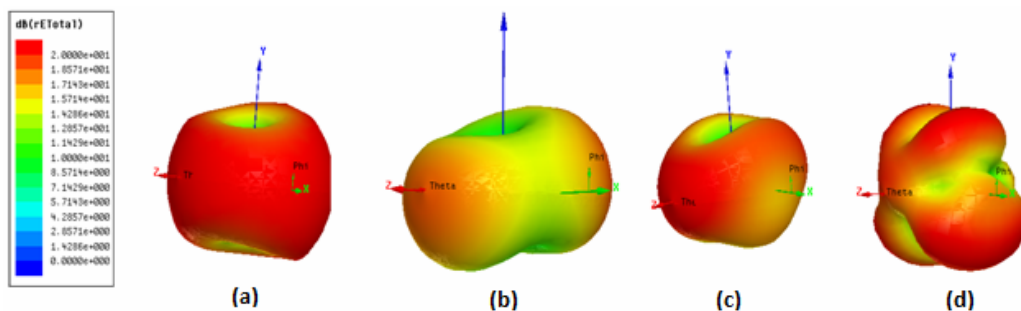


Fig.3.46. Simulated radiation patterns of a notched serrated monopole antenna at (a)3.6GHz(b)5.8GHz(c)6.7GHz and (d)9.8GHz ($L=20\text{mm}$, $L_1=15\text{mm}$, $L_2=12\text{mm}$, $d=2\text{mm}$, $W_1=8\text{mm}$, $W=3\text{mm}$, $h=1.6\text{mm}$, $L_n=5.5\text{mm}$, $W_n=4\text{mm}$)

Fig.3.47 depicts the simulated VSWR of the band notched antenna for different slot lengths L_n . As observed, the notch bandwidth and frequency can be tuned by varying the length (L_n) of the U-shaped slot.

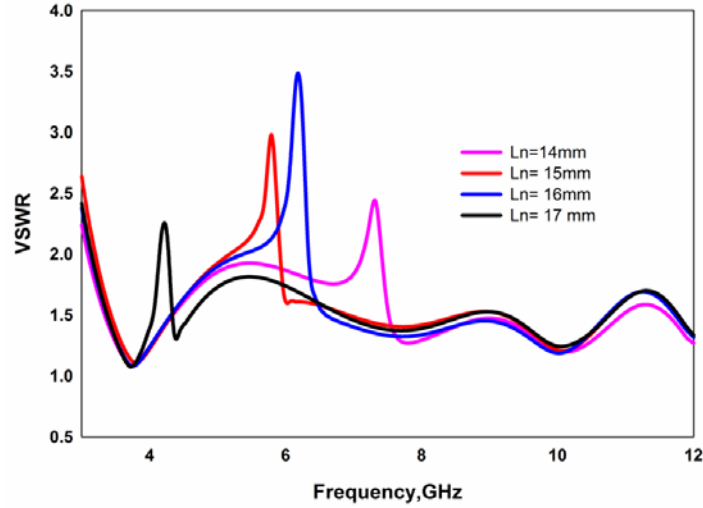


Fig.3.47. VSWR values of band notched serrated monopole antenna for different L_n .
 ($L=20\text{mm}, L1=15\text{mm}, L2=12\text{mm}, d=2\text{mm}, W1=8\text{mm}, W=3\text{mm}, h=1.6\text{mm}, Wn=4\text{mm}$)

It is observed from the figure that center frequency of the notched band is determined by the slot length L_n and is approximately

$$L_n \approx \lambda_{g,5.8\text{GHz}} / 2$$

at the rejection frequency where $\lambda_g = \lambda_0 / \sqrt{\epsilon_{eff}}$ and $\epsilon_{eff} = (\epsilon_r + 1) / 2$.

The radiation patterns of the antenna at the notched frequency in two principle planes are shown in Fig.3.48. Pattern at 5.8GHz has been normalized w.r.t that at 3.6GHz for comparison. A reduction in gain of $\approx 10\text{dBi}$ is observed along all directions.

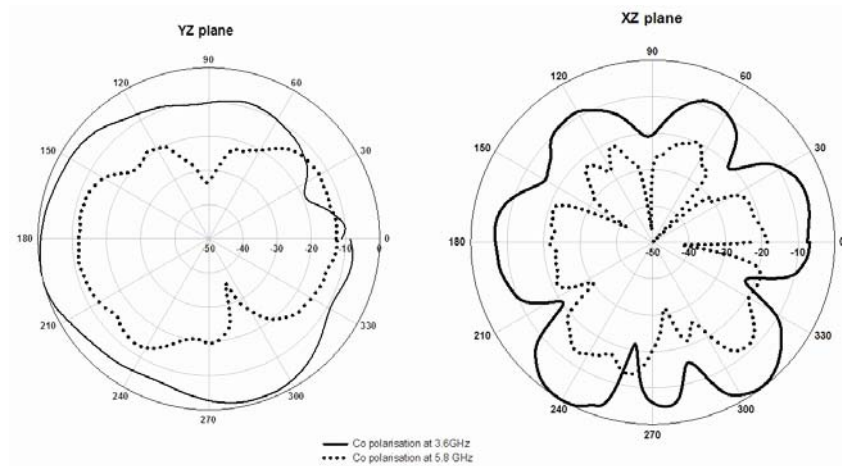


Fig.3.48. Measured radiation pattern of band notched serrated monopole antenna
($L=20\text{mm}$, $L_1=15\text{mm}$, $L_2=12\text{mm}$, $d=2\text{mm}$, $W_1=8\text{mm}$, $W=3\text{mm}$, $h=1.6\text{mm}$, $L_n=5.5\text{mm}$, $W_n=4\text{mm}$)

The gain and radiation efficiency of the antenna is measured and plotted in Fig.3.49. An average gain of 3dBi is noted throughout the operating band except at the notched frequency a reduction in gain greater than 5dBi is obtained. The antenna has a radiation efficiency of more than 80% in the pass band and a reduction in the rejected band.

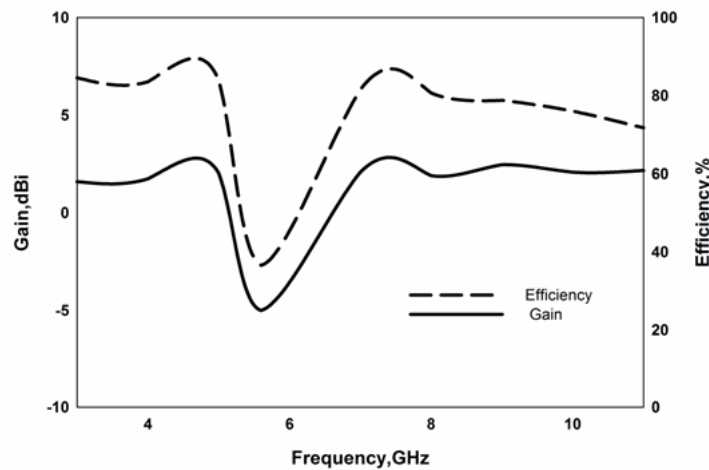


Fig.3.49. Gain and efficiency of the band notched serrated monopole antenna
($L=20\text{mm}$, $L_1=15\text{mm}$, $L_2=12\text{mm}$, $d=2\text{mm}$, $W_1=8\text{mm}$, $W=3\text{mm}$, $h=1.6\text{mm}$, $L_n=5.5\text{mm}$, $W_n=4\text{mm}$)

3.3.2 Reconfigurable Antennas

It is clear that the functionality of wideband planar monopole antennas with band-notched behavior can be significantly improved if the excitation of the slot mode is electronically controlled. Electronic control of the slot mode resonance can be accomplished by means of an RF switching device that controls the flow of current to the inner part of the slot. Therefore, the antenna filtering capability can be further improved by making this band-notched behaviour switchable [20]-[21]. Since the existence of interfering systems depends on the antenna environment, the filtering function exhibited by planar monopoles with fixed band-notched behaviour might not be necessary in some cases. In this case, depending on whether interference from other systems is present or not, the antenna filtering feature can be activated at will.

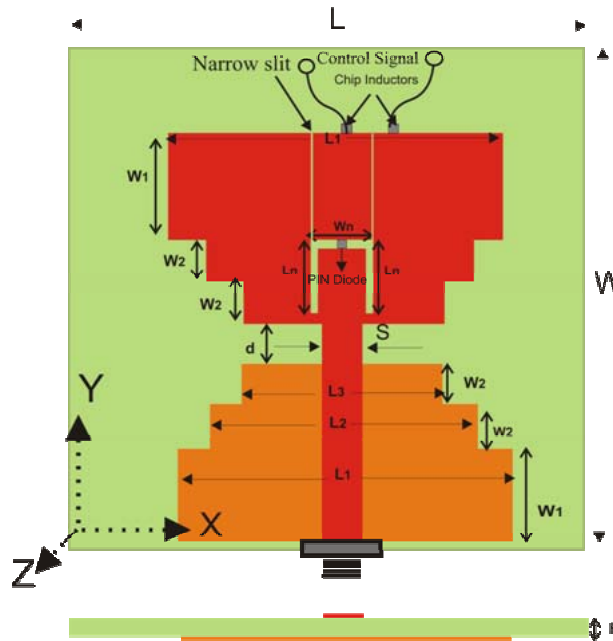


Fig.3.50. Geometry of the UWB band notched planar monopole antenna loaded with a PIN diode, and the RF-DC isolation network ($L=20\text{mm}$, $L_1=15\text{mm}$, $L_2=12\text{mm}$, $d=2\text{mm}$, $W_1=8\text{mm}$, $W=3\text{mm}$, $h=1.6\text{mm}$, $L_n=5.5\text{mm}$, $W_n=4\text{mm}$)

The structure of the proposed antenna is shown in Fig. 3.50, where the switching device has been inserted in the upper part of the slot, so as to minimize the effect over the antenna performance. When the switch is in the ON state, and assuming an ideal shunt for this switching state, the antenna behavior is the same as that observed in Fig. 3.43, where the slot mode is excited and a rejected band is generated. On the other hand, when the switch is in the OFF state, the antenna is equivalent to Antenna III, and the band rejection is consequently prevented.

3.3.2.1 Implementation of the switch by means of a PIN diode

In principle, the implementation of the RF switch can be carried out by means of a Micro-Electro-Mechanical System (MEMS) or a high frequency PIN diode. MEMS switches are becoming increasingly applied to antenna design [22]-[24], and constitute an appealing alternative, since they offer very low power consumption and very low ohmic losses [25]. However, their commercial cost is still prohibitive nowadays, so their use in this case is not an attractive option, if we consider their application in a very low cost antenna, such as a planar monopole. Therefore, the use of PIN diodes seems to be the best alternative for the application under study, due to their low-cost, reliability, compact size, and small resistance and capacitance in both the ON and OFF states.

Several recent reconfigurable antennas based on the use of PIN diodes can be found in literature, mainly dealing with slot antennas [26]-[27] and microstrip antennas [28]-[29].

Figure 3.50 schematically shows the required setup for the switch connection and biasing. In the proposed configuration, a PIN diode is integrated across the slot at the current minimum position. Two narrow slits are used to

avoid DC short in the patch. The resonance of $\lambda/2$ slot is not much affected by these slits. The RF isolation of the patch from the control signal lines is achieved by integrating two chip inductors without perturbing the surface current on the patch. This avoids spurious radiations from the control signal lines.

The PIN diode acts as a short when it is forward biased. When the diode turns ON, the proposed slot mode does not exist. In simulation, PIN diode is modeled using equivalent forward resistance and it leads to the disappearance of the notch band.

To verify the performance of the proposed design, reflection and radiation characteristics of the antenna are measured using HP8510C Vector Network analyzer. Simulated and measured return loss curves of the antenna with ON and OFF states of the PIN diode are shown in Fig.3.51.

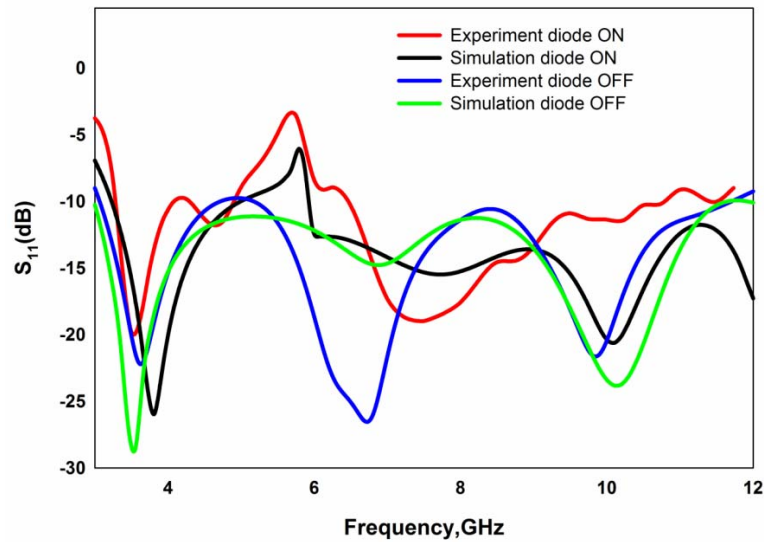


Fig.3.51. Measured and simulated reflection coefficients of the reconfigurable UWB antenna ($L=20\text{mm}, L_1=15\text{mm}, L_2=12\text{mm}, d=2\text{mm}, W_1=8\text{mm}, W=3\text{mm}, h=1.6\text{mm}, L_n=5.5\text{mm}, W_n=4\text{mm}$).

3.4 A Compact CPW fed serrated UWB antenna

The coplanar waveguide (CPW) feeding mechanism has many advantages over microstrip type feed lines, such as low dispersion, low radiation leakage, the ability to selectively control the characteristic impedance, and the ease of integration with active devices. The antenna fed by a microstrip line may result in misalignment because of the required etching on both sides of the dielectric substrate. The alignment error can be eliminated if a CPW feed is used. So in this section, the above mentioned microstrip monopole antenna is modified to a CPW fed monopole to cater to the needs of modern communication systems without compromising the antenna characteristics.

3.4.1 Geometry of CPW fed serrated antenna

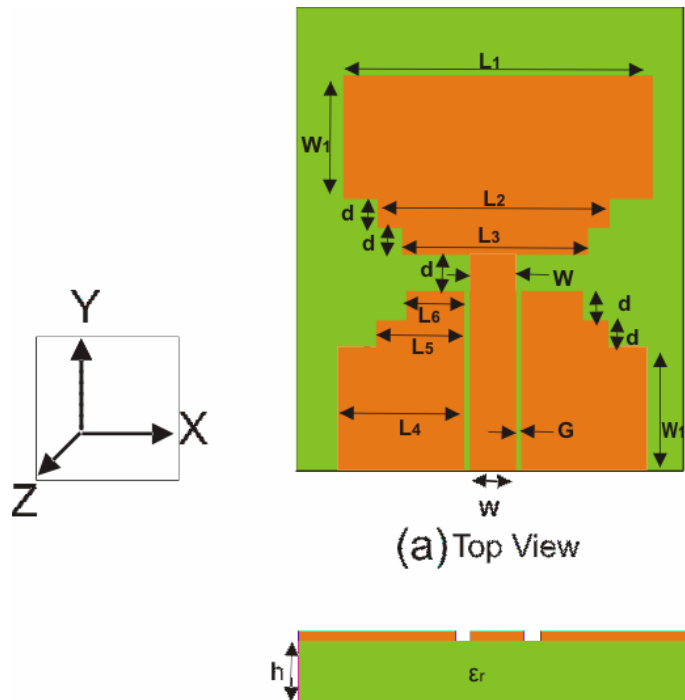


Fig.3.52 Geometry of the CPW fed serrated monopole antenna
 ($L_1=20\text{mm}, L_2=15\text{mm}, L_3=12\text{mm}, L_4=8.15, L_5=5.65, L_6=4.15, d=2\text{mm},$
 $W_1=8\text{mm}, W=3\text{mm}, G=0.35\text{mm}, h=1.6\text{mm}, \epsilon_r=4.4$)

Fig. 3.52 shows the geometry of the proposed antenna. It consists of a rectangular radiation patch with two pairs of symmetrical serrations each on patch and ground.

The antenna is printed on a substrate with dielectric constant $\epsilon_r = 4.4$, loss tangent $\tan \delta = 0.02$ and thickness $h = 1.6$ mm. The staircase radiating element consists of three rectangles of lengths L_1, L_2, L_3 and widths W_1, W_2, W_3 . The ground plane also consists of a combination of three rectangles of lengths L_4, L_5, L_6 and widths W_1, W_2, W_3 respectively on either side of the transmission lines. The gap 'd' between the patch and the ground plane is 2 mm. Length of the feed line L_f is optimized to be 12mm. The strip width (W) and gap(G) of the Coplanar Waveguide(CPW) feed are derived using standard design equations for 50 Ω impedance. Total dimensions of the antenna are only 20mmx26mmx1.6mm.

3.4.2 Reflection Characteristics of CPW fed Serrated Monopole Antenna

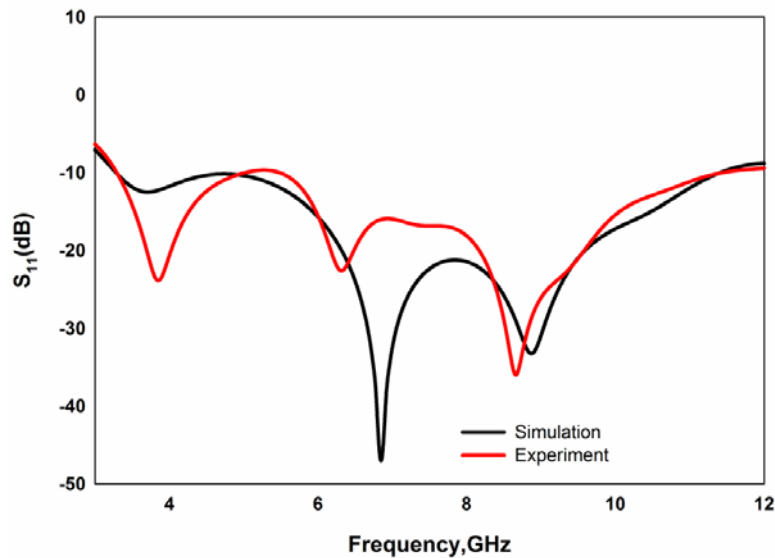


Fig.3.53. Simulated and measured reflection coefficient of the CPW fed serrated monopole antenna
($L_1=20\text{mm}, L_2=15\text{mm}, L_3=12\text{mm}, L_4=8.15, L_5=5.65, L_6=4.15,$
 $d=2\text{mm}, W_1=8\text{mm}, W=3\text{mm}, G=0.35\text{mm}, h=1.6\text{mm}, \epsilon_r=4.4$)

Measured and simulated reflection characteristics of the antenna are shown in Fig.3.53. A good agreement is seen between them. Antenna has three resonances at 3.85GHz, 6.36GHz and 8.73GHz and ultra wide band performance is obtained by merging these resonances. A 2:1VSWR band width from 3.1GHz to 11.4GHz is obtained.

3.4.3 Design of CPW fed Serrated Monopole Antenna

1) Design a 50 Ω CPW line on a substrate with permittivity ϵ_r . Calculate ϵ_{re} using $\epsilon_{re} = (\epsilon_r + 1)/2$ where ϵ_{re} is the effective permittivity of the substrate.

2) Design the stair case patch using the dimensions

$$L_1 = 0.77 \lambda_c \text{ (3.9)}$$

$$L_2 = 0.579 \lambda_c \text{ (3.10)}$$

$$L_3 = 0.463 \lambda_c \text{ (3.11)}$$

And

$$W_1 = 0.3 \lambda_c \text{ (3.12)}$$

$$W_2 = W_3 = 0.077 \lambda_c \text{ (3.13)}$$

where λ_c is the wavelength corresponding to centre frequency of the operating band.

3) Calculate ground plane dimensions using

$$L_4 = 0.314 \lambda_c \text{ (3.14)}$$

$$L_5 = 0.216 \lambda_c \text{ (3.15)}$$

And

$$L_6 = 0.16 \lambda_c \text{ (3.16)}$$

- 4) Calculate the length of the transmission L_f and the gap between patch and ground plane d using

$$L_f = 0.463 \lambda_c \dots\dots\dots(3.17)$$

And

$$d = 0.077 \lambda_c \dots\dots\dots(3.18)$$

In order to justify the design equations, the antenna parameters are computed for different substrates (Table 3.5) and are tabulated in Table 3.6.

Table 3.5 Antenna Description

	Antenna 1	Antenna 2	Antenna 3	Antenna 4
Laminate	Rogers 5880	FR4 Epoxy	Rogers RO3006	Rogers6010LM
h(mm)	1.57	1.6	1.28	0.635
ϵ_r	2.2	4.4	6.15	10.2
ϵ_{re}	1.6	2.7	3.575	5.6
W(mm)	4	3	2.58	2.05
G(mm)	0.17	0.35	0.45	0.5

Table 3.6 Computed Geometric Parameters of the Antenna

Parameter (mm)	Antenna 1	Antenna 2	Antenna 3	Antenna 4
L_1	25.7796	20	17.3635	13.8463
L_2	19.3849	15	13	10.411
L_3	15.501	12	10.44	8.325
L_4	10.53	8.15	7.0807	2.877
L_5	7.231	5.65	4.8708	5.3946
L_6	5.364	4.15	3.608	5.646
W_1	10.044	8	6.765	3.884
d	2.577	2	1.736	1.3846
L	15.5	12	10.44	8.325

Fig 3.54 shows the reflection coefficients of different antennas as given in Table 3.4. In all the cases antenna is operating in the UWB region.

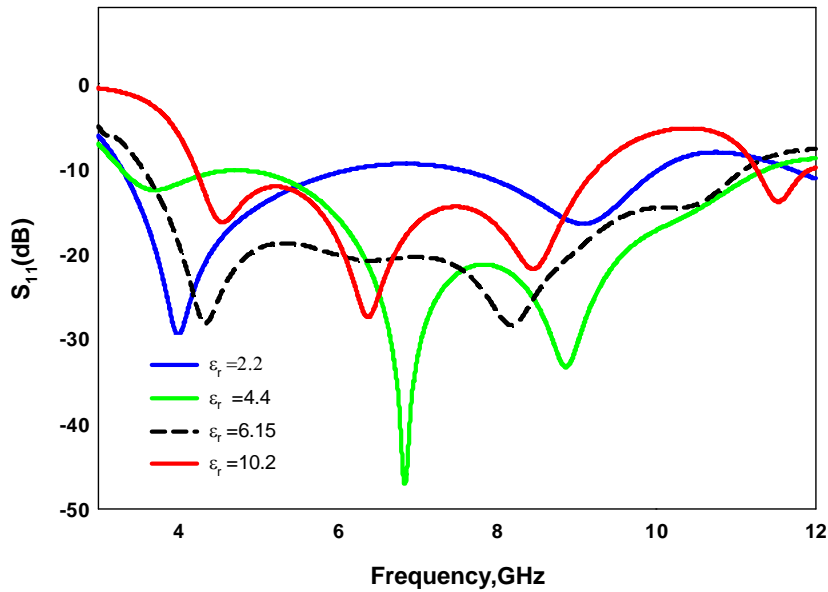


Fig.3.54. Reflection coefficients of the serrated CPW fed serrated monopole antenna for different substrates

Simulated radiation patterns and surface current distribution of the antenna at the resonant frequencies are plotted in Fig.3.55. Analyzing the current distributions it is obvious that first resonance corresponds to $\lambda/4$ variation along the edge of the steps. Second and third resonances are found to be higher order harmonics of the first resonance.

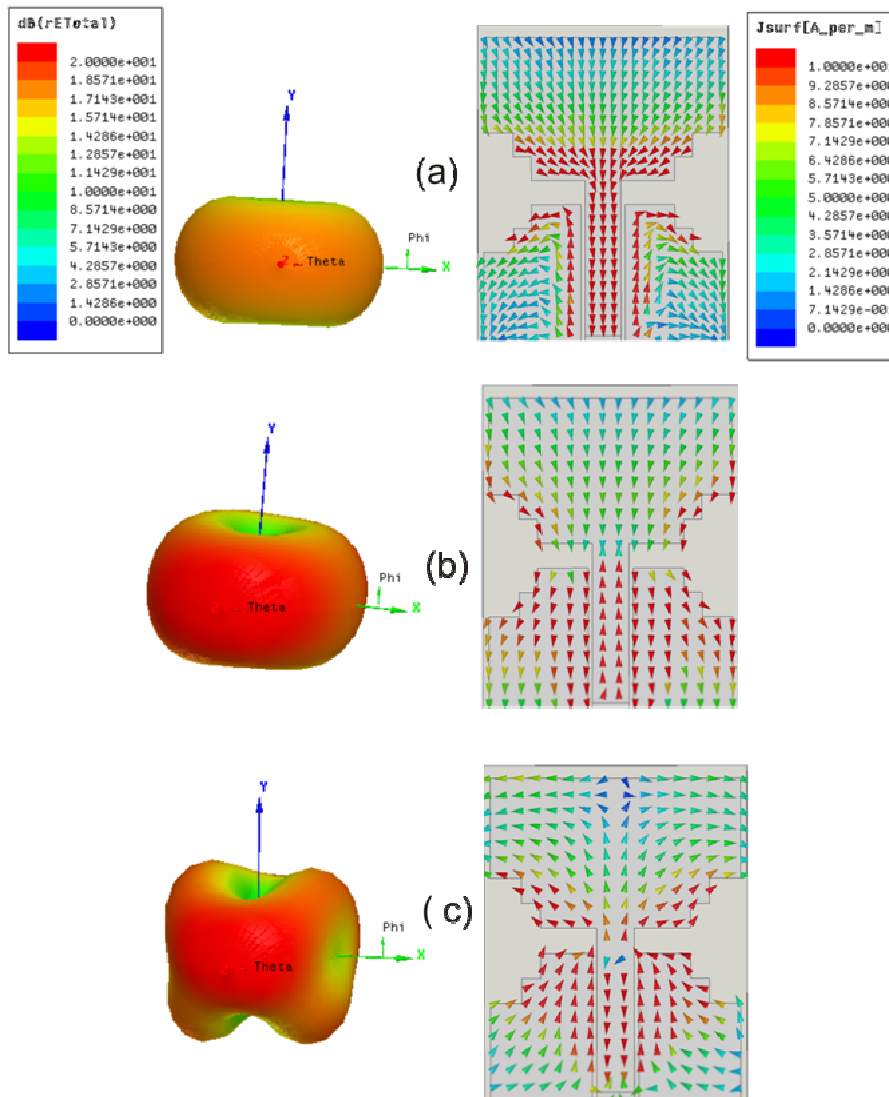


Fig.3.55. Simulated radiation pattern and surface current distribution of the CPW fed serrated monopole antenna at the (a)3.63GHz (b)6.87GHz and (c)8.98GHz ($L_1=20\text{mm}, L_2=15\text{mm}, L_3=12\text{mm}, L_4=8.15, L_5=5.65, L_6=4.15, d=2\text{mm}, W_1=8\text{mm}, W=3\text{mm}, G=0.35\text{mm}, h=1.6\text{mm}, \epsilon_r=4.4$)

Measured radiation patterns of the antenna at the resonant frequencies are shown in Fig.3.56. In YZ plane figure of eight shaped pattern is obtained and in

the XZ plane pattern is omni directional. A cross polar isolation better than 15dB is obtained in YZ plane.

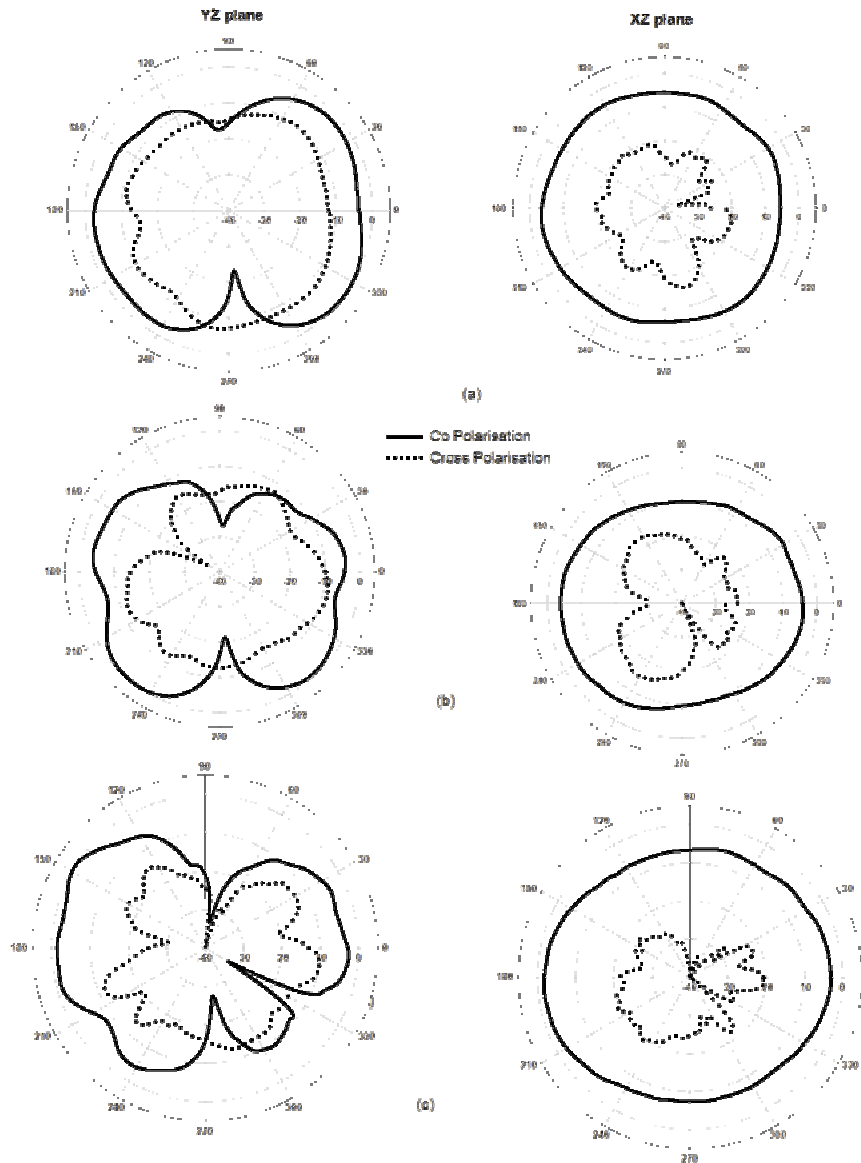


Fig.3.56. Measured radiation patterns of the CPW fed serrated antenna at (a) 3.85GHz (b)6.36GHz and(c) 8.73GHz
 $(L_1=20\text{mm}, L_2=15\text{mm}, L_3=12\text{mm}, L_4=8.15, L_5=5.65, L_6=4.15,$
 $d=2\text{mm}, W_1=8\text{mm}, W=3\text{mm}, G=0.35\text{mm}, h=1.6\text{mm}, \epsilon_r=4.4)$

Fig. 3.57 illustrates the measured antenna gain and radiation efficiency from 3.0 to 11.5 GHz for the proposed antenna. As shown in the figure, gain is almost constant in the entire band with variation less than 1dB. So the antenna exhibits stable gain across the operation band. Average efficiency of the antenna is 90%.

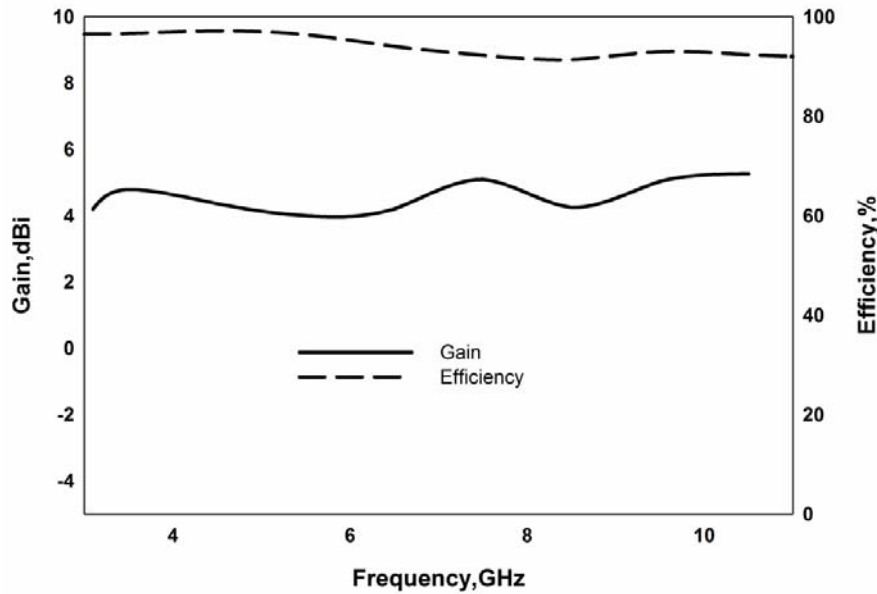


Fig.3.57. Gain and efficiency of the CPW fed serrated antenna
 $(L_1=20\text{mm}, L_2=15\text{mm}, L_3=12\text{mm}, L_4=8.15, L_5=5.65, L_6=4.15,$
 $d=2\text{mm}, W_1=8\text{mm}, W=3\text{mm}, G=0.35\text{mm}, h=1.6\text{mm}, \epsilon_r=4.4)$

3.5 Time Domain Analysis of UWB Monopole Antennas

Since UWB systems directly transmit narrow pulses rather than employing a continuous wave carrier to convey information, the effect of the antenna on the transmitted pulse becomes a crucial issue. In such a system, the antenna behaves like a band pass filter and reshapes the spectra of the pulses. The signal waveforms arriving at the receiver usually do not resemble the waveforms of the source pulses at the transmitter. The antenna, hence, should be designed with care to avoid undesired distortions. In other words, a good

time domain performance is a primary requirement of UWB antenna, as mentioned in Chapter 2.

3.5.1 Group Delay of UWB Monopole Antennas

In ultra wideband systems, the information is transmitted using short pulses. Hence, it is important to study the temporal behavior of the transmitted pulse. The communication system for UWB pulse transmission must limit distortion, spreading and disturbance as much as possible. Group delay is an important parameter in UWB communication, which represents the degree of distortion of pulse signal. The group delay is measured by placing two identical antennas in the far field. A nondistorted structure is characterized by a constant group delay, i.e., linear phase, in a relevant frequency range. The nonlinearities of a group delay indicate the resonant character of the device, which implicates the ability of the structure to store the energy.

The comparison of the group delays for the face to face and side by side orientations of the antennas are shown in Fig.3.58. In the case of ground modified antenna, both face to face and side by side orientations exhibits a group delay variation of 4ns. In the case of micro strip fed serrated antenna, a group delay variation of 3ns is obtained for both the orientations. Band notched antenna shows a decrease in group delay at the notch frequency compared to other frequencies. Group delay variations are minimum for CPW fed serrated monopole antenna and is less than 3ns for both orientations. These values of group delays indicate that the proposed antennas have linear phase characteristics and hence superior pulse handling capabilities as demanded in modern communication systems.

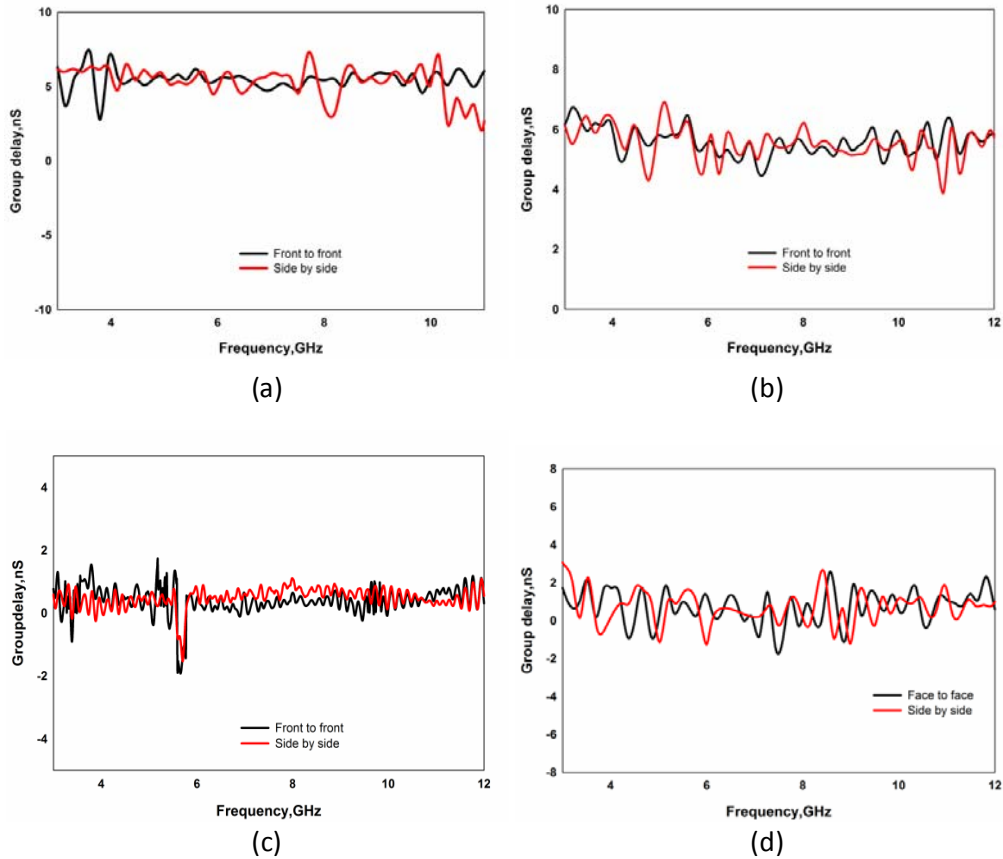


Fig.3.58. Measured group delay for face to face and side by side orientations of (a) ground modified monopole antenna (b) Microstrip fed serrated monopole antenna (c) Band notched serrated monopole antenna and (d) CPW fed serrated monopole antenna.

3.5.2 Transfer functions of UWB Monopole Antennas

The procedure for transfer characteristics measurements are as explained in section 2.5.4 of Chapter 2. Transmitting and receiving antennas are positioned in their far fields. Measurements are performed at steps of 45°. The measured antenna transfer function magnitudes are plotted in the azimuth plane and shown in Fig.3. 59.

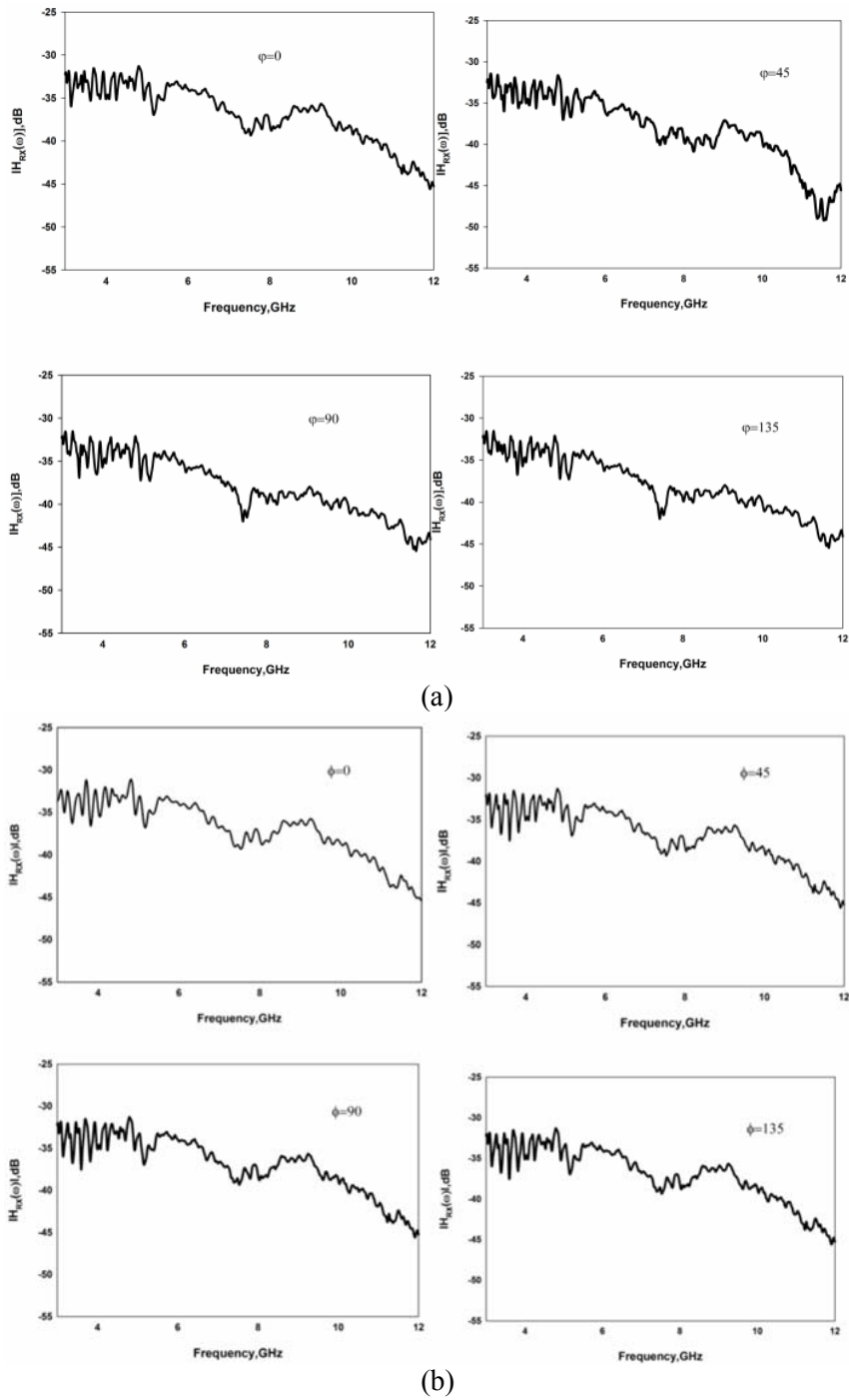
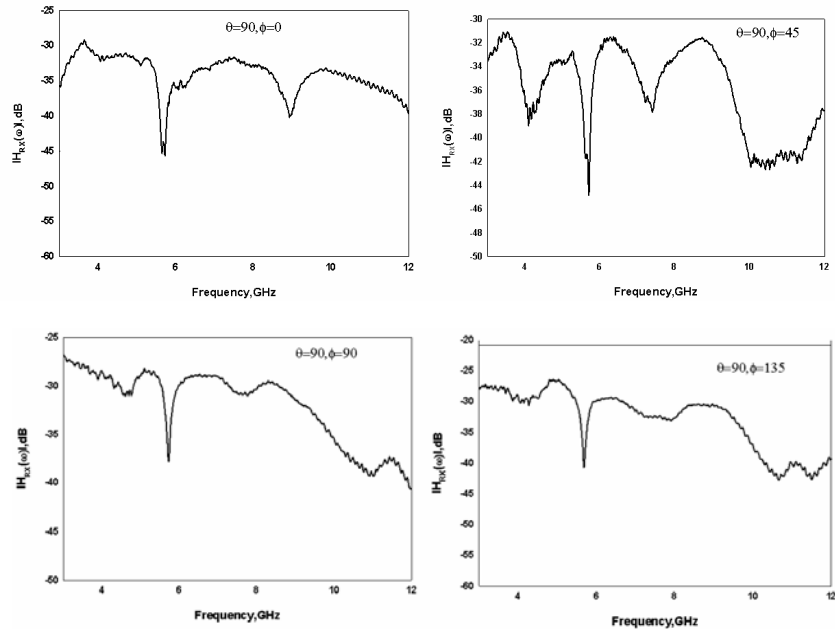
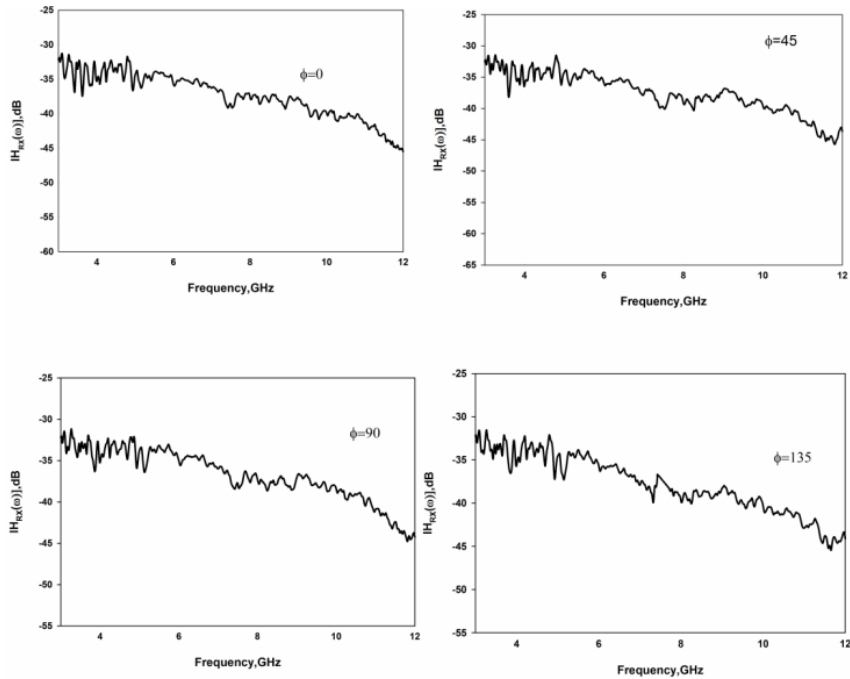


Fig.3.59. Measured transfer function in the azimuth plane for (a) ground modified monopole antenna (b)Microstrip fed serrated monopole antenna



(c)



(d)

Fig.3.59. Measured transfer function in the azimuth plane for (c) Band notched serrated monopole antenna and (d) CPW fed serrated monopole antenna.

Measured transfer functions indicates that in the case of ground modified antenna, transfer function is decreased for all the angles verifying the radiation pattern distortion observed at higher frequencies. Microstrip fed serrated antenna also shows a decrease in transfer function but less than that of ground modified antenna. In the case of band notched antenna, a sudden decrease in transfer function is observed at the notch frequency. Compared to other three antennas, CPW fed antenna shows minimum distortion in transfer function.

3.5.3 Impulse Responses of UWB Monopole Antennas

Impulse responses are calculated from measured transfer functions by taking IFFT and are plotted in Fig.3.60. Most of the responses resembles the delta function. Pulse dispersion and ringing is higher in band notched antenna.

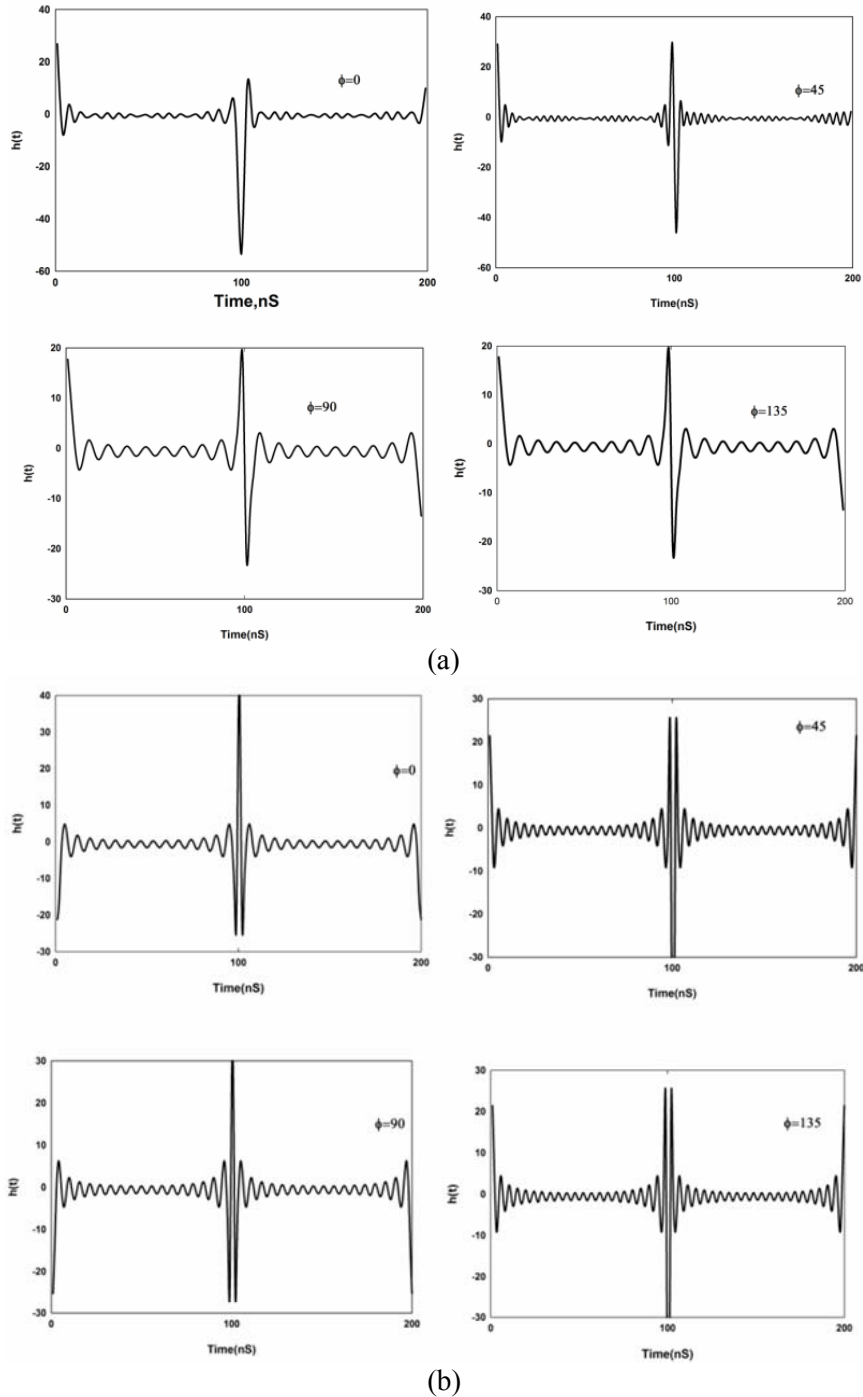
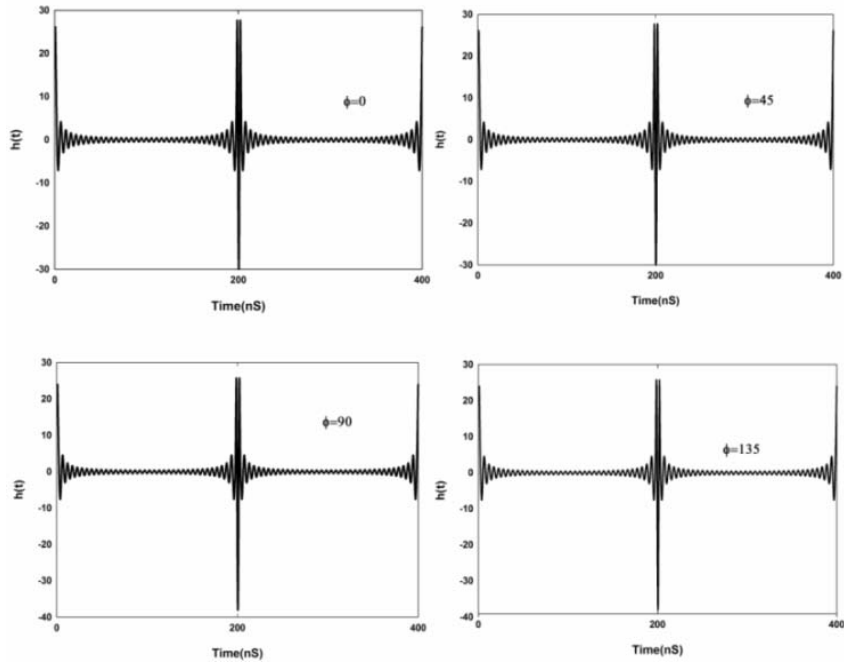
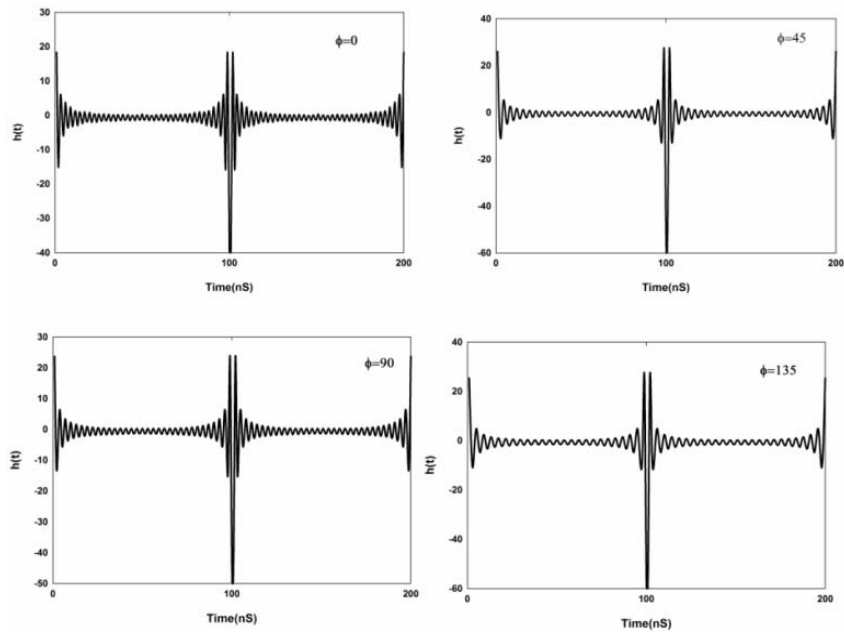


Fig.3.60. Measured impulse responses in the azimuth plane (a) ground modified monopole antenna (b) Microstrip fed serrated monopole antenna



(c)



(d)

Fig.3.60. Measured impulse responses in the azimuth plane (c) Band notched serrated monopole antenna and (d) CPW fed serrated monopole antenna.

3.5.4 Received Signal Waveforms of UWB Monopole Antennas

Transient response of the antenna is studied by modeling the antenna by its transfer function. The transmission coefficient S_{21} is measured in the frequency domain for the face-to-face and side-by-side orientations. The transfer function is then computed. The channel is assumed to be a Linear Time Invariant (LTI) system to verify the capability of the proposed antenna for transmission and reception of these narrow pulses.

The transfer function(Eqn.2.11) is transformed to time domain by performing the inverse fourier transform. Fourth derivative of a Gaussian function is selected as the transmitted pulse. The output waveform at the receiving antenna terminal can therefore be expressed by convoluting the input signal and the transfer function. The input and received wave forms for the face-to-face and side-by-side orientations of the antenna are shown in Fig.3.61. It can be seen that in the case of ground modified antenna, microstrip fed antenna and band notched antenna some ringing is observed for the received pulses. In the case of CPW fed serrated antenna, in both face to face and side by side orientations, received waveform match with each other very well.

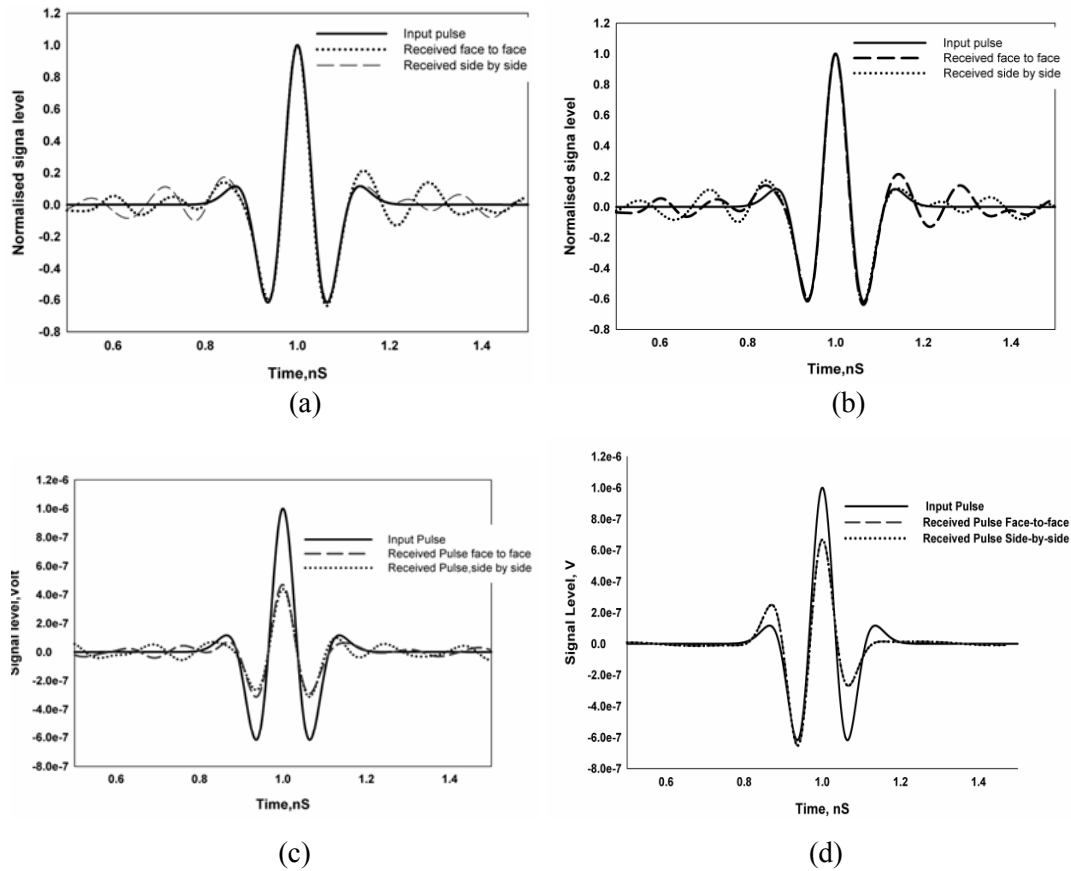


Fig.3.61. Input and received pulses for the face to face and side by side orientations of (a) ground modified monopole antenna(b) Microstrip fed serrated monopole antenna(c) Band notched serrated monopole antenna and (d) CPW fed serrated monopole antenna

3.5.5 Fidelity Factor of UWB Monopole Antennas

Fidelity factor for two identical antennas are tabulated as given in chapter 2. Fidelity factor in different orientations of the antennas are shown in the Fig.3.62. Maximum fidelity for ground modified antenna is 94.61%. Maximum fidelity factor of microstrip fed serrated antenna is 96.18% and that of band notched serrated monopole is 95.85% while that of CPW fed serrated monopole is 95.289%.

These values for the fidelity factor show that the antennas imposes negligible effects on the transmitted pulses.

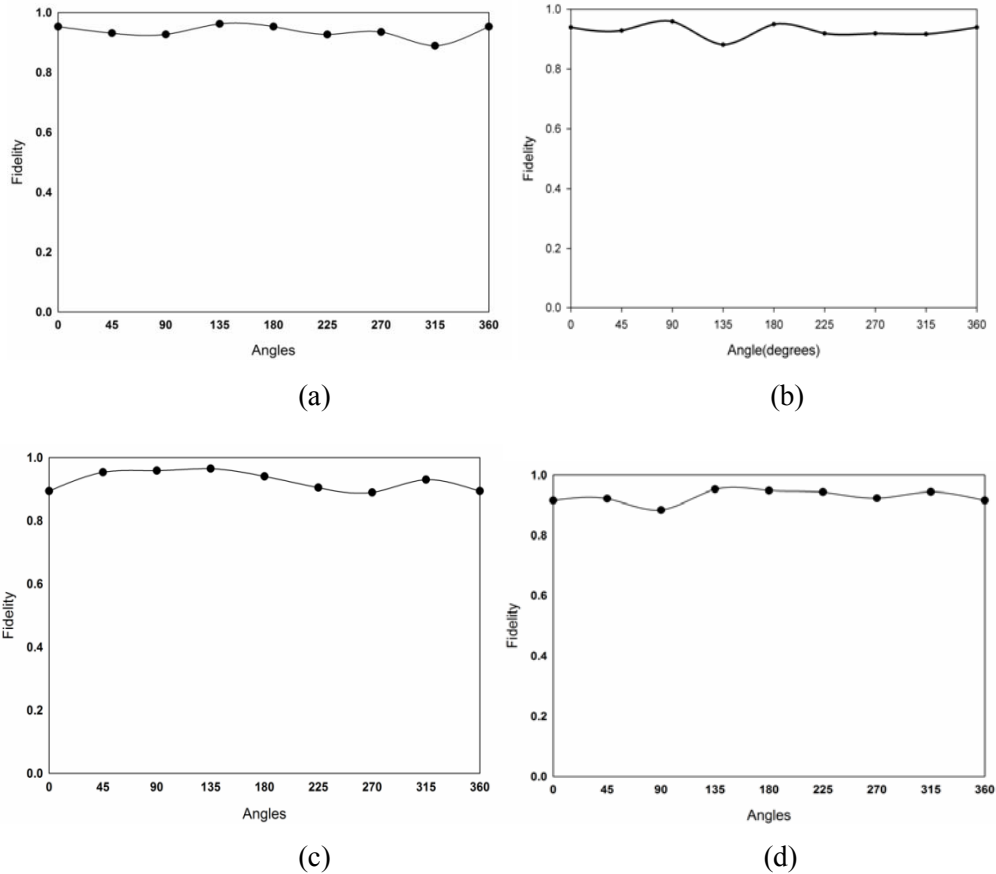


Fig.3.62. Fidelity factor for various angles of (a) ground modified monopole antenna(b) Microstrip fed serrated monopole antenna(c) Band notched serrated monopole antenna and (d) CPW fed serrated monopole antenna.

3.5.6 EIRP of UWB Monopole Antennas

Since FCC UWB operating bandwidth definition is based on power emission limits, investigation of the effective isotropic radiated power (EIRP) emission level of the antenna with a given excitation signal is essential. Fig.3.63 shows the measured EIRP emission level of the antenna excited with a

fourth order gaussian pulse. As it is clear from the figure, EIRP of all the antennas satisfies the FCC indoor and outdoor masks for the entire UWB band.

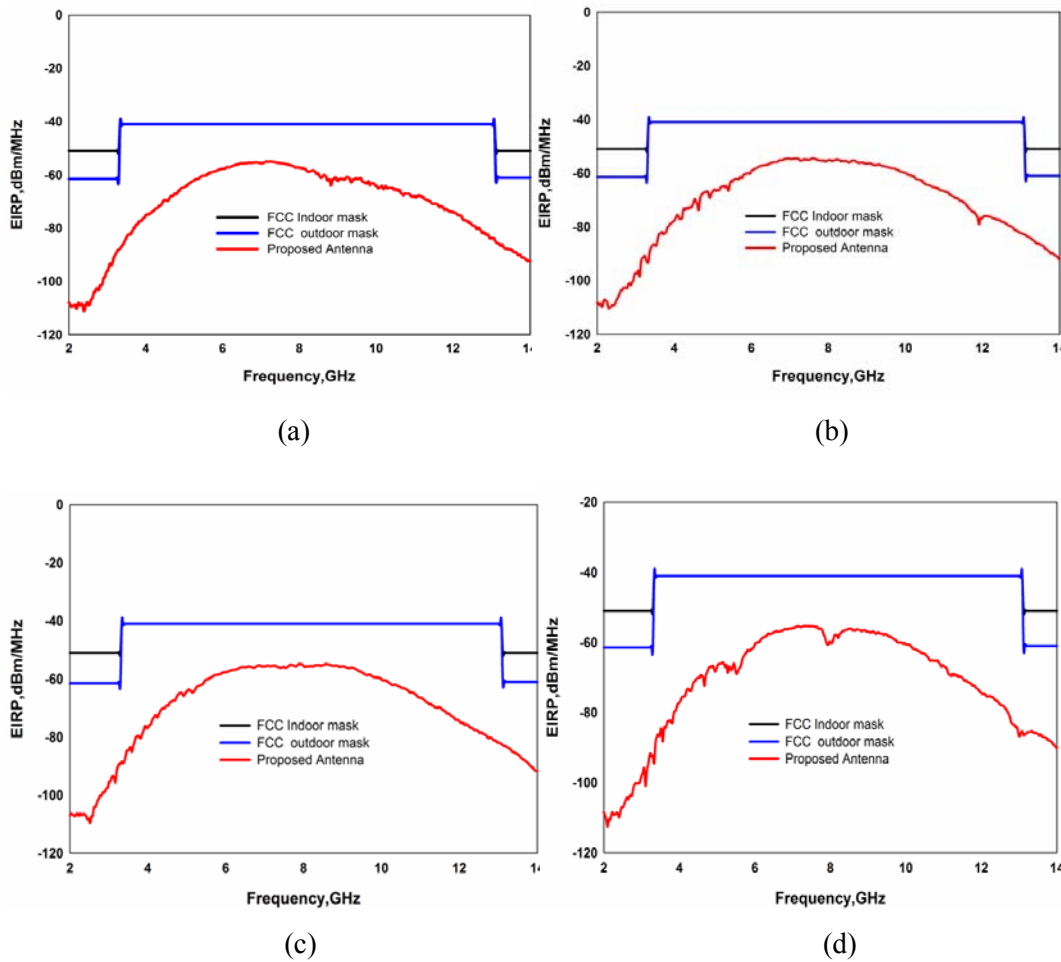


Fig.3.63. EIRP emission level of (a) ground modified monopole antenna (b) Microstrip fed serrated monopole antenna (c) Band notched serrated monopole antenna and (d) CPW fed serrated monopole antenna.

Photographs of antennas discussed in this chapter are shown in Fig.3.64.

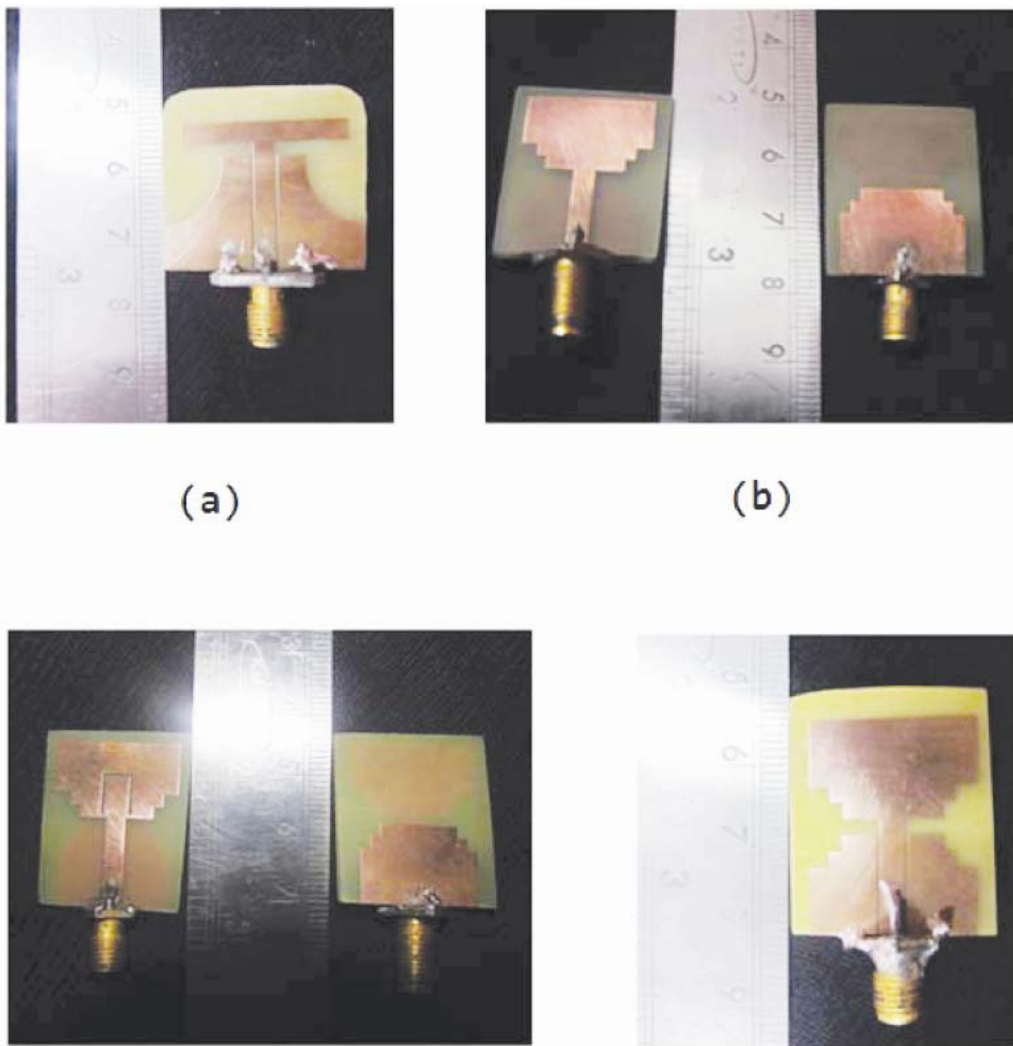


Fig.3.64. Photographs of (a) ground modified monopole antenna(b) Microstrip fed serrated monopole antenna(c) Band notched serrated monopole antenna and (d) CPW fed serrated monopole antenna.

3.5.7 Chapter Summary

In this chapter two designs of UWB planar monopole antennas, namely ground modified monopole and serrated monopole are presented. The ground modified monopole antenna has wide band operation (3.1GHz to 12GHz), simple structure and nearly omnidirectional radiation patterns at the lower end of the spectrum. The antenna is compact in size (30x22mm²) and fed using a CPW feed. The antenna appears to be an ideal candidate for the 3.1 to 10.6GHz UWB operation from the frequency domain studies. Since the antenna operates over a multi-octave bandwidth, it would be excellent to transmit pulses of the order of a nanosecond in duration with minimal distortion.

The serrated monopole antenna presented has a reduced size (20x22mm²) and wide band operation (2.8 to 11.2GHz). It appears to be ideal for UWB handheld applications with compact size, stable & omnidirectional antenna patterns. A band notched serrated antenna to notch out the 5.8GHz WLAN band by etching an inverted U slot from the patch is also presented. Electronic reconfiguration of the notch band by integrating a PIN diode across $\lambda/2$ inverted 'U' slot is also demonstrated. A CPW fed serrated monopole antenna of same dimension as that of microstrip fed monopole is also developed and presented. Time domain analysis of all antennas is also discussed at the end of this chapter.

References

- [1] R.Garg,P.Bhartia,I.Bahl and A.Ittipiboon,2001, "Microstrip Antenna Design Handbook",Norwood,MA:Artech House.
- [2] C.Y. Huang, W.C. Hsia," Printed elliptical antenna for ultra-wideband communications", *Electron Lett* ,2005.
- [3] J. Jung, W. Choi, and J. Choi, "A small wideband microstrip-fed monopole antenna", *IEEE Microwave Wireless Compon Lett* 15, pp.703–705,2005.
- [4] X.L. Bao, M.J. Ammann, "Investigation on UWB monopole antenna with rectangular slitted ground plane", *Microwave Opt Technol Lett* ,pp. 1585–1587,2007.
- [5] X. Zhang, W. Wu, Z.H. Yan, J.B. Jiang, and Y. Song, "Design of CPW-fed monopole UWB antenna with a novel notched ground", *Microwave Opt Technol Lett*, pp.88–91 2009.
- [6] Q. Wu, R. Jin, J. Geng, and M. Ding, "Pulse preserving capabilities of printed circular disk monopole antennas with different grounds for the specified input signal form", *IEEE Trans Antennas Propag*,pp. 2866–2873,2007.
- [7] J.-P. Zhang, Y.-S. Xu and W.-D. Wang,"Microstrip-fed semielliptical dipole antennas for ultrawideband communications",*IEEE Trans. Antennas Propag.*, vol. 56, no. 1, pp. 241–245, 2008.
- [8] Vasylchenko, W. D. Raedt and G. A. E. Vandenbosch,"Design and parametric analysis of a very compact UWB antenna with band rejection feature", *Proc.of iWAT2008*, vol. 3, pp. 430–433, 2008.

- [9] C.-Y. Hong, C.-W. Ling, I.-Y. Tarn and S.-J. Chung,” Design of a planar ultrawideband antenna with a new band-notch structure”, IEEE Trans. on Antennas and Propagat., vol. 55, no. 12, pp. 3391–3397,2007.
- [10] K. Yin and J. P. Xu” Compact ultra-wideband antenna with dual bandstop characteristic”, Electron. Lett., vol. 44, no. 7, pp. 453–454,2008.
- [11] S.-W. Qu, J. L. Li and Q. Xue,” A band-notched ultrawideband printed monopole antenna”, IEEE Antennas Wireless Propag. Lett., vol. 5, pp. 495–498, 2006.
- [12] E. Pancera, D. Modotto, A. Locatelli, F. M. Pigozzo and C. De Angelis,”Novel design of UWB antenna with band-notch capability”, European Microwave Week 2007, ECWT, Munich, 2007.
- [13] J. Kim, C. S. Cho and J. W.Lee, “5.2GHz notched ultra wide band antenna using slot-type SRR”, Electron. Lett., vol. 42, no. 6, pp. 315–316, 2006.
- [14] W. J. Lui, C. H. Cheng and H. B. Zhu,” Compact frequency notched ultra-wideband fractal printed slot antenna”, IEEE Micro. Wireless Comp. Lett., vol. 16, no. 4, pp. 224–226, 2006.
- [15] K. H. Kim, Y. J. Cho, S. H. Hwang and S. O. Park,” Band-notched UWB planar monopole antenna with two parasitic patches”, Electron. Lett., vol. 41, no. 14, pp. 783–785, 2005.
- [16] Young Jun Cho, Ki Hak Kim, Dong Hyuk Choi, Seung Sik Lee, and Seong-Ook Park ,”A Miniature UWB Planar Monopole Antenna With 5-GHz Band-Rejection Filter and the Time-Domain Characteristics”, IEEE Transaction on Antennas and Propagation, Vol. 54, No. 5, May 2006.

- [17] Tzyh-Ghuang Ma and Sung-Jung Wu,” Ultrawideband Band-Notched Folded Strip Monopole Antenna”, IEEE Trans. Antennas Propag, Vol. 55, No. 9, September 2007.
- [18] Reza Zaker, Changiz Ghobadi, Javad Nourinia,” Novel modified UWB planar monopole antenna with variable frequency band notch function”, IEEE Antennas and Wireless Propagation Letters, 7, pp.112-114. 2008.
- [19] Keyvan Bahadori, Yahya Rahmat-Samii,” A miniaturized elliptic-card UWB antenna with WLAN band rejection for wireless communications”, IEEE Trans. Antennas Propag, 55(11), pp.3326-3332. 2007.
- [20] E. Antonino, M. Ferrando, M. Cabedo and C.A. Suarez, “Ultra-wideband antenna with switchable band-notched behaviour”, 1st European Conference on Antennas and Propagation, Nice (France). November 2006.
- [21] E. Antonino, M. Cabedo, M. Ferrando and M. Baquero, “Novel UWB antennas with switchable and tunable band-notched behavior”, IEEE Antennas and Propagation Society International Symposium 2007, Honolulu (EEUU),10-15 June 2007.
- [22] N. Kingsley, D. E. Anagnostou, M. Tentzeris and J. Papapolymerou, “RF MEMS Sequentially Reconfigurable Sierpinski Antenna on a Flexible Organic Substrate With Novel DC-Biasing Technique”, Journal of Microelectromechanical systems, Vol. 16, No. 5, Oct. 2007.
- [23] D. E. Anagnostou et al., “Design, fabrication, and measurements of an RFMEMS- based self-similar reconfigurable antenna,” IEEE Trans. Antennas Propag., vol. 54, no. 2, pt. 1, pp. 422–432, Feb. 2006.

- [24] B. Cetiner, J. Qian, H. Chang, M. Bachman, G. Li, and F. DeFlaviis, “Monolithic integration of RF MEMS switches with a diversity antenna on PCB substrate,” *IEEE Trans. Microw. Theory Tech.*, vol. 51, no. 1, pp. 332–334, Jan. 2003.
- [25] C. Goldsmith, J. Randall, S. Eshelman, T. H. Lin, D. Denniston, S.Chen, and B. Norvell, “Characteristics of micromachined switches at microwave frequencies,” in *IEEE Microwave Theory and Techniques Symp. Dig.*, vol. 2, 1996, pp.1141–1144.
- [26] D. Peroulis, K. Sarabandi and L. P. B. Katehi, “Design of Reconfigurable Slot Antennas”, *IEEE Trans. Antennas Propagat.*, vol. 53, no. 2, pp. 645-654, February 2005.
- [27] N. Symeon, R. Bairavasubramanian, C. Lugo, I. Carrasquillo, D.C. Thompson, G.E. Ponchak, J. Papapolymerou, M.M. Tentzeris, “Pattern and frequency reconfigurable annular slot antenna using PIN diodes”, *IEEE Trans. Antennas Propag.*, vol. 54, no. 2, pt. 1, pp. 439-448, Feb. 2006.
- [28] S.H. Chen, J.-S. Row, K.L. Wong, “Reconfigurable Square-Ring Patch Antenna With Pattern Diversity”, *IEEE Trans. Antennas Propag.*, vol. 55, no. 2, pp. 472-475, Feb. 2007.
- [29] W.L. Liu, T.R. Chen, S.H. Chen and J.S. Row, “Reconfigurable microstrip antenna with pattern and polarisation diversities”, *Electronics Letters*, Vol. 43, Is. 2, pp: 77 – 78, Jan. 18, 2007.

.....❧.....

PLANAR TRIANGULAR SLOT ULTRA WIDEBAND ANTENNA

Contents	4.1	<i>Review on UWB planar Slot Antennas</i>
	4.2	<i>Triangular slot UWB antenna</i>
	4.3	<i>5.8GHz Band Notched Triangular Slot Antenna</i>
	4.4	<i>Time Domain Antenna Analysis</i>
	4.5	<i>Chapter Summary</i>

Earlier part of this chapter is devoted for the detailed literature review about the planar slot antenna. The evolution of a reduced size UWB slot antenna design is presented. This antenna overcomes the disadvantage of pattern deterioration at the higher frequencies of antennas described in previous chapters. For ease of fabrication and better integration, a CPW feed is employed. The surface current distributions on the antenna and their radiation patterns at the resonant modes are analyzed in detail. From the detailed experimental and simulation studies, the design equations for the planar slot UWB antenna are derived. To reduce the interference with the conventional WLAN, a notch band is also introduced. Time domain analysis of these antennas is also conducted to study the suitability of these antennas for pulse based applications.

4.1 Review on UWB planar Slot Antennas

A slot antenna comprises of a slot of appropriate shape on a thin sheet of metal. The slot radiates electromagnetic energy bidirectionally when excited by a voltage source. Slot antenna is considered as the compliment of dipole antenna and regarded as the magnetic of monopoles in view of the EM duality. Slot antenna can be fabricated on a metallic strip very easily. Usually the slot length is half of the wavelength at the desired frequency and the width is a small fraction of wavelength. The antenna is frequently compared to a conventional half- wave dipole consisting of two metal strips. The physical dimensions of the metal strips are just compliment of the slot antenna sheet. This type of antenna is called the complementary dipole. The electric field distribution in the slot can be obtained from the relationship between the slot and complementary wire antennas, as established by Babinet [1].

A U-shaped slotted patch was experimentally investigated in [2] and an impedance bandwidth of 27% from 1.565-2.065 GHz, was obtained. Several researchers have attempted similar approaches with microstrip patch antennas, a detailed account of which has been compiled in [3] and [4].

Another technique is to excite a narrow rectangular slot with a simple microstrip feed line as in [5] and [6]. In [5], the feed point is shifted from the center of the slot and is short circuited through the dielectric substrate. A similar technique of feed point shifting close to the slot end was used in [6]. In both cases, the offset of the feed point lead to perfect impedance match in a narrow frequency band and obtained an impedance bandwidth of approximately 20%.

When a T-shaped microstrip tuning stub is used to excite a wide rectangular aperture, a relatively broad bandwidth is noted (58%) from 1.5 to 3.2GHz [7]. Similarly, modifications in the shape of the slot can also result in broadband

operation as in [8] where a semi-circular slot and a protruding square shape is used to realize a bandwidth of 46%.

A kind of tapered slot antenna with planar structure, which was called the Vivaldi antenna, was proposed by P. J. Gibson [9] in 1979. This antenna has a wide bandwidth and a medium gain, but worked as an end-fire antenna. Its longitudinal dimension is large and impedance bandwidth is inherently limited by the microstrip to slotline transition. A printed two-side-antipodal exponential tapered slot antenna proposed by E. Gazit [10] has resolved the transition problem, though with a relatively higher cross-polarization level. Later, the balanced antipodal Vivaldi tapered slot antenna introduced by J. D. S. Langley [11] restrained the cross polarization to be less than -17 dB, with a bandwidth of 15 : 1, covering frequencies from 1.3–20 GHz.

In recent years, many researchers have been engaged in the printed wide-slot antenna and have realized the ultra wide band property through the combination of changing the slot shape and using different feeding structures. The wide-slot antenna is fed by a cross-shaped feeding with a cross shaped stub at the end instead of the common open microstrip feeder. It is equivalent to introducing a resonance circuit and hence resulting in an impedance bandwidth of 98% [12]. The slot antenna fed by a fan shaped stub together with a strip line has achieved a bandwidth of 114% by optimizing the length of the stub and the size of the fan-shape [13].

In [14], a rectangular patch in the middle of the rectangular slot is used to achieve a measured impedance bandwidth of 111%. By adding a rectangular copper sheet on one side of the microstrip to adjust the port impedance of the antenna, its impedance bandwidth extends to 135.7%, covering frequencies 2.3–12 GHz [15]. The printed wide-slot antenna also has been designed to use

various shapes of the guide strip terminal of its CPW feeder to excite the slot, and accordingly obtain the broadening of its impedance bandwidth.

Another type of printed slot antenna is the printed bowtie slot antenna, which has by virtue of simple configuration, wide bandwidth, low cross polarization level and high gain [16, 17]. In [16], impedance bandwidth is widened by using a linearly tapered slot at the joint of the coplanar waveguide and the bow-tie slot. A tapered coplanar waveguide feeder can be applied for achieving an impedance bandwidth of 123% [17].

A novel planar tapered-slot-fed annular slot antenna [18] proposed by T.G. Ma utilizes a unique tapered-slot feeding structure and simultaneously possesses ultra wide bandwidth, almost uniform radiation patterns, and low profile.

An improved design of the U-shaped stub rectangular slot antenna with a tuning pad for enhancing the impedance bandwidth is proposed by D.C. Chang [19]. By properly tuning the physical size of the copper pad, a wide impedance bandwidth can be achieved for UWB applications. For 10 dB return loss, impedance bandwidth of the antenna is from 2.3 to 12 GHz (135.7%).

Pengcheng Li presented two novel designs of planar elliptical slot antennas[20]. This printed antenna fed by either microstrip line or coplanar waveguide with U-shaped tuning stub with the elliptical/circular slots offered ultrawideband characteristics.

Evangelos S.et.al presented novel circular and elliptical CPW-fed slot and microstrip-fed antenna designs targeting the 3.1–10.6 GHz band[21]. The antennas are comprised of elliptical or circular stubs that excite similar-shaped slot apertures. Four prototypes have been examined, fabricated and experimentally tested. The

three being fed by a CPW and the fourth by a micro strip line. They exhibited a very satisfactory behavior throughout the 7.5 GHz band in terms of impedance match (VSWR 2), radiation efficiency and radiation pattern characteristics.

T.G.Ma.et.al presented a new coplanar waveguide- fed tapered ring slot antenna for ultra wideband (UWB) applications[22]. This antenna consists of a 50 Ω coplanar waveguide feeding line, wideband coplanar waveguide-to-slot line transition, and a pair of curved radiating slots. The impedance bandwidth is from 3.1 GHz to more than 12 GHz. The actual operating bandwidth is, however, limited by the distortion of radiation patterns. Such pattern distortion can be attributed to the antenna mode transition and is investigated with the help of the radiation patterns in the traditional sense as well as a dimensionless normalized antenna transfer function.

An ultrawideband (UWB) stripline slot antenna is analysed in frequency and time domain by C. Marchais et al [23]. Experiments were carried out to investigate its return loss, radiation behavior, and time-domain response. The antenna offers 130% impedance bandwidth. Moreover, its 108% radiation bandwidth covers the UWB band with a linear radiated far-field phase.

Gopikrishna et al. presented a novel ultra-wideband (UWB) antenna consisting of a linear tapered slot in the ground plane and a microstrip to slotline transition [24]. The antenna possesses a wide bandwidth from 2.95–14 GHz and shows stable radiation patterns with an average gain of 3dBi throughout the band. Measured group delay and transmission characteristics indicate that the antenna has good pulse handling capabilities.

A novel ultra wideband (UWB) printed wide-slot antenna was presented by Shi Cheng et al [25]. The presented design comprises of PICA-like structures,

etched from a double-layer substrate. Compared to the original PICA, it is lower in profile, more compact and maintains comparable performance. The results show that the proposed antenna provides at least 13:1 impedance bandwidth at 10-dB return loss.

A new coplanar waveguide-fed slot antenna for ultrawideband (UWB) applications is presented by Aidin Mehdipour [26]. The UWB characteristics of the antenna are achieved through the electromagnetic coupling between two adjacent slot arms. The antenna operates with VSWR lower than 2.2 in frequency band 3.1 GHz -10.6 GHz.

D.D. Krishna et al. presented an ultra-wideband (UWB) printed slot antenna, suitable for integration with the printed circuit board (PCB) for Wireless Universal Serial-Bus (WUSB) dongle applications [27]. The design comprises of a near-rectangular slot fed by a coplanar waveguide printed on a PCB of width 20 mm. The proposed design has a large bandwidth covering the 3.1– 10.6 GHz UWB band, with omnidirectional radiation patterns.

Two new low-cost, compact antennas, which operate in the upper half of the direct sequence spread spectrum UWB (DS-UWB) band, are presented by Tharaka Dissanayake [28]. These antennas are not only impedance matched, but also retain very good pattern stability over the operating band. One L-slot antenna has a planar ground plane and the other modified L-slot antenna has a ground plane consisting of a planar section and two sidewalls. Measured radiation pattern is presented to demonstrate the effect of ground plane on radiation patterns. Wideband radiation characteristics and the pattern stability of these antennas are investigated with the help of pattern stability factor (PSF).

Sunil Kumar Rajgopal presented an ultra wideband (UWB) pentagon shaped planar microstrip slot antenna that can find applications in wireless

communications [29]. Combination of the pentagon shape slot, feed line and pentagon stub are used to obtain 124% (2.65–11.30 GHz) impedance bandwidth which exceeds the UWB requirement of 110% (3.10–10.60 GHz). A ground plane of 50mm x 80 mm size is used which is similar to wireless cards for several portable wireless communication devices. The proposed antenna covers only the top 20 mm or 25% of the ground plane length, which leaves enough space for the RF circuitry. Three variations of the antenna design using the straight and rotated feed lines on two different substrates are considered. Effect of the conducting reflecting sheet on back of the antenna is investigated, which can provide directional radiation patterns but with reduced matching criteria.

A simple and compact CPW-fed ultra-wideband monopole-like slot antenna [30] was presented by X. Qing. The antenna comprises a monopole-like slot and a CPW fork-shaped feeding structure, which is etched on a FR4 printed circuit board (PCB) with an overall size of 26 mm x 29 mm x 1.5 mm. The simulation and experiment show that the proposed antenna achieves good impedance match, consistent gain, stable radiation patterns and consistent group delay over the operating bandwidth of 2.7–12.4 GHz (128.5%). Furthermore, through adding two more grounded open-circuited stubs, the proposed antenna design features band-notched characteristic in the band of 5–6 GHz while maintaining the desirable performance over lower/upper UWB bands of 3.1–4.85 GHz/6.2–9.7 GHz.

Jorge R. Costa presented a simple and compact printed antenna that exhibits adequate transient performance for ultra wideband (UWB) applications and it is further adequate for polarization diversity schemes[31]. The antenna is based on an original combination of two crossed exponentially tapered slots plus a star-shaped slot to produce a stable radiation pattern with very stable polarization over the 3.1–10.6 GHz FCC assigned band. Figure of merit like

output pulse fidelity and time window containing 90% of the transmitted energy are analyzed over the entire solid angle and showed to remain quite stable, in line with envisaged UWB system requirements. Compact dual-antenna arrangements are also analyzed in view of potential use for UWB multiple-input–multiple-output implementations.

A method to design a microstrip-fed antipodal tapered- slot antenna, which has ultra wideband performance and miniaturized dimensions was proposed by M. Amin Abbosh [32]. The proposed method modifies the antenna structure to establish a direct connection between the microstrip feeder and the radiator. That modification, which removes the need to use any transitions and/or baluns in the feeding structure, is the first step in the proposed miniaturization. In the second step of miniaturization, the radiator and ground plane are corrugated to enable further reduction in the antenna's size without jeopardizing its performance. The simulated and measured results confirm the benefits of the adopted method in reducing the surface area of the antenna, while maintaining the ultra wideband performance.

Chow-Yen-Desmond Sim proposed a novel compact microstrip-fed slot antenna [33]. By properly loading a notch to the open-ended T-shaped slot and extending a small section to the microstrip feed line, multiple resonant frequencies are excited and merged to form large enough 10-dB return loss bandwidth (measured from 3.1 to 11.45 GHz) for ultra wideband (UWB) applications.

In applications where size, weight, cost, performance, ease of installation, and aerodynamic profile are constraints, low profile antennas like microstrip and printed slot antennas are required. Printed slot antennas fed by CPW have several advantages over microstrip patch antennas. Slot antennas exhibit wider bandwidth, lower dispersion and lower radiation loss than microstrip antennas,

and when fed by a coplanar waveguide. They also provide an easy means of parallel and series connection of active and passive elements that are required for improving the impedance match and gain [34].

4.2 Triangular slot UWB antenna

The release of Ultra Wideband (UWB) for unlicensed applications by the FCC (Federal Communication Commission) received much attention by the industries and academia. This is due to low power consumption, high secured data rate support [35]. With the rapid developments of such UWB systems, a lot of attention is being given for designing the UWB antennas. The design of an antenna at the UWB band is quite challenging one because it has to satisfy the stringent requirements such as very large impedance bandwidth, omnidirectional radiation pattern, constant gain, high radiation efficiency, constant group delay, low profile and easy to manufacture [36]. Interestingly the planar slot antennas with CPW fed possess the above said features with simple structure, less radiation loss, less dispersion and easy integration with monolithic microwave integrated circuits (MMIC) [37]. Hence, the CPW fed planar slot antennas [38-45] are identified as the most promising antenna design for wideband wireless applications. In planar slot antennas two parameters affect the impedance bandwidth of the antenna, the slot width and the feed structure. The wider slot provides more bandwidth and the optimum feed structure gives the good impedance matching.

In this session, design of a triangular slot antenna with ultra wide impedance bandwidth is presented. The antenna 1 is a simple triangular slot antenna (Fig.4.1(a)). Then the transmission line is extended by a length S as shown in Fig. 4.1(b) (Antenna 2). Then a rectangle of length L and width W is top loaded on the signal strip resulting in the development of final UWB design (Antenna 2). The evolution of the antenna is shown in Fig.4.1.

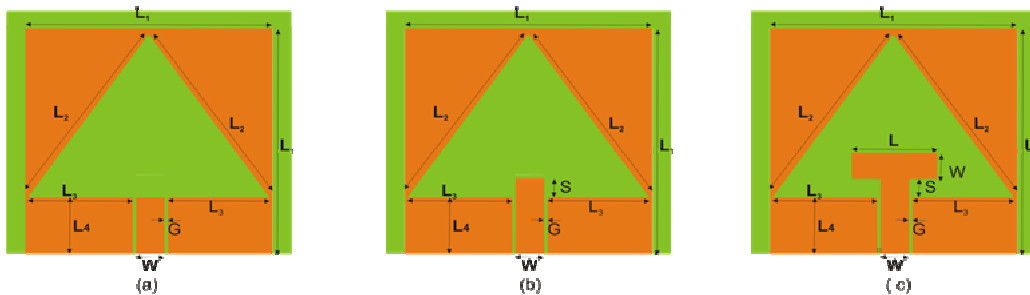


Fig.4.1 Evolution of Triangular slot UWB antenna(a)Triangular slot antenna(b) Signal strip extende Triangular slot Antenna(c)Triangular slot UWB antenna .
 ($L_1=26\text{mm}$, $L_2=22.65\text{mm}$, $L=9\text{mm}$, $L_3=10.85\text{mm}$, $L_4=7\text{mm}$, $S=2\text{mm}$, $W=3\text{mm}$, $h=1.6\text{mm}$, $\epsilon_r=4.4$ and $G=0.35\text{mm}$)

4.2.1 Triangular slot Antenna (Antenna 1)

The antenna consists of an isosceles triangular slot of side L_2 and base $2L_3+W+2G$ etched on a square substrate of size $L_1 \times L_1$ having dielectric constant $\epsilon_r = 4.4$, loss tangent $\tan \delta = 0.02$ and thickness $h = 1.6$ mm. The strip width (W) and gap (G) of the CPW feed are derived using standard design equations for 50Ω input impedance[47]. The top and side view of the antenna geometry is illustrated in Fig. 4.1.

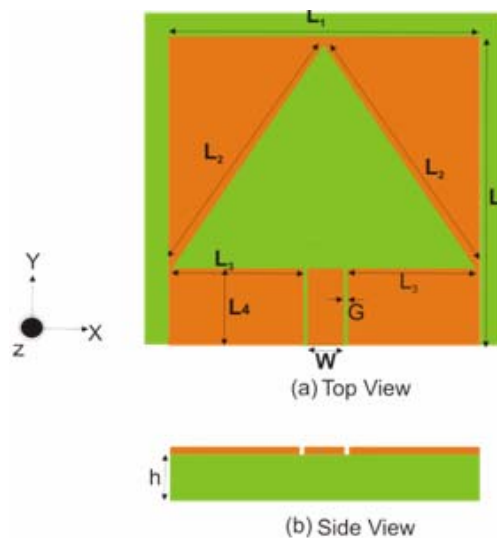


Fig.4.2. Geometry of the Antenna 1($L_1 =26\text{mm}$, $L_2=22.65\text{mm}$, $L_3=10.85\text{mm}$, $L_4=7\text{mm}$, $W = 3\text{mm}$, $G = 0.35\text{mm}$, $h = 1.6\text{mm}$ and $\epsilon_r = 4.4$)

The reflection and transmission coefficients of the antenna shown in Fig.4.3 indicates that antenna has a poorly matched resonance at 14GHz. The reflection coefficient is only -3.8dB. The S_{21} study shows that there is some radiation at this frequency but it is not efficient. With an aim to bring matching in the operating band, transmission line of antenna 1 is extended by a length S as described in the next session.

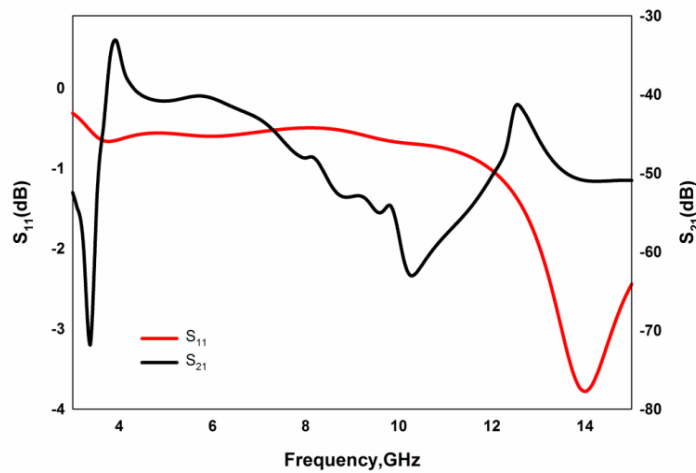


Fig.4.3. Reflection and transmission coefficients of antenna 1
 $(L_1=26\text{mm}, L_2=22.65\text{mm}, L_3=10.85\text{mm}, L_4=7\text{mm}, W=3\text{mm},$
 $G=0.35\text{mm}, h=1.6\text{mm}$ and $\epsilon_r=4.4)$

4.2.2 Signal strip extended Triangular slot Antenna (Antenna 2)

In the previous section we have seen that the antenna produces a poorly matched resonance at 14 GHz. In order to improve the matching, signal strip of antenna 1 is extended by a length S resulting in Antenna 2. Since S is inside the slot compactness of the antenna is not at all affected.

The antenna includes an isosceles triangular slot of side L_2 and base $2L_3+W+2G$ etched on a square substrate of size $L_1 \times L_1$ having dielectric constant $\epsilon_r = 4.4$, loss tangent $\tan \delta = 0.02$ and thickness $h = 1.6$ mm. Signal

strip is extended by a length S . The top and side view of the antenna geometry is illustrated in Fig. 4.4.

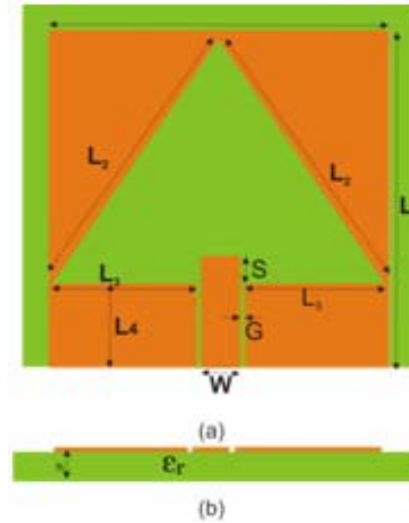


Fig.4.4. Geometry of the Antenna 2
 ($L_1 = 26\text{mm}$, $L_2 = 22.65\text{mm}$, $L_3 = 10.85\text{mm}$, $L_4 = 7\text{mm}$, $W = 3\text{mm}$,
 $S = 2\text{mm}$, $G = 0.35\text{mm}$, $h = 1.6\text{mm}$ and $\epsilon_r = 4.4$)

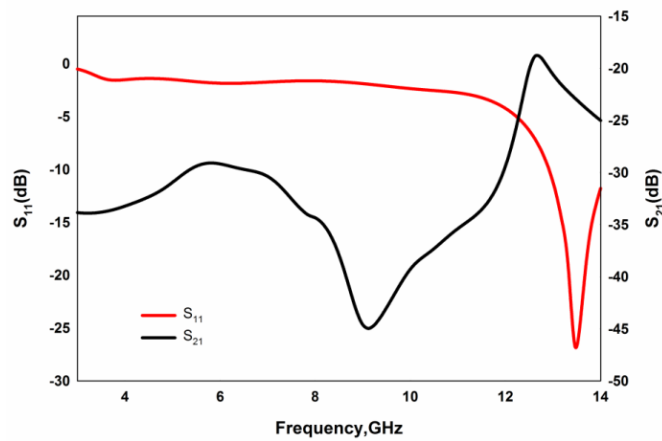


Fig.4.5. Reflection and transmission coefficients of antenna 2
 ($L_1 = 26\text{mm}$, $L_2 = 22.65\text{mm}$, $L_3 = 10.85\text{mm}$, $L_4 = 7\text{mm}$, $W = 3\text{mm}$,
 $G = 0.35\text{mm}$, $h = 1.6\text{mm}$ and $\epsilon_r = 4.4$)

Reflection and transmission coefficients of the antenna plotted in Fig.4.5 indicate that there is a single resonance at 13.5GHz with bandwidth ranging

from 13-14GHz. Also there is a tendency for matching around 4 GHz. ie, is improved matching is obtained than antenna 1. The transmission characteristics again confirms this result. At 13.5GHz, power received is nearly -19dBi which is very much greater than antenna 1.

To improve matching at low frequency region and to produce additional resonance in the middle frequency range, a rectangular stub is incorporated on the signal strip resulting in the development of final antenna. The combined effect of the triangular slot and rectangular stub results in the UWB operation. This is carried out in detail in the next session.

4.2.3 Triangular Slot UWB Antenna (Antenna 3)

In this section, a printed compact Coplanar Waveguide(CPW) fed triangular slot antenna for Ultra Wide Band (UWB) communication systems is presented. Design equations are implemented and validated for different substrates. The simulation and experimental studies reveal that the proposed antenna exhibits good impedance match, stable radiation patterns and constant gain throughout the operating band.

4.2.3.1 Geometry of the Triangular slot UWB Antenna

The geometry of the proposed antenna is shown in Fig.4.6. The antenna consists of an isosceles triangular slot of side L_2 and base $2L_3+W+2G$ etched on a square substrate of size $L_1 \times L_1$ having dielectric constant $\epsilon_r = 4.4$, loss tangent $\tan \delta = 0.02$ and thickness $h = 1.6$ mm. A rectangle of length L and width W is connected as shown in the figure. The spacing between the rectangle and the edge of the ground plane is S . The antenna is distinctive in its structure and it has simple design with less number of design parameters compared to the existing antennas in the literature.

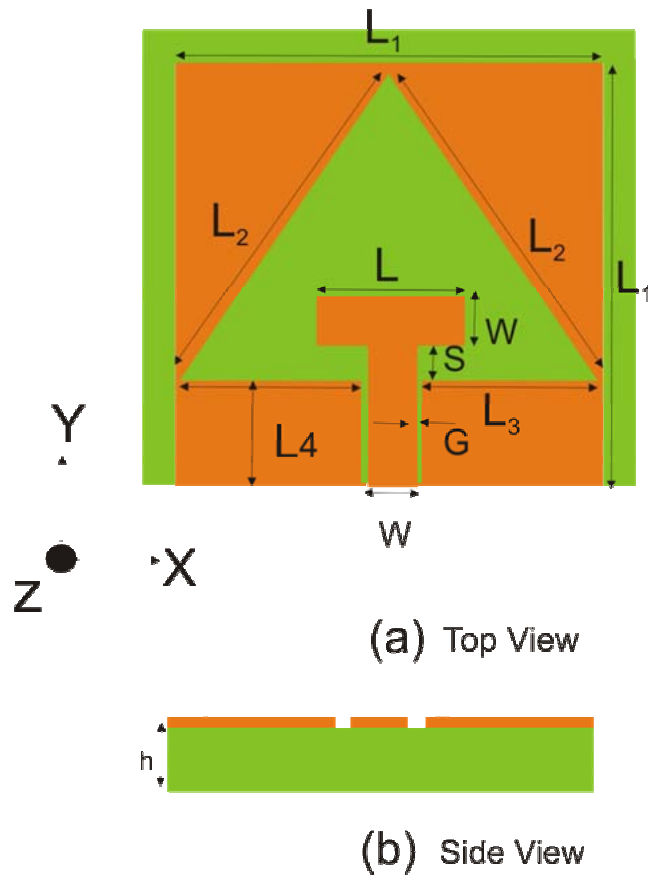


Fig. 4.6. Geometry of the triangular slot UWB antenna.
 ($L_1=26\text{mm}$, $L_2=22.65\text{mm}$, $L=9\text{mm}$, $L_3=10.85\text{mm}$, $L_4=7\text{mm}$,
 $S=2\text{mm}$, $W=3\text{mm}$, $h=1.6\text{mm}$, $\epsilon_r=4.4$ and $G=0.35\text{mm}$)

4.2.3.2 Reflection Characteristics of the Triangular slot UWB Antenna

Fig.4.7 illustrates the simulated and measured reflection coefficient of the optimal design of the antenna with parameters as in Fig.4.6. The -10dB bandwidth appears to span an extremely wide frequency range from 3.1GHz to 11.1GHz. The wide bandwidth is obtained by merging three resonances centered at 3.38GHz, 4.8GHz and 9.5GHz respectively. This is elaborately explained in the remaining sessions.

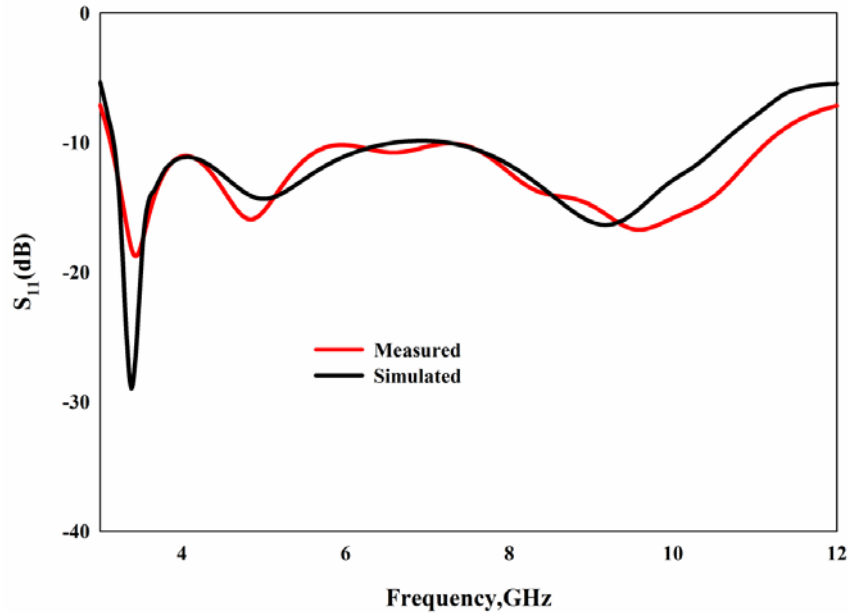


Fig.4.7. Simulated and measured reflection coefficients of the triangular slot UWB antenna ($L_1=26\text{mm}$, $L_2=22.65\text{mm}$, $L=9\text{mm}$, $L_3=10.85\text{mm}$, $L_4=7\text{mm}$, $S=2\text{mm}$, $W=3\text{mm}$, $h=1.6\text{mm}$, $\epsilon_r=4.4$ and $G=0.35\text{mm}$)

4.2.3.3 Parametric Analysis of the Triangular slot UWB Antenna

Further insight on the antenna performance is obtained by carrying out a detailed parametric analysis. The variation of reflection coefficients with different antenna parameters are given below.

4.2.3.3.1 Effect of rectangle length L

In order to study the effect of strip length L on the return loss characteristics, a thorough parametric analysis has been performed. Fig 4.8 shows the variation of reflection characteristics and input impedance for different strip lengths L. It is observed that without the strip ($L=3$), there are only two poorly matched resonances within the UWB frequency range.

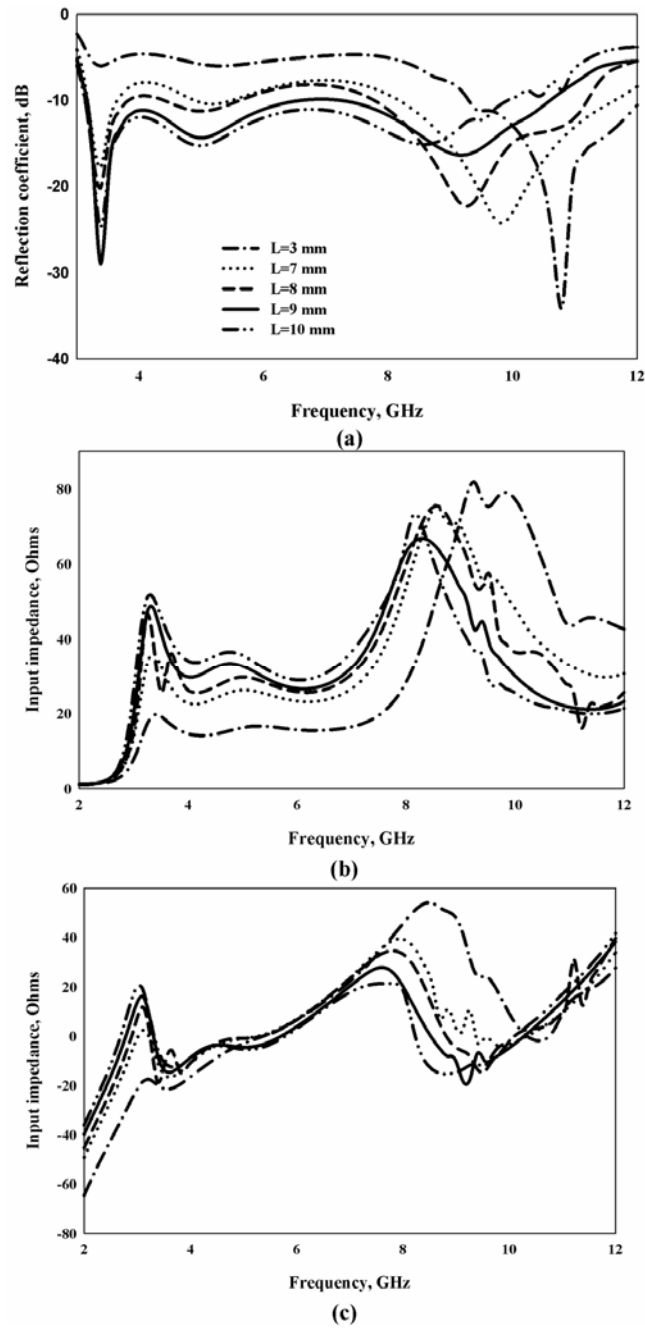
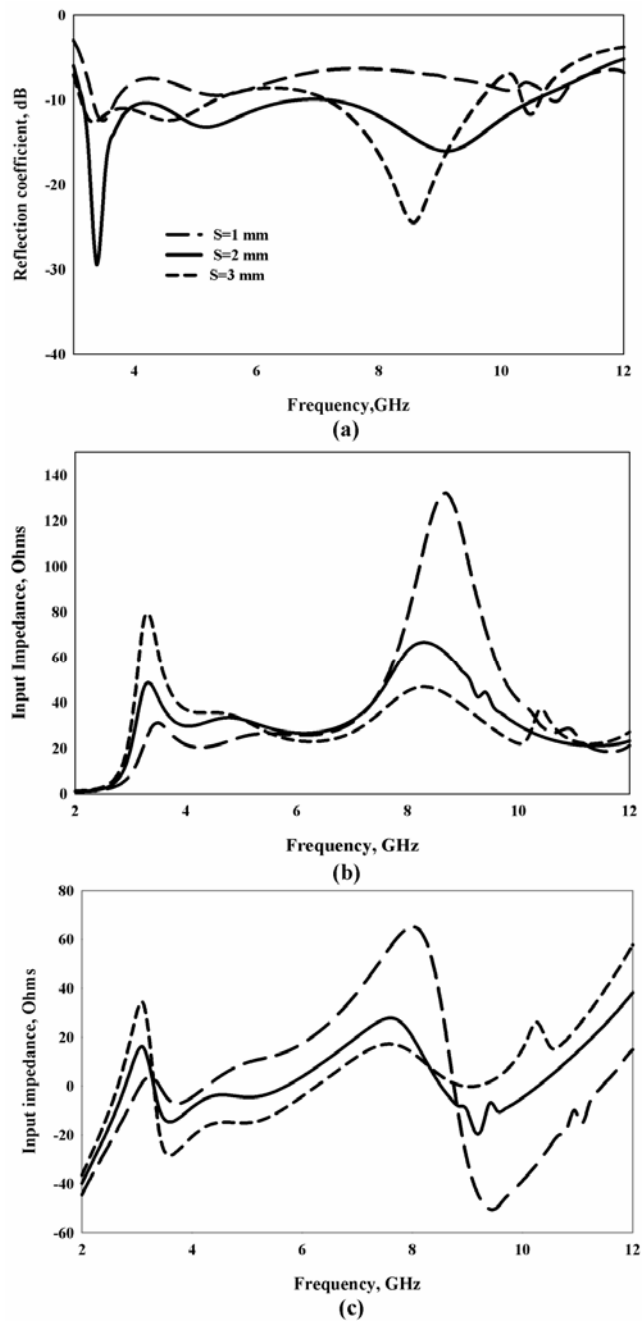


Fig.4.8. Reflection coefficient and impedances of the triangular slot antenna for different L (a)Reflection coefficient (b)Real part of impedance (c)Imaginary part of impedance
 ($L_1=26\text{mm}$, $L_2=22.65\text{mm}$, $L_3=10.85\text{mm}$, $L_4=7\text{mm}$, $S=2\text{mm}$, $W=3\text{mm}$, $h=1.6\text{mm}$, $\epsilon_r=4.4$ and $G=0.35\text{mm}$)

As L increases, matching corresponding to the first and second resonances increases. The strip produces a third resonance and at the optimum strip length, three resonances merge together to form UWB frequency response. It can also be seen that without the strip, the antenna has very low input impedance and is highly capacitive. Increase in L improves the input impedance corresponding to the first and second resonances. Also the imaginary part is shifted towards the inductive side. The strip produces extra capacitive reactance and at the optimum design, it merges the resonances to give UWB operation. From parametric studies L is found to be $0.346 \lambda_c$ where λ_c is the wavelength corresponding to centre frequency of the operating band.

4.2.3.3.2 Effect of gap distance S .

Variation of S , which adjusts the coupling between the radiating element and the ground plane is also studied. Variation of return losses and input impedances of the antenna for different S are shown in Fig. 4.9. It is found that good impedance matching can be obtained by enhancing the coupling between the slot and feed. When the coupling is increased to a certain value, the optimum operating bandwidth can be obtained. However, if the coupling is increased more, the impedance matching deteriorates, showing that over coupling also degrades the impedance matching. For $S=1\text{mm}$, matching is very poor for the first two resonances and real part of impedance is low (24Ω), but impedance improves with increase in S and a value of 50Ω is achieved at $S=2\text{mm}$. Also increase in S increases the inductive reactance. When $S=3\text{mm}$, real part of impedance is further increased and the imaginary part is shifted towards inductive side. From detailed analysis value of S is optimised to be $0.076 \lambda_c$ where λ_c is the wavelength corresponding to centre frequency of the operating band.



**Fig. 4.9. Reflection coefficients and impedances of the triangular slot antenna for different S.(a) Reflection coefficient(b) Real part of impedance(c)Imaginary part of impedance.
 ($L_1=26\text{mm}$, $L_2=22.65\text{mm}$, $L=9\text{mm}$, $L_3=10.85\text{mm}$, $L_4=7\text{mm}$, $W=3\text{mm}$, $h=1.6\text{mm}$, $\epsilon_r=4.4$ and $G=0.35\text{mm}$)**

4.2.3.3.3 Effect of triangular side L_2

Effect of variation of L_2 on reflection coefficient is also conducted and shown in figure 4.10. It is found that L_2 mainly affects the resonances and the bandwidths are less affected. Optimum performance is obtained for $L_2=22.6\text{mm}$. From exhaustive analysis value of L_2 is found to be $0.87 \lambda_c$ where λ_c is the wavelength corresponding to centre frequency of the operating band.

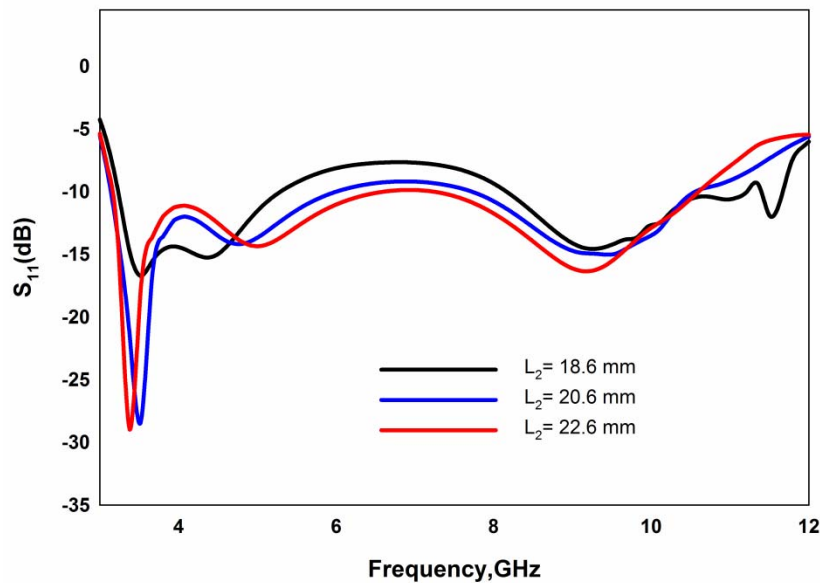


Fig.4.10. Reflection coefficient of the triangular slot antenna for different L_2 values
 ($L_1=26\text{mm}$, $L_2=22.65\text{mm}$, $L=9\text{mm}$, $L_3=10.85\text{mm}$, $L_4=7\text{mm}$,
 $W=3\text{mm}$, $h=1.6\text{mm}$, $\epsilon_r=4.4$ and $G=0.35\text{mm}$)

4.2.3.3.4 Effect of L_3

The effect of variation of reflection coefficient with different L_3 values are also conducted and is shown in Fig. 4.11. It is found that compared to L_2 , L_3 affects the resonant frequencies also. From detailed analysis value of L_3 is found to be $0.417 \lambda_c$ where λ_c is the wavelength corresponding to centre frequency of the operating band.

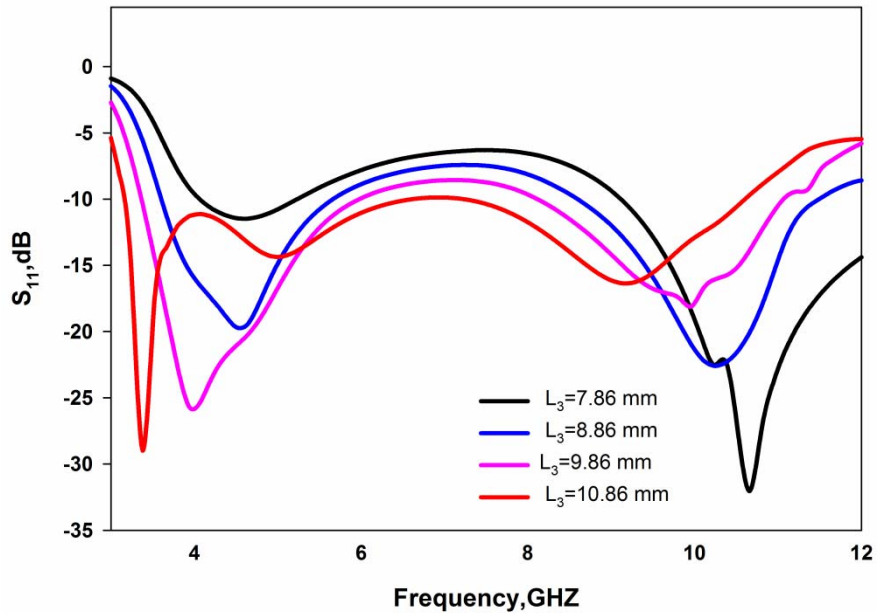


Fig.4.11 Reflection coefficient of the triangular slot antenna for different L_3 values ($L_1=26\text{mm}$, $L_2=22.65\text{mm}$, $L_3=9\text{mm}$, $L_4=7\text{mm}$, $W=3\text{mm}$, $h=1.6\text{mm}$, $\epsilon_r=4.4$ and $G=0.35\text{mm}$)

4.2.3.5 Field distributions and Radiation patterns of the Triangular slot UWB Antenna

From the spectrum of impedance performance, it can be seen that there are three resonances at 3.38, 4.8, and 9.5 GHz. These resonances correspond to the different modes of field distribution and play important roles on the explanation of the radiation patterns. The electric field distributions of these resonant modes are then simulated and the corresponding radiation patterns are investigated at 3.8, 4.8, and 9.5GHz, as shown in Figs. 4.12–4.14, respectively. Fig. 4.12 shows the first resonant mode at 3.38 GHz, where the electric fields are concentrated at the upper center part with polarization mainly in the y-axis. This set of field distribution is locally similar to that of mode in a rectangular waveguide [46], and considered as the fundamental mode of the antenna. The radiation pattern of this mode is like a small dipole oriented in the y-axis

leading to a bidirectional pattern in the E-plane (yz plane) and omni directional pattern in the H-plane (xz plane), as shown in Fig. 4.15(b).

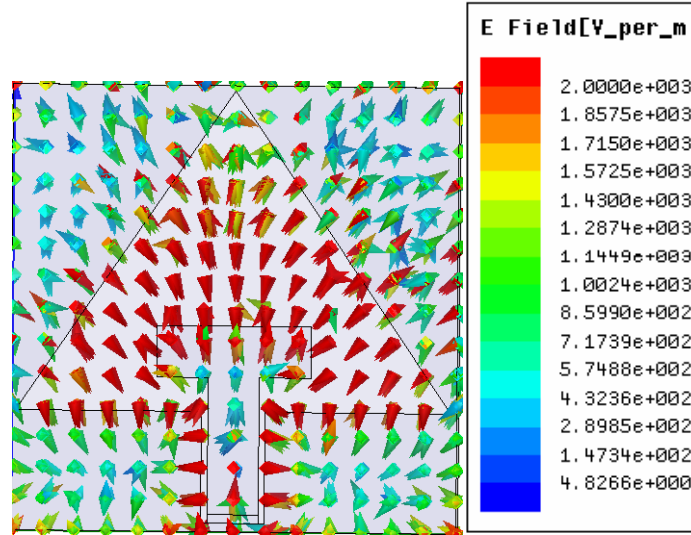


Fig.4.12 Distribution of electric fields at first resonant mode at 3.38GHz
**($L_1=26\text{mm}$, $L_2=22.65\text{mm}$, $L=9\text{mm}$, $L_3=10.85\text{mm}$, $L_4=7\text{mm}$,
 $S=2\text{mm}$, $W=3\text{mm}$, $h=1.6\text{mm}$, $\epsilon_r=4.4$ and $G=0.35\text{mm}$)**

Fig. 4.13 shows the second resonant mode at 4.8 GHz where both x- and y-component fields exist. Note that the x-component fields of the left and right sides of the stub are in the opposite directions that cancel out each other at far fields in the symmetric E-plane. Therefore, the E-plane patterns are almost unchanged and still have good polarization isolation (x-polarized level better than 20 dB), as shown in Fig. 4.15(c). However, the x-component fields generate cross-polarized patterns in the H-plane, as shown in figure.

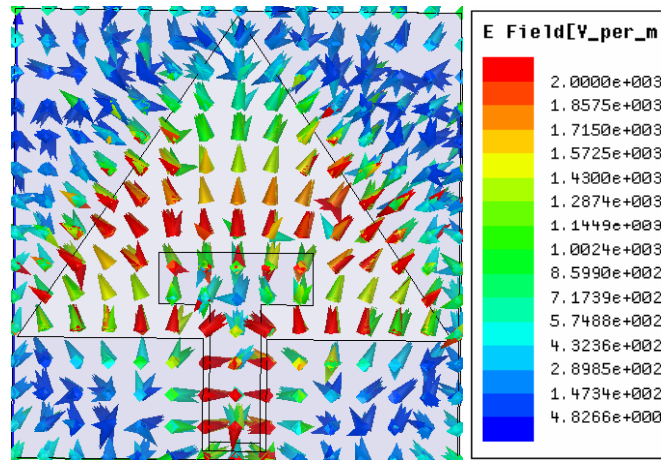


Fig.4.13 Distribution of electric fields at second resonant mode at 4.8GHz
 ($L_1=26\text{mm}$, $L_2=22.65\text{mm}$, $L=9\text{mm}$, $L_3=10.85\text{mm}$, $L_4=7\text{mm}$, $S=2\text{mm}$,
 $W=3\text{mm}$, $h=1.6\text{mm}$, $\epsilon_r=4.4$ and $G=0.35\text{mm}$)

Fig. 4.14 shows the third resonant mode at 9.5 GHz, where the y-component fields are partially shifted to lower part and concentrated to the left and right sides of the CPW feed. This field distribution contains multiple higher order modes and makes the peak of E-plane patterns shift slightly from the z-axis, as shown in Fig. 4.15(d).

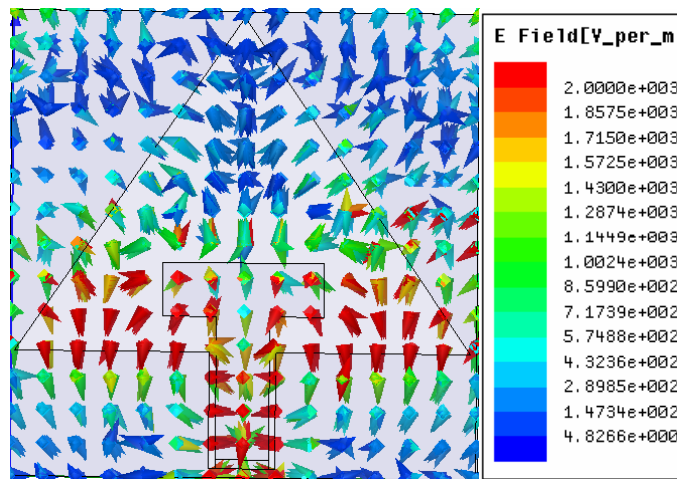


Fig.4.14. Distribution of electric fields at third resonant mode at 9.5 GHz
 ($L_1=26\text{mm}$, $L_2=22.65\text{mm}$, $L=9\text{mm}$, $L_3=10.85\text{mm}$, $L_4=7\text{mm}$, $S=2\text{mm}$,
 $W=3\text{mm}$, $h=1.6\text{mm}$, $\epsilon_r=4.4$ and $G=0.35\text{mm}$)

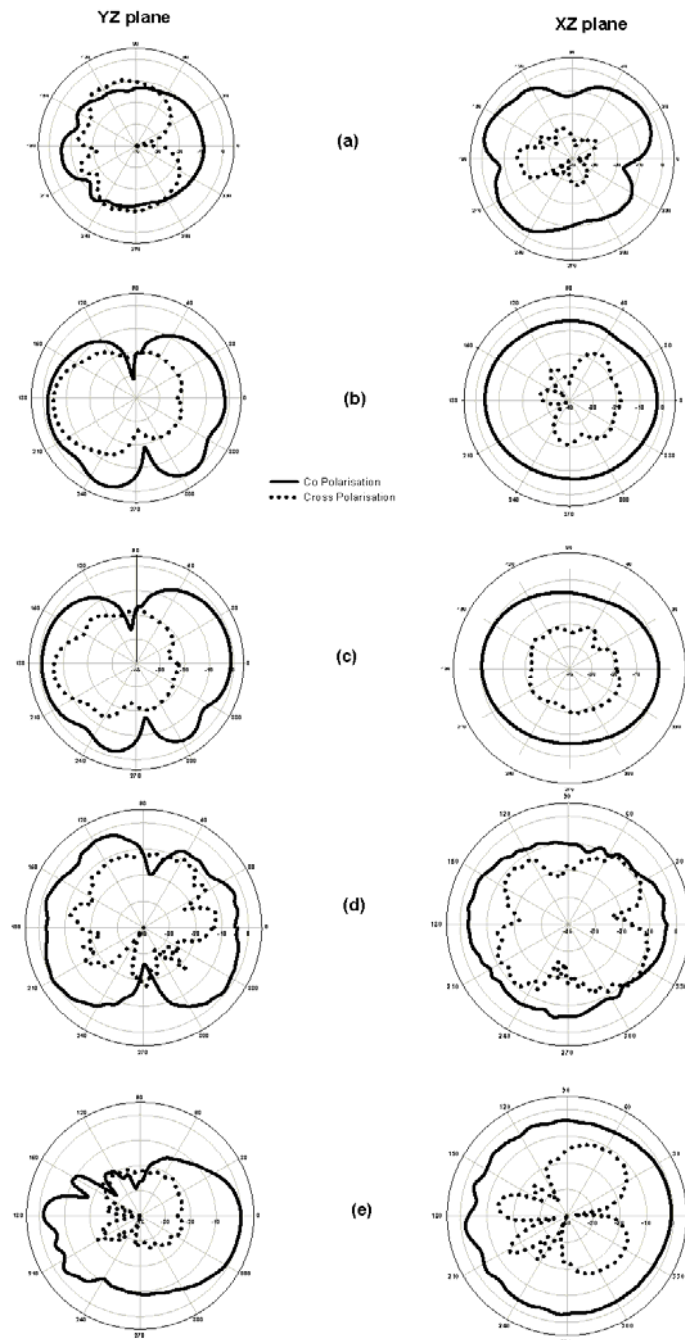


Fig.4.15 Measured radiation pattern of the triangular slot antenna at the frequencies (a)3.1GHz (b) 3.38 GHz(c)4.8GHz (d)9.5GHz and (e)10.6GHz
 ($L_1=26\text{mm}$, $L_2=22.65\text{mm}$, $L=9\text{mm}$, $L_3=10.85\text{mm}$, $L_4=7\text{mm}$, $S=2\text{mm}$, $W=3\text{mm}$, $h=1.6\text{mm}$, $\epsilon_r=4.4$ and $G=0.35\text{mm}$)

From the measured radiation pattern of the antenna shown in Fig.4.15, it is clear that the antenna exhibits omnidirectional pattern in the higher frequencies also. This is also confirmed by the time domain measurements of the antenna discussed in section 4.4.

4.2.3.6 Design of the Triangular slot UWB Antenna

Since we are interested in the ultra wide band width, centre frequency of operating band is taken into account while deriving the design equations. The criteria for designing the antenna is as follows.

- 1) Design a 50Ω CPW line on a substrate with permittivity ϵ_r . Calculate the effective permittivity of the substrate ϵ_{reff} using $\epsilon_{\text{reff}} = (\epsilon_r + 1)/2$.
- 2) Ground plane plays a major role in determining the first and second resonances. The dimensions of the ground plane are calculated as follows.

$$L_1 = (\lambda_c) \text{ ----- (4.1)}$$

$$L_4 = (0.27 \lambda_c) \text{ ----- (4.2)}$$

where λ_c is the wavelength corresponding to centre frequency of the operating band.

- 3) Sides of the triangle L_2 and L_3 are calculated using

$$L_2 = (0.87 \lambda_c) \text{ ----- (4.3)}$$

and

$$L_3 = (0.417 \lambda_c) \text{ ----- (4.4)}$$

- 4) Length of the rectangular stub L and the gap between stub and ground plane separation S are calculated using

$$S = 0.076 \lambda_c \text{ ----- (4.5)}$$

and

$$L = 0.346 \lambda_c \text{ ----- (4.6)}$$

In order to justify the design equations, the antenna parameters are computed for different substrates (Table 4.1) and Table 4.2 shows the computed geometric parameters of the antenna.

Table 4.1 Antenna Description

	Antenna 1	Antenna 2	Antenna 3	Antenna 4
Laminate	Rogers 5880	FR4 Epoxy	Rogers RO3006	Rogers6010LM
h(mm)	1.57	1.6	1.28	0.635
ϵ_r	2.2	4.4	6.15	10.2
ϵ_{re}	1.6	2.7	3.575	5.6
W(mm)	4	3	2.58	2.05
G(mm)	0.17	0.35	0.45	0.5

Table 4.2 Computed Geometric Parameters of the Antenna

Parameter (mm)	Antenna 1	Antenna 2	Antenna 3	Antenna 4
L_1	33.8	26	22.5	18
L_2	29.47	22.6	19.65	15.6
L_3	14.1	10.85	9.4	9
L_4	9.11	7	6	4.85
S	2.6	2	1.735	1.36
L	11.71	9	7.8	6.22

Fig 4.16 shows the reflection coefficients of different antennas as given in Table 4.2. In all the cases antenna is operating in the UWB region.

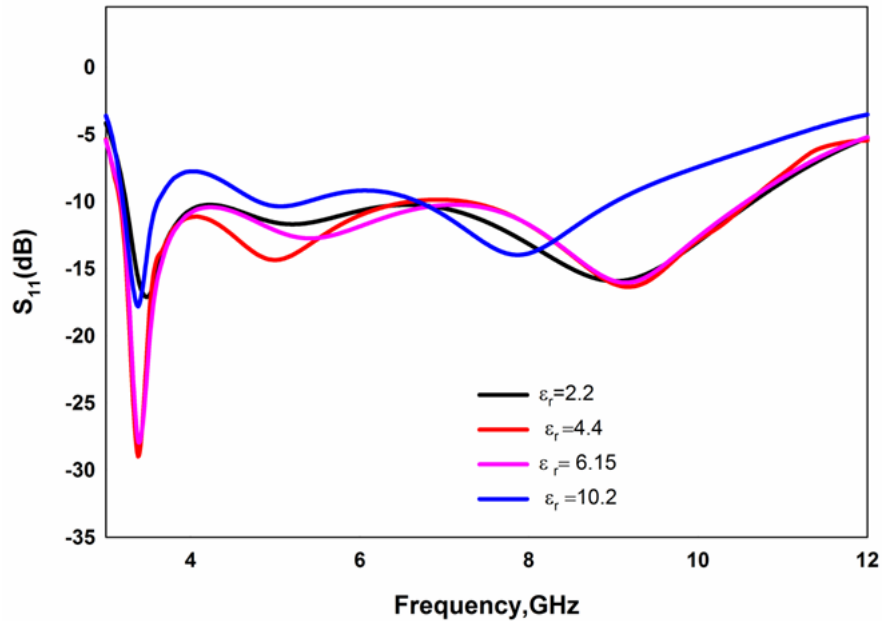


Fig.4.16. Reflection coefficient of the Triangular slot UWB antenna with computed geometric parameters for different substrates

4.2.3.7 Current distribution and radiation pattern of the triangular slot UWB antenna

The $|S_{11}|$ can only depict the performance of an antenna as a lumped load at the end of the feeding line. The elaborated electromagnetic behaviour of the antenna can only be revealed by examining the current distributions or radiation patterns. The typical current distributions of the antenna at the resonant frequencies and the corresponding radiation patterns are displayed in Fig. 4.17. From the current distribution, it is clear that both first and second resonances are produced by the symmetrical path ABC and DEC. Third resonance corresponds to a $\lambda_g/4$ variation along the path FG. Compared to ground

modified monopole and serrated monopole antennas, the antenna exhibits near omni-directional pattern in the entire UWB spectrum.

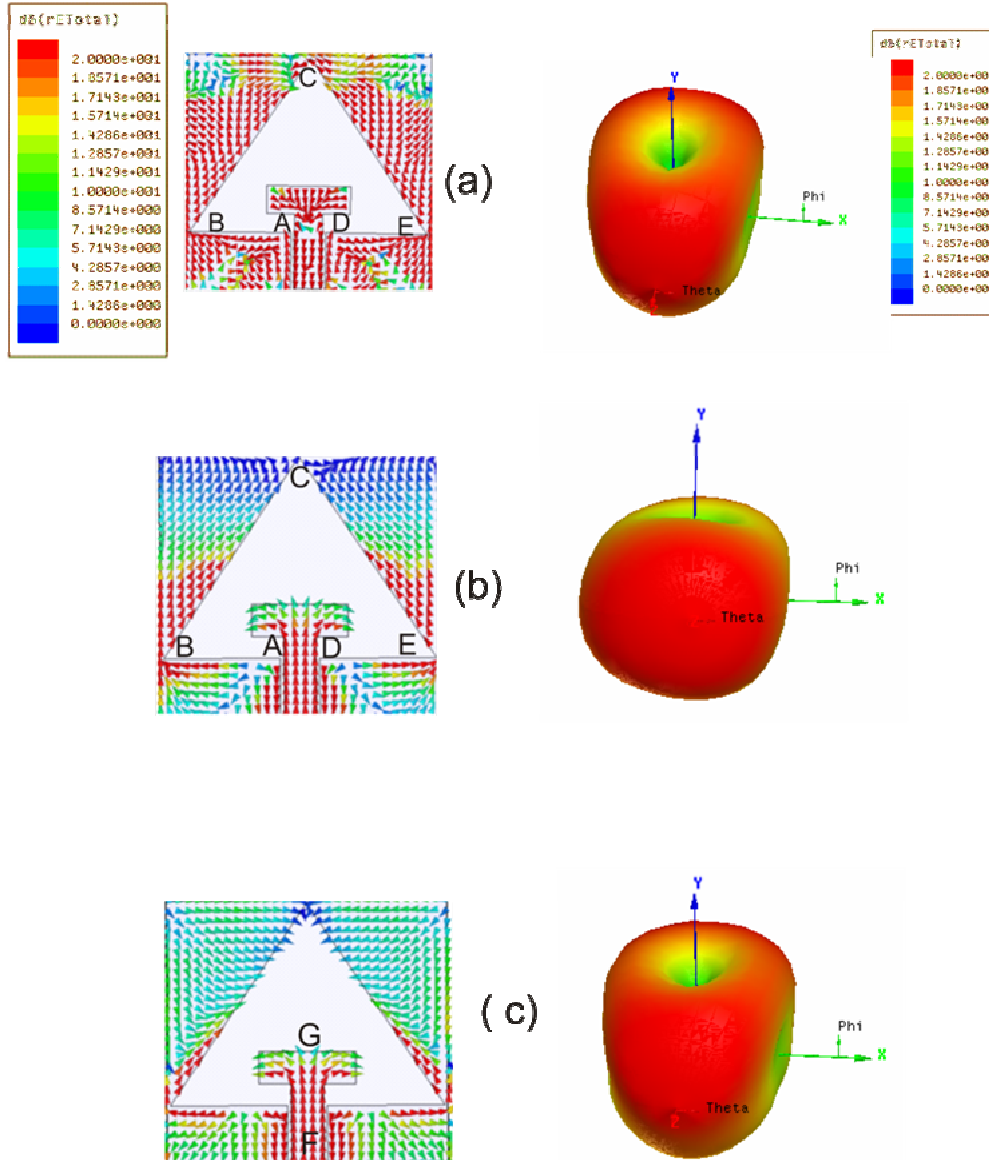


Fig.4.17 Simulated surface current distribution and radiation patterns of the triangular slot antenna at (a) 3.38GHz(b)4.78GHz and (c)9.6GHz ($L_1=26\text{mm}$, $L_2=22.65\text{mm}$, $L=9\text{mm}$, $L_3=10.85\text{mm}$, $L_4=7\text{mm}$, $S=2\text{mm}$, $W=3\text{mm}$, $h=1.6\text{mm}$, $\epsilon_r=4.4$ and $G=0.35\text{mm}$)

4.2.3.8 Gain and Efficiency of the triangular slot UWB antenna.

The gain and efficiency are two important figure of merit of the antenna. The gain of the antenna is measured using gain comparison method while the efficiency of the proposed antenna is measured using Wheeler cap method. The measured gain and efficiency of the antenna are depicted in Fig.4.18. A peak gain of 5.5dBi is observed at 11GHz and it is also worth to note that the antenna provides almost uniform gain throughout the band. Average efficiency of the antenna is found to be 72%.

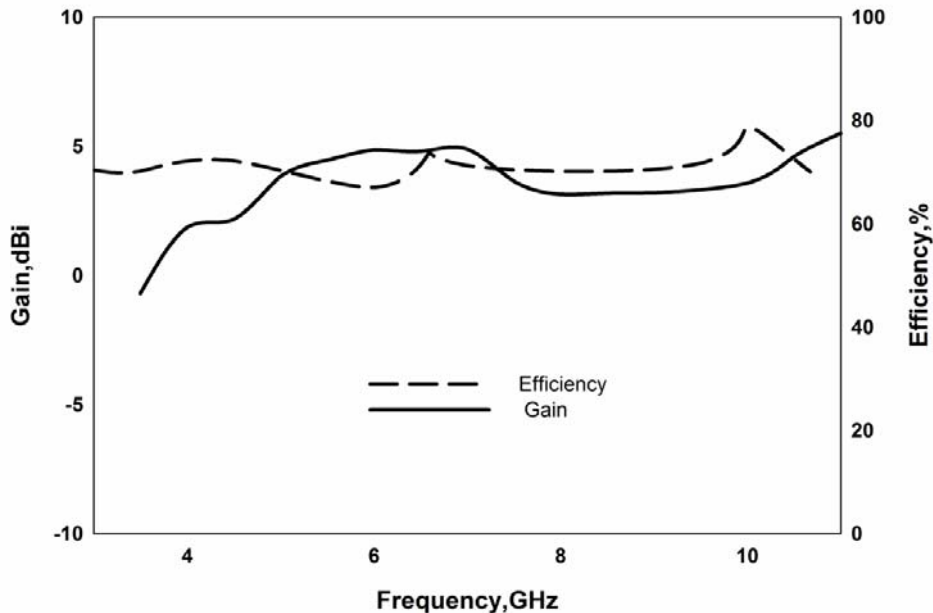


Fig.4.18. Gain and efficiency of the triangular slot UWB antenna ($L_1=26\text{mm}$, $L_2=22.65\text{mm}$, $L=9\text{mm}$, $L_3=10.85\text{mm}$, $L_4=7\text{mm}$, $S=2\text{mm}$, $W=3\text{mm}$, $h=1.6\text{mm}$, $\epsilon_r=4.4$ and $G=0.35\text{mm}$)

4.3 5.8GHz Band Notched Triangular Slot Antenna

In the proposed antenna, to avoid interference with electronic systems operating in the IEEE802.11a and HIPERLAN/2 bands, a band reject mechanism is achieved by incorporating two open ended slits as shown in

Fig.4.19 are made at the top edge of the T stub, where the effective length of each slit is around quarter wavelength for the 5.8 GHz resonance. Dimensions of the triangular slot antenna remain same as in Fig.4.7.

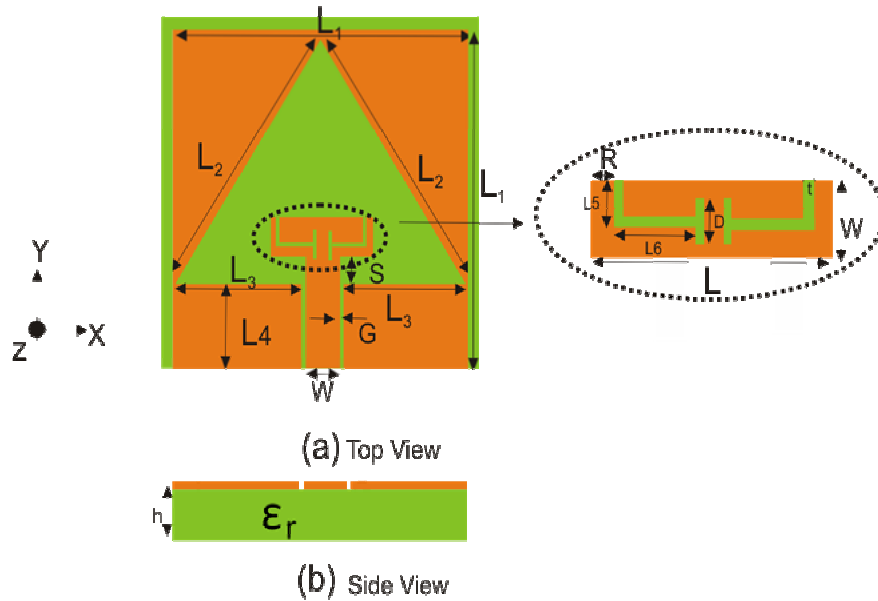


Fig. 4.19. Geometry of the band notched triangular slot antenna
 $(L_1=26\text{mm}, L_2=22.65\text{mm}, L_3=10.85\text{mm}, L_4=7\text{mm}, S=2\text{mm},$
 $W=3\text{mm}, h=1.6\text{mm}, \epsilon_r=4.4, G=0.35\text{mm}, L_5=2.25\text{mm}, L_6=3.5\text{mm},$
 $D=1.5\text{mm}, t=0.5\text{mm and } R=0.5\text{mm})$ (a)Top View(b)Side view

4.3.1 Reflection characteristics of Band Notched Triangular Slot Antenna

Fig.4.20 plots the measured and simulated reflection coefficient of the UWB slot antenna with the narrow slit inscribed. It shows good rejection at 5.8GHz. A notch band from 5GHz to 6.1GHz is obtained.

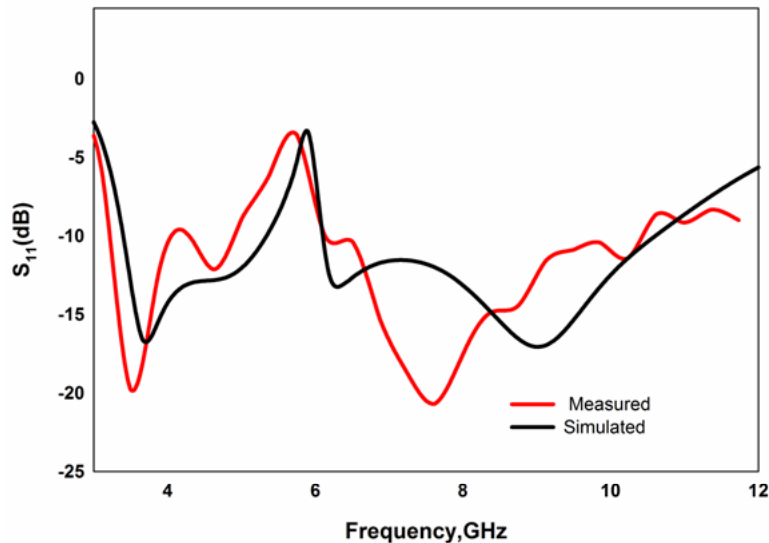


Fig.4.20. Measured and Simulated reflection coefficient of the band notched triangular slot antenna ($L_1=26\text{mm}$, $L_2=22.65\text{mm}$, $L_3=10.85\text{mm}$, $L_4=7\text{mm}$, $S=2\text{mm}$, $W=3\text{mm}$, $h=1.6\text{mm}$, $\epsilon_r=4.4$, $G=0.35\text{mm}$, $L_5=2.25\text{mm}$, $L_6=3.5\text{mm}$, $D=1.5\text{mm}$, $t=0.5\text{mm}$ and $R=0.5\text{mm}$).

To design the open ended slits for band notch, the equation to be followed is

$$L_5 + L_6 + D = \lambda_{g,5.8}/4 \text{ ----- (4.7)}$$

where $\lambda_{g,5.8}$ is the guide wavelength computed at 5.8 GHz. The optimum values for these parameters are, $L_5 = 6.45\text{mm}$, $L_6 = 0.9\text{mm}$, $R=0.5\text{mm}$, $D = 0.25\text{mm}$ and $t=0.5\text{mm}$.

The slits function as shorted transmission lines having an electrical length of approximately $\lambda_g/4$ at 5.8 GHz, giving a high input impedance.

The band-notched property is also observed in Fig.4.21, where the simulated 3D radiation patterns plotted at 3.38GHz, 6.0GHz, and 9.6GHz remains similar to the corresponding plots of the triangular slot antenna(Fig.4.6), without the slit except for the notched frequency at 5.8GHz. At 5.8GHz, a distinct reduction in radiation is noted for all directions.

Fig.4.21(e) shows that the surface current distribution appears stronger around the slit at the notched frequency of 5.8GHz. This leads to destructive interference of the excited surface currents in the patch.

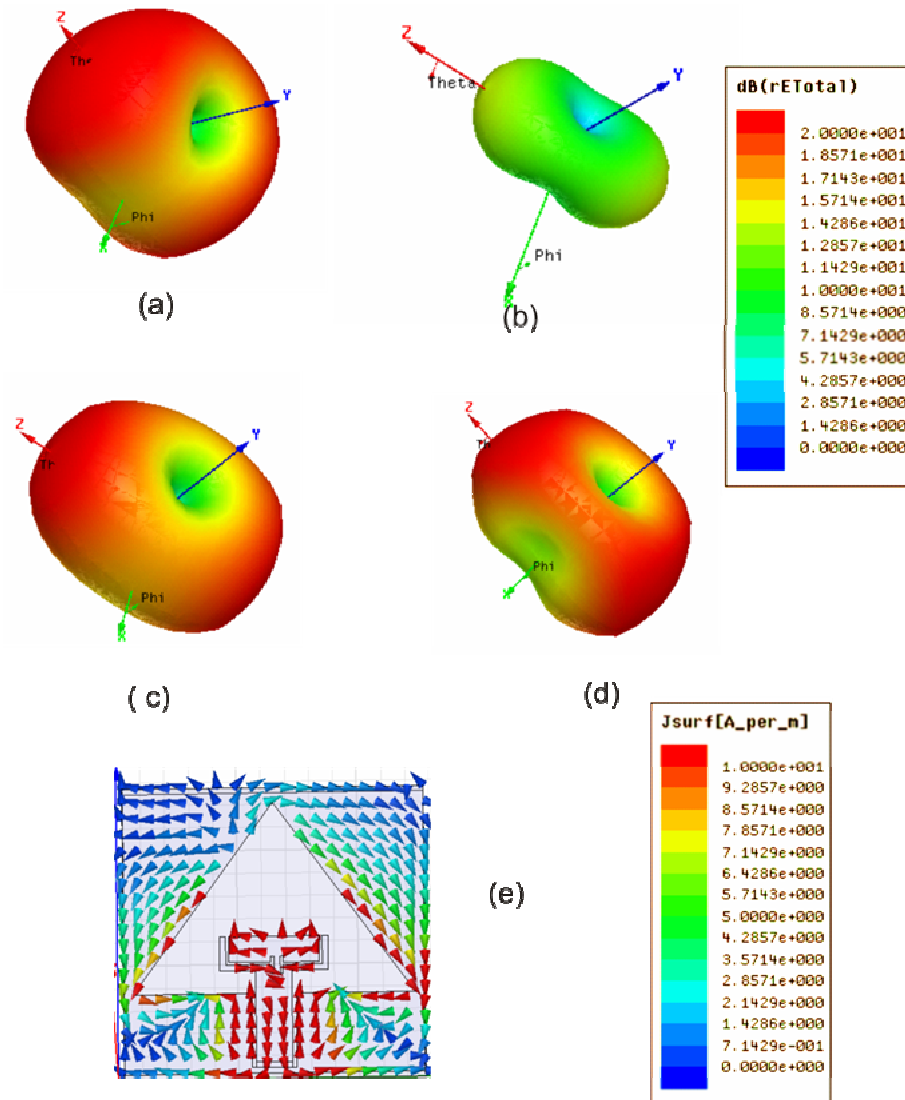


Fig.4.21. Simulated radiation patterns of band notched triangular slot antenna at (a)3.66GHz (b)5.8GHz(c)6.32GHz and (d)9GHz (e)Current distribution at 5.8GHz

$(L_1=26\text{mm}, L_2=22.65\text{mm}, L_3=10.85\text{mm}, L_4=7\text{mm}, S=2\text{mm}, W=3\text{mm}, h=1.6\text{mm}, \epsilon_r=4.4, G=0.35\text{mm}, L_5=2.25\text{mm}, L_6=3.5\text{mm}, D=1.5\text{mm}, t=0.5\text{mm}$ and $R=0.5\text{mm}$).

Measured gain and efficiency of the band notched triangular slot antenna is plotted in Fig.4.22. An average gain of 3dBi is noted throughout the operating band except at the notched frequency where a gain of -6dBi is obtained. The antenna designed has a radiation efficiency of more than 70% in the pass band and a reduction in the rejected band.

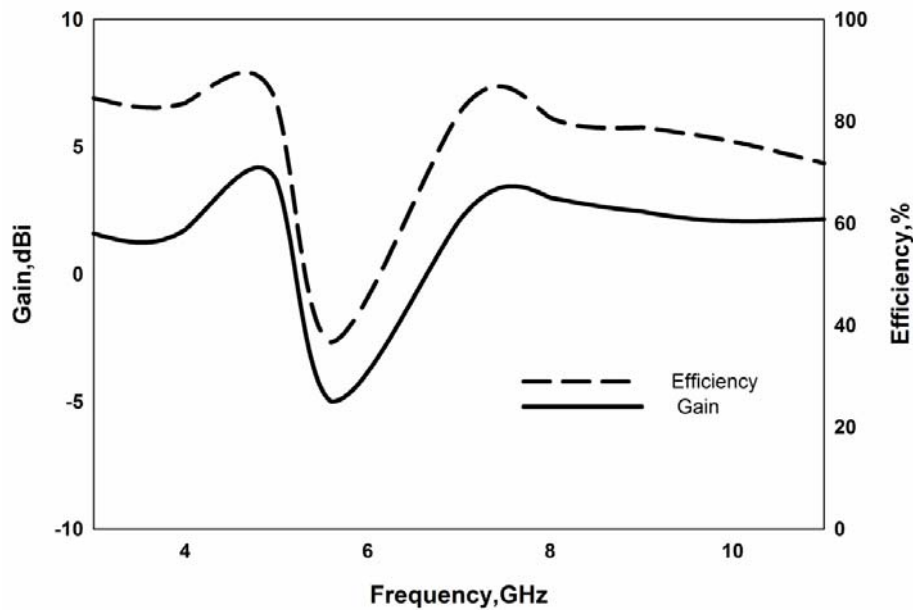


Fig.4.22. Measured gain and efficiency of the band notched triangular slot UWB antenna
 $(L_1=26\text{mm}, L_2=22.65\text{mm}, L_3=10.85\text{mm}, L_4=7\text{mm}, S=2\text{mm}, W=3\text{mm}, h=1.6\text{mm}, \epsilon_r=4.4, G=0.35\text{mm}, L_5=2.25\text{mm}, L_6=3.5\text{mm}, D=1.5\text{mm}, t=0.5\text{mm}$ and $R=0.5\text{mm}$).

The measured radiation patterns in the YZ and XZ planes of the antenna at the notched frequency are plotted in Fig.4.23. The pattern at 5.8GHz has been normalized w.r.t that at 3.4GHz. We can observe a reduction in gain by 10dB along all directions.

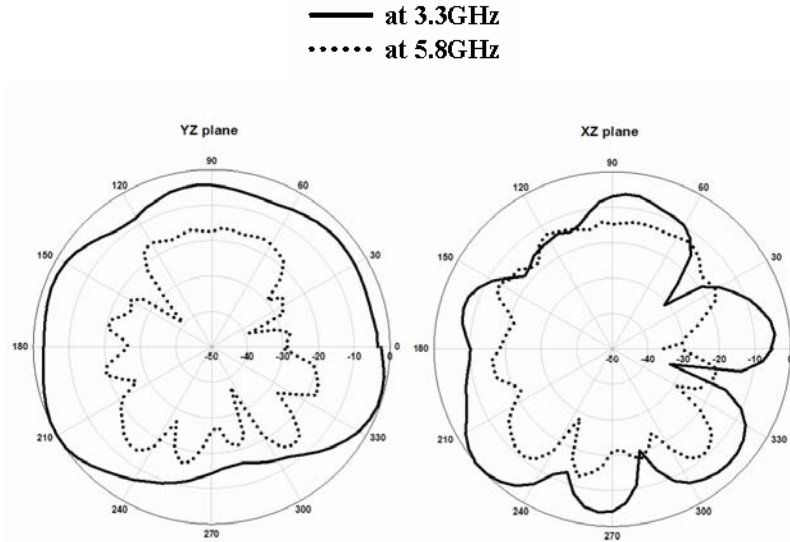


Fig.4.23. Measured radiation pattern of the notched triangular slot antenna

$(L_1=26\text{mm}, L_2=22.65\text{mm}, L_3=10.85\text{mm}, L_4=7\text{mm}, S=2\text{mm}, W=3\text{mm}, h=1.6\text{mm}, \epsilon_r=4.4, G=0.35\text{mm}, L_5=2.25\text{mm}, L_6=3.5\text{mm}, D=1.5\text{mm}, t=0.5\text{mm}$ and $R=0.5\text{mm}$).

4.4 Time Domain Analysis of Triangular Slot UWB Antennas

In the previous sessions we have analyzed the frequency domain parameters of triangular slot and band notched triangular slot antennas. Since time domain analysis is also important for UWB antennas as frequency domain analysis, the following section describes the time domain analysis of the above mentioned UWB antennas.

4.4.1 Group delay of Triangular Slot UWB Antennas

Group delays of the triangular slot and band notched slot antennas are measured for the face to face and side by side orientations and are shown in Fig.4.24. In the case of triangular slot antenna, group delay variations are less than 1nS for both the orientations. In the case of band notched antenna, a sudden decrease in group delay is observed at the notch frequency.

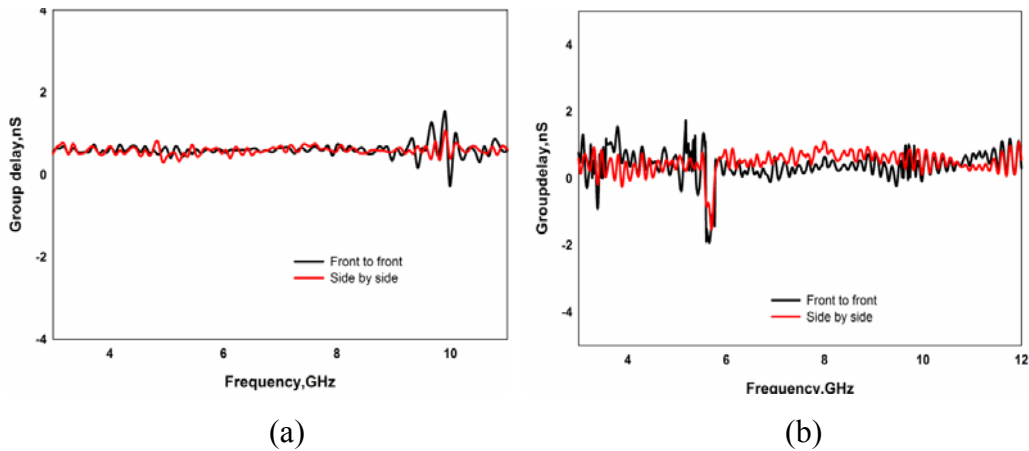


Fig.4.24. Group delays of (a)triangular slot UWB antenna and (b)Band notched triangular slot UWB antenna.

4.4.2 Transfer functions of Triangular Slot UWB Antennas

In UWB application, to minimize the potential interferences between the UWB system and the narrowband systems, the variations of the transfer function magnitude and the group delay should be as acute as possible in the notch-bands and need to be constant in the un-notched bands. A transmitting/ receiving antenna system satisfying these requirements will suppress the interferences coming from the narrowband systems and lead little distortion on useful signals.

Transfer functions of both antennas are measured as given in chapter 2 and are shown in Fig.4.25. It is found that transfer functions of triangular slot antenna remains almost constant in the entire operating band. But, in the case of band notched antenna, a sudden decrease in transfer function is obtained at the notch frequency.

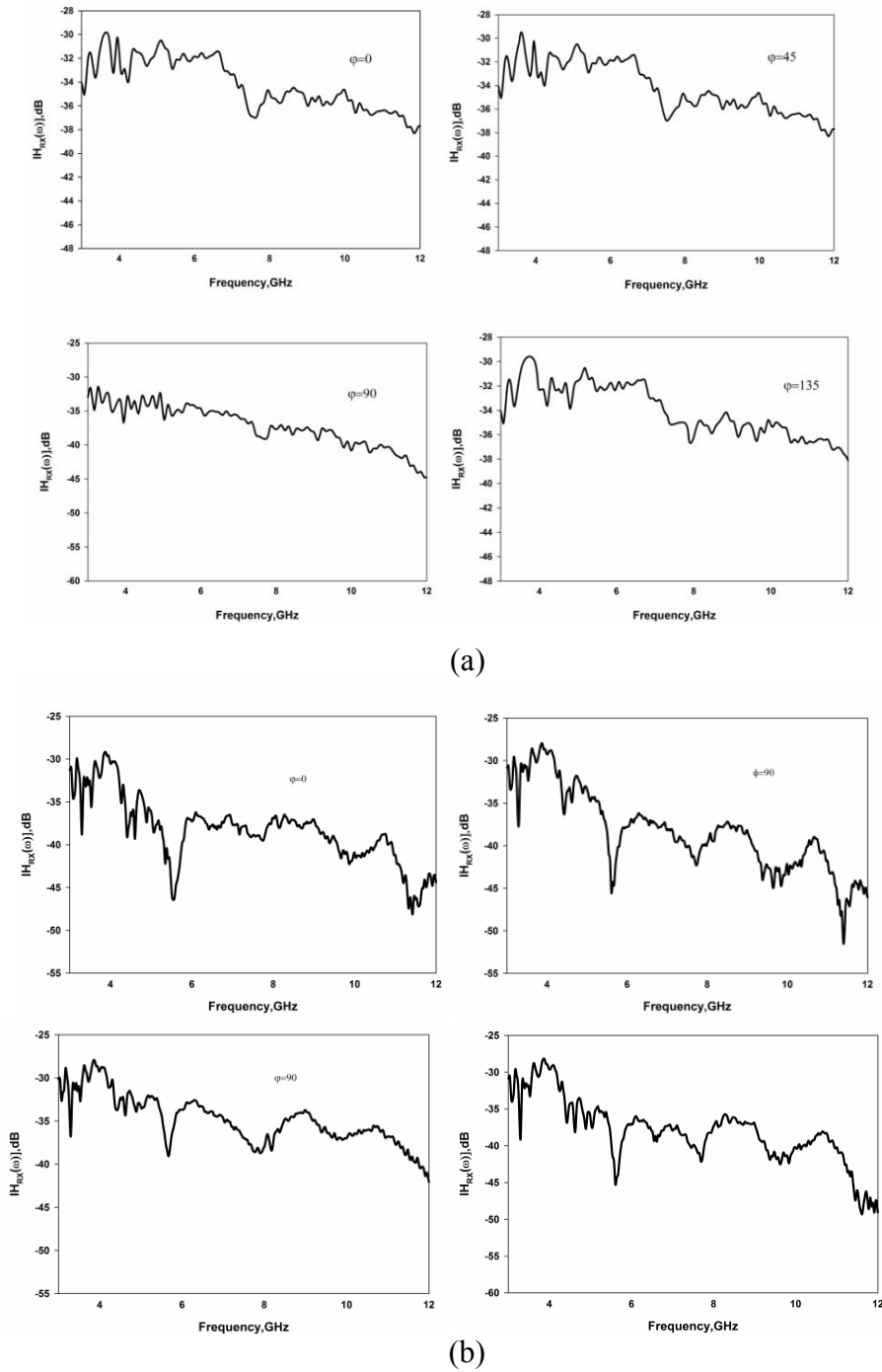


Fig.4.25. Measured transfer functions of (a) triangular slot UWB antenna and (b) Band notched triangular slot UWB antenna.

4.4.3 Impulse Responses of Triangular Slot UWB Antennas

Impulse responses are calculated from the measured transfer functions for various orientations of the receiving antennas and are plotted in Fig.4.26. In the case of band notched antenna ringing is more than the antenna without band notch.

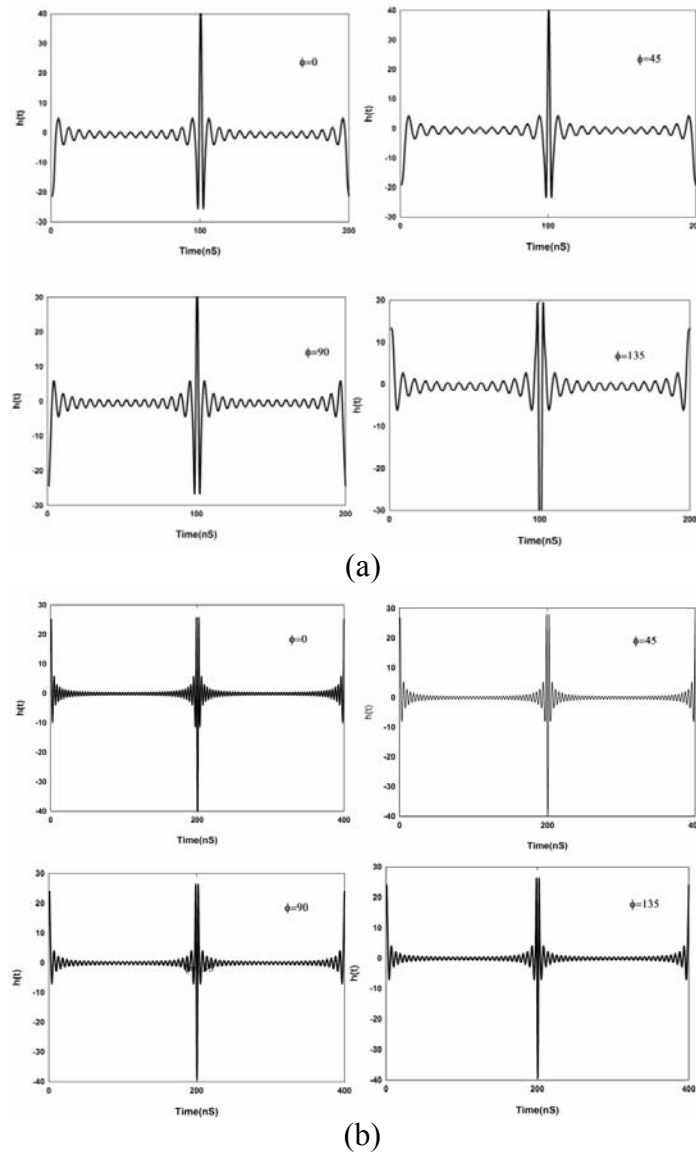


Fig.4.26. Measured impulse responses of (a)Triangular slot UWB antenna and (b)Band notched triangular slot UWB antenna

4.4.4 Received signal waveforms of Triangular Slot UWB Antennas

For a UWB system, as shown in figure 2.2, the received signal is required to match the source pulse with minimum distortions because the signal is the carrier of useful information. The received waveform is determined by both the source pulse and the system transfer function which has already considered the effects from the entire system including the transmitting and receiving antennas.

Received pulses are plotted for triangular slot and band notch antennas by convoluting input pulses and the impulse responses in Fig.4.27. In the case of triangular slot antenna, received waveforms for the two scenarios, ie. face to face and side by side, match with each other very well, which corresponds to the omnidirectional radiation patterns of the antenna. The signal waveform generally follow the shape of the source pulse and only have slight distortion. But in the case of band notched antenna, slight ringing is observed for the received pulses. Measurements indicate that very little distortion was introduced by the antennas and the antennas practically did not affect the transmitted pulses in a destructive way.

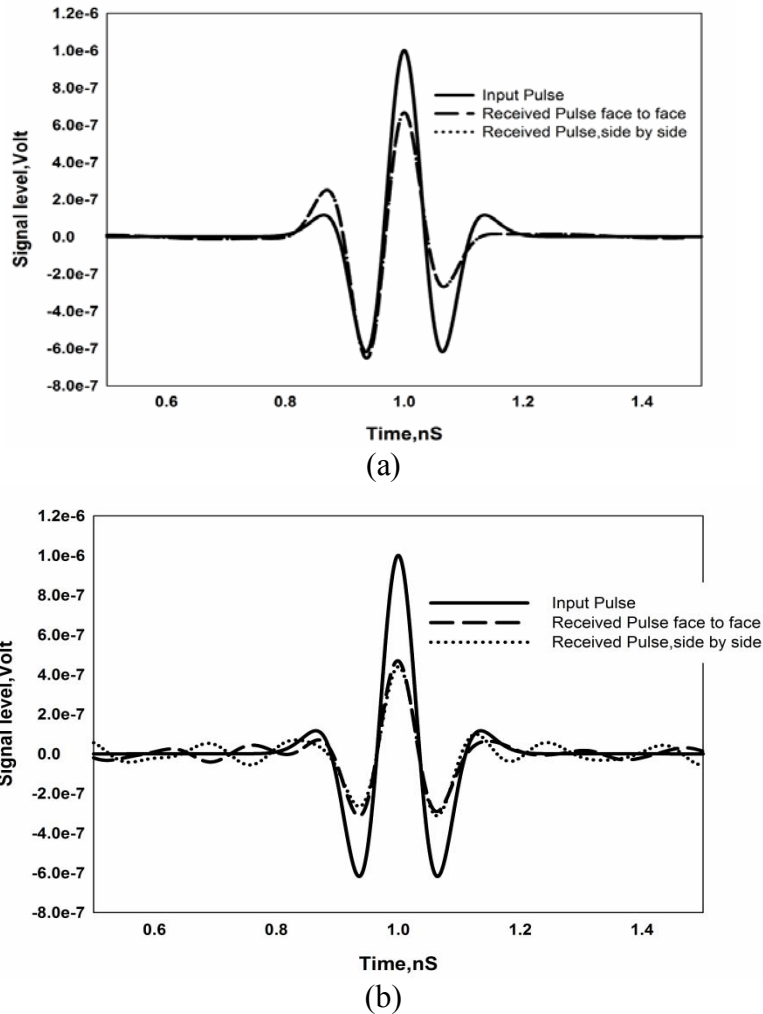


Fig.4.27 Measured received pulses of (a) triangular slot antenna and (b) Band notched triangular slot antenna

4.4.5 Fidelity of Triangular Slot UWB Antennas

Fidelities of the antennas are measured as explained in section 2.2 and are shown in Fig.4.28. Maximum fidelity for triangular slot antenna is found to be 97.4%. And for band notched antenna maximum fidelity is found to be 94.61%. Thus triangular slot antenna exhibits maximum fidelity to other antennas discussed in this thesis.

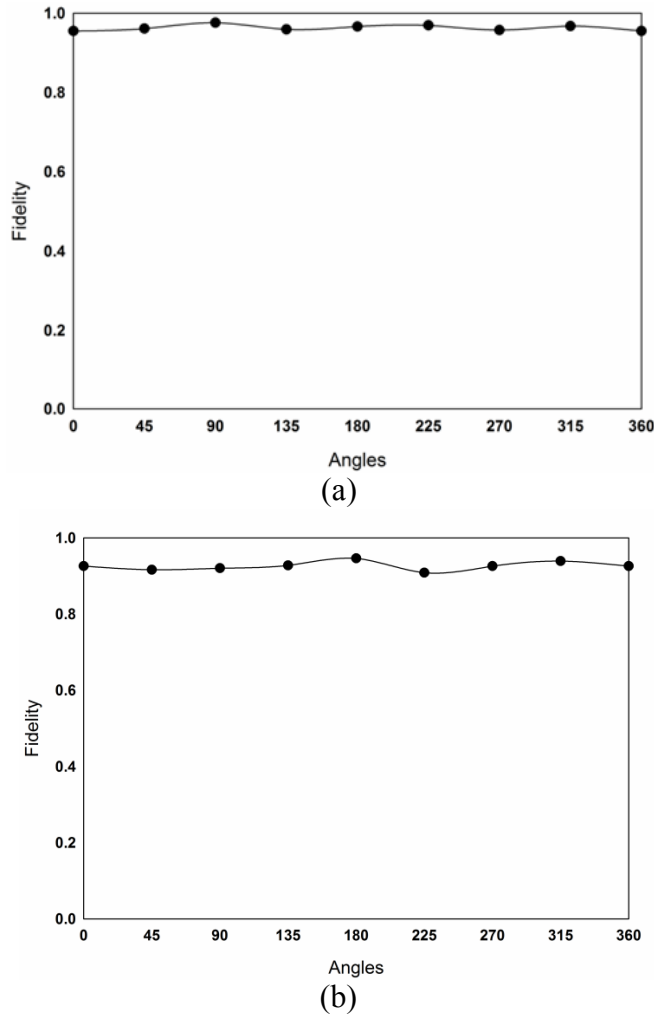


Fig.4.28. Fidelities of (a) triangular slot UWB antenna and (b) Band notched triangular slot UWB antenna

4.4.6 EIRP of Triangular Slot UWB Antennas

According to FCC regulations, UWB systems must comply with stringent EIRP limits in the frequency band of operation. EIRP is the amount of power that would have to be emitted by an isotropic antenna to produce the peak power density of the antenna under test. Measured EIRPs of triangular slot antennas are shown in Fig.4.29. It is clear from the figure that EIRPs of the antennas satisfies both the indoor and outdoor masks of FCC.

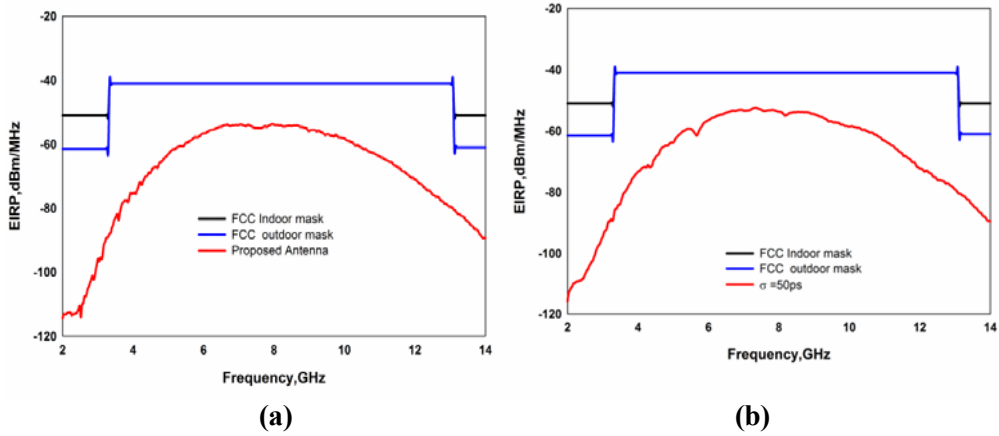


Fig.4.29 Measured EIRPs of (a) triangular slot UWB antenna and (b)Band notched triangular slot UWB antenna

Photographs of the triangular slot antennas are shown in Fig.4.30.

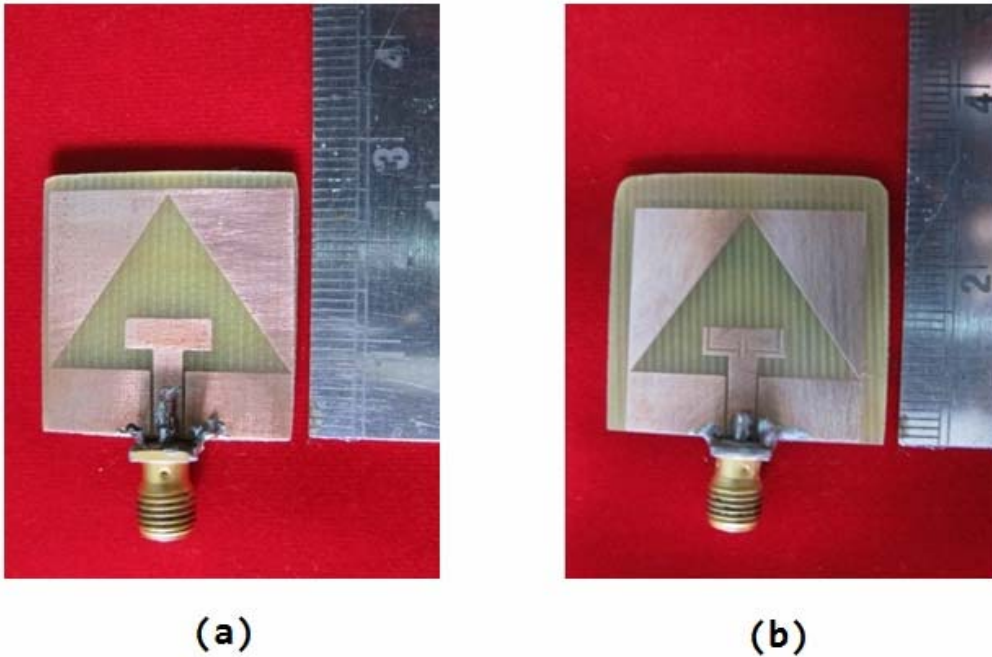


Fig.4.30. Photographs of (a)Triangular slot antenna(b)Band notched triangular slot antenna

4.5 Chapter Summary

Design of a compact ultra wideband triangular slot antenna operating from 3.1 to 11.1GHz is presented in this chapter. The antenna has simple structure and nearly omni directional radiation pattern. It is very interesting to note that this antenna has only 26x26mm² in size and fed by a CPW.

The antenna appears to be an ideal candidate for the 3.1 to 10.6GHz UWB operation from the frequency domain studies. Since the antenna operates over a multi-octave bandwidth, it would be excellent to transmit pulses of the order of nanosecond duration with minimal distortion.

In the last section of this chapter, the designed UWB antenna is adapted to coexist with 5.8GHz WLAN band with minimum interference. A thin half wavelength open ended slit is inscribed on the rectangular patch to filter out the 5.8GHz WLAN band with minimum interference. The time domain performance of these antennas for validating their suitability for pulsed applications is also carried out at the end of the chapter.

References

- [1] J.D. Kraus, "Antennas Since Hertz and Marconi", IEEE Trans. Ants. Prop, AP-33, 131-137, 1985
- [2] Huynh T., Lee K. F," Single layer single patch wideband microstrip antenna", IEE Electronics Letters, 31, 1310-1312, August 1995.
- [3] Wong, Kin-Lu, "Compact and broadband microstrip antennas", John Wiley & Sons Inc., New York, 2002.
- [4] Godara, Lal Chand, "Handbook of Antennas in Wireless Communications", Florida, CRC Press,2002.

- [5] Yoshimura, Y. A microstrip slot antenna, IEEE Transactions on Microwave Theory and Techniques, 20, pp.760-762, August 1972.
- [6] Pozar, David M. “Reciprocity method of analysis for printed slot antenna and slot coupled microstrip antennas”. IEEE Transactions on Antennas and Propagation, AP-34(12), pp.1439-1466,1986.
- [7] M. K. Kim, K. Kim, Y. H. Suh and I. Park, “A T-shaped microstrip-line-fed wide slot antenna”, Proc. IEEE AP-S Int. Symp., pp. 1500–1503, 2000.
- [8] W.-S. Chen, C. C. Huang and K. L. Wong, “A novel microstripline fed printed semicircular slot antenna for broad band application”, Microw. Opt. Techno. Lett., vol. 26, no. 4, pp. 237–239, 2000.
- [9] Gibson P J, The Vivaldi aerial, Proceedings of the 9th European Microwave Conference, Brighton,pp. 101–105,1979.
- [10] Gazit E. Improved design of the Vivaldi antenna, Proceedings of Institute of Electrical Engineering, pp.89–92,1988.
- [11] Langley J. D. S, Hall P S. Newham P, Novel ultra-wide-bandwidth Vivaldi antenna and low cross polarization, Electronics Letters, pp.2004–2005,1993.
- [12] Y. Kim and D.-H. Kwon, CPW-fed right-angled dual tapered notch antenna for ultra-wideband communication , Electronics Letters, pp.674-675,2005.
- [13] Y.W. Jang, “Broadband cross-shaped microstrip-fed slot antenna”, Electronics Letters, ,pp.2056-2057,2000.
- [14] F.W. Yao, S.S. Zhong and X.L. Liang, “Wideband slot antenna with a novel microstrip feed”, Microwave Opt. Tech. Lett., pp.275-278,2005.

- [15] S. Sadat and M. Fardis, "A compact microstrip square-ring slot antenna for UWB applications", IEEE Antennas Propagat. Symp., Albuquerque, New Mexico, pp.4629-4633, 2006.
- [16] S.A. Evangelos and A.Z. Anastopoulos," Circular and elliptical CPW-Fed slot and microstrip-fed antennas for ultrawide band applications" , IEEE Antennas and Wireless Propagat. Lett., vol.5:pp. 294-297,2006.
- [17] J.W. Niu and S.S Zhong," A CPW-fed broadband slot antenna with linear taper", Microwave and Opt. Tech. Lett., pp.218-221,2004.
- [18] Tzyh-Ghuang Ma, and Shyh-Kang Jeng," Planar Miniature Tapered-Slot-Fed Annular Slot Antennas for Ultrawide-Band Radios " , IEEE Transactions on Antennas and Propagation, Vol. 53, No.3, March 2005.
- [19] Chang D C, Liu J C, Liu M Y," Improved U-shaped stub rectangular slot antenna with tuning pad for UWB applications", Electronics Letters, pp.1095–1097,2005 .
- [20] Pengcheng Li, Jianxin Liang and Xiaodong Chen, Study of Printed Elliptical/Circular Slot Antennas for Ultrawideband Applications, IEEE Transactions on Antennas and Propagation, Vol. 54, No. 6, June 2006.
- [21] Evangelos S. Angelopoulos, Argiris Z. Anastopoulos, "Circular and Elliptical CPW-Fed Slot and Microstrip-Fed Antennas for Ultra wideband applications", IEEE Antennas and wireless propagation letters, Vol. 5, 2006 .
- [22] Tzyh-Ghuang Ma and Chao-Hsiung Tseng, "An Ultrawideband Coplanar Waveguide-Fed Tapered Ring Slot Antenna", IEEE Transactions on Antennas and Propagation, Vol. 54, No. 4, April 2006.

- [23] C. Marchais, G. Le Ray, and A. Sharaiha, "Stripline Slot Antenna for UWB Communications, IEEE Antennas and Wireless Propagation Letters, Vol. 5, 2006.
- [24] M. Gopikrishna, D.D. Krishna, C.K. Aanandan, P. Mohanan and K. Vasudevan, "Compact linear tapered slot antenna for UWB applications", Electronic Letters, Vol. 44 No. 20, 25th September 2008.
- [25] Shi Cheng, Paul Hallbjörner, and Anders Rydberg, "Printed Slot Planar Inverted Cone Antenna for Ultrawideband Applications", IEEE Antennas and Wireless Propagation Letters, vol. 7, 2008.
- [26] Aidin Mehdipour, Karim Mohammadpour-Aghdam, Reza Faraji-Dana, and Mohammad-Reza Kashani-Khatib, "A Novel Coplanar Waveguide-Fed Slot Antenna for Ultrawideband Applications", IEEE Transactions on Antennas and Propagation, Vol. 56, No. 12, December, 2008.
- [27] D.D. Krishna, M. Gopikrishna, C.K. Aanandan, P. Mohanan and K. Vasudevan, "Ultra-wideband slot antenna for wireless USB dongle applications", Electronic Letters, Vol. 44, No. 18, 28th August 2008.
- [28] Tharaka Dissanayake and Karu P. Esselle, "UWB Performance of Compact L-shaped Wide Slot Antennas", IEEE Transactions on Antennas and Propagation", Vol. 56, No. 4, April 2008.
- [29] Sunil Kumar Rajgopal and Satish Kumar Sharma, "Investigations on Ultrawideband Pentagon Shape Microstrip Slot Antenna for Wireless Communications", IEEE Transactions on Antennas and Propagation, Vol. 57, No. 5, MAY 2009.

- [30] X. Qing Z.N. Chen, “Compact coplanar waveguide-fed ultra-wideband monopole-like slot antenna”, *IET Microw. Antennas Propag.*, Vol. 3, Iss. 5, pp. 889–898 2009.
- [31] Jorge R. Costa Carla R. Medeiros, and Carlos, A. Fernandes,” Performance of a Crossed Exponentially Tapered Slot Antenna for UWB Systems”, *IEEE Transactions on Antennas and Propagation*, Vol. 57, No. 5, May 2009.
- [32] Amin M. Abbosh, “Miniaturized Microstrip-Fed Tapered-Slot Antenna With Ultrawideband Performance”, *IEEE Antennas and Wireless Propagation Letters*, Vol. 8, 2009.
- [33] Chow-Yen-Desmond Sim, Wen-Tsan Chung, and Ching-Her Lee, “Compact Slot Antenna for UWB Applications”, *IEEE Antennas and Wireless Propagation Letters*, Vol. 9, 2010.
- [34] Wong, K.-L., “Compact and Broadband Microstrip Antennas”, JohnWiley and Sons Inc., New York, NY, 2002.
- [35] FCC NEWS(FCC 02-48), Feb. 14,2002. FCC News release.
- [36] M. Ghavami, L.B. Michael and R. Kohno, “Ultra Wideband Signals and Systems in Communication Engineering”, New York: John Wiley and Sons, USA, 2004.
- [37] K.L. Wong, “Compact and Broadband Microstrip Antenna”, John Wiley and sons. Inc., NY, USA, 2001.
- [38] A.U. Bhohe, C.L. Holloway, M. Piket-May and R. Hall, “ Coplanar waveguide fed wideband slot antenna,” *Electronics Letters*, vol. 36, no. 16, pp.1340-1342, Aug. 2000.

- [39] Alpesh U. Bhoje, Christopher L. Holloway et al, “ Wide- Band Slot antennas with CPW Feed Lines: Hybrid and Log-Periodic Designs ,” IEEE Trans. Antennas and Propag, vol. 52, no. 10, pp. 2545-2554, Oct. 2004.
- [40] J. Yeo, Y. Lee and R. Mittra, “Wideband slot antennas for wireless communications,” IEE Proc.-Microwave. Antennas Propag.(J), vol. 151, no. 4, pp.351-355, August 2004.
- [41] J.Y. Chiou, J.Y. Sze and K.L. Wong, “ A broad-band CPW-fed strip-loaded square slot antenna,” IEEE Trans. Antennas and Propag., vol.51, no.4. April 2003.
- [42] H.D. Chen, “Broadband CPW-fed square slot antenna with a widened tuning stub,” IEEE Trans. Antennas and Propag., vol. 51, no 8, Aug. 2003.
- [43] Denidni and M.A. Habib, “ Broadband printed CPW-fed circular slot antenna,” Electronics Letters, vol. 42, no. 3, pp. 135-136, Feb. 2006.
- [44] T.N. Chang and G.A. Tsai, “A wideband coplanar waveguide-fed circularly polarised antenna,” IET Microw. Antennas Propag., vol. 2, no. 4, pp. 343–347, 2008.
- [45] Shun-Yun Lin et al, “A Novel Compact Slot Antenna for Ultra-Wideband Communications,” IEEE Antennas and Propagation Intl. Symposium, pp. 5123-5126, June 2007.
- [46] Yi-Cheng Lin, IEEE, and Kuan-Jung Hung, Compact Ultrawideband Rectangular Aperture Antenna and Band-Notched Designs, IEEE Trans. Antennas and Propag, Vol. 54, No. 11, November 2006.

.....❧.....

CONCLUSIONS AND FUTURE PERSPECTIVE

5.1 *Thesis Summary and Conclusions*

5.2 *Suggestions for Future Work*

This chapter sums up the results and highlights the achievements of the research work carried out. This is followed by few suggestions for future work. The results presented in the thesis have been published by the author in different international journals and conferences.

5.1 Thesis Summary and Conclusions

The aim of the thesis was to investigate the design requirements of compact planar antennas for ultra wide band applications. Two types of antennas belonging to this class were identified: monopole and slot antennas. Three novel compact antennas were designed, namely ground modified monopole, serrated monopole and triangular slot antenna. The evolution of the designed antennas were investigated in detail to have an insight into their wideband behavior.

The design aspects, based on the geometrical parameters of the antenna, were first investigated. The simulation studies, in terms of their return loss and current/field distribution on the antenna at different resonances, reveal their dependence on the antenna dimensions. Dimensional parameters, critically determining the resonances and wideband impedance matching of the antenna, were identified and simple relations were deduced. This can help the antenna designer to design the antenna on any substrate for the desired frequency range of operation. The deduced geometry can act as a precursor to the final design optimized using any of the simulation softwares.

The designs also incorporate thin slot resonators inscribed within the radiator to reject narrow frequency bands. Such embedded filters avoid the use of additional filters in the circuits which may not be desired for portable wireless systems with space constraints.

A brief summary of the different antennas designed are;

1. Ground modified monopole antenna

This antenna has a wide band of operation (3.1GHz to 12GHz), simple structure and an omnidirectional radiation patterns especially at the lower end of the spectrum. This UWB monopole design is arrived from an

existing narrow band design by a geometric manipulation of the ground plane, whose design aspects are presented in Chapter 3. As mentioned in the detailed literature review of monopole antennas, there are several design practices to realize UWB in such antennas, which may even complicate the antenna design. In the present work a novel method is proposed which include removing quarter circles from the ground plane which can be mathematically accounted to design the ground modified Monopole antenna on laminates with any permittivity.

2. Serrated monopole Antennas

A microstrip fed serrated monopole antenna is designed first which has a reduced size of $20 \times 22 \text{mm}^2$ and wide band of operation (3.09 GHz to 11.6 GHz) is developed. The UWB response is achieved by a microstrip fed staircase patch with an identical inverted ground plane. Antenna appears to be perfectly ideal for UWB hand held applications with compact size, stable & omnidirectional antenna pattern. The antenna gain averages around 2.5dBi and an average efficiency of 85% is noted in the operating band. A band notched antenna to notch out the 5.8GHz WLAN band by etching an inverted U slot from the patch is also presented. Electronic reconfiguration of the notch band by integrating a PIN diode across $\lambda/2$ inverted 'U' slot is also demonstrated. A CPW version of the antenna is also developed and studied at the end of the chapter.

3. Triangular slot Antennas

A triangular slot antenna having the size of $26 \times 26 \text{mm}^2$ overcomes the disadvantage of pattern deterioration at higher frequency region found in the case of ground modified and serrated monopoles is also presented. The antenna features all the desirable characteristics demanded by UWB

communication systems such as adequate impedance bandwidth and stable radiation patterns throughout the ultra-wide band. This design also include an open ended slots inscribed on the tuning stub to notch out the 5.8GHz WLAN band.

The antennas designed for UWB operation from 3.1 to 10.6GHz has been further analyzed for their time domain response in the final section of the chapters to confirm their suitability for pulsed UWB applications. The transfer function measurements are performed for the azimuthal planes and their impulse responses are deduced. The band-notched antenna designs record a clear increase in ringing. The antenna effects on nano-second pulses are measured in terms of the fidelity factor and values $> 90\%$ in the azimuth plane is recorded for all antennas. The triangular slot antenna gives a superior performance with a fidelity $>95\%$ in the azimuth.

All of the designs proposed in this thesis can be conveniently used for ultra wide band systems. However, in the case of ground modified monopole and serrated monopoles, a distortion in the pattern is observed at higher frequencies since the region of radiation does not remain constant. This distortion in the frequency domain gets reflected in the transient response of the antenna and the performance varies with azimuth angle.

The triangular slot antenna, by virtue of their near omnidirectional pattern over the whole bandwidth, exhibits relatively uniform transient response for different space coordinates. The performance of all the designed UWB antennas is, however, within tolerable limits which makes them suitable for pulsed UWB applications.

5.2 Suggestions for Future Work

The following are some of the prospects for future work:

The transfer functions are determined from the measurements. But they can also be found from simulation by placing virtual probes around the antennas. For better understanding of the 3- dimensional antenna radiation properties, an automated measurement setup may be devised in future to measure at different spherical coordinates of the antenna.

A direct time domain measurements may also be performed in future for all the designed antennas using the pulsed power measurements available in PNA's. The antenna can be designed on low temperature co-fired ceramic (LTCC) substrates in future which have the advantage of direct integration with mono lithic microwave circuits.

Further miniaturization of the antennas designed is a feasible future prospect, the techniques to achieve ground-independent UWB antenna performance may be stressed in order to enhance their prospect of adoption in practical applications. Diversity UWB antenna may also investigated for the same reasons. When the antenna is built on a portable device, the impact from human body may also be considered.

UWB systems operate at extremely low power level which limits its transmission range. In order to enhance the quality of the communication link and improve channel capacity and range, directional systems with high gain are required. Therefore, research on UWB directional antenna and antenna array may be carried out.

Due to the low power level operation of UWB systems, a typical UWB receiver requires a low-noise amplifier. Antenna integration with low-noise amplifier may be investigated in future.

.....❧.....

International Journals

- [1] **Shameena.V.A**, Suma M.N ,Rohith K. Raj, Bybi.P.C and P. Mohanan, Compact Ultra wide band serrated antenna with notch band ON/OFF control”, *IEE Electronics Letters*, Volume 42, Issue 23, November 9,2006.
- [2] **Shameena.V.A**, Sarah Jacob, Mridula.S, Anju Pradeep, Lindo.A.O and P.Mohanan “A Compact CPW fed Slot Antenna for Ultra Wide Band applications”, *AEUE, International Journal of Electronics and Communication*, Vol.56,pp.189-194, March 2012.
- [3] **Shameena.V.A**, Sarah Jacob, Mridula.S, C.K.Aanandan, K.Vasudevan and P.Mohanan, A Compact modified ground CPW fed antenna for UWB Applications”, *Microwave Review Journal* ,Vol.17, No.1, September2011.
- [4] Laila.D,Sujith.R, **Shameena V.A**,Deepak.U,Nijas.C.M and P.Mohanan” CPW fed antenna for mobile handset with metal wire mesh”, *IJCA Proceedings on International Conference on VLSI, Communications and Instrumentation (ICVCI): 25-27,2011*.
- [5] Sreejith M.Nair, **Shameena V.A**, R. Dinesh, and P. Mohanan,”Compact Semicircular Directive Dipole Antenna for UWB Applications”, *IEE Electronics Letters*, Vol.47, No.23, November 10, 2011.
- [6] Sreejith M.Nair, **Shameena V.A**,Nijas C.M, C.K.Aanandan, K.Vasudevan and P. Mohanan, “Compact Slot line fed Enhanced Gain Dipole Antenna for 5.2 GHz/5.8 GHz Applications”, Accepted for publication, *International Journal of RF&Microwave Computer-Aided Engineering*.
- [7] Sreejith M.Nair, **Shameena V.A**,Nijas C.M,C.K.Aanandan,K.Vasudevan and P. Mohanan, “Compact Slot line fed Dual Band Dipole Antenna for 2.4/5.2 GHz WLAN Applications”, Accepted for publication, *International Journal of RF&Microwave Computer-Aided Engineering*.

- [8] Sarah Jacob, **Shameena V.A**, Mridula S, C.K.Aanandan,K.Vasudevan and P. Mohanan”Planar UWB antenna with modified slotted ground plane”, Accepted for publication, *International Journal of RF&Microwave Computer-Aided Engineering*.
- [9] Sreejith M.Nair, **Shameena V.A**,Nijas C.M, C.K.Aanandan,K.Vasudevan and P. Mohanan,”Novel Chipless RF Identification Technology for On – touch Data Transfer Applications”, Communicated to *Microwave and Optical Technology Letters*.
- [10] **Shameena V.A**, U. Deepak, R. Sujith, D. Laila, R. Dinesh, and Pezholil Mohanan ,”Band Notched Ultra Wide Band Slot Antenna”, *31st PIERS*, Kuala Lumpur, Malaysia,27-30 March, 2012.
- [11] **Shameena.V.A**,Sarah Jacob, Mridula.S, C.K.Aanandan, K.Vasudevan and P.Mohanan,”A Compact modified ground CPW fed antenna for UWB Applications” *URSI GASS,2011*,Istanbul,Turkey.
- [12] **Shameena V.A**,Sarah Jacob,C.K.Aanandan,K.Vasudevan and P.Mohanan “A Compact CPW fed serrated UWB antenna” *ICCSP,2011*,NIT Calicut, Kerala.
- [13] **Shameena V.A**, S.Mridula, C.K.Aanandan, K.Vasudevan and P.Mohanan “A compact CPW fed slot antenna for ultra wide band applications” *IEEE APS-2009*, Charleston,South Carolina, USA.
- [14] D. Laila, R. Sujith, C. M. Nijas, **Shameena V.A**, R. Dinesh, and Pezholil Mohanan, A Metamaterial Antenna with Reduced Radiation Hazards towards Human Head, *31st PIERS*, Kuala Lumpur, Malaysia,27-30 March, 2012.
- [15] Laila.D,Sujith.R, **Shameena V.A**,Deepak.U,Nijas.C.M and P.Mohanan” CPW fed antenna for mobile handset with metal wire mesh” *ICVCI-2011, St.Gits,Kottayam*.
- [16] Anju pradeep, **Shameena V.A**, S.Mridula,Binu Paul and P.Mohanan “Notch band optimization of planar ultra wide band antenna using GA”, *URSI GA-2008*.

- [17] **Shameena.V.A**, Deepthi.K.V, Gijo Augustine, BinuPaul, C.K.Aanandan, K.Vasudevan and P.Mohanan “CREMASOFT-Microwave measurement automation software”, *Proc. of the National Symposium on Microwave Antennas and Propagation, (APSYM-06). India*
- [18] **Shameena.V.A**, and P.Mohanan ”A compact CPW fed antenna for ultra wide band applications” *Proc. of the National Symposium on Microwave Antennas and Propagation, (APSYM-08). India*
- [19] Sarah Jacob,S.Mridula, **Shameena.V.A** and P.Mohanan “Planar UWB Antenna” *Proc. of the National Symposium on Microwave Antennas and Propagation, (APSYM-10). India*

.....❧.....

Citations

- A. Shameena.V.A, Suma M.N ,Rohith K. Raj, Bybi.P.C and P. Mohanan, Compact Ultra wide band serrated antenna with notch band ON/OFF control”, *IEE Electronics Letters*, Volume 42, Issue 23, November 9,2006.
- [1] “Antenna device with crenellated ground plane”, WIPO Patent WO/2008/132495A1.
- [2] E.Antonino-Daviu, M. Cabedo-Fabrés, , M. Ferrando-Bataller ,”Modal Analysis and Design of Band-Notched UWB Planar Monopole Antennas”, *IEEE Transactions on Antennas and Propagation*,Vol.59,Issue 8,August 2011,Vol.58,Issue 5,May 2010.
- [3] J.R. Kelly, P.S. Hall, P. Gardner and F. Ghanem ,“Integrated narrow/band-notched UWB antenna”, *Electronics Letters*, 10th June 2010 Vol. 46 No. 12.
- [4] Joseph Manoj, “Microstrip-fed compact dual band planar antenna”, Ph.D thesis, Cochin University of Science and Technology.
- [5] Kelly, J.R,Hall, P.S,Gardner, P,”Band-Notched UWB Antenna Incorporating a Microstrip Open-Loop Resonator” ,*IEEE Transactions on Antennas and Propagation*,Vol.59,Issue 8,August 2011.
- [6] C.-Y.-D. Sim ,”Planar UWB Antenna With 5GHz Band Rejection Switching Function At Ground Plane”, *Progress In Electromagnetics Research*, Vol. 106, 321-333, 2010.
- [7] E.Antonino-Daviu, M. Cabedo-Fabres, M. Ferrando-Bataller and Vicent M. Rodrigo-Pefiarrocha,”Active UWB Antenna with Tuneable Band-notched Behaviour”, *Electronics Letters*, August 31,2007.
- [8] Alexander Vasylychenko, Luis A. Cuevas, Xavier Rottenberg, Walter De Raedt and Guy A. E. Vandenbosch”A Planar Monopole UWB Antenna with Switchable Band-Rejection Feature”, *ICUWB 2009* (September 9-11, 2009).

.....✂.....

Curriculum Vitae

SHAMEENA V.A

Senior Research Fellow,
Centre for Research in Electromagnetics and Antennas (CREMA)
Department of Electronics, Cochin University of Science and Technology,
Cochin 682 022, Kerala, India
Phone: 91-484-2576418 Mobile: 91-8089770410 Fax: 91-484-2575800
E-mail: shameenava@gmail.com.

OBJECTIVE

To get a challenging position in an organization to pursue research activities in the field of Electromagnetics and antennas.

SUMMARY

- **5 years** of research experience in Microwave communication, especially in Antennas, Electromagnetics and Dielectric measurements.
- **Publications – 19; International journal – 9; Conferences – 10**
- **Citations - 8**
- Proficiency in Design and Development of various types of antennas

HONORS, AWARDS & ACHIEVEMENTS

- Awarded with **Research Fellowship in Sciences for Meritorious students** by University Grants Commission (UGC), Govt.of India in 2011.
- Awarded student grant from CSIR, the Govt. of India for presenting a research work at 30th URSI General Assembly and Scientific Symposium held at Istanbul, Turkey during 13-20 August 2011

AREAS OF INTEREST

Planar Antennas, Microwave communication, Metamaterial Antennas, Electromagnetics, Biological effects of Microwaves, Dielectric resonator antennas, Ferroelectric tunable devices, Microwave material characterisation etc.

TECHNICAL SKILLS

- Experienced in using **HP 8510C** Vector Network Analyzer, **PNA E8362B** Network Analyzer, **R&S ZVB20**, Anritsu Spectrum Analyzer, Anechoic chamber measurements etc.
- Experience in Antenna and RF/Microwave circuit design tools like **Ansoft HFSS, CST MWS and IE3D**.

- Experience in design and testing of compact low frequency antennas, **uniplanar antennas**, and printed monopole antennas.
- Involved in the designing of various ultra compact wide band uniplanar antennas for multiband applications highly suitable for compact mobile phones.
- Involved in the design of **radiation hazardless antenna** suitable for mobile handset.
- Designed various Uniplanar antennas for applications compatible for use in Laptops and similar wireless devices.
- Hands-on experience in **building of antenna prototypes** using photolithography and antenna experimental work.

SCIENTIFIC PROGRAMMES ATTENDED

Date (Year)	Organising Body	Title and Purpose of Events
16-18, November SYMPOL 2011	Department of Electronics, Cochin University of Science and Technology	International conference on Ocean Electronics- SYMPOL-2011 Organizing committee member
13-20 August 2011	International Union of Radio Science(URSI)	URSIGASS-2011,Istanbul, Turkey. Presented a poster
4-5 March, 2011	University Grants Commission(UGC) and Cochin University of Science and Technology	National Seminar on Frontier Technologies in RF Engineering. As a Participant
10-12 February,2011	National Institute of Technology,Calicut,Kerala.	To present a research paper
14-16 December, APSYM 2010	Department of Electronics, Cochin University of Science and Technology	Antennas and Propagation Symposium -2010 Organizing committee member
18-20, November SYMPOL2009	Department of Electronics, Cochin University of Science and Technology	International conference on Ocean Electronics- SYMPOL-09 Organizing committee member
10-12, December, APSYM 2008	Department of Electronics, Cochin University of Science and Technology	Antennas and Propagation Symposium -2008 Organizing committee member and Presented a research paper

RESEARCH EXPERIENCE INCLUDING RESEARCH PROJECTS

Research Fellow at Centre for Research in Electromagnetics and Antennas (CREMA), Department of Electronics, Cochin University of Science and Technology, Cochin, from March 2006 onwards.

EDUCATION

Course	Year of Passing	University	Institution	Class
M.Sc Electronics	2003-2005	Cochin University of Science and Technology(CUSAT), Cochin, Kerala, India	Department of Electronics, CUSAT, Kerala, India	First class with Distinction CGPA 8.64
B.Sc Physics	2000-2003	Calicut University Kerala, India	S.N.College,Nattika	First class (84.7%)

PERSONAL

Date of birth : 1st June 1983
Sex : Female
Nationality : Indian
Passport Number : F-2904233

Permanent Address : Valiyakath house
P.O.Karayamuttom
Via-Valapad – 680567,
Kerala, India.
Ph: +91 487 2396573

Cell : 91-8089770410

E-mail : shameenava@gmail.com

.....*SR*.....

Index

A

Anechoic Chamber, 39,42,45,70
Ansoft, 39,46,71

B

Blue tooth,6,7,8,9,30,35
bandnotch,33,79,121,123,124,125,126,127,128,129,140,141,144,146,147,148,149,150,151,152,157,183,184,185,186,187,188,189,190,191,192,193,194,195,205

C

calibration ,45
Cellular ,5,7
characteristic impedance,81,132
communication,1,2,3,4,5,6,7,8,9,10,11,12,14,21,24,25,26,27,28,29,30,31,34,35,36,37,52,56,59,61,62,65,68,71,72,74,75,76,77,80,105,108,121,132,140,151,153,155,161,163,165,169,196,197,198,199,200,201,202,206,207
Coplanar waveguide,62,63,64,65,81,82,83,93,122,132,133,158,159,161,162,165,169,198,199,202,203
CREMA SOFT, 43,45

D

Dielectric constant, 93,133,164,166, 168
Dipole,3,4,20,21,62,74,151,156,176

E

Efficiency,
4,13,16,43,44,45,60,62,101,105,120,121,128,139,183,187
Electromagnetic, 2,9,12,13,15,28,31,42,46,61,73,118,121,126,156,160,181,201
electronic gadgets, 62

experimental, 13,15,39,45,59,64,66,67,69,79,81,87,89,94,110,155,156,159,168
EIRP,24,25,56,57,58,59,73,149,150,196,197

F

far field, 42,56,58,64,140,141,178
Fidelity,33,39,55,56,70,148,149,195,164,206

G

gain, 7,17,27,31,32,42,45,46,47,48,50,55,57,58,62,65,66,70,79,101,105,120,121,127,128,139,183,187,157,158,159,161, 163,168,183
Group delay,16,40,49,50,70,140,141,162,163,165,190,191

H

harmonics, 136
HFSS, 39,46,71
HP8510C, 41,131

I

ISM, 8
Impulse Response,13,16,33,50,54,55,56,59,144,145,146,193,194,206

L

LTCC, 207

M

metamaterials, 4,37
microstrip,3, 32,34,35,60,62,63,66,104,105,112,118,123,130,132,141,143,145,146,147,148,149,150,151,154,156,157,158,159,161,162,163,196,197,205
MMIC, 60
multiband, 21,22,24,35,76

O

omnidirectional, 59,66,67,72,73,77,78, 80,99,101,114, 152,160,179,192, 204, 205,206

P

Pin
diode,33,79,129,130,131,150,154,205
Photolithography,40
Planar Antennas,30,56,61,62,70,73
polarization,2,16,17,19,20,42,58,63,66, 84,86,107,108,157,158,162,175,176,197

R

Reconfigurable
antennas,153,154,129,130,131
RF isolation, 131

S

Serration,104,111,112,113,114,115,11 6,117,118,120,124,125,126,127,128,13 2,133,134,136,138,139,140,141,143,14 5,146,147,148,149,150,79,32,33
surface current,32,110,111,124,125, 131,136,79,84,92,98,155,182,186

T

THRU calibration,45
Time domain,31,33,13,14,41,46,53,54, 55,67,71,72,39,139,140,145,150,155,1 59,188,196,206,207
Transfer function,33,48,49,54,55,65, 70,141,143,145,159,189,190,191,192,2 06,207

V

VSWR,61,63,64,65,66,68,70,83,94,11 3,123,127,134,159,160

W

WLAN,11,33,79,121,122,150,153,196, 155,205,206.

.....❧.....